The Synthesis and Characterization of Novel *N*-Ferrocenyl Benzoyl Amino Acid and Dipeptide Derivatives.

by

David M. Savage B.Sc. (Hons)

A thesis presented for the degree of Doctor of Philosophy

at

Dublin City University

Ollscoil Chathair Bhaile Átha Cliath

School of Chemical Sciences

May 2003

To Mam and Dad

DECLARATION

I hereby certify that this material, which I now submit for assessment on the programme of study leading to the award of Ph.D is entirely my own work and has not been taken from the work of others save and to the extent that such work has been cited and acknowledged within the text of my work.

Signed: David M Savage. ID No. 99145472.

David M. Savage

Date: 22/8/03

Acknowledgements

I want to thank Dr Peter T M Kenny and Dr John F Gallagher, firstly, for giving me the opportunity to conduct research under their supervision, and secondly, for being so supportive and patient during my time in DCU

I also want express my gratitude to

The Irish-American partnership and the DCU School of Chemical Sciences for funding this research

Dr Yoshiteru Ida at the School of Pharmaceutical Sciences, Showa University, Hatanodai, Shinagawa-ku, Tokyo 142-8555, Japan, for obtaining mass spectrometric data

Dr Robert Forster, for the use of electrochemical equipment, Dr Alan Kennedy, Dr Darren Walsh and Lorraine Keane, for advice and expertise in obtaining and interpreting the electrochemical data

To all the technical staff especially Damien McGuirk, Mick Burke and Ambrose May

Thanks also to all the fourth year undergraduate students especially French exchange student Helene who worked on this project

A special thanks to my colleagues, Noel Brennan, Frankie Anderson, Steven Alley and Paula Kelly, members of the Kenny and Gallagher research group

All my fellow postgraduate researchers particularly, Ben, Colm, Ollie, Mairead, Cathal, Darragh, Andrea, Ray, Rob, Jai Feng, Rachel, Yang, Nameer, and Ian, in X249, Peter, Scott, Adrian, Helen, Jennifer, Karl, Johnny, Wesley, Marco, Kev and Fiona 1 & 2, in X246

Thanks to all my mates outside the world of academia (sorry I have been away so long, see you all soon!!!)

A big thank you to Edel for being so helpful and patient with me

Thanks also to my brother and sisters, John, Ruth and Claire

Finally to my parents, Maurice and Maire, thanks for supporting me morally and financially and every other imaginable way through the last 26 years A more wonderful set of parents do not exist Without their help none of what I have achieved would have been possible

Abstract

A series of novel *N*-(ferrocenyl)benzoyl amino acid and dipeptide derivatives have been synthesized and characterized It is intended that the incorporation of organometallic fragments onto amino acids and dipeptide moieties will lead to the development of new materials with innovative applications In this project, a ferrocenyl benzoyl moiety has been attached to amino acid or dipeptide fragments using standard peptide chemistry Though there are more than one potential uses for these new amino acid derivatives, the presence of both hydrogen bond donating amide and redox active moieties would suggest that they should be cheap and effective ionophoric compounds and this may be their most financially exploitable application In addition, investigations are ongoing to ascertain the biological activity of these compounds

The synthesis of the *N*-(ferrocenyl)benzoyl amino acid and dipeptide derivatives was achieved by coupling the free *N*-terminus of an amino acid ester (glycine, L-alanine, L-leucine, L-phenylalanine, β-alanine, 4-aminobutyric acid, ± 2-ammobutyric acid, isobutyric acid) or dipeptide esters (glycine-glycine, glycine-L-alanine, glycine-L-leucine, glycine-L-phenylalanine, L-alanine-glycme, L-alanine-L-alanine, L-alanine-L-leucine, L-alanine-L-phenylalanme, β-alanine-β-alanine) to the carboxyl group of the *ortho*, *meta* or *para* ferrocenyl benzoic acid by using the standard 1,3-dicyclohexylcarbodiimide (DCC), 1-hydroxybenzotriazole (HOBt) protocol

These compounds were fully characterized by a range of spectroscopic techniques including, IR, UV-Vis, ^{1}H, ^{13}C, DEPT 135 and HMQC NMR in addition to FAB-MS, ESI, MALDI-TOF and tandem MS X-ray crystal structures were also obtained in some cases

Cyclic voltammetric and ^{1}H NMR titration experiments were carried out in order to determine the anion sensing and/or recognition abilities of the *N*-(ferrocenyl)benzoyl glycine, β-alanine, glycine-glycine and β-alanine-β-alanine compounds In the ^{1}H NMR spectra, downfield shifts of the amide proton in order of 1 ppm were noted upon addition of $H_2PO_4^{2-}$ to a solution of *N*-(ferrocenyl)benzoyl-β-alanine-β-alanine ethyl ester This is an indication that *N*-(ferrocenyl)benzoyl amino acids and dipeptide derivatives may be applicable as effective anion sensing compounds

Table of Contents

Chapter 4. Anion Binding studies.

Chapter 1.

Literature Review

1 1 Introduction

Though organometallic complexes, in which low oxidation state metals are coordinated to a range of organic based ligands, have been known for over two hundred years,[1] the inadvertent discovery of ferrocene by two independent research groups in 1951 marked the beginning of modern organometallic chemistry [2,3] In the immediate aftermath of its discovery, ferrocene (originally called dicyclopentadienyliron) was initially formulated as containing two Fe-C σ bonds However, this structure was not at all consistent with its stability toward air and heat Following subsequent physical and spectral experiments, Wilkinson *et al*, proposed a revolutionary bonding theory in order to explain these apparent anomalies *i e* the π systems of the two respective cyclopentadienyl ligands interact with the empty *d* orbitals of the iron atom thus resulting in a sandwich type structure [4] Subsequent X-ray diffraction studies of ferrocene confirmed that Wilkinson's theory was indeed correct [5] This breakthrough caused a renaissance in the field of organometallic chemistry resulting in the development of a thriving discipline whose practitioners have produced a host of intriguing structures some of which have found application in various disciplines including organic synthesis and catalysis [6]

In recent years, a characteristic development has been the gradual merging of once distinct fields of research The emergence of bio-organometallic chemistry *i e* the attachment of organometallic compounds to biomolecules, as a subject of interest, is a case in point [7] The attraction of biomolecules to the chemist may be accounted for by the fact that they are usually plentiful in nature and are hence, relatively cheap In addition, biomolecules are generally stable under physiological conditions, yet are inherently but specifically reactive [7] Scientists have realized that in terms of structure and reactivity, the attachment of organometallic fragments to biomolecules may well pave the way towards the synthesis of a multitude of novel compounds that could have potentially many applications

The literature review that follows, seeks to give an overview of the chemistry of ferrocene and the applications of certain ferrocenyl compounds that are relevant to the research reported later in this thesis

1.2 The chemistry of ferrocene.

1 2 1 The Effective Atomic Number rule in relation to ferrocene

The stability of ferrocene can be accounted for by the fact it obeys the effective atom number (EAN) rule The EAN rule states that a stable complex with the electronic configuration of the next highest noble gas is obtained, when the sum of metal *d* electrons plus the electrons donated from its ligands adds up to 18 Ferrocene is an 18 electron complex, and the 18 electrons can be accounted for by the addition of 6 electrons of Fe^{2+} to 12 electrons donated by the two respective cyclopentadienyl anions [8]

1 2.2 Bonding in the ferrocene molecule.

Bonding in ferrocene, involves ring to metal donation of π electrons, from the filled *p* molecular orbital on the ring into a vacant *d* orbital on the metal (Fe^{2+}), coupled with a degree of metal to ring back bonding from the filled orbitals on the metal to the π^* orbital on the (η^5-C_5H_5) ring, (the 10 p orbitals of the two rings give rise to ten molecular orbitals which are related to the 10 molecular orbitals of the individual rings) The five *p* orbitals on the planar cyclopentadienyl group can be combined to produce 5 molecular orbitals of which one is strongly bonding (a), two are weakly bonding and are degenerate (e_1), and two are degenerate and weakly anti-bonding (e_2) For the ferrocene bonding description, there are two cyclopentadienyl groups, so their sum and difference are considered They are a_{1g}, a_{2u}, e_{1g}, e_{2g}, e_{2u} Therefore, there are three sets of π orbitals of which only the e_{2g} and e_{2u} are unfilled If these molecular orbitals are considered along with the metal orbitals, a molecular orbital picture becomes apparent for the ferrocene molecule The metal orbitals have the following symmetries, 4s and $3d_z^2$ corresponding to A_{1g}, $3d_{xz}$ and $3d_{yz}$ corresponding to e_{1g}, $3d_{xy}$ and $3d_{x^2-y^2}$ corresponding to e_{2g}, $4p_z$ corresponds to A_{2u}, $4p_x$ and $4p_y$ corresponds to e_{1u} and the metal has no orbital of e_{2u} symmetry Although the ring and metal orbitals may have compatible symmetries, the degree of overlap between them is dependent on energy differences and distribution in space For example, the a_{1g} bonding molecular orbital is mainly ligand based and it is stable relative to the metal orbitals 4s and $3d_z^2$, so therefore they have little interaction Similarly, the a_{2u} level has virtually no interaction with the higher lying Fe $4p_z$ orbital which has formally the correct symmetry to combine The best matched orbitals in terms of symmetry and energy are a_{1g} and Fe $3d_{xz}$ and $3d_{zy}$, and consequently the two strong π

bonds created form most of the strength of the ferrocene molecule [8] The molecular orbital diagram for ferrocene is shown in Figure 1 1

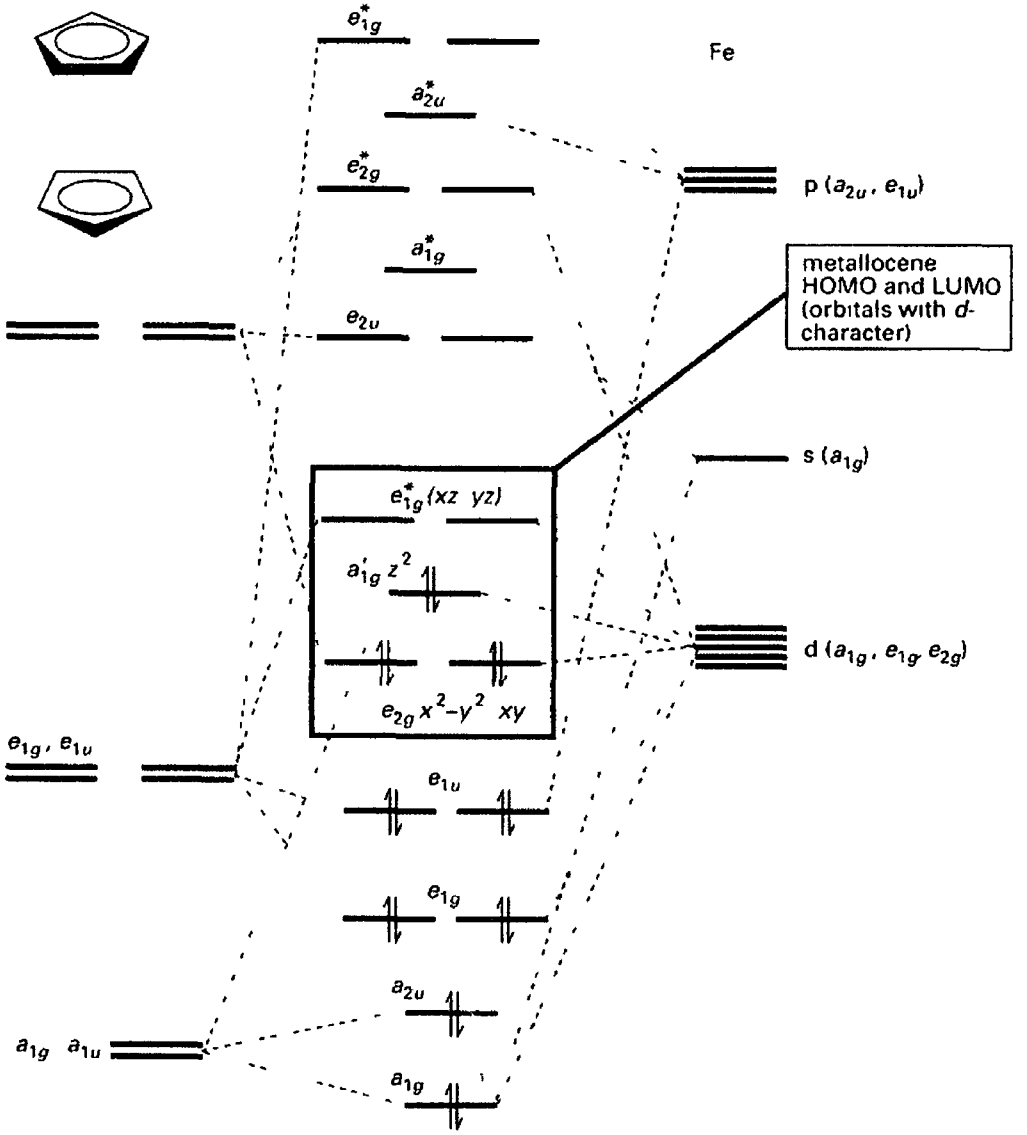

Fig 1 1 Molecular orbital diagram for ferrocene [8]

1 2 3 An examination of the molecular orbital diagram in relation to the 18-electron rule.

Ferrocene is the most stable metallocene It has the ideal number of electrons for a (η^5-C_5H_5)M(η^5-C_5H_5) complex *i e* 18 electrons Nine pairs of electrons are accommodated precisely by filling all the bonding and non-bonding molecular orbitals and none of the anti-bonding molecular orbitals The frontier orbitals can be regarded as bonding (e_2),

non-bonding (a_1) and anti-bonding (e_1*) (Figure 1 2) Molecular energy level diagrams indicate that the chemically relevant frontier orbitals are neither strongly bonding nor anti-bonding, this allows for the existence of metallocenes that diverge from the eighteen electron rule *e g* cobaltocene (19 electron) and nickelocene (20 electron)

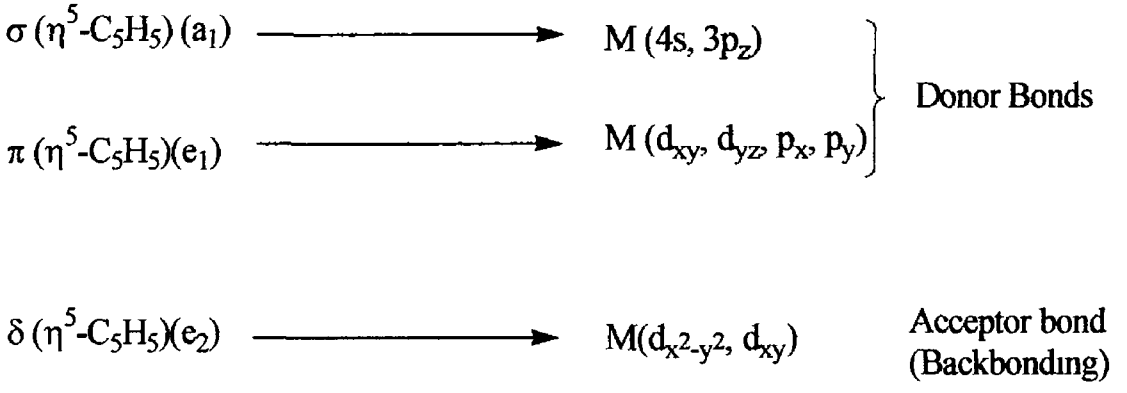

Fig 1.2 Electronic distribution in ferrocene [8]

1.2 4 The organic chemistry of ferrocene

Ever since the discovery of ferrocene in 1951, research concerning the synthesis of ferrocenyl derivatives has increased rapidly [6] Confirmation that the cyclopentadienyl rings of ferrocene were aromatic suggested that the chemistry of ferrocene was analogous to that of other aromatic compounds and hence, many ferrocenyl derivatives were prepared using classic aromatic synthetic procedures [9] For example, the Friedel-Crafts acylation and various metallation procedures have been applied successfully to the ferrocene system [9] Due to the stability that ferrocene shows (in terms of the strength of the metal to ligand bonds), there is a vast range of organic chemistry possible and therefore, it is feasible to carry out many transformations on the cyclopentadienyl ligands using harsh conditions without disrupting the structural integrity of the ferrocene molecule [6] For these reasons, countless papers have appeared in the chemical literature since 1951 reporting a multitude of reactions and synthetic procedures involving ferrocene thus laying testimony to its popularity and synthetic versatility Some of these reactions are summarized in Figure 1 3

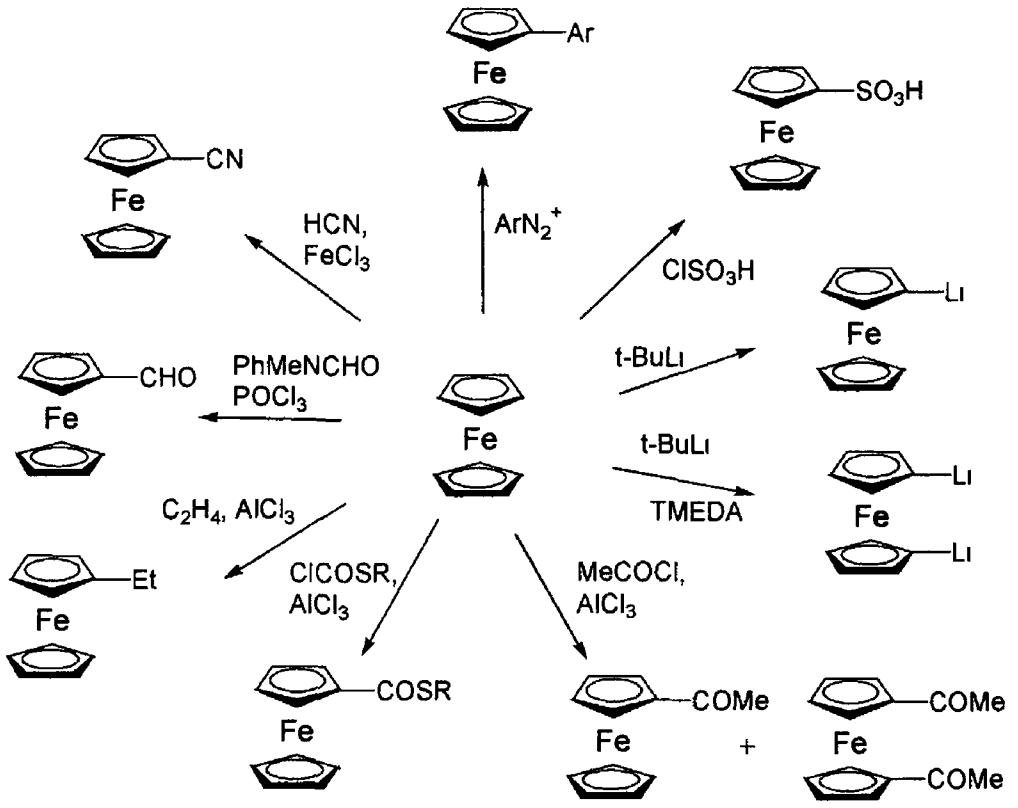

Fig 1.3 Some organic reactions of ferrocene [8]

1 2.4.1 Electrophilic substitution of ferrocene

Electrophilic substitution reactions dominate the chemistry of ferrocene and some possible modes of reaction have been proposed [8]

A reaction mechanism has been suggested where the initial interaction occurs between the electrophilic agent and the weakly bonding electrons of the iron atom This is followed by a transfer of the electrophile to the *endo* face of the (η^5-C_5H_5) *i e* the side nearest the iron atom Subsequent proton elimination gives the substituted product

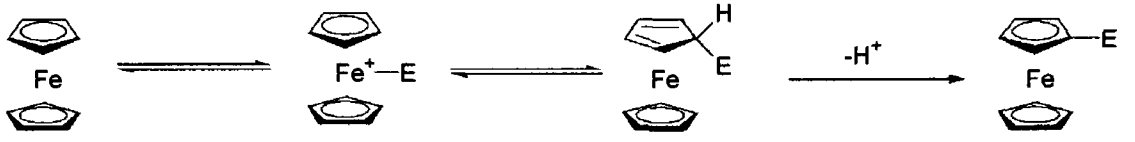

Fig 1 4 A mode of reaction for the electrophilic substitution of ferrocene that proceeds *via* the transition states in which the electrophile is bonded to iron atom [8]

Alternatively, it has also been proposed that the electrophilic agent can react directly with the cyclopentadienyl ring and does not have any direct interaction with the iron atom

Unlike the reaction scheme in Figure 1 4, the electrophile is added to the *exo* (least hindered) face of the ferrocene molecule

Although there are examples in the literature of an intramolecular migration of a group from the metal atom to the *endo* face of attached π-hydrocarbon ligands, studies carried out by Rosenblum and Abbate in 1966 indicate that electrophilic substitution reactions involving ferrocene are more likely to proceed *via* the route outlined in Figure 1 5 [10]

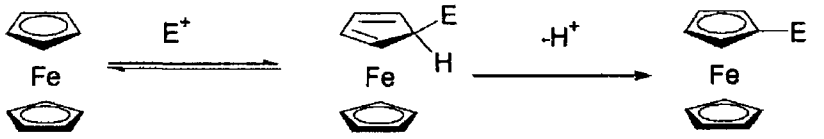

Fig 1 5 A reaction mechanism for the electrophilic substitution of ferrocene where the electrophile reacts directly with the (η^5-C_5H_5) ring *via* the *exo* transition state

A third possible route outlined in Figure 1 6 involves the addition of an electrophile directly to the *endo* face of the (η^5-C_5H_5) ligand

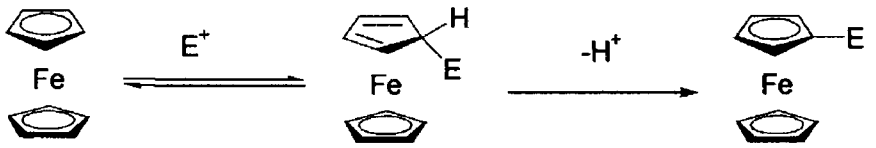

Fig 1 6 A mode of reaction for the electrophilic substitution of ferrocene where the electrophile reacts directly with the (η^5-C_5H_5) ring *via* the *endo* transition state

Each of the routes is plausible and probably all occur It has been suggested that the stereochemistry of electrophilic substitution and the kinetic features of the reaction are governed to large extent by the nature of the electrophile [8] For example, where reagents are more electrophilic than the proton, the rate determining step is the addition of the electrophile which favours the attack from *exo* direction, but for reagents that are less electrophilic than the proton the *endo* pathway is favoured and deprotonation is rate limiting

1 2.4 2 The arylation of ferrocene.

The arylation of ferrocene is achieved by treating ferrocene with an aryl diazonium salt (Figure 1 3) [8] The exact details regarding the mechanism of this reaction are unknown Investigations carried out independently by Pauson, Wemmayer and Nesmeyanov indicated that this reaction is of a free radical nature, citing the Bachman-Gomberg reaction as an analogous example [11-13] This assertion has received a wide consensus [14 15] In the reaction between ferrocene and an aryl diazonium salt, Pauson suggested a mechanism involving an initial electron transfer process in which ferrocene effects reduction of the diazonium cation to a diazonium radical which subsequently decomposes with evolution of nitrogen gas and generation of the aryl radical (Figure 1 7) [11] The characteristic appearance of a blue-green colour is consistent with the formation of ferricenium salts

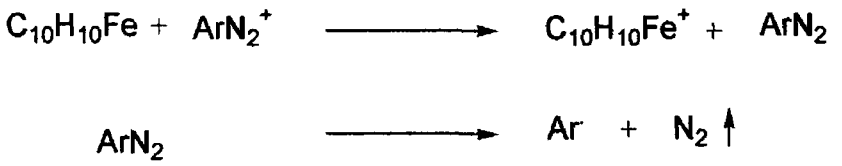

Fig 1 7 Proposed reaction scheme to account for the generation of aryl radical species [11]

Rosenblum *et al* later suggested that this reaction proceeds *via* a transient species formed between the diazonium cation and the iron atom of ferrocene (Figure 1 8) [14]

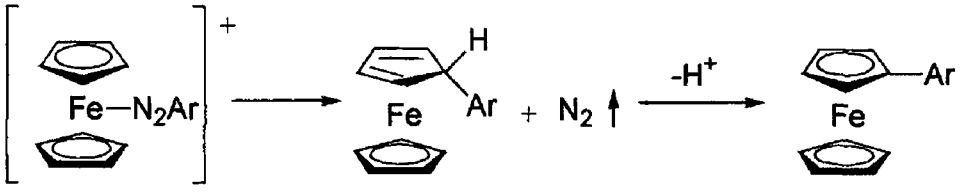

Fig 1 8 The transient transition state as proposed by Rosenblum *et al* [14]

The generation of arylferrocenes must therefore arise from the decomposition of the transient species shown in Figure 1 8 This involves the internal migration of the aryl group and the simultaneous loss of N_2 to give an endocyclic σ product It is unknown if the migrating species is a cationic or radical species [14]

1.3 Redox properties of ferrocene

The redox properties of ferrocene and its derivatives refers to its ability to lose one electron at potentials that are a function of the electron donating ability of the substituents attached to the cyclopentadienyl ring [6] A large variety of macrocycles, cryptands and cavitands containing the ferrocene unit have been synthesised and characterised [16-18] In the majority of cases, complexation by the ligands affects the electrochemistry of the redox centre, particularly when the guest species is either in close proximity to the iron atom or coordinated by functional groups that are conjugated with the ferrocene system In many cases the sole reason for the incorporation of a ferrocenyl moiety into an organometallic system is for exploitation of its redox properties [19] For example, ferrocene is readily oxidised to the dicyclopentadienyl iron (III) cation (ferricenium) and this can be achieved in a number of ways,

1 Electrochemically
2 Photochemically
3 Various oxidising agents

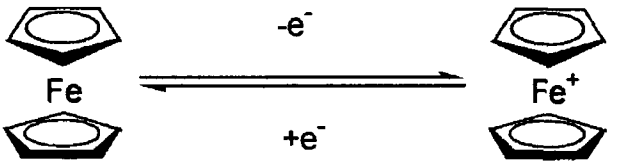

Fig 1 9 Oxidation/reduction of ferrocene

Oxidation is reversible both chemically and electrochemically and the potential shows sensitivity to nature of substituents, for example, alkyl groups tend to aid oxidation, whereas aryl groups tend to hinder oxidation [6]

This redox activity has resulted in the incorporation of ferrocene into supramolecular systems to act as switches or receptors Since selective binding of the systems can affect redox potential of the metallocene unit, this offers huge applications in the field of chemical sensors [6]

1.4 Biologically active ferrocenyl compounds

In the past ten years, much research has been carried out, studying transition metal complexes that incorporate biogenic entities [20] This has yielded a two way learning process On the one hand, biologists and biochemists have found out that certain organometallic compounds are stable, often even under physiological conditions On the other hand, organometallic chemists have recognized the potential and chemical diversity of biologically relevant ligands [7]

Since the introduction of antibiotics for the therapy of infectious diseases, bacteria have rapidly developed immunity towards the actions of drugs *Pathogenic organisms*, resistant to one or more drugs have become increasingly prevalent over the last few decades to the point where the difficulties in controlling infections with antibiotics have risen enormously For example, there has been a dramatic increase in the incidence of mycobacterial infection coupled with the resistance of mycobacteria against frontline anti-tuberculosis drugs [21] Serious problems are caused by the emergence of MRSA (multi-resistant staphylococci and glycopeptide resistant enterococci [22]) and over the last thirty years the instance of malaria in the developing world has risen sharply due to overuse of the conventional malarial drug chloroquine [23] These problems urgently require the development of new drugs, preferentially those with new mechanisms of action

Interest is rapidly growing in the use of transition metal complexes in medicine and other biological areas [23] An example is the successful application of platinum complexes such as cisplatin *i e* *cis*-$[PtCl_2(NH_3)_2]$, a potent anti-tumour agent [24] More interesting for the purposes of this review is the research carried out by Kopf-Maier and Georgopoulou where their respective investigations of ferrocenium salts have shown that they also exhibit anti-tumour activity [25,26]

Krieg *et al* have synthesised a series of *N*-ferrocenyl amino steroid molecules **1** (Figure 1 10) in an attempt to develop novel antimicrobial agents [27] Squalamine, a naturally occurring amino steroid, 7-aminocholesterol and their derivatives were described as having interesting antibiotic activities After the novel steroidal (*N*-ferrocenylmethyl)amines were screened *in vitro* for antimicrobial activity against a broad spectrum of test organisms including fungi, mycobacteria, multi-resistant staphylococci, and enterococci, four stereo-isomers of (16-ferrocenylmethyl)amino-estratrienes exhibited noteworthy broad activity against all organisms tested

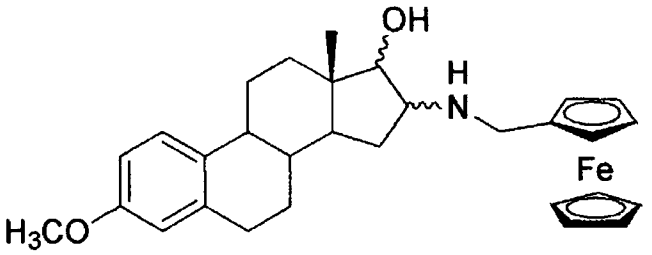

1

Fig 1 10 The general structure of novel *N*-ferrocenyl steroid molecules that displayed outstanding anti-microbial activity against a range of organisms [27]

Malaria is a tropical disease that causes approximately of 3 million deaths per year The drug chloroquine has been employed as treatment for this disease However, increasing resistance to chloroquine has prompted the search for new anti-malarial substances Biot *et al* have developed a series of the anti-malarial drug, chloroquine, that incorporates the ferrocenyl moiety **2a-2e** (Figure 1 11) [28] The synthesis and subsequent investigations of the ferrocenyl derivatives of such drugs was as a result of the organism *Plasmodium falciparum* developmg resistance to previously potent anti-malarial drugs like chloroquine Attracted by its stability and non-toxicity to mammals, it was postulated that a ferrocenyl moiety would be ideal for incorporation in new chloroquine based treatments

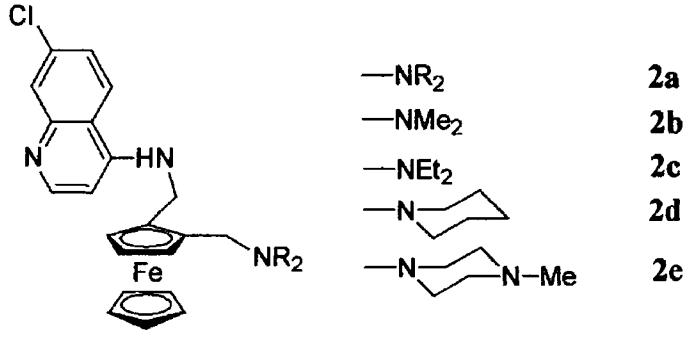

Fig 1 11 7-Chloro-4-[[[2-{(*N*,*N*-R_2-ammo)-methyl}ferrocenyl]methyl]amino]-quinoline derivatives [28]

The inclusion of the ferrocenyl moiety proved to be successful in so far as it was active against a chloroquine-resistant strain of *Plasmodium falciparum in vitro* Biot *et al*

concluded that the structure-activity relationships demonstrate that the anti-malarial effect of the derivatised structure increased due to the presence of ferrocene [28]

Maryanoff *et al* have applied the concept of bio-isosterism to their research [29] This principle has often been used by medicinal chemists as a means of reducing toxicity or improving bio-activity of known drugs For example, in drug molecules containing aromatic rings, the substitution of heterocyclic moieties for a phenyl group is a common strategy Maryanoff and his co-workers became intrigued with ferrocene as a bio-isosteric replacement for either the phenyl or pyrrole group in the anti-inflammatory compound tolmetin, (which is used to treat arthritis)

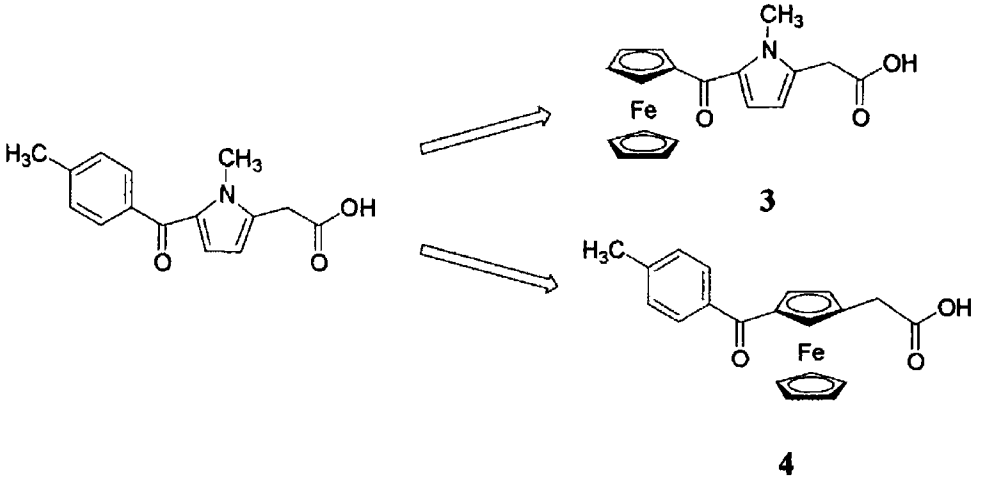

Fig 1 12 Bio-isosteric derivatives of tolmetin incorporating ferrocene [29]

The ferrocenyl derivatives of tolmetin **3** and **4** (Figure 1 12) were tested for anti-arthritic activity However, their investigations, that saw the phenyl and heterocyclic group replaced with the ferrocenyl moiety has led to a loss of pharmacological and biochemical activity and therefore, it was concluded that the bio-isosterism of the ferrocene unit in this instance is generally poor

Ma and co-workers have synthesised a series of ferrocenyl compounds (an example of which, **5**, can be seen in Figure 1 13) which have incorporated the thiazole ring moiety [30] The thiazole functional group is fairly widespread in biologically active compounds For example, it appears in thiamine, a co-enzyme required for the oxidative decarboxylation of α-keto acids and tetrahydrothiazole appears in the skeleton of penicillin, which is still one of the most important antibiotics Therefore, it is clear that compounds containing the

thiazole moiety have much potential as bio-active compounds The thiazole functionalized compounds were synthesised by reactmg thiourea with chloroacetyl ferrocene to form 4-ferrocenyl-2-thiazoamme This species was subsequently condensed with aromatic aldehydes to give a series of novel imines These imines were subsequently reacted with thioglycollic acid causing a cyclisation reaction and forming ferrocenyl thiazolidone derivatives

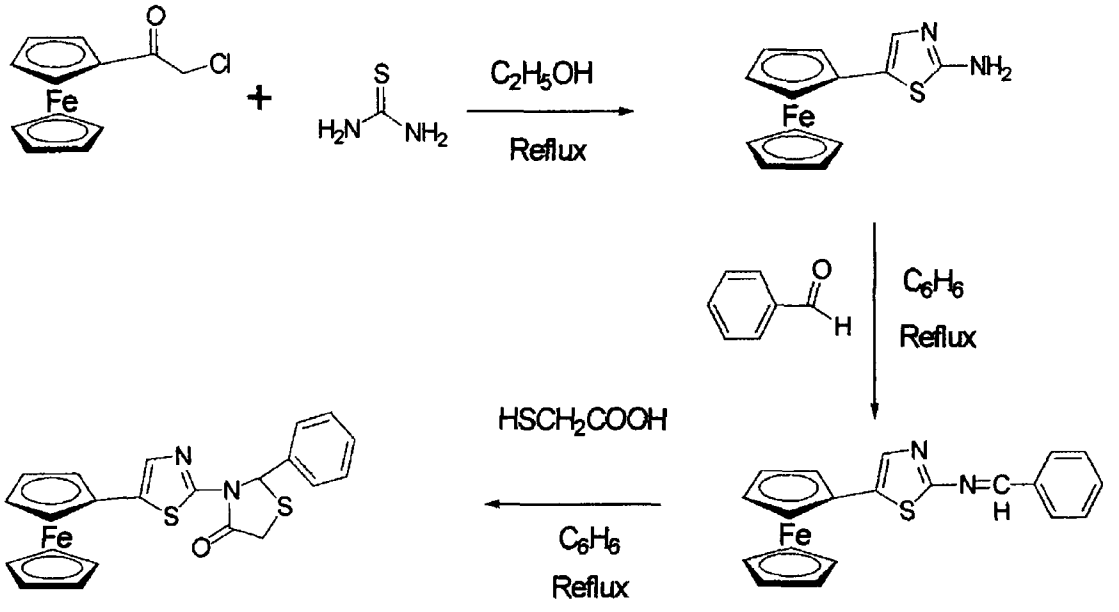

5

Fig 1 13 An example of the ferrocenyl thiazoamine and ferrocenyl thiazolidone derivatives [30]

Not only has ferrocene been incorporated into compounds with potential medicinal properties, but there is an example in the literature of the ferrocenyl moiety forming part of a new class of insect growth regulator It had been established previously that *N-tert*-butyl-*N,N'*-diacylhydrazines mimics the action of a 20-hydroxyecdysone which activates the ecdysone receptor which in turn leads to lethal premature molting [31] Subsequent investigations indicated that molecular hydrophobicity is favourable and therefore the *N-tert*-butyl-*N,N'*-dibenzoylhydrazine derivative was synthesised and its anti-larval properties investigated Runqiu *et al* expected the substitution of the phenyl group with the ferrocenyl moiety to induce 'great changes' in molecular properties such as solubility and hydrophobicity and hence it was hoped that the larvicidal activity of the ferrocenoyl derivatives would be enhanced significantly [32] It had also been reported that

biscarbamoyl sulfide derivatives of methylcarbamate insecticides still retained the good insecticidal activity of the parent methylcarbamate, but were substantially less toxic to mammals [31] Bearing this in mind, Runqiu and co-workers have introduced a thiocarbamate moiety into *N-tert*-butyl-*N'*-ferrocenoyl-*N*-benzoylhydrazine These compounds **6a**, **6b**, **7a**, **7b**, **8a** and **8b** (Figure 1 14) have excellent insect growth regulators' activity and retains the good insecticidal activity of the parent methylcarbamate and the *N-tert*-butyl-*N'*-ferrocenoyl-*N*-benzoylhydrazine Tests have shown that the toxicity of the methylcarbamate to mammals was reduced at the same time

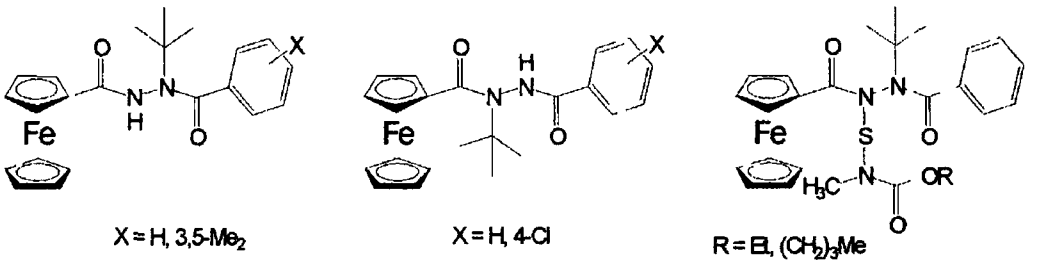

6a, 6b **7a, 7b** **8a, 8b**

Fig 1 14 The *N-tert*-butyl-*N'*-ferrocenoyl-*N*-benzoylhydrazine derivatives [32]

When the larvae of the chosen insect (the southern army worm) were treated with the above compounds, results indicated that while very potent insecticide compounds were synthesised, toxicity levels towards mammals were still high

1.5 Anion Recognition.

In comparison to the field of cation recognition, anion recognition is a subject that has only since the 1960s, received any significant profile [33,34] Anions are ubiquitous in our environment and play a vital role in nature, for example DNA (deoxyribonucleic acid) is a polyanion, co-factors of enzymes are anions, and ATP (adenosine triphosphate), life's major source of energy is an anion Various diseases have also been linked to anions and how they are bound *in vivo e g* cystic fibrosis is known to be caused by a misregulation of chloride channels and Alzheimer's disease has been linked to anion binding enzymes [34] Environmentally, nitrates and phosphates (constituents of modern fertilizers) which are potent polluting agents of aquatic habitats need to be extracted and/or monitored carefully [35]

The relatively late development of this subject may be explained by the difficulty by which anions are complexed This difficulty is brought about by a number of factors

1 They have low charge to area ratio

2 Anions may be sensitive to pH

3 Anions have a wide range of geometries and shapes [34,36]

Effective anion recognition can be achieved by rational design of receptors Ensuring complementary geometry between the receptor and the anion is crucial in the pursuit of selectivity The series of non-covalent interactions that are exploited in this process are as follows,

a Electrostatic interactions

b Hydrogen bonding

c Both electrostatic interactions and hydrogen bonding [34 36]

1.5 1 Non redox active anion receptors.

In 1968 the first synthetic receptor **9** for inorganic anions was reported (Figure 1 15) [37] This receptor was size selective for chloride ion and its intended mode of operation was for the positively charged ammonium moiety of the host molecule to bind the negatively charged anion guest molecule by electrostatic interaction

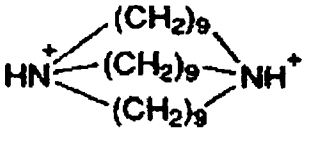

9

Fig 1 15 The first reported anion binding molecule [37]

Other early examples of anion receptors include the macrocyclic quaternary ammonium hosts **10a**, **10b** and **11** (Figure 1 16) which were prepared by Schmidtchen *et al* [38] In subsequent investigations these compounds were found to complex anions in water For example, the cavity of receptor **11** has a diameter of 4 6Å and forms a strong bond and encapsulates iodide, which has an anionic diameter of 4 12Å However these compounds were associated with counter ions which compete for binding space, hence neutral zwitterionic species were synthesised and it was found that these form stronger bonds with Cl^-, Br^-, and I

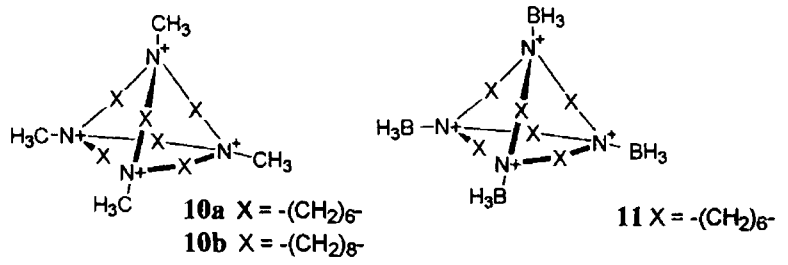

Fig 1 16 Quaternary carbon receptors that only utilize electrostatic interactions [38]

Having seen how counterions interfere with the action of host-guest complexation, scientists realized that it would be desirable to make a new type of anion receptor that did not rely on the action of electrostatic forces The exploitation of intermolecular forces like hydrogen bonding was investigated as a possible alternative or complementary strategy for complexing anions

Hydrogen bonds are particularly strong dipole-dipole forces that exist between hydrogen and electronegative atoms such as oxygen, sulphur, nitrogen or fluorine and these forces are known to be directional [39] This allows for the possibility of designing receptors with specific shapes that are capable of differentiating between anionic guests with different geometries or hydrogen bonding requirements [40]

Among the many examples of receptors which complex anions by exclusive means of hydrogen bonding, Pascal and co-workers produced one of the first amide based anion receptors **12** (Figure 1 17) [39] This development was evidence of the further evolution of this subject because for the first time a neutral anion receptor was synthesised This receptor showed evidence of binding fluoride ions in d_6-DMSO

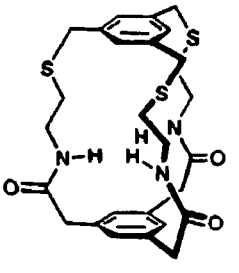

12

Fig 1 17 First amide based anion receptor as prepared by Pascal *et al* [39]

Vahyaveetil and co-workers produced a series of acyclic tripodal receptors **13** and **14** containing amide groups (Figure 1 18) [40] These receptors had C_3 symmetry and hence were specially designed for the complexation of tetrahedral anionic species by exclusive

means of hydrogen bonding Compounds **13** and **14** represented the first time that host compounds were prepared to complement the dimensions and shape of a potential guest molecule

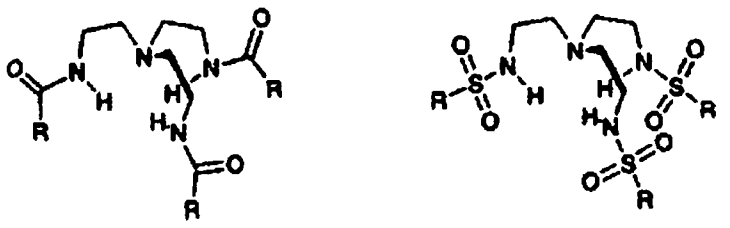

13 **14**

Fig 1 18 Tripodal acyclic receptors [40]

A cystine based cyclic oligourea was demonstrated to act as a versatile neutral receptor for both inorganic and organic anions operating exclusively through hydrogen bonds [41] Ranganathan and coworkers were interested in transport mechanisms used in various natural processes that utilize neutral protein based vehicles, and were keen to synthesize a receptor that would have multiple hydrogen bonding pockets distributed uniformly throughout in its cyclic backbone that would not only be structurally similar to natural models but would also show high selectivity in multifunction anion complexation ^{1}H NMR studies have shown that while the smaller cyclic tri-urea **16** (Figure 1 19) prefers to complex with spherical (halide) and trigonal planar (nitrate) anions, the larger oligomer tetra-urea **15** can trap the tetragonal planar squarate dianion with modest efficiency Also of relevance to this authors research is the use of amino acid moieties as constituents of an anion receptor

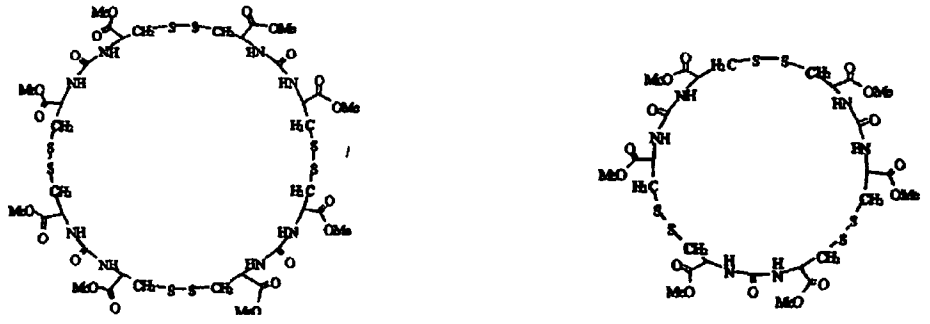

15 **16**

Fig 1 19 The cyclic tri and tetra-urea anion receptors [41]

1.5 2 Redox active anion receptors.

Molecular receptors have been designed that have the ability to selectively bind and sense the anion recognition event *via* a macroscopic physical response As a result, innovative electrochemical and spectral sensory reagents for anions, based on novel transition metal organometallic and co-ordination receptor systems have been synthesized Incorporating these signaling probes into various acyclic, macrocyclic and calixarene ligand frameworks leads to new receptor systems capable of responding to anion complexation

1 5 2 1 Cobaltocenium redox active anion receptors.

The design of receptors that have the ability to selectively bind and sense the anion recognition event *via* a macroscopic physical response has been the subject of much research since the mid 1990s [35] This macroscopic physical response has been facilitated by the incorporation of inorganic redox centres, and these have been successfully incorporated into various host frameworks and shown to electrochemically detect charged guest species [35]

In 1989, Beer and Keefe reported the synthesis of the first redox-responsive class of anion receptor based on the redox active, pH independent and positively charged cobaltocenium moiety [42]

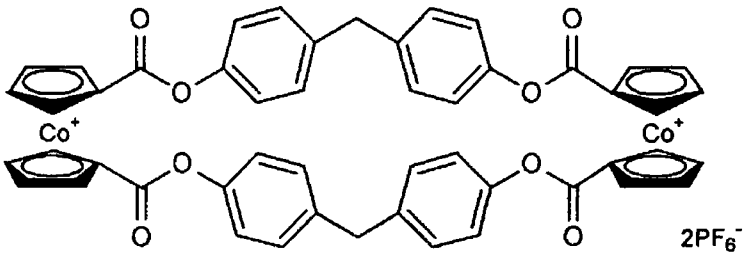

17

Fig 1 20 The first reported cobaltocenium anion receptor [42]

This ester linked macro-cyclic cobaltocenium receptor **17** (Figure 1 20) was capable of binding bromide ions *via* favourable electrostatic interactions However, there were drawbacks associated with this receptor, for example, its ester linkages were susceptible to acid hydrolysis, it was poorly soluble in organic solvents, and it was difficult to synthesize

Some of these difficulties were addressed when Beer and co-workers synthesised a series of novel cobaltocemium based acyclic receptors where the ester linkages were replaced with amide linkages [43 44] This series consisted of derivatives containing *para, meta, ortho* substituted aniline groups (Figure 1 21), bis and tripodal substituted compounds (Figures 1 22 and 1 23)

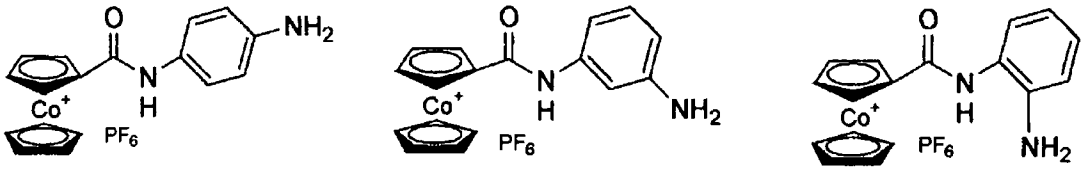

Fig 1 21 Cobaltocemum redox active receptors [43,45]

The introduction of the aniline amino group for receptors **18, 19** and **20** has resulted in enhanced binding (except in **18** due to the fact that the aniline ammo group is too far removed from the binding site to contribute to anion complexation) The addition of tetrabutylammonium salts $NBu_4^+X^-$, ($X = Cl^-, Br^-, NO_3^-, HSO_4^-, H_2PO_4^-$) to CD_3CN or d_6-DMSO solutions of these receptors resulted in remarkable downfield shifts of the respective receptor's protons in their ^1H NMR spectra Of particular note were the substantial downfield shifts of the amide protons, $\Delta\delta = 1\ 28$ ppm for **18** and 1 52 ppm for **19** on addition of one equivalent of chloride These results suggest a significant -CO-NH X^- hydrogen bonding interaction is contributing to the overall anion complexation process [43]

From the ^1H NMR data, stability constants calculated for dihydrogenphosphate were found to be 1200 and 320 M^{-1} for **18** and **19**, respectively, which was approximately an order of magnitude higher than that measured for chloride This difference in the stability constant value can be attributed to the dihydrogenphosphate anion being better able to form hydrogen bonds with the receptor than the chloride anion

Cyclic voltammetry experiments have shown that these receptors were able to bind and electrochemically recognize several different anions *i e* Cl^-, Br^-, NO_3^-, HSO_4^- The addition of anions to solutions of cobaltocenium resulted in cathodic shifts of the reversible Cp_2Co^+/Cp_2Co redox couple For the addition of chloride, values of 30 and 85 mV and with dihydrogenphosphate larger magnitudes of 200 and 240 mV were observed

These results indicate not only that the anion was being bound by the receptor, but also that there is considerable contribution towards this complexation process from hydrogen bonding The importance of hydrogen bonding was highlighted with **21** and **22** (Figure 1 22) when the tertiary amide cobaltocenium analogues were shown not to respond electrochemically to anions Hence, these experiments demonstrate that both the cobaltocenium and the amide moieties are necessary for the successful complexation of anions

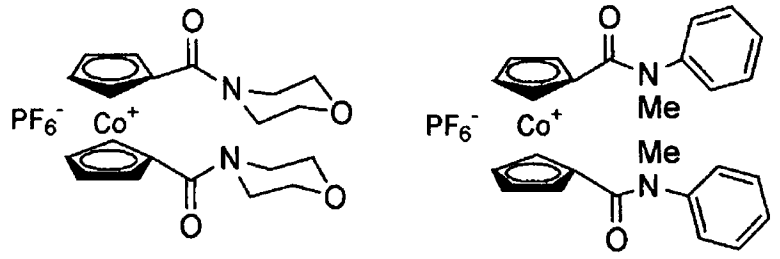

Fig 1 22 Cobaltocenium receptors with appended tertiary amide groups, hence these compounds are not capable of hydrogen bonding with anions

Evidence of a macrocyclic effect was obtained with the two compounds **23** and **24** (Figure 1 23) ^{1}H NMR titrations with chloride in DMSO-d_6 gave stability constants of 250 M^{-1} for the macrocyclic compound and 20 M^{-1} for its acyclic analogue [43 45]

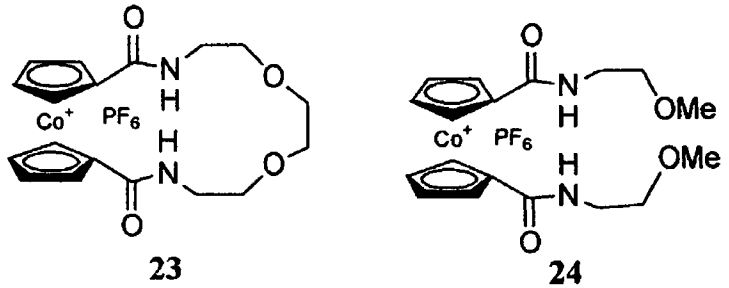

Fig 1 23 A cyclic and acyclic cobaltocenium based anion receptor [43 45]

Having established that cobaltocemum with its appended amide units are effective anion receptors, Beer and co-workers set about preparing more selective anion receptors This was achieved when they synthesized a novel series of ditopic *bis* (cobaltocemum) receptor molecules **25-28** (Figure 1 24) [46]

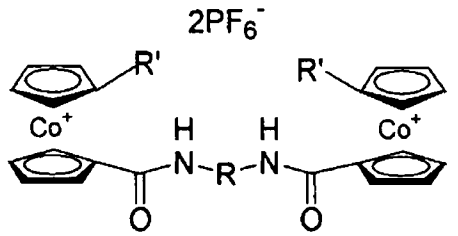

R' = -CO_2Et

R = -$(CH_2)_2$- **25**

R = -$(CH_2)_3$- **26**

R = -$(CH_2)_4$- **27**

R = -$(C_6H_4$-CH_2-$C_6H_4)$- **28**

Fig 1 24 Cobaltocenium redox active anion receptors [46]

Proton NMR studies showed that receptors **25** and **26** formed 1 1 complexes while receptors **27** and **28** formed 2 1 complexes However, as the length of the alkyl chain increases the stability of the complex decreases All of these ditopic cobaltocenium receptors were found to display electrochemical recognition with dihydrogen phosphate anion again giving the largest cathodic shift

Calixarenes are attractive host molecules on which to construct additional recognition sites for anions Beer and co-workers synthesised *bis*-cobaltocene calixarene derivatives **29-31** (Figure 1 25), designed for the complexation and electrochemical recognition of anionic guests [47 48] These derivatives were shown to form very stable 1 1 anion complexes in deuterated DMSO and receptor **29** was found to bind chloride anion preferentially to dihydrogenphosphate ion When the substituents on the basic calix[4]arene frame were modified, dramatic changes in binding patterns were observed For example, derivative **30** exhibits $H_2PO_4^-$ >> Cl^- selectivity trend which is the opposite of receptor **29**

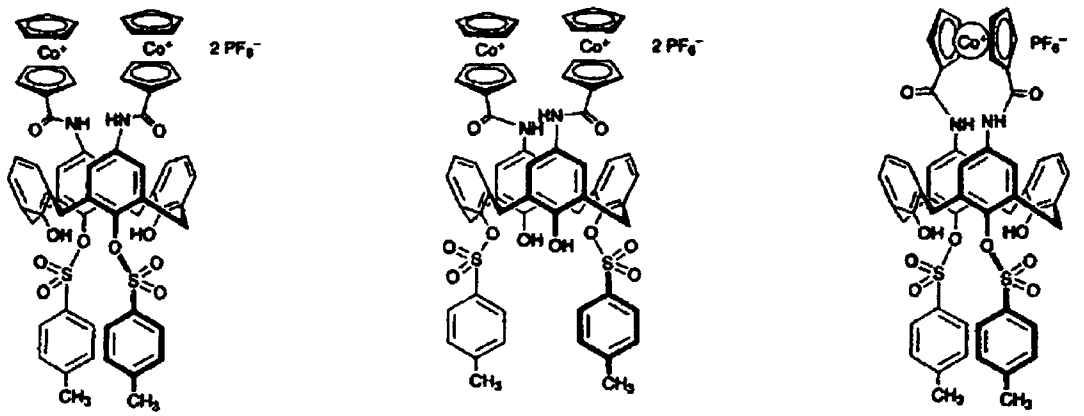

29 **30** **31**

Fig 1 25 Cobaltocenium calix[4]arene receptors [47 48]

1.5.2.2 Ferrocenyl redox active anion receptors.

The redox active ferrocenyl moiety has also been exploited in the electrochemical sensing of anions Ferrocene units appended with secondary amides have been utilized for anion recognition In their neutral state, these receptors have no inherent electrostatic attraction with anions making the ^{1}H NMR determined stability constants of the host-guest species lower in magnitude than the analogous cobaltocenium systems Electrostatic interaction can however, be turned on by electrochemical oxidation of the ferrocene derivative to the cationic ferrocenium derivative and consequently these molecules exhibit interesting electrochemical anion sensing and recognition properties Hence, the ferrocene group can be considered a molecular switch, as electrostatic interaction between the redox active moiety and the anion can be switched on or off by electrochemical oxidation or reduction respectively

Beer *et al* synthesized a complex containing two ferrocenyl and one cobaltocenium moieties **32** (Figure 1 26) Their subsequent research indicated that ferrocene-containing amines or amides are capable of binding and sensing anions in their own right ^{1}H NMR titrations suggested that the receptor formed 1 1 solution complexes with each of the anionic guests Cyclic voltammetry titration experiments indicated in addition to the cathodic perturbations seen for the cobaltocenium/cobaltocene redox couple, a ferrocene/ferrocenium couple was also observed This discovery has led to the synthesis of other ferrocenyl anion receptors [49]

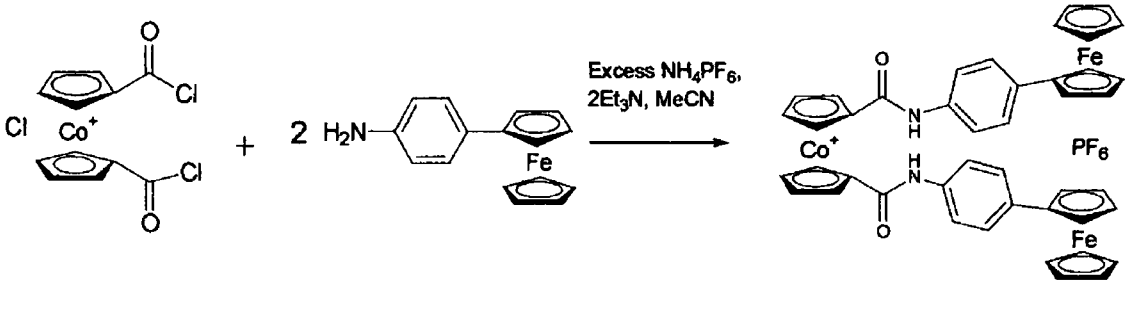

32

Fig 1 26 Beer and co-workers first ferrocene containing anion receptor [49]

^{1}H NMR experiments, where receptors **33a**, **33b**, and **34** (Figure 1 27) were titrated against tertiary butyl ammonium salts of various anions, resulted in significant downfield shifts of the respective amide protons [49] In addition, electrochemical investigations

showed considerable anion induced cathodic perturbations of the respective ferrocenyl oxidation current peaks for compounds **33a**, **33b** and **34** These ^{1}H NMR and electrochemical data strongly suggest that compounds **33a**, **33b** and **34** are anion sensing molecules and that both amide and ferrocenyl moieties participate in the complexation process Competition experiments were also preformed to establish the relative affinities of the $H_2PO_4^{2-}$, HSO_4^- and Cl^- anions for the respective receptors This data showed that the receptors **33a**, **33b** and **34** all have greatest affinity for $H_2PO_4^-$, even in a ten-fold excess of HSO_4^- and Cl [49]

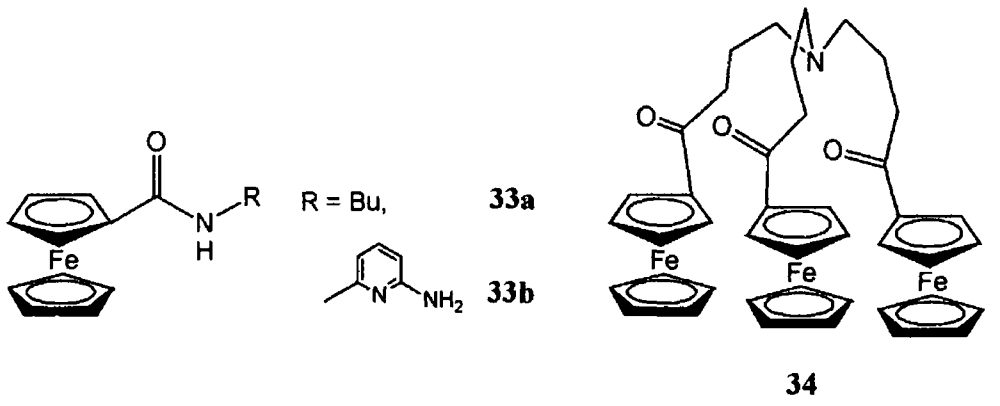

Fig 1 27 Ferrocene containing anion receptors [49]

In subsequent studies, Beer and co-workers attempted to explain why these compounds were effective anion sensors In order to accomplish this, it was necessary to identify the essential components for anion binding in the ferrocenyl anion receptors [50] Compounds **35** and **36** (Figure 1 28) were chosen as simple but typical and fundamental examples Compound **35** is an amide substituted ferrocenyl receptor while compound **36** provides additional pyridine and amine groups (which are good proton acceptors and donor sites for the formation of hydrogen bonds) Two important conclusions were reached during their investigations

(a) Both the ferrocene and amide moieties are needed to bind anions

(b) Of the 2 receptors that were examined, compound **36** (*i e* the receptor with the extra capacity to donate/accept hydrogen bonds *via* the pyridinyl nitrogen, amide and amine moieties) was the more effective

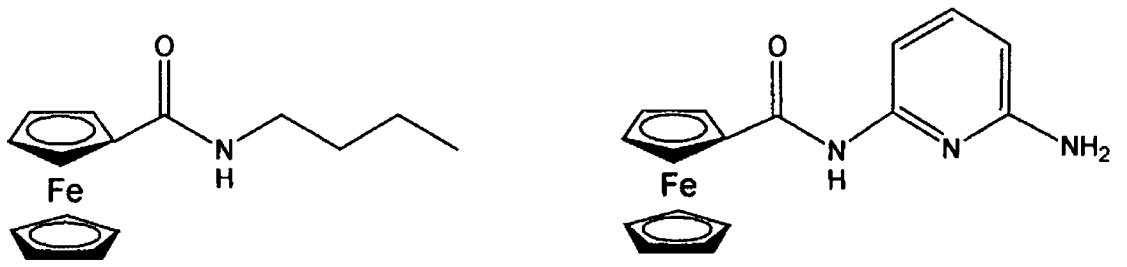

35 **36**

Fig 1 28 *N*-Ferrocenoyl amide receptors [50]

Electrochemical competition studies were performed that showed that both receptors can electrochemically recognize anions with a selectivity order $H_2PO_4^- > HSO_4^- > Cl^-$ The electrochemically induced ion pairs between an anion and the oxidized receptor molecule results mainly from the anion affinity for Fc^+ However, this does not agree with ^1H NMR studies where the attraction is due solely to hydrogen bond interactions between the amide proton and the anion In this case the neutral receptor **36** had more affinity for HSO_4^- than for $H_2PO_4^-$ The complexation between a neutral receptor molecule and a proton bearing anion is thermodynamically more favoured for receptor **36** (which contains both proton donor and acceptor sites) than for receptor **35**, which contains only a proton donor site *i e* an amide proton In the neutral state, it has been shown that compound **36** has a thermodynamic binding selectivity of $HSO_4^- > H_2PO_4^- > Cl^-$

Beer and co-workers then synthesized another series of receptors based on neutral amide systems **37-43** (Figure 1 29) with the intention of assessing their anion recognition properties [51]

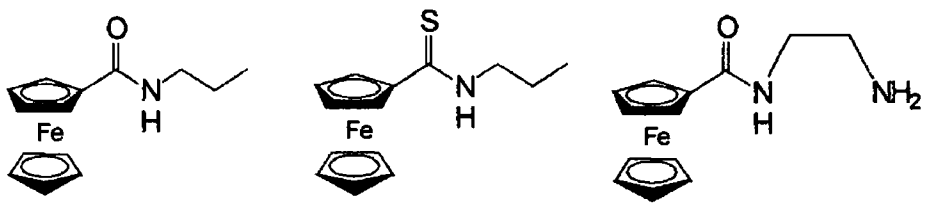

37 **38** **39**

Fig 1.29 Neutral *N*-ferrocenoyl receptors [51]

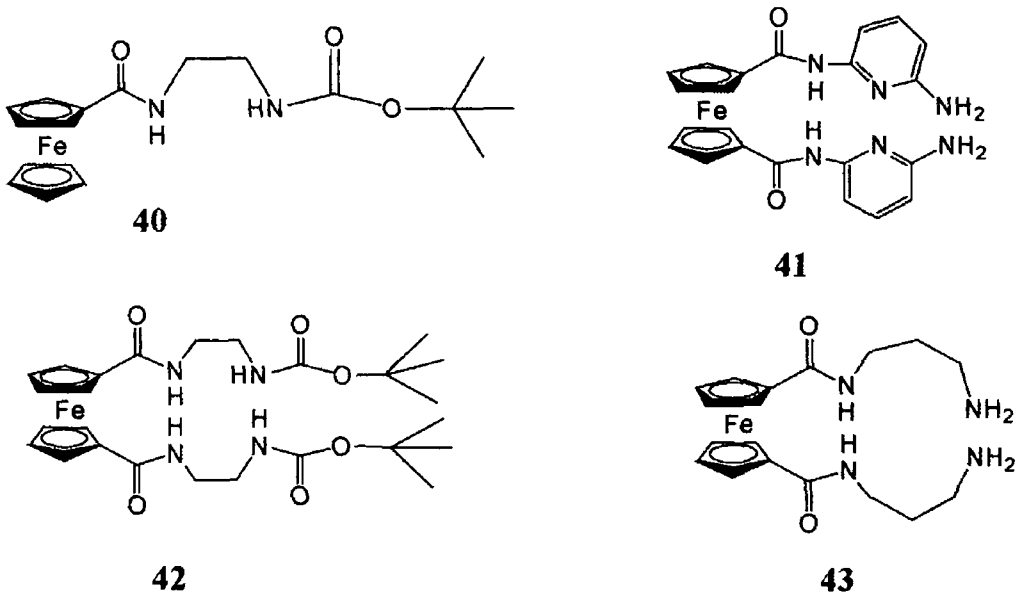

Fig 1 29 Neutral *N*-ferrocenoyl receptors (continued) [51]

The thioamide receptor **38** was found to be particularly effective at complexing chloride ions in comparison to its carboxyamide analogue **37** This paralleled an earlier discovery that showed thiourea compounds to be more effective at complexing anionic species than urea analogues [52] This observation can be justified as the thioamide proton is more acidic in comparison to the carboxyamide proton *i e* the thioamide proton will form hydrogen bonds more readily

Both amide and amine functionalities were present in the bifunctional receptor **39** The presence of the amine group in addition to the amide gave receptor **39** the means by which it could form hydrogen bonds more efficiently with a guest molecule It was proposed that this receptor utilized two different modes of anion binding The ability of the bidentate anion receptor **39** to recognize anionic species was investigated using halide ions On treatment with anionic solution, the amide proton was shifted further downfield (in the ^{1}H NMR spectrum) than the amine protons, however this effect became less pronounced as the size of the anion increased

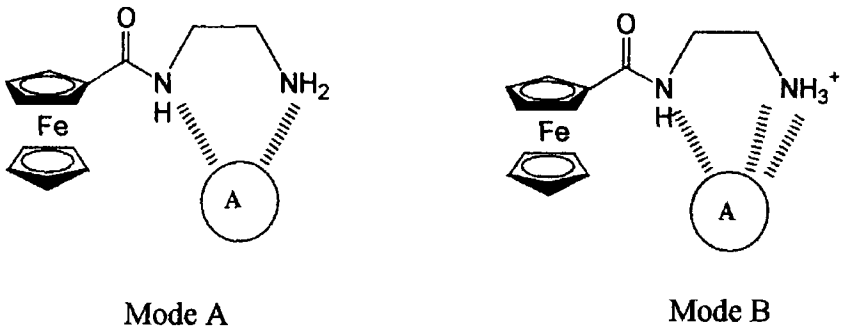

Mode A Mode B

Fig 1 30 The two modes of binding proposed for receptor **39** [51]

Two modes of binding are shown in Figure 1 30 Mode A acts for non acidic guests It depends on the receptor to donate the hydrogen bond from the amide and to a lesser extent from the amine Mode B alternatively operates for more acidic guests The anion loses a proton to the basic amine that forms a positively charged ammonium moiety By means of both electrostatic and hydrogen bond interactions the anion is then bound This type of bonding shows higher affinity for HSO_4^- than for $H_2PO_4^-$ It is thought that the H_2PO_4 mode of binding with the above receptors utilizes a combination of modes A and B [51]

As seen in the case of compound **36**, pyridine moieties have been included in receptor molecules so as to give the receptor an added binding site that is capable of accepting or donating hydrogen bonds Carr and co-workers have synthesized two redox active sensors **44** and **45** (Figure 1 31) that incorporate the *N*-ferrocenoyl and pyridine moieties and hence are capable of sensing neutral carboxylic acid guests *via* hydrogen bonding interactions [53 54]

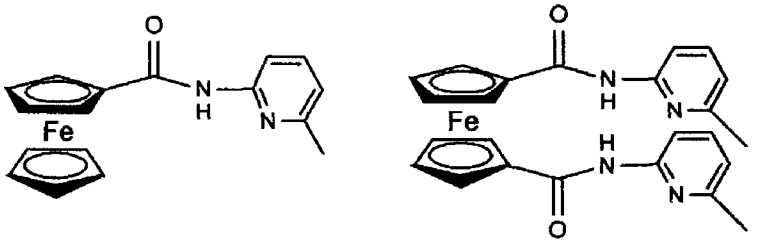

44 **45**

Fig 1 31 Carr and co-workers *N*-ferrocenoyl amide receptors [54]

Two ferrocenyl compounds containing mono and bis-amido pyridine moiety **44** and **45** were synthesised ^{1}H NMR and X-ray diffraction studies reveal that the complex of

structure **44** and glutaric acid consists of hydrogen bonding interactions between the amide hydrogen and the pyridyl nitrogen [54]

Similarly pyrrole moieties have also been identified as possible anion binding units [55] Sessler *et al*, have reported the synthesis of three new pyrrole rich *ansa*-ferrocene systems **46a-c** (Figure 1 32) wherein the length and nature of bridging arm has been varied [56] They have postulated that both of these factors play a role in regulating the dihydrogen phosphate anion affinities as well as modulating the nature of the ferrocene/ferrocenium based electrochemical response Crystal structure studies have shown that a water molecule was bound in the cavity This indicates that there was both N-H O and O-H O hydrogen bond interactions between host and guest $H_2PO_4^-$ has two OH groups that could interact with the oxygen of the ether group in the linker To examine these interactions further, host derivatives with 0, 1 and 2 ether oxygens were prepared It was subsequently found that the binding affinity for the $H_2PO_4^-$ anion increases according to the amount of oxygens in the ether linker group Electrochemical results indicate that much of the binding interaction is as a result of hydrogen bonding between the two hydroxyl groups of H_2PO_4 and the oxygens of the ether linker groups

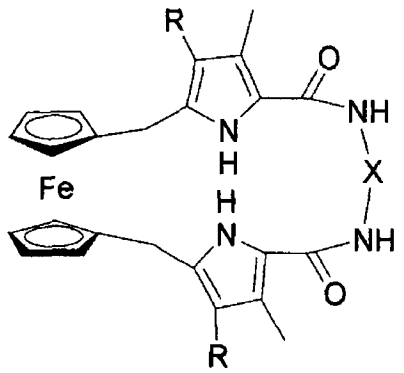

$X = (CH_2)_5$ **46a**
$X = CH_2CH_2OCH_2CH_2$ **46b**
$X = CH_2(CH_2OCH_2)_2CH_2$ **46c**

Fig 1 32 The *ansa*-ferrocene receptors which complex $H_2PO_4^-$ anion [56]

More recently Sessler and co-workers have been interested in anion complexation and detection based on a calix[4]pyrrole system **47** (Figure 1 33) which is known to interact *via* hydrogen bonds with a variety of halides and oxo-anions [57] Previous research attempted to use ferrocene as an electrochemical reporting group and has yielded unusual and sometimes contradictory reports, and therefore, it was decided to employ the ferrocene moiety in a much more intimate role in the anion complexation process A

calix[4]pyrrole molecule was prepared that would allow for the possibility of direct Fc-H A anion binding interactions as well as N-H A⁻ hydrogen bond interactions ^{1}H NMR data provided evidence that there was formation of hydrogen bonds between the cyclopentadienyl protons and the anions in solution Electrochemical data indicated that this receptor senses anionic species with $H_2PO_4^-$ and F^- causing the most dramatic cathodic shifts

47

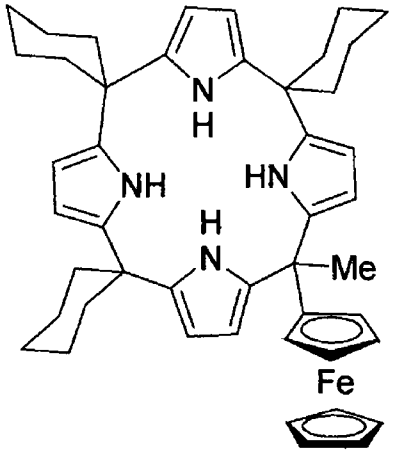

Fig 1 33 The calix[4]pyrrole receptor **47** which has been shown to both electrochemically sense and hydrogen bond anions [57]

The potential of *N*-ferrocenoyl amide derivatives as redox active host molecules for anions has become apparent over the past few years Consequently, experimentation with the architecture of such systems, in order to improve their specificity was a feature of the studies undertaken by Reynes *et al* [58] They prepared a series of compounds **48-52** (Figure 1 34) These compounds are based on the well established combination of ferrocene as the electrochemical signaling unit, and secondary amide groups as hydrogen bond donors Reynes and co-workers were particularly interested in

1 The contribution made to the anion binding process by varying the number of ferrocene groups
2 The "preorganization" of the binding site

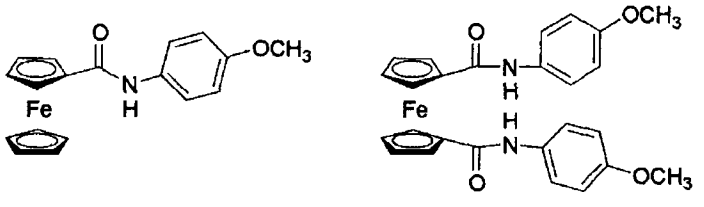

48

49

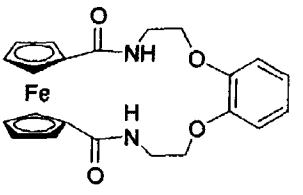

50

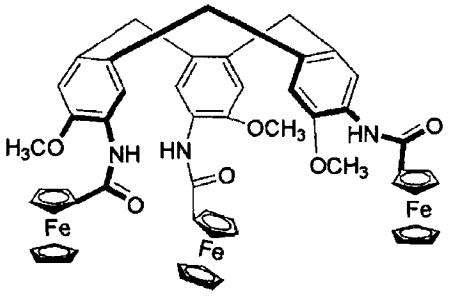

51

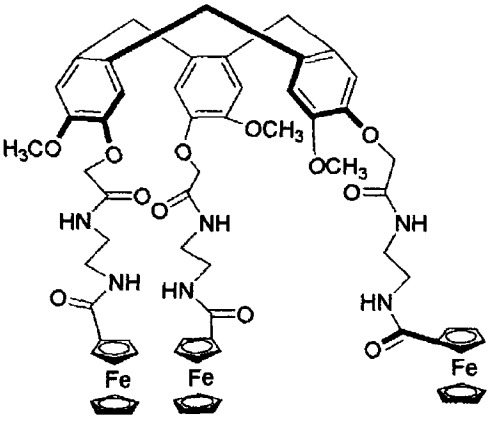

52

Fig 1 34 The *N*-ferrocenoyl anion receptors synthesized [58]

The addition of anions to solutions of these anion receptor molecules caused significant perturbations in their respective ^{1}H NMR spectra The signals of the respective amide protons of receptors **48-52** were shifted downfield indicating once again that there is significant contribution to anion binding from hydrogen bond interactions between host and guest molecules For example, on addition of $H_2PO_4^-$, downfield shifts of up to 2 ppm were recorded The electrochemical investigations also yielded evidence that anion complexation was occurring On addition of anions to solutions of these receptors, two types of electrochemical behaviour have been observed,

1 The gradual negative shift in the Fc/Fc^+ redox potential
2 The growth at a less positive potential of a new redox wave at the expense of the original wave for the free ligand were observed

These observations are typical of effective anion sensing molecules The receptors with more than one ferrocenyl group were found to be especially effective electrochemical sensors and led to the conclusion that the number of binding sites and ferrocenyl groups in the receptor and its topology determine the electrochemical recognition behaviour and

therefore it is not surprising that the cyclic receptors **51** and **52** (Figure 1 34) yielded the best results

Alternative and/or complementary anion binding strategies have been investigated by Beer and co-workers The combination of additional Lewis acid transition metal centres (*i e* additional metals other than the iron atom in ferrocene) with the redox responsive ferrocenoyl amide moiety may lead to new acyclic and macrocyclic hetero-polymetallic receptors that exhibit greater anion thermodynamical stability and new selectivity trends This was accomplished by coordinating a variety of Lewis acidic transition metal (*i e* a metal that can accept electron density) centres to a new ferrocene phosphine amide ligand to yield the compounds **53-57** (Figure 1 35) [59]

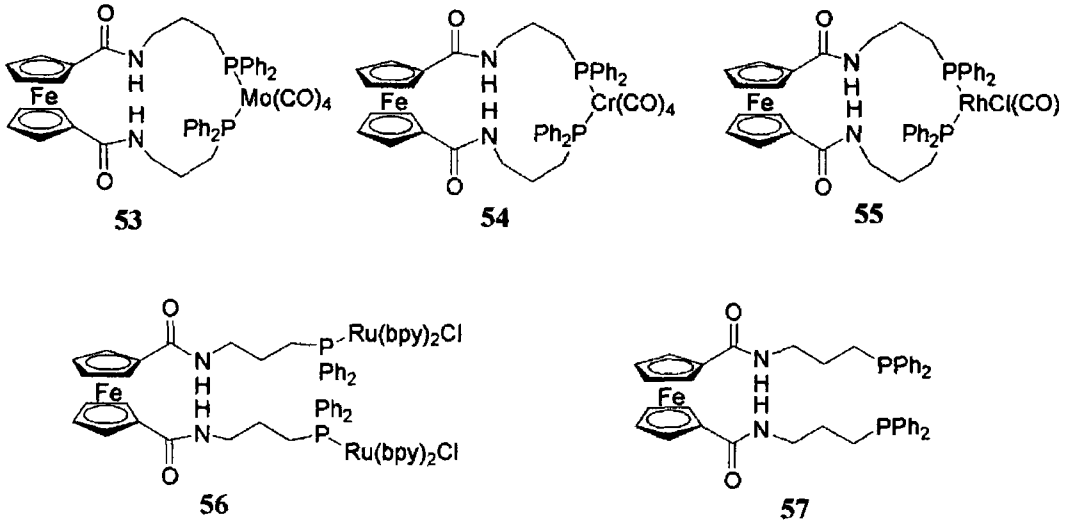

Fig 1 35 Transition metal coordinated ferrocene phosphine amide receptors [59]

^{1}H NMR and resultant EQNMR studies of titration curves revealed several remarkable features As was anticipated, the presence of phosphine coordinated Lewis acidic transition metal increases the strength of the interaction with the anionic Lewis bases The largest increase in magnitude of binding occurs with the charged ruthenium(II) receptor **56**, again emphasizing the importance of attractive electrostatic forces in the anion complexation process The Cl anion was found to be bound one order of magnitude more by the molybdenum **53** and chromium **54** derivatives than by receptor **57**, this may mean that the macrocycle plays a role in anion binding The preference for anion varied from receptor to receptor For receptors **53** and **54** it was found that anion

binding decreases in the order $Cl^- > Br^- > I^-$ which reflects the decrease in charge density of the anion The ruthenium(II) receptor **56** bound Cl^- and I^- anion equally well but showed more affinity for Br^- In the case of receptors **53** and **54** this was attributed to their respective macrocyclic cavities being too small Similarly, it was found that receptor **55** could not accommodate Br^-, I^- or $H_2PO_4^-$ as its macrocycle was too small It was concluded that anion binding seems to be enhanced by the presence in the receptor of a Lewis acid metal Electrochemical studies indicated that these new receptors could also electrochemically sense various anions *via* significant cathodic perturbations of the respective ferrocene and transition metal oxidation wave

1 5 2 3 Ferrocenyl functionalized poly-aza and aza-oxa anion and cation receptors

Scientists interested m the synthesis of artificial anion sensing devices have noted that in nature, the anion binding event generally occurs in an aqueous environment, therefore it would be of major benefit if water soluble anion receptors could be made Water soluble poly-aza ferrocenyl macrocyclic ligands have been prepared which can bind both cationic and anionic species depending on the pH of solution (this is schematically represented in Figure 1 36) These receptors can interact with cations *via* the well-known coordinating ability of the amine group On the other hand, ferrocenyl functionalized polyamines can bind anions in three different ways

(a) Electrostatic interaction *via* positively charged protonated amino groups

(b) By hydrogen bonding

(c) By electrostatic interactions *via* oxidised ferrocenium cations [60 61]

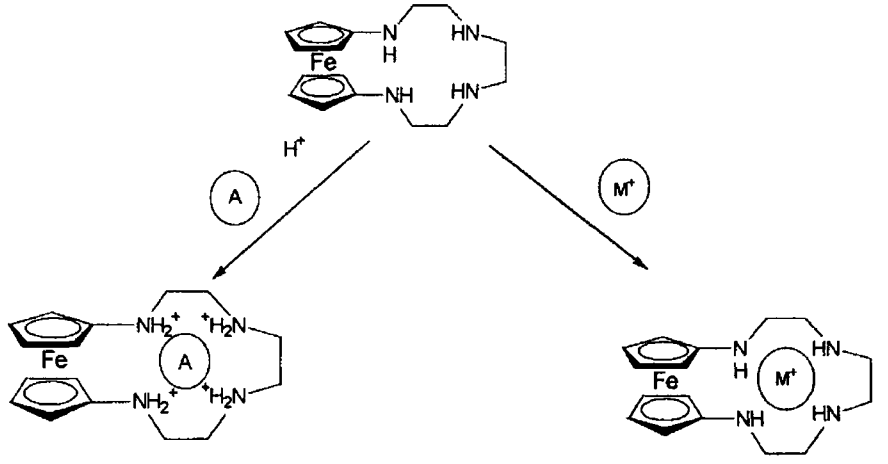

Fig 1 36 The poly-aza ferrocenyl compounds that complex either anions or cations [60]

Electrochemical experiments indicated that at high pH, that these ferrocenyl poly-aza receptors could recognize transition metal cations Cu^{2+}, Ni^{2+} and Zn^{2+} in polar organic, solvents and water [61] In aqueous pH range of 6-8, the respective pKa values of receptors **58-61** (Figure 1 37) allow the protonated poly-ammonium forms of these ligands to complex and electrochemically sense anions such as adenosine triphosphate (ATP) and $H_2PO_4^-$ in an aqueous environment Thus, these new poly-aza ferrocene macro-cyclic ligands represent novel dual-purpose pH dependent prototype amperometric sensors for the electrochemical recognition of transition metal cations and phosphate anions in water

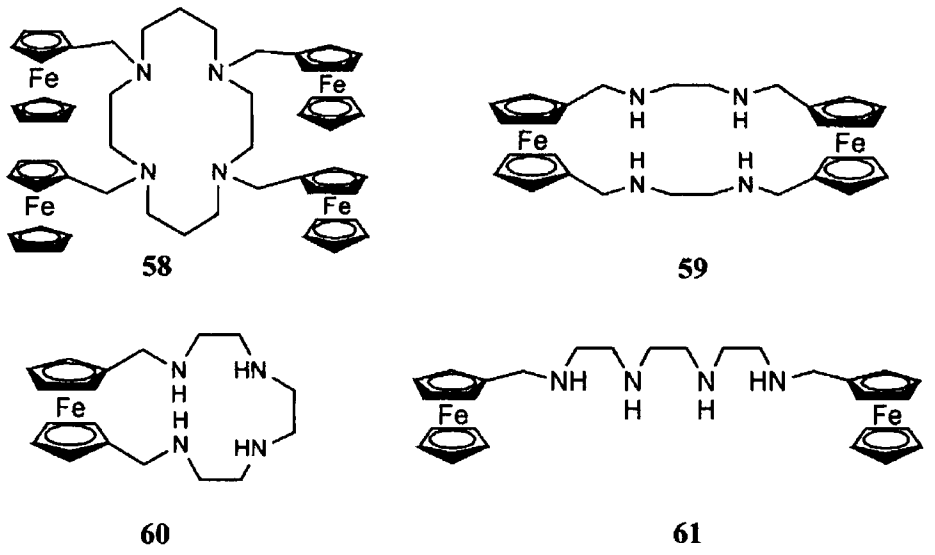

Fig 1 37 Ferrocene functionalized polyaza compounds [61]

More recently open chain ferrocenyl functionalized polyamines **62-64** (Figure 1 38) have been synthesized and have been shown to be effective anion and cation receptors in aqueous solutions As with the ferrocenyl cyclic poly-aza compounds, the complexation of anions or cations is achieved by the contribution of one or more of the following factors

1 By electrostatic interaction *via* positively charged protonated ammo groups
2 By hydrogen bonding
3 By electrostatic interaction via oxidized ferrocenium cation

Hydrogen bonding or electrostatic interactions (*via* positively charged protonated amino groups) can be tuned by varying the pH of solution For example, amine groups can act as either hydrogen bond donors or acceptors, hence binding properties of these poly-aza

compound can be alternated by protonatmg or deprotonatmg the amine or ammonium groups respectively [62]

These receptors were tested electrochemically with metal cations *i e* Ni^{2+} Cu^{2+}, Zn^{2+}, Cd^{2+} and Pb^{2+} at five different pH values from 3 to 9 in aqueous solutions A degree of selectivity was noted for different receptor compounds, for example, compound **62** was selective for Cu^{2+} and Ni^{2+}, **63** showed selectivity for Cu^{2+} and Zn^{2+} and electrochemical data suggested that compound **64** had affinity for Cu^{2+}, Ni^{2+} and Cd^{2+} ions They were also tested in the presence of anionic species The pH for these experiments was fixed at 4 9 The biologically important anion ATP was found to interact with receptor **63** and caused a significant cathodic perturbation in the cyclic voltammogram Receptor **62** was found to be an ineffective anion sensing molecule, however, **64** did show some affinity for ATP, phosphate and sulfate

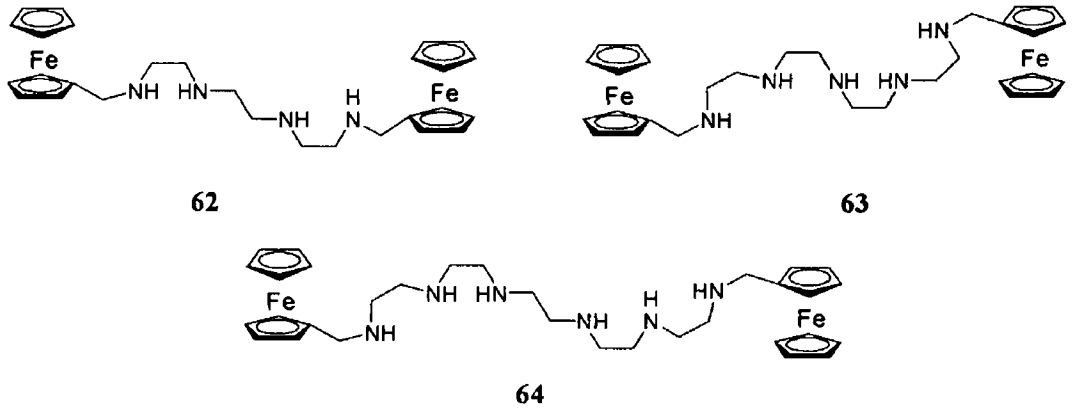

Fig 1 38 Open chain ferrocene functionalized polyamine receptors [62]

A series of further ferrocenyl functionalized cyclic and open chain polyaza and aza-oxa compounds **65-70** (Figure 1 39) have been prepared by Beer and co-workers [63] The emphasis of this investigation was on the complexation of biologically and environmentally relevant anions *i e* ATP, phosphate and sulfate in water and other aqueous solution A series of cyclic voltammetric experiments were carried out where the electrochemical shift in the presence of ATP and phosphate has been measured in water and in 1,4-dioxane-water solutions as a function of pH In the aqueous media the electrochemical response found against ATP, phosphate and sulfate was relatively unremarkable with maximum cathodic shifts of 30-40 mV This compares with the response in acetonitrile induced by phosphate and sulfate where large cathodic shifts of

up to 200 mV were found [63] It was determined however, that at certain pH values, the compounds **65-70** selectively detect sulphate and phosphate in the presence of competing anions in the aqueous environment

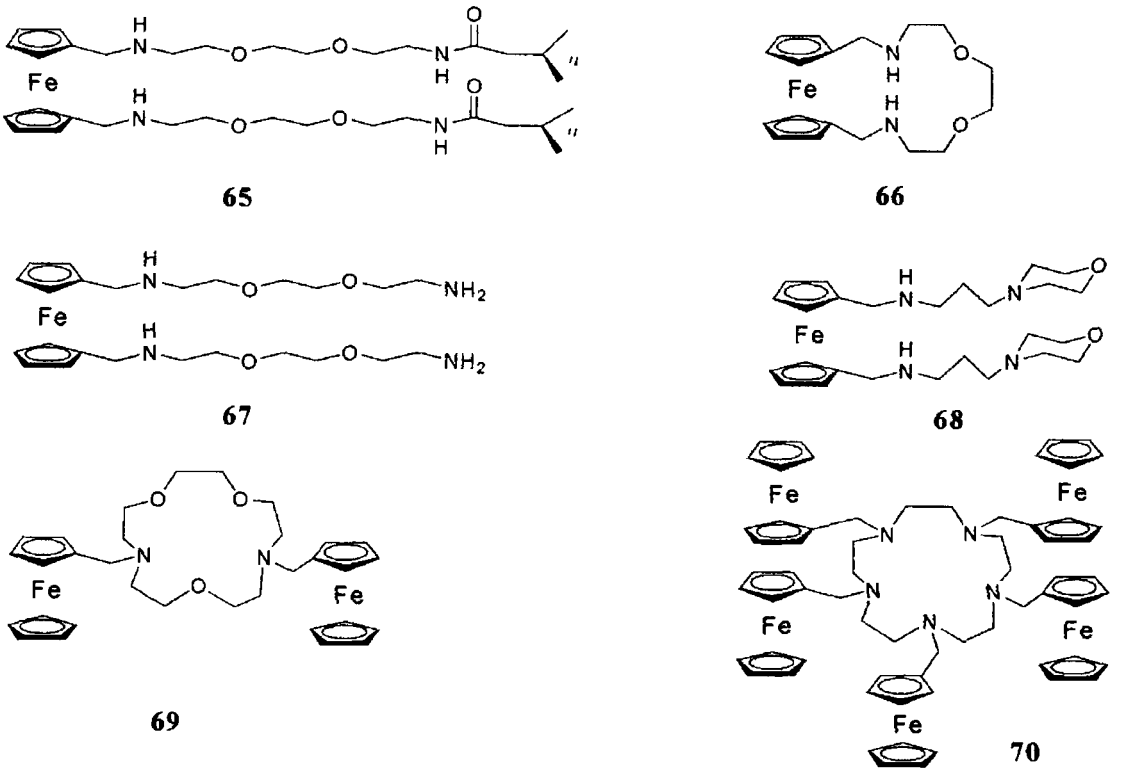

Fig 1 39 Six ferrocene functionalized poly-aza receptors which were used to investigate interactions with various anions in water [63]

Martinez-Mañez and co-workers have extended their research by preparing and testing the anion and cation sensing abilities of ferrocenyl functionalized cyclic and acyclic aza-oxa receptors **71-74** (Figure 1 40) [64]

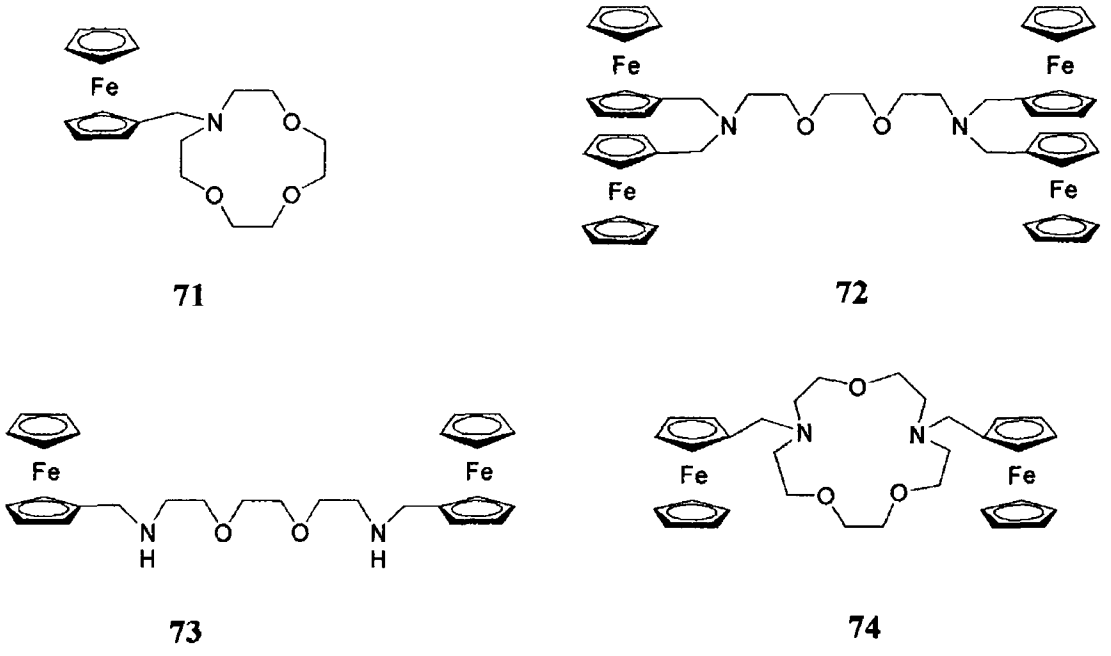

Fig 1 40 Ferrocenyl functionalized poly aza-oxa receptors [64]

When the pH was lowered by the addition of *p*-toluenesulfonic acid, the amine moieties were protonated and in aqueous solutions anodic shifts of between 80 and 200 mV (versus SCE) were observed This result suggests that the ferrocenyl groups respond on addition of H^+ ions to solutions of these receptors In the presence of sulfate all receptors show a cathodic shift of the reduction wave The $H_2PO_4^-$ anion induces larger electrochemical shifts in both the cathodic and anodic peaks than HSO_4^- However, no affinity at all was shown for either Cl or Br^- Hence these receptors show selectivity for $H_2PO_4^-$ over HSO_4 , Cl^- and Br

As already stated, the development of anion recognition as an area of study was based on the fact that many biologically important molecules are anions [65] However, examples of receptors for molecules like amino acids (which exist as zwitterions) are very rare Beer and co-workers synthesised a bis-(ferrocene carboxamide) substituted di-aza 18-crown-6 receptor **75** (Figure 1 41) and carried out electrochemical and proton NMR investigations [65] It was noted that prior binding of a metal cation aided the subsequent binding of anions

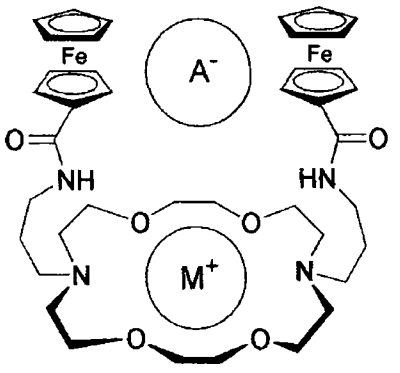

75

Fig 1 41 Ferrocenoyl zwitterionic receptor [65]

Interaction of the receptor with the metal cation was strong, but the anion only interacted weakly with the receptor It was found that the binding of anions is significantly enhanced by the presence of a bound cation *i e* Ba^{2+}, K^{+} with selectivity for HSO_4^- over Cl^- due to favourable electrostatic forces This novel receptor is capable of electrochemically recognizing the complexed anions, cations and anion/cation pairs

1.5.2 4 Ferrocenyl functionalized receptors incorporating a biogenic moiety

The commercial success of potentially useful compounds is dependent on a number of factors Firstly, it is an imperative that the compound carries out the function that it is supposed to but it is equally important that the starting materials should be easily accessible and inexpensively acquired Natural products like porphyrins and amino acids are inexpensive, robust, and very common in nature and hence they are attractive molecules to work with For the purposes of molecular recognition these compounds are ideal, as in many cases this is the role that they carry out in nature [41]

Amino acids are particularly attractive anion binding compounds In the human body proteins are extensively exploited for the transport and regulation of anionic species The presence of amide bonds in peptides enables anionic guest species to be bound *via* hydrogen bond interactions The *N*-ferrocenoyl mono and dipeptide ester derivatives which Kenny, Gallagher and co-worker have made have not only exploited the hydrogen bonding ability of peptides but also the well established redox properties of ferrocene [66 67] For the monopeptide derivatives **76a-c** (Figure 1 42), a series of electrochemical and ^1H NMR titrations were carried out with $H_2PO_4^-$, HSO_4^-, Br^-, and BF_4^- $H_2PO_4^-$ shows most affinity for the *N*-ferrocenoyl glycine derivatives, the trend being $H_2PO_4^- >> HSO_4 > Cl^-$

> BF_4^- Downfield shifts of the amide proton in the ^1H NMR spectra and cathodic shifts of up to 120 mV were observed when the *N*-ferrocenoyl glycine derivatives **76a-c** were treated with $H_2PO_4^-$ [66]

The dipeptide derivative **77a** (Figure 1 42) that incorporates glycine was found to sense halide and dihydrogen phosphate anions with marked selectivity, the trends being $H_2PO_4^-$ >> Cl > Br^- >> HSO_4^- ^1H NMR investigations showed that downfield shifts of the CONH amide proton ranged from $\Delta\delta$ 0 25-2 0 ppm when the solution of receptor **76a** in $CDCl_3$ was treated with anions added as their tetra-alkyl ammonium salts Treatment of the *N*-ferrocenoyl compound with $H_2PO_4^-$ causes the largest cathodic perturbation (in the order of 110 mV) of the ferrocene-ferricenium redox couple The anion binding studies with **76b** and **76c** showed that much less anion complexation occurred, perhaps indicating that the amino acid alkyl side-chains have an inhibitory effect on anion complexation

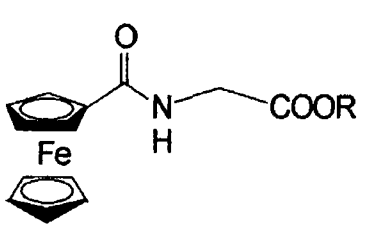

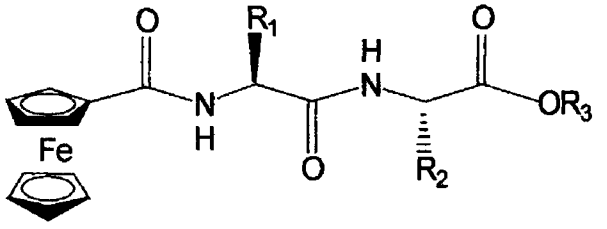

$R = CH_3$	**76a**	$R_1 = H, R_2 = H, R_3 = Me$	**77a**
$R = C_2H_5$	**76b**	$R_1 = {}^tBu, R_2 = {}^tBu, R_3 = Et$	**77b**
$R = CH_2Ph$	**76c**	$R_1 = Me, R_2 = Bn, R_3 = Et$	**77c**

Fig 1 42 *N*-Ferrocenoyl amino acid derivatives [66 67]

Porphyrins like peptides are common in nature and are perhaps best known for their role in carrying oxygen in hemoglobin/myoglobin and for their role in chlorophyll in the process of photosynthesis [68] Owing to its well-known redox activity, the porphyrin macrocycle is an attractive building block on which to append additional recognition sites for anion binding The attachment of ferrocenyl amide hydrogen bonding groups to various atropisomers of *meso*-5,20,15,20-tetra-*kis*-(*o*-ferrocenyl-carbonyl amino phenyl substituted) porphyrin creates novel cavities that contain unique topological amide hydrogen bonding environments This is in combination with a Lewis acid metal such as zinc(II), complexed in the porphyrin macrocyclic cavity produced a new selective redox-active sensory reagent for anions The ^1H NMR spectra shows large downfield shifts of

the amide proton in the receptor-anion complex suggesting that the metalloporphyrin binds anionic guests very strongly *via* hydrogen bond interactions In addition, it is noteworthy that the stability constant evaluations in CH_2Cl_2 display selectivity trends that are dependent upon the topological arrangements of the ferrocene amide group of a particular atropisomer For example, the α,α,α,α-isomer **78** (Figure 1 43) is bromide selective, whereas the α,α,α,β-isomer **79** (Figure 1 43) exhibits the selectivity sequence $NO_3^- > Cl^- > HSO_4^-$

Electrochemical investigations recognize anions *via* significant cathodic perturbations of the respective porphyrin oxidation and ferrocene/ferricenium redox couples [69 70]

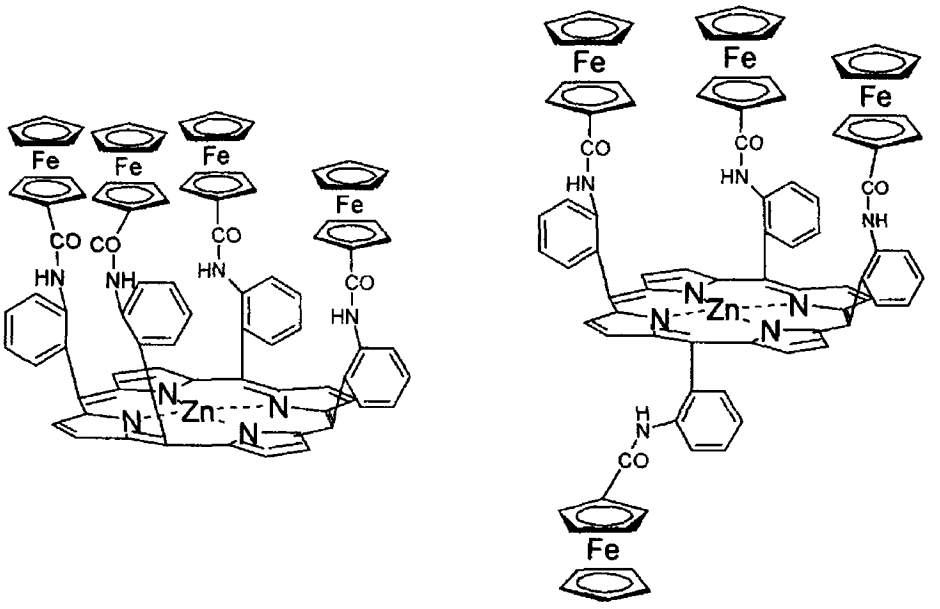

78 **79**

Fig 1 43 Metalloporphyrins that were found to be effective anion sensing molecules [69 70]

1.6 *N*-Ferrocenoyl peptides.

Conjugates of biomolecules such as amino acid and peptides with covalently bound organometallic compounds have recently gained considerable attention [71 72] For example, chemists have been drawn to this type of compound because of the vital roles that amino acids, peptides and proteins play in nature Similarly, the chemical properties of ferrocene in terms of reactivity, structural impact and redox behaviour are also currently areas of major interest [73-77] The incorporation of transition metal complexes like ferrocene into such highly structured biomolecules is envisioned not only to provide new biomaterials

and efficient redox systems but also to give scientists an insight into what may happen in electron transfer processes that occur in nature [78]

A transition metal can be intimately involved in electron transfer processes either as an electron storage device, as part of an electron transfer chain or as the reaction centre itself [78] Though some work has been carried out in order to understand what may influence the electron transfer processes that occur in metalloproteins, not much is known about what exactly happens However, recent experiments have shown that the manner in which the peptide chain is arranged in the vicinity of the redox centre has a major bearing electron transfer processes

Kraatz and co-workers have published a number of research papers in the field of ferrocenyl peptides in an attempt to understand the extent to which the ^{1}H NMR and electrochemical properties of the ferrocenyl group differ when appended peptide groups are varied These studies arose as a result of preliminary investigations, which suggested that the ferrocenyl moiety may be employed as a structural probe [78] They were also particularly interested in the electron transfer properties of rigid and flexible assemblies, addressing the role of the peptidic backbone in the electron transfer process and assessing the influence of amino acid side chains in modifying the electron transfer characteristic of a peptide chain [78-81 83]

In the course of their research Kraatz and coworkers performed electrochemical experiments that provided strong evidence that the redox properties of the ferrocene moiety is dependent on the length and structure of an oligopeptide chain [79] It was found that as an oligoproline chain grows, the ferrocene becomes easier to oxidize This was attributed to the formation of a poly-proline helix, and this assertion was supported by the fact that when the helix is fully formed (*i e* Fc-Pro_n-OR, n = 3,4 where Pro is proline) no further changes in the redox potential are seen Another tripeptide (consisting of two prolines and a phenylalanine residue) was made and corresponding electrochemical experiments yielded the information that in this case the ferrocene was much harder to oxidize than in the previous example This is probably because no amino acid helix was seen to form These results suggest firstly that electrochemically it is possible to distinguish a ferrocenyl oligoproline **80** (Figure 1 44) from a ferrocenyl oligopeptide (Pro-Pro-Phe) **81** (Figure 1 44) chain and secondly that secondary structure of a peptide chain may have a major influence on the redox potential [79]

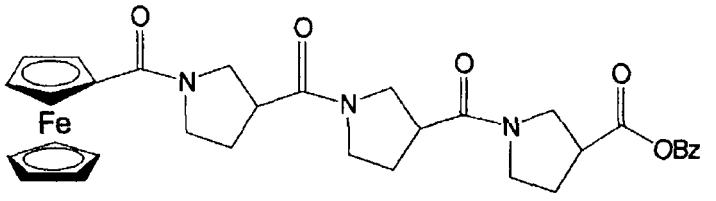

80

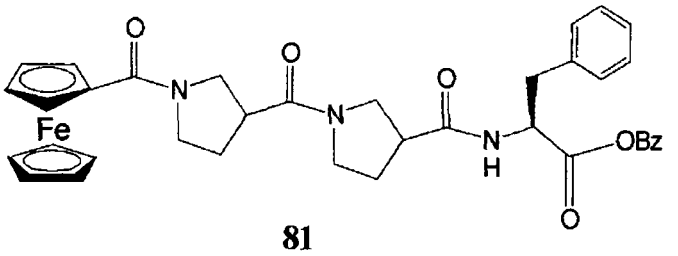

81

Fig 1 44 *N*-Ferrocenoyl tripeptide molecules incorporating proline and phenylalanine [79]

Kraatz and co-workers subsequently prepared a novel series of bis-oligoprolinoyl ferrocenyl derivatives (Figure 1 45) [80] In addition to the required product **82**, the 1-oligoprolinoyl-1'-OBt-ferrocenyl byproduct **83** (Figure 1 45) was obtained inadvertently These conformations prevent steric interactions of the amino acid side groups NMR studies show that the two oligoproline residues on the respective cyclopentadienyl rings give rise to one set of signals In addition, the chemical shift of the α-protons of the proline residues are in a region of the spectrum characteristic for the peptide chain being in the helical poly-proline conformation These compounds also display single reversible oxidation waves, which are dependent on the oligoproline chain length as was observed previously for the mono-substituted Fc-oligoprolines *i e* as the oligoproline chain grows in length and is able to adopt a stable helix conformation, the ferrocene moiety becomes easier to oxidize This work served to show that the appended amino acid/peptide chain influences the redox potential of the ferrocenyl moiety (primarily because of its sensitivity to changes in the secondary structure of appended peptides)

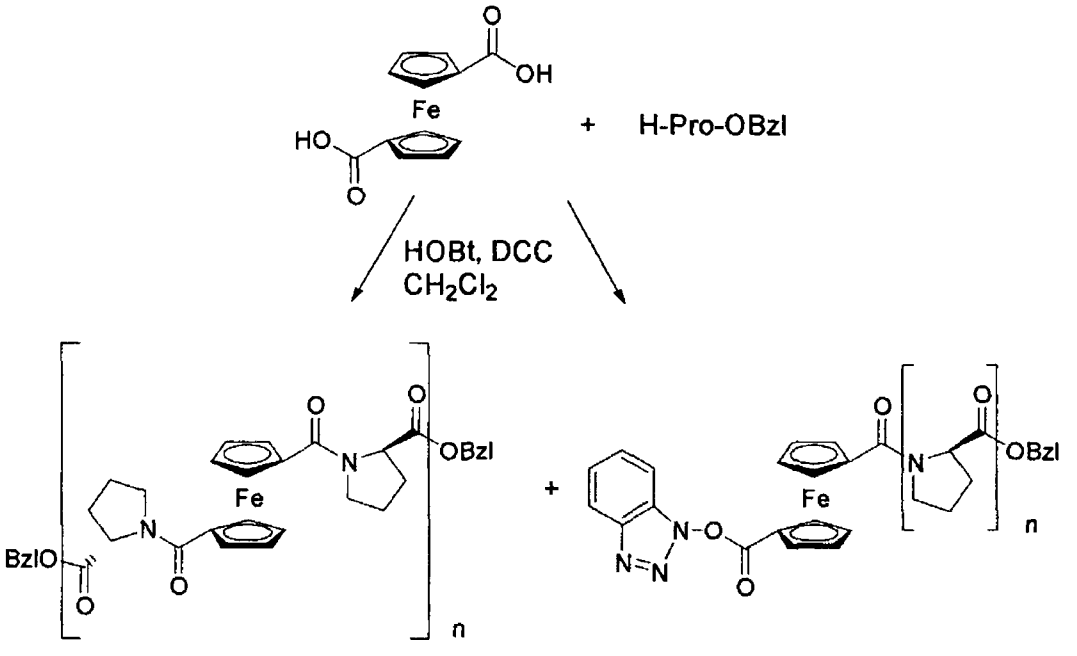

82 **83**

Fig 1 45 Syntheses of 1,1'-di(oligoprolinoyl)-ferrocenes **82** and 1-oligoprolinoyl-1'-benzotriazole ester-ferrocenes **83** [80]

N-Ferrocenyl peptide derivatives have a characteristic ability to interact with a guest molecule *via* hydrogen bond interactions Kraatz and co-workers have also reported the synthesis of three ferrocenoyl dipeptide derivatives **84-86** (Figure 1 46) and have described their interaction with 3-aminopyrazole [81] 3-aminopyrazole was chosen as a guest molecule as previous research had suggested that pyrazoles could be used as templates to induce the β-sheet motif by forming hydrogen bonds with the peptide backbone [82] Hence, experiments that monitor electronic changes in redox centres, depending on secondary peptide structure in its environment could be carried out It was noted, that of the three dipeptide derivatives used, the leucine-phenylalanine derivative **86** formed the strongest interaction with 3-aminopyrazole It was suggested that this was due to the presence of the relatively bulky isopropyl and benzyl groups of the leucine and phenylalanine residues respectively In comparison to the glycine-glycine **84** and alanine-alanine **85** derivatives, the flexibility of the peptide backbone of the leucine-phenylalanine derivative **86** is restricted and hence, the binding site is more defined In addition, Kraatz and his coworkers found that due to the 'sterically demanding'

sidegroups of compound **86**, the β-sheet conformation had already started to form Electrochemical and ^{1}H NMR experimental data were in agreement about the strength of the interaction of the 3-aminopyrazole with the respective ferrocenyl dipeptides For example, shifts in the redox potential varied from no change for receptor **84** to 30 mV for receptor **86** (versus the ferrocene/ferricenium redox couple) These electrochemical data were paralleled by downfield shifts of 2 5 ppm in the ^{1}H NMR spectrum for receptor **86** It can therefore be stated conclusively that the ferrocene moiety is sensitive to structural changes, which in this case was caused by the binding of 3-aminopyrazole *via* hydrogen bond interactions with the *N*-ferrocenyl-L-leucine-L-phenylalanine derivative **86** [81]

i

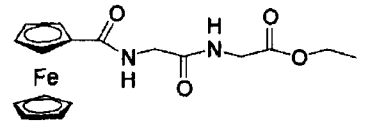

84

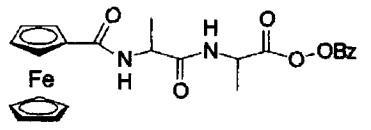

85

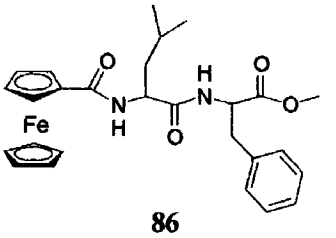

86

ii

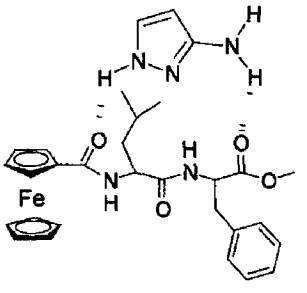

Fig 1 46 (i) The *N*-ferrocenoyl dipeptide derivatives used in the experiments with 3 aminopyrazole (ii) The interaction of 3-aminopyrazole with *N*-ferrocenoyl leucine–phenylalanine methyl ester **86** [81]

More recently, Kraatz and co-workers have prepared two ferrocenyl oligopeptides "constructs" with a second peptide chain [83] It is proposed that this structure has the ability to interact strongly with aspartic proteases such as HIV 1 protease Two 1,1'-*bis*-peptides were designed Compound **87a** and **b** (Figure 1 47) have the identical peptide sequence to that found in pepstatin, a potent naturally occurring inhibitor of aspartic proteases Work is ongoing to evaluate the electrochemistry of the two compounds and their ability to bind aspartate proteases [83]

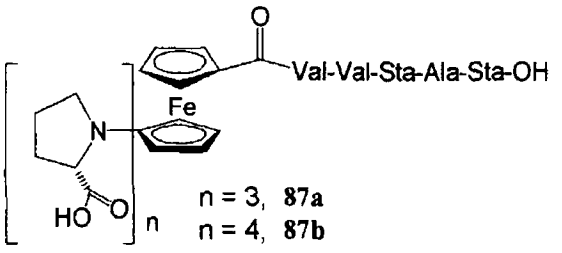

Fig 1 47 A potential bioactive *N*-ferrocenoyl polypeptide compound [83]

The ferrocenyl group has been known to mediate electron transfers between electrodes and the redox sites of proteins By attaching ferrocenyl groups onto proteins, their redox activities have been regulated by external potentials In 1997 Kira *et al* reported the synthesis and subsequent resolution of L-ferrocenylalanine (ferAla) **88** (Figure 1 48) [84] Kira and his colleagues claimed that the redox activity of a ferrocenyl functionalized amino acid/peptide is only fully exploited when the ferrocenyl moiety is appended to an amino acid at a specific, known position Hence, they have suggested an alternative 'improved' synthetic route to that proposed by Osgerby and Pauson [85] The ferAla derivative was subsequently incorporated in a hexapeptide and its conformation was determined The spectral data showed that the polypeptide under investigation also adopts an α-helical conformation which may result from the incorporation of bulky ferAla units This unusual amino acid may find application in peptide mimetic studies, for example, it has been suggested that the incorporation of the ferrocenyl functionalized alanine derivative may add artificial redox functions to synthetic polypeptides or to genetically engineered proteins

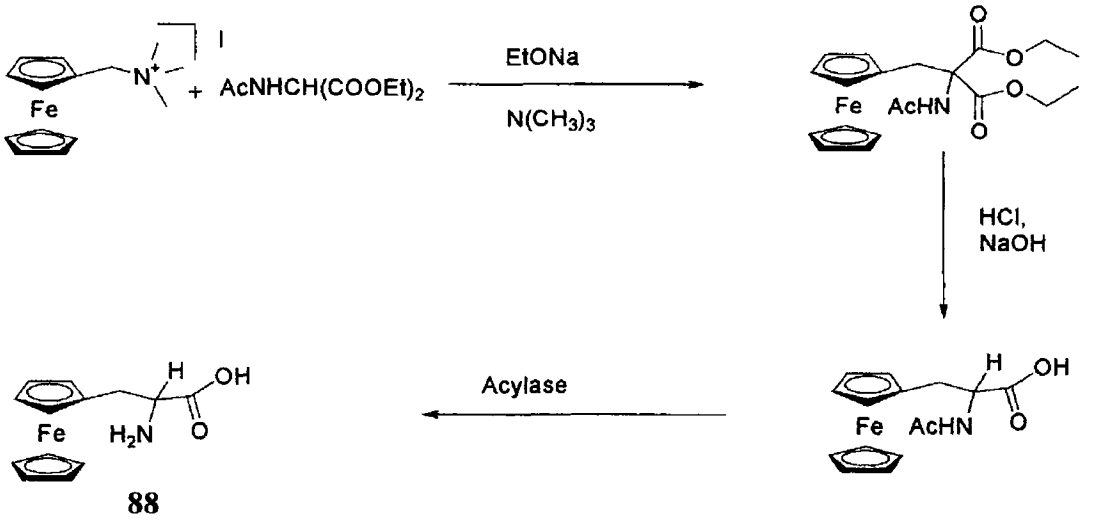

88

Fig 1.48 Synthetic path for L-ferrocenylalanine [84]

Moriuchi and co-workers have prepared a series ferrocenyl functionalized amino acid and dipeptide derivatives **89-93** (Figure 1 49) for the purpose of gaining an insight into protein folding Their research primarily focused on the design of secondary structure mimetics composed of dipeptides [86 87] Ferrocene was employed as a scaffold on which to build peptide strands The inter cyclopentadienyl spacing distance is approximately 3 3 Å and this distance is ideal for intramolecular hydrogen bonding between peptide strands appended to the respective cyclopentadienyl rings of the ferrocenyl moiety Hence, these compounds served as models of ordered structures based on two rigid intramolecular hydrogen bonds (between the N-H and C=O functions of the respective amino acids) and a helical molecular arrangement in the crystal packing Moriuchi *et al* have postulated that the manner in which these ferrocenyl peptide molecules self organize may provide an insight into the way in which protein folding occurs [87] This research serves to emphasise that the architectural control of molecular self organization is of great importance with respect to gaining an insight into the mechanisms of protein folding and the development of new functional materials

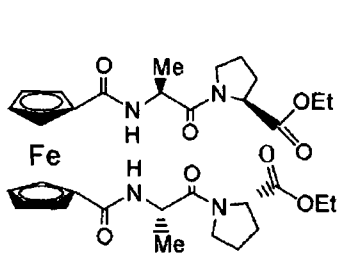

89

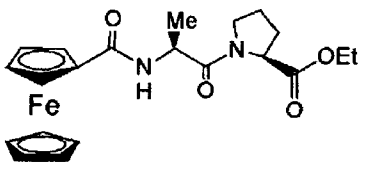

90

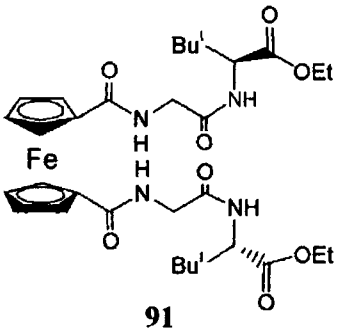

91

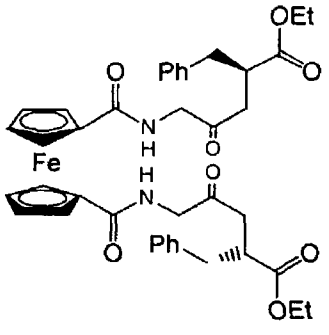

92

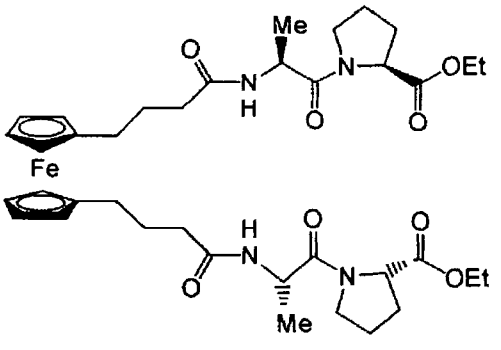

93

Fig 1 49 The *N*-ferrocenoyl compounds made by Nomoto *et al* in the study of their interactions [87]

Metal ions have been known to exhibit a variety of properties in proteins, the most important of which is the stabilization of the structures required for biological functions [88] This knowledge has inspired Moriuchi and his colleagues to design and synthesize the ferrocene bearing dipeptide chain (-L-Alanine-L-Proline-NHPy) **94** (Figure 1 50) with an additional pyridyl moiety, which is capable of participating in hydrogen bonding and binding metal salts

The ferrocene bearing dipeptide chain was demonstrated to create a highly organized assembly through the intermolecular hydrogen bonded network in an anti-parallel manner The appended pyridinyl moiety was found to be capable of participating in hydrogen bonding and binding to the metal salt The two ferrocenyl dipeptide strands of the palladium complex could rotate with respect to each other about the palladium centre by the ball bearing motion of the two pyridinyl rings [88]

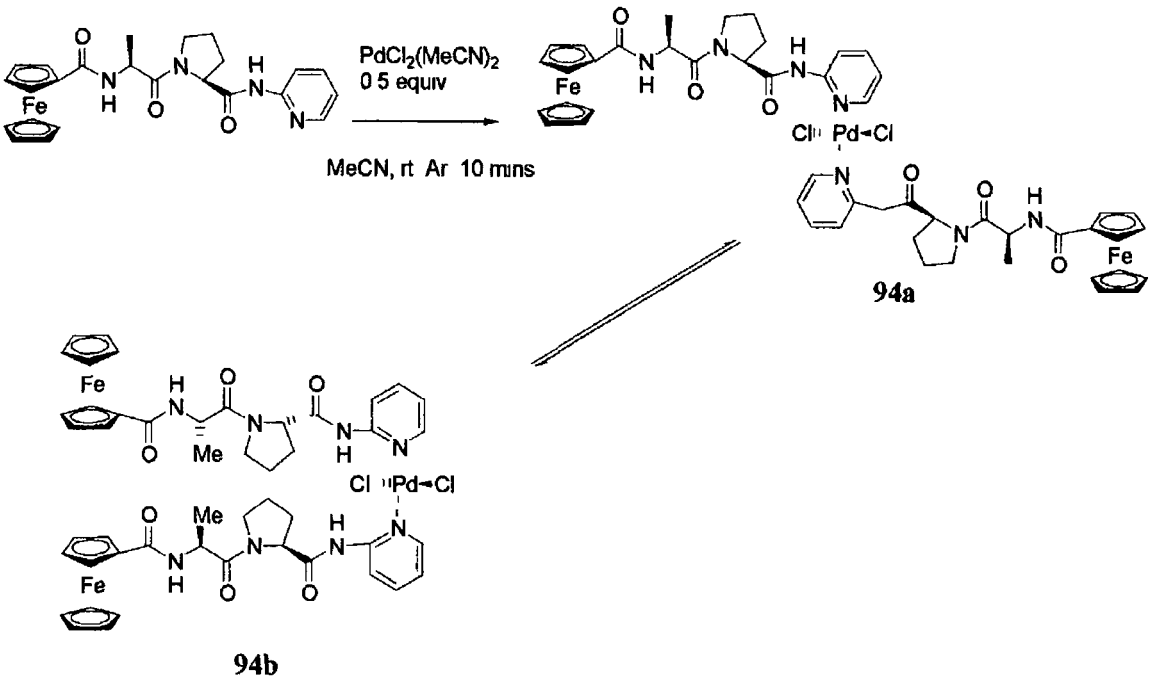

Fig 1 50 *N*-ferrocenyl dipeptide and *N*-ferrocenyl dipeptide palladium complex [88]

In a subsequent related study, Moriuchi *et al* prepared analogous ferrocene bearing podand dipeptide chains (-L-Ala-L-Pro-NHPy) (Figure 1 51) [89] It was intended, that by employing previously described well known rigid intramolecular hydrogen bonds (between the N-H and C=O functions of the respective podand peptide chains) more highly ordered systems may be prepared with respect to earlier investigations [87] In

addition, the metal coordination sites on the pyridine rings are envisaged to further stabilize the conformation of the ferrocene bearing podand dipeptide strands ^{1}H NMR data strongly suggested that the complexation of the palladium salt by the pyridmyl nitrogens further stabilized the complex by restraining the conformation of the respective peptide strands, hence facilitating stronger hydrogen bonds between the N-H and the C=O functions of the podand dipeptide chains, as the signal due to the alanine amide protons in complex **96** appears further downfield with respect to the signal of the alanine amide protons in complex **95**

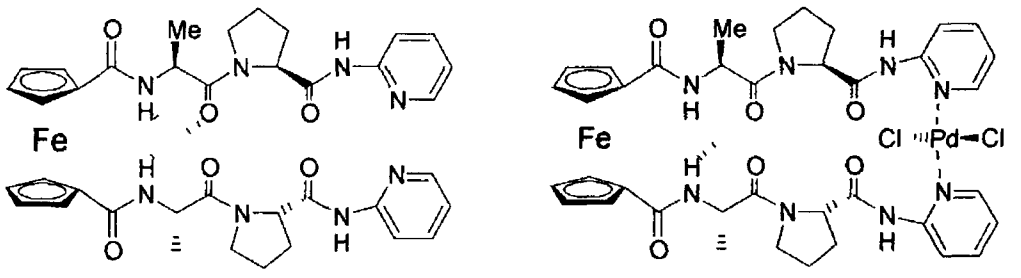

95 **96**

Fig 1 51 Ferrocenes bearing podand dipeptide chains [89]

1.7 Conclusion

Since the discovery of ferrocene in 1951, this sandwich type compound has not only revitalised the field of organometallic chemistry as a subject of interest, but it has also provided chemists with a versatile building block on which new materials with novel functions can be built For example, due to the growing immunity of pathogenic organisms to conventional antibiotic treatments along with society's general requirement for new bio-chemicals, diversification of existing and established biologically active compounds continue apace Ferrocene is an ideal isosteric substitute for phenyl and heterocyclic rings, and hence drug and other biologically active compounds bearing the ferrocenyl moiety are becomng more popular

The field of supramolecular chemistry has also exploited the well known redox capabilities of ferrocene ^{1}H NMR and electrochemical studies have shown that ferrocenyl compounds with appended hydrogen bond donor sites can bind anionic species These compounds may potentially provide the basis on which anion sensing devices may be developed

Peptide mimetic models that incorporate the ferrocenyl moiety have been prepared in order to facilitate the study of protein function and structure It is thought that the presence of an electrochemically active moiety on a peptide may aid the acquisition of information regarding the secondary structure that a peptide/protein may adopt and hence, a better understanding of protein function may be obtained

The synthesis and characterization of *N*-ferrocenyl benzoyl amino acid and dipeptide derivatives is reported in this thesis Investigations have been carried out in order to determine the anion sensing abilities of these compounds and studies to determine their biological activity is currently in progress

Chapter 1 references

1 Elschenbroich Ch , Salzer, A , '*Organometallics*', **1992**, VCH, Weinheim
2 Kealy, T J , Pauson, P L , *Nature*, **1951**, *168*, 1038
3 Miller, S A , Tebboth, J F , Tremaine, J , *J Chem Soc* , **1952**, *74*, 632
4 Wilkinson, G , Rosenblum, M , Whiting, M C , Woodward, R , *J Chem Soc* , **1952**, *74*, 2125
5 Huheey, J E , '*Inorganic Chemistry*' **1977**, 2nd Edition, Harper Int
6 Togni, A , Hayashi, T , *Ferrocenes*, **1994**, VCH, Weinheim
7 Severin, K , Bergs, R , Beck, W , *Angew Chem Int Ed* , **1998**, *37*, 1634
8 Long, N J , *Metallocenes*, **1998**, Blackwell Sciences
9 Woodward, R B , Rosenblum, M , Whiting, M C , *J Chem Am Soc* , **1952**, *74*, 3458
10 Rosenblum, M , Abbate, F W , *J Chem Am Soc* , **1966**, *88*, 4178
11 Broadhead, G D , Pauson, P L , *J Chem Soc* , **1955**, 367
12 Weinmayer, V , *J Chem Am Soc* , **1955**, *77*, 3012
13 Nesmayanov, A N , Perevalova, E G , Golovnya, R V , *Doklady Acad Nauk SSSR*, **1954**, *99*, 539
14 Rosenblum, M , Glenn-Howells, W , Banerjee, A K , Bennett, C , *J Chem Am Soc* , **1962**, *84*, 2726
15 Little, W F , Lynn, K N , Williams, R , *J Chem Am Soc* , **1963**, *85*, 3055
16 Saji, T , *Chem Lett* , **1986**, 274
17 Hammond, P J, Bell, A P , Hall C D , *J Chem Soc Perkin Trans I*, **1983**, 707
18 Beer, P D , Nation, J E , McWhinnie, S L W , Harmann, M E , Hursthouse, M B , Ogden, M I , White, A H , *J Chem Soc , Dalton Trans*, **1991**, 2485
19 Beer, P D , Cadman, J , *Coord Chem Rev* , **2000**, *205*, 131
20 Kopf-Maier, P , Kopf, H , *Chem Rev* , **1987**, 1137
21 Bloom, B , Murray, J , *Science*, **1992**, *257*, 1055
22 Johnson, A , Uttley, A , Woodward, N , *Clin Microbiol* , **1990**, Rev 3, 280
23 Jaouen, G , Vessieres, A , Butler, I , *Acc Chem Res* , **1993**, *26*, 391
24 Rosenberg, B , Van Camp, L , Trosko, J E , Mansour, V H , *Nature*, **1969**, *222*, 385
25 Kopf-Maier, P , Kopf, H , Neuse, E , *Angew Chem Int Ed Eng* , **1994**, *23*, 446
26 Georgopoulos, A , Mingos, D , White, A , Williams, D , Horrocks, B , Houlton, A , *J Chem Soc Dalton Trans* , **2000**, 2969
27 Krieg, R , Wyrwa, R , Mollman, U , Görls, H , Schönecker, B , *Steroids*, **1998**, *63*, 531
28 Biot, C , Glorian, G , Maciejewsji, L A , Brocard, J S , *J Med Chem* **1997**, *40*, 3715
29 Maryanoff, B E , Keeley, S L , Perisco, F J , *J Med Chem* , **1983**, *26*, 226
30 Ma H , Hou Y , Bai, Y , Lu, J , Yang, B , *J Organomet Chem* , **2001**, *627-639*, 742
31 Wing, D , *Science*, **1988**, *241*, 467
32 Runqui, H , Qingmin, W , *J Organomet Chem* , **2001**, *637-639*, 94
33 Antonisse, M M G , Reinhoudt, D N , *J Chem Soc Chem Comm* , **1998**, 448
34 Scheerder, J , Engbersen, J F J , Reinhoudt, D N , *Recuil des Travaux des Pays Bas*, **1996**, 115
35 Beer, P D , Gale, A , *Angew Chem Ed Int Eng* , **2001**, *40*, 486
36 Schmidchen, F P , Berger, M , *Chem Rev* , **1997**, *97*, 1609
37 Park, C H , Simmons, H E , *J Am Chem Soc* , **1968**, *90*, 2431
38 Schmidchen, F P , Muller, G , *J Chem Soc Chem Comm* , **1984**, 1115

39 Pascal, R A , Spergel, J , Van Engen, D , *Tetrahedron Lett*, **1986**, *27*, 4099
40 Valiyaveettil, S , Engbersen, J F J , Verboom, W , Reinhoudt, D N , *Angew Chem Int Ed Eng* , **1993**, *32*, 900
41 Ranganathan, D , Lakshm C , *J Chem Soc Chem Comm* , **2001**, 1250
42 Beer, P D , Keefe, A D , *J Organomet Chem* , **1989**, *C40*, 375
43 Beer, P D , Drew, M G B , Graydon, A R , Smith, D K , Stokes, S E , *J Chem Soc , Dalton Trans* , **1995**, 403
44 Beer, P D , Hazlewood, C , Hesek D , Hodacova J , Stokes, S E , *J Chem Soc , Dalton Trans* , **1993**, 1327
45 Beer, P D , *J Chem Soc Chem Comm* , **1996**, 689
46 Beer, P D , Drew, M G B , Hesek, D , Nam, K C , *Organometallics*, **1999**, *18*, 933
47 Beer, P D , Drew, M G B , Hesek, D , Shade, M , Szemes, F , *J Chem Soc Chem Comm* , **1996**, 2161
48 Beer, P D , Drew, M G B , Hesek, D , Nam, K C , *J Chem Soc Chem Comm* , **1997**, 107
49 Beer, P D, Chen, Z , Goulden, A J , Graydon, A R , Stokes, S E , Wear, T , *J Chem Soc Chem Comm* , **1993** 1834
50 Chen, Z , Graydon, A R , Beer, P D , *J Chem Soc Faraday Trans* , **1996**, *92*, 97
51 Beer, P D , Graydon, A R , Johnson, A O M , Smith, D K , *Inorg Chem* , **1997** *36*, 2112
52 Nishizawa, S , Buhlmann, P , Iwao, M , Umezawa, Y , *Tetrahedron Lett* , **1995**, *36*, 6483
53 Carr, J D , Lambert, L , Hibbs, D E , Hursthouse, M B , Abdul-Malik, K M , Tucker, J H R , *J Chem Soc Chem Comm* , **1997**, 1649
54 Carr, J D , Coles, S J , Hassan, W W , Hursthouse, M B , Abdul-Malik, K M , Tucker, J H R , *J Chem Soc Dalton Trans* **1999**, 57
55 Anzanbacher Jr , P , Jursikova, K , Sessler, J L *J Chem Am Soc* , **2000**, *122*, 9350
56 Sessler, J L , Zimmerman, R S , Kirkovitz, G J , Gebauer, A , Scherer, M , *J Organomet Chem* , **2001**, *637-639*, 343
57 Gale, P A , Hursthouse, M B , Light, M E , Sessler, J L , Warriner, C L , Zimmerman, R S , *Tetrahedron Lett* , **2001**, *42*, 6759
58 Reynes, O , Maillard, F , Moutet, J-C , Royal G , Saint-Aman, E , Stanciu, G , Dutosta J-P, Gosse, J , Mulatier, J-C , *J Organomet Chem* , **2001**, *637-639*, 356
59 Kingston, J E , Ashford, L , Beer, P D, Drew, M G B , *J Chem Soc Dalton Trans* , **1999**, *251*
60 Beer, P D , Chen, Z , Drew, M G B , Johnson, A O M , Smith, D K , Spencer, P , *Inorg Chim Acta*, 1996, *246*, 143
61 Beer, P D , Cadman, J , Lloris, J M , Martinez-Manez, R , Padilla, M E , Pardo, T , Smith, D K , Soto, J , *J Chem Soc Dalton Trans* , **1999**, 127
62 Lloris, J , Martinez-Mañez, R , Padilla-Tosta, M , Pardo, T , Soto, J , Tendero, M , *J Chem Soc Dalton Trans* , **1998**, 3657
63 Beer, P D , Cadman, J , Lloris, J , Martinez-Mañez, R , Soto, J , Pardo, T , Marcos D M , *J Chem Soc Dalton Trans* , **2000**, 1805
64 Lloris, J , Martinez-Mañez, R , Soto, J , Pardo, T , *J Organomet Chem* , **2001**, *637-639*, 151
65 Beer, P D , Chen, Z , Ogden, M I , *J Chem Soc Faraday Trans* , **1995**, *91*, 295
66 Gallagher, J F , Kenny, P T M , Sheehy, M J , *Inorg Chem Comm* , **1999**, *2*, 200
67 Gallagher, J F , Kenny, P T M , Sheehy, M J , *Inorg Chem Comm* , **1999**, *2*, 327

68 Zumdahl, S , '*Chemistry*', **1993**, Heath Publishing
69 Beer, P D , Drew, M G B , Hesek, D , Jagessar, R , *J Chem Soc Chem Comm* , **1995**, 1187
70 Beer, P , Drew, M G B , Jagessar, R , *J Chem Soc Chem Dalton Trans* , **1997**, 881
71 Sherman, S E , Lippard, S J , *Chem Rev* , **1987**, *87*, 1153
72 Ryabov, A D , *Angew Chem Int Ed Eng* , **1991**, *30*, 931
73 Brosch, O , Weyhermuller, T , Metzler-Nolte, N , *Inorg Chem* , **1997**, *38*, 5308
74 Schnert, J , Hess, A , Metzler-Nolte, N , *J Organomet Chem* , **2001**, *637-639*, 349
75 Hess, A , Brosch, O , Weyhermuller, T , Metzler-Nolte, N , *J Organomet Chem* , **1999**, *589*, 75
76 Van Staveren, D , Weyhermuller, T , Metzler-Nolte, *J Chem Soc Chem Dalton Trans* , **2003**, 210
77 Maricic, S , Berg, U , Frejd, T , *Tetrahedron*, **2002**, *58*, 3085
78 Kraatz, H-B , Lusztyk, J , Enright, G D , *Inorg Chem* , **1997**, *36*, 2403
79 Kraatz, H-B , Leek, D , Houman, A , Enright, G D , Lusztyk, J , Wayner, D , *J Organomet Chem* , **1999**, *589*, 38
80 Xu, Y , Saweczko, P , Kraatz, H-B , *J Organomet Chem* , **2001**, *637-639*, 335
81 Saweczko, P , Kraatz, H-B , *Coord Chem Rev* , **1999**, *190-192*, 185
82 Kirster C N , Schrader T H , *J Am Chem Soc* , **1997**, *119*, 12019
83 Xu, Y , Kraatz, H-B , *Tetrahedron Lett* , **2001**, 2601
84 Kira, M , Matsubara, T , Shinohara, H , Sisido, M , *Chem Lett* , **1997**, 89
85 Osgerby, J M , Pauson, P L , *J Chem Soc* , **1958**, 656
86 Nomoto, A , Moriuchi, T , Yamazaki, S , Ogawa, A , Hirao, T , *J Chem Soc Chem Comm* , **1998**, 1963
87 Moriuchi, T , Nomoto, A , Yamazaki, S , Ogawa, A , Hirao T , *J Chem Am Soc* , **2001**, *123*, 68
88 Moriuchi, T , Yoshida, K , Hirao, T , *J Organomet Chem* , **2001**, *637-639*, 75
89 Moriuchi, T , Yoshida, K , Hirao, T , *Organometallics*, **2001**, *20*, 3101

Chapter 2

Results and discussion

2 1 Introduction

Organometallic compounds have been found to be incorporated in a wide variety of attractive materials that may potentially have diverse applications [1] One such organometallic compound, ferrocene, is recognized as a promising candidate for incorporation in novel materials due to its stability, its spectroscopic, its electrochemical properties and its ease of use [2] As a direct consequence of these properties, research in the area of ferrocenyl derivatives has seen a dramatic increase in attention over the past decade, primarily for the ultimate goals of achieving novel sensor compounds, peptide mimetic models and unnatural drugs [3]

In this project, the primary aim was the synthesis and characterisation of unusual biological materials that combine three key moieties *i e*

a An electroactive core

b A conjugated linker that may act as a chromophore

c An amino acid derivative that can interact with other molecules *via* hydrogen bonding

These three key moieties are the constituents of *N*-(ferrocenyl)benzoyl amino acid derivatives, the general structure of which is shown in Figure 2 1

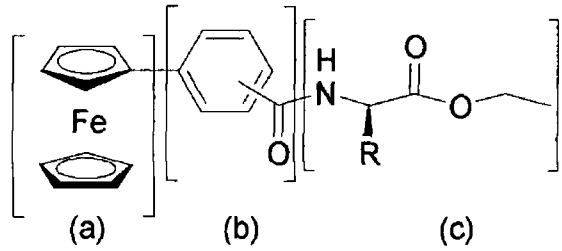

Fig 2 1 General structure for the *N*-(ferrocenyl)benzoyl amino acid ester derivatives

The series of compounds presented herein comprises a ferrocenyl moiety linked directly to the amino acid residue through an *ortho-*, *meta-* or *para-* benzoyl group such that molecular *cleft* between the ferrocenyl moiety and the amino acid residue is enlarged with respect to earlier investigations [4,5]

2 2 The synthesis of the *N*-(ferrocenyl)benzoyl amino acid ester derivatives

Coupling reactions allow the facile introduction of the ferrocenyl benzoyl group onto an amino acid The incorporation of the ferrocenyl benzoyl moiety onto a series of amino acid methyl and ethyl esters was thus achieved Ferrocenyl benzoic acid was added to a stirred solution of equimolar amounts of the amino acid ester hydrochloride, treated with triethylamine (Et_3N), dicyclohexylcarbodiimide (DCC) and 1-hydroxybenzotriazole (HOBt) at 0°C in dichloromethane The procedure is similar to that as used by Degani *et al* to incorporate ferrocene carboxylic acid onto proteins [6] The synthetic route employed in the synthesis of an *N*-{*para*(ferrocenyl)benzoyl} amino acid derivative is outlined in Figure 2 2 The condensation of ferrocenyl benzoic acid with amino acid esters of L-phe, L-leu, L-ala, gly, β–ala, 4-amino butyric acid, ±2-amino butyric acid and isoamino butyric acid ethyl ester proceeded with yields ranged between 40 and 68% and all gave spectroscopic data in accordance with their proposed structures

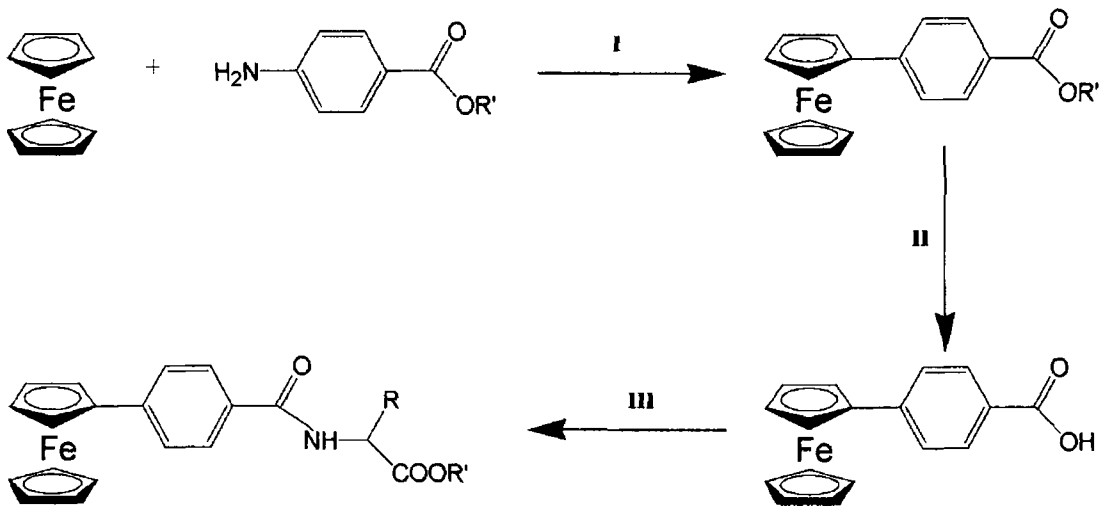

I = $NaNO_2$, HCl, 5°C II = NaOH/MeOH, H_2O, III = DCC, HOBt, Et_3N, AA ester

Fig 2 2 The general reaction scheme for the synthesis of *N-para*-(ferrocenyl)benzoyl amino acid esters (A similar protocol is used for the *ortho-* and *meta-* derivatives)

2 2 1 The preparation of ferrocenyl benzoic acid

The synthesis of ferrocenyl benzoic acid employed conventional diazonium salt chemistry Treatment of methyl/ethyl aminobenzoate with sodium nitrite in the presence of hydrochloric acid yielded the diazonium salt of the ester This was reacted with ferrocene *in situ* to furnish the *ortho-*, *meta-* and *para-* ferrocenyl methyl/ethyl benzoates

which were isolated as viscous oils Prior to any further reaction the ester groups were cleanly cleaved using a 10% sodium hydroxide solution to yield ferrocenyl benzoic acid The ^{1}H NMR spectra of the ferrocenyl benzoic acid showed the appearance of a weak, broad singlet at approximately δ 13 and this peak is consistent with the presence of the carboxylic acid proton In addition, the disappearance of the characteristic ester peaks in both the ^{1}H and ^{13}C NMR spectra also suggested that the base hydrolysis step had cleaved the ester group to yield the ferrocenyl benzoic acid The IR spectra for the *ortho*, *meta* and *para* ferrocenyl benzoic acid derivatives show peaks at approximately 1680cm^{-1} and 3500 cm^{-1} corresponding to the carbonyl and hydroxyl groups of a carboxylic acid moiety

2 2 2 Amino acids

Amino acids are the constituent moieties of proteins and hence are molecules of much interest From a synthetic point of view, they have been extensively utilized in pursuit of novel materials including peptide mimetic models, supramolecular compounds and amino acid based disease treatments [7-9]

As their name implies, amino acids are bifunctional compounds that contain both a basic amino group and a carboxylic acid group Therefore, the synthetic value of amino acids as building blocks stems from the fact that they can be linked together (or to other suitable compounds *e g* ferrocenyl benzoic acid) *via* a condensation reaction between amino and carboxyl moieties resulting in the formation of an amide bond

The reaction of ferrocenyl benzoic acid with an amino acid ester (Figure 2 2) was required to form the amide bond that links the two moieties To ensure this outcome and prevent the formation of an anhydride linkage, the carboxyl terminus of the amino acid was protected as either a methyl or ethyl ester However, there are a variety of alternative carboxyl protecting techniques available that can be employed to fulfill the requirements of a particular situation

2 2 3 Carboxyl protecting groups.

2 2 3 1 Methyl/Ethyl esters

Chemically, there is essentially little difference in the reactivity of the methyl or ethyl esters and therefore anything that is said of one holds true for the other

Amino acids react easily with thionyl chloride in methanol to give the corresponding methyl ester hydrochloride (Figure 2 3) [10] The amino acid ester hydrochloride salts can

be neutralized to give the free base but these generally deteriorate rapidly and therefore, the free base is generally generated *in situ* when required, usually by using a tertiary amine

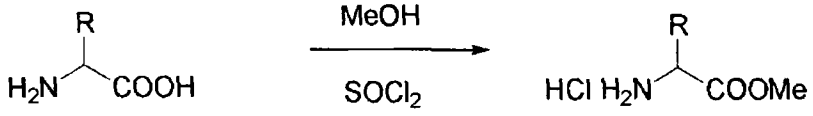

Fig 2 3 The protection of the carboxyl terminus of an amino acid by conversion to a methyl ester

Methyl esters are completely stable towards HBr, acetic acid, trifluoroacetic acid (TFA) or catalytic hydrogenolysis and therefore the selective removal of amino protecting groups from peptide methyl ester derivatives presents no difficulties Due to the stability of the methyl ester protecting group, its own removal may present difficulties Saponification is sometimes satisfactory, however, the base that is required for this process may cause racemization (Figure 2 4)

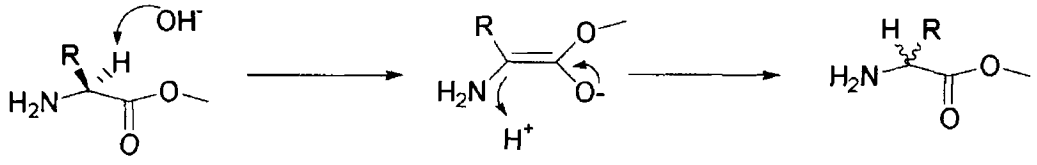

Fig 2 4 The process of racemization that may occur instead of the desired cleavage reaction due to the presence of base required for saponification

2 2 3 2 Benzyl esters

Amino acid benzyl esters are best prepared by the 4-toluenesulphonic acid catalyzed esterification with benzyl alcohol and they are subsequently isolated as their 4-toluenesulphonic salts [11] Like the methyl/ethyl esters, their corresponding free bases are unstable The benzyl ester group can be removed by saponification and by hydrazinolysis, but more importantly they are cleaved by HBr and HF, the mechanism of which is schematically shown in Figure 2 5

The benzyl ester group is generally stable to acidic media and therefore can be carried through a variety of functional group interconversions unscathed

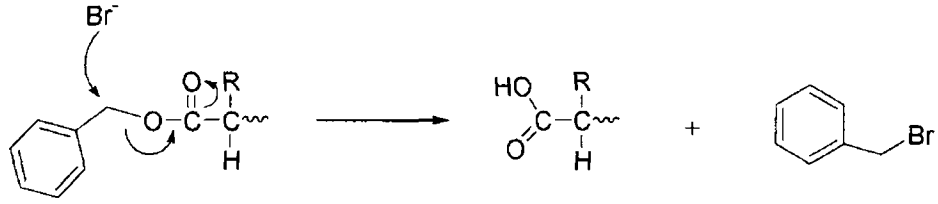

Fig 2 5 The removal of the benzyl protecting group

2 2 3 3 Phenyl esters

Phenyl ester carboxy-protection was devised to facilitate smooth carboxy deprotection in the presence of acid sensitive groups [12] The amino acid phenyl esters are prepared (Figure 2 6) using phenol and DCC and are usually crystalline

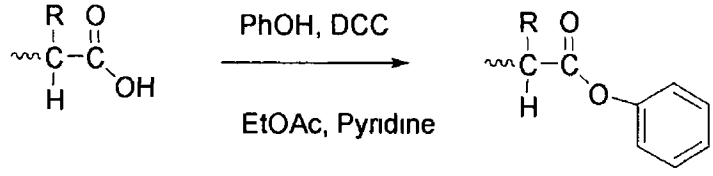

Fig 2 6 The protection of the carboxyl group using the phenyl ester group

The phenyl ester group is stable to acids and catalytic hydrogenolysis but is very vulnerable to attack by peroxide ions The reaction with peroxide ions is completed at a pH of 10 5 and takes about 15 minutes The acid is obtained *via* a peroxy acid transition state (Figure 2 7)

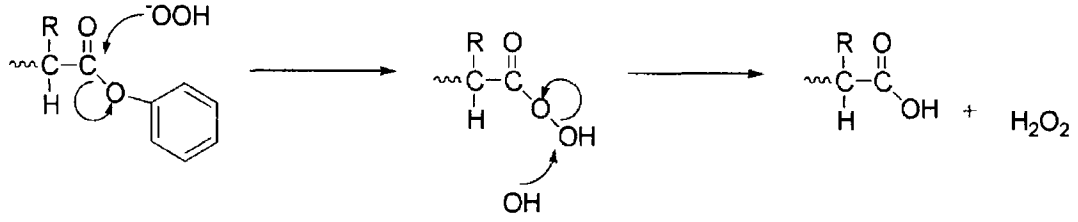

Fig 2 7 The removal of phenyl ester protecting group [12]

2 3 Amide bond formation/Coupling reactions

The key step in peptide synthesis is the formation of the peptide bond [13] The peptide bond can be formed from the reaction between a carboxylic acid and an amino group at high temperatures However, high temperatures may damage sensitive functional groups on susceptible peptides Peptide synthesis is in fact performed at or below room temperature, and coupling methods, which require the application of heat, are not thought to be useful [14] Therefore, in order to form a peptide bond, either the amino or carboxyl group

must be activated so as to produce the desired amide In general it is the carboxyl group that is activated and there are many activation reagents and procedures available to facilitate this process [14]

2 3 1 Activation and coupling reagents

2.3 1 1 Acyl chlorides

The activation of acylammo acids by conversion to the corresponding acyl chlorides, followed by reaction with amino acids is probably the most obvious and simple approach to peptide synthesis (Figure 2 8) In fact, this was the couplmg method of choice in the early days of peptide synthesis [14]

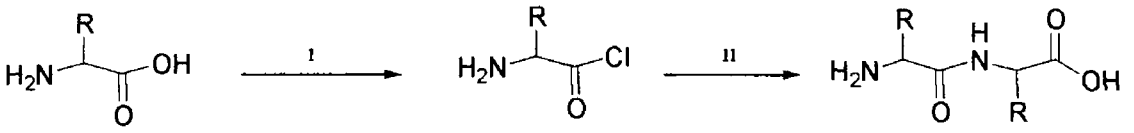

i = PCl_5, PhH ii = Amino Acid, MgO, aq Dioxane

Fig 2 8 The synthesis and application of amino acid chlorides

The synthesis of the acyl chloride traditionally employed reagents such as $SOCl_2$ or PCl_5, however, these reagents are too severe to be compatible with sensitive peptides A further complication is that most simple acyl ammo acid chlorides cyclize spontaneously to yield oxazolones Although oxazolones are active with respect to aminolysis, the base present (originally to neutralize the HX by-product, where X is a halogen) can cause significant racemization (Figure 2 9) Therefore, due to the general requirement for chirally pure materials, this procedure is not widely employed anymore [14]

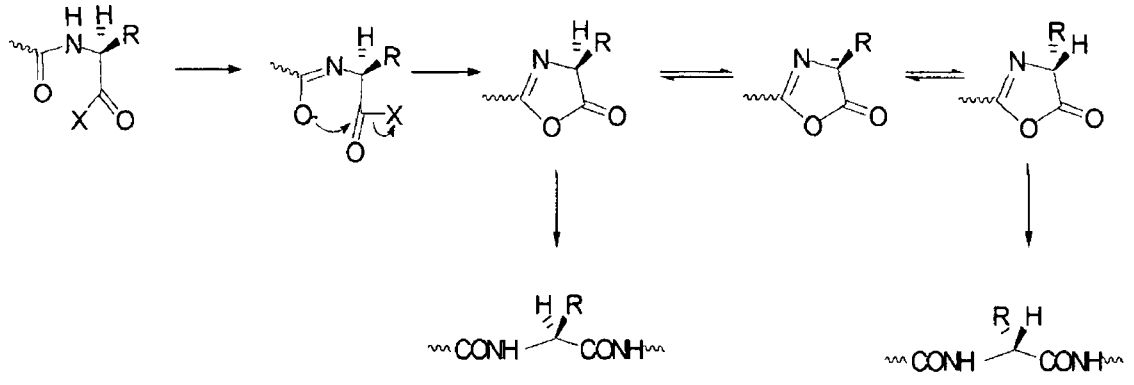

Fig 2 9 The process of racemization *via* the oxazolones transition state [14]

2 3 1 2 Phosphonium reagents

Acyloxyphosphomum species, which can be generated by the attack of carboxylate anions on suitable phosphomum cations react readily with nucleophilic moieties at the acyl carbon This has led to the development of phosphonium reagents for use as direct coupling reagents For example, benzotriazolyl-1-oxy(dimethylamino) phosphomum hexafluorophosphate (BOP) has been employed with great success as a coupling reagent [15] The BOP reagent reacts with the carboxylate function of an amino acid to yield an amino acid benzotriazole ester and this moiety can easily undergo aminolysis (Figure 2 10)

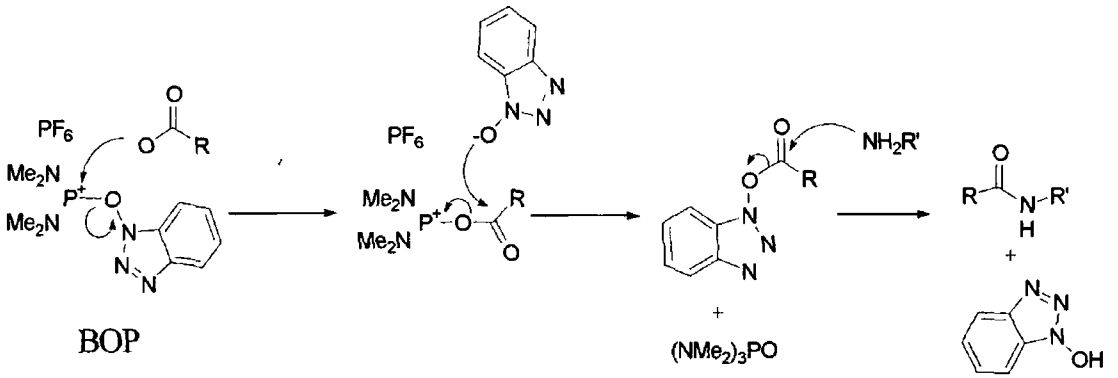

Fig 2 10 The mechanism by which the BOP reagent operates [15]

The BOP reagent has been found to be widely applicable and gives excellent yields However, the byproduct, hexamethylphosphoramide (HMPA) is very toxic Therefore, derivatives of the BOP reagent have been developed to avoid these problems For example reagents like PyBOP and the uronic salt *O*-benzotriazolyl bis-(dimethylamino)uromum tetrafluoroborate (TBTU) (Figure 2 11) are seen a likely candidates to replace BOP [14 16]

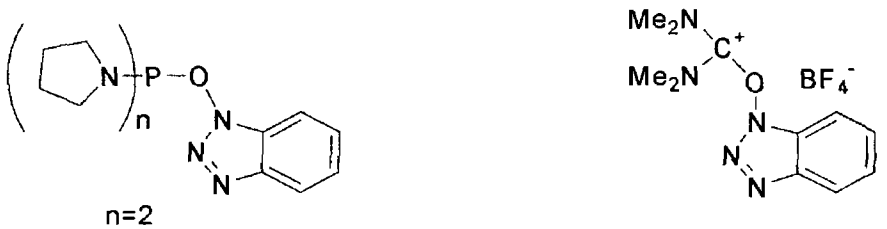

Fig 2 11 The phosphonium (PyBOP) and uronic (TBTU) coupling reagents

2 3 1 3 Active esters

Attempts to use aminolysis for peptide synthesis were first made in the early days of peptide synthesis [13] These attempts were generally unsuccessful Subsequently, it was realized that the reaction would be facilitated by the use of more efficient ester leaving groups Hence, a variety of 'active esters' have been developed and investigations have been carried out to establish their utility [13]

Active esters are generally introduced onto an amino protected amino acid/peptide using the DCC/HOBt protocol The attraction of this method lies in the fact that few byproducts are generated and as there is no base present, racemization is not so much of a problem In addition, the ease in which some of the byproducts may be removed is a factor that may influence their use For example, for a water insoluble protected peptide, a succinimido ester coupling is especially convenient as *N*-hydroxysuccinimide is very water soluble, similarly, for water soluble peptides, a halophenyl ester may be appropriate as they are ether soluble

2 3 1 4 Carbodiimides

Carbodiimides have become very important reagents for the synthesis of peptides ever since Sheehan and Hess reported their synthetic results in 1955 [17 18] Their experimental results showed DCC to be a very effective coupling reagent and it has since become and remained one of the most important coupling reagents available [19]

DCC operates by converting the carboxylic acid group into a reactive acylating agent, which undergoes further nucleophilic acyl substitution with the amine (Figure 2 12) The first activating step is the nucleophilic attack of the carboxylate group on the carbon of the carbodnmide function to yield an *O*-acylisourea The highly reactive *O*-acylisourea can undergo aminolysis by the nucleophilic attack of the amine on the carbonyl carbon leading to the formation of the amide and the dialkylurea byproduct Alternatively, another carboxylic acid function can react with the *O*-acylisourea intermediate forming an amino acid anhydride intermediate [20 21] This is also a potent alkylating agent and can react with the amino component leading to amide bond formation

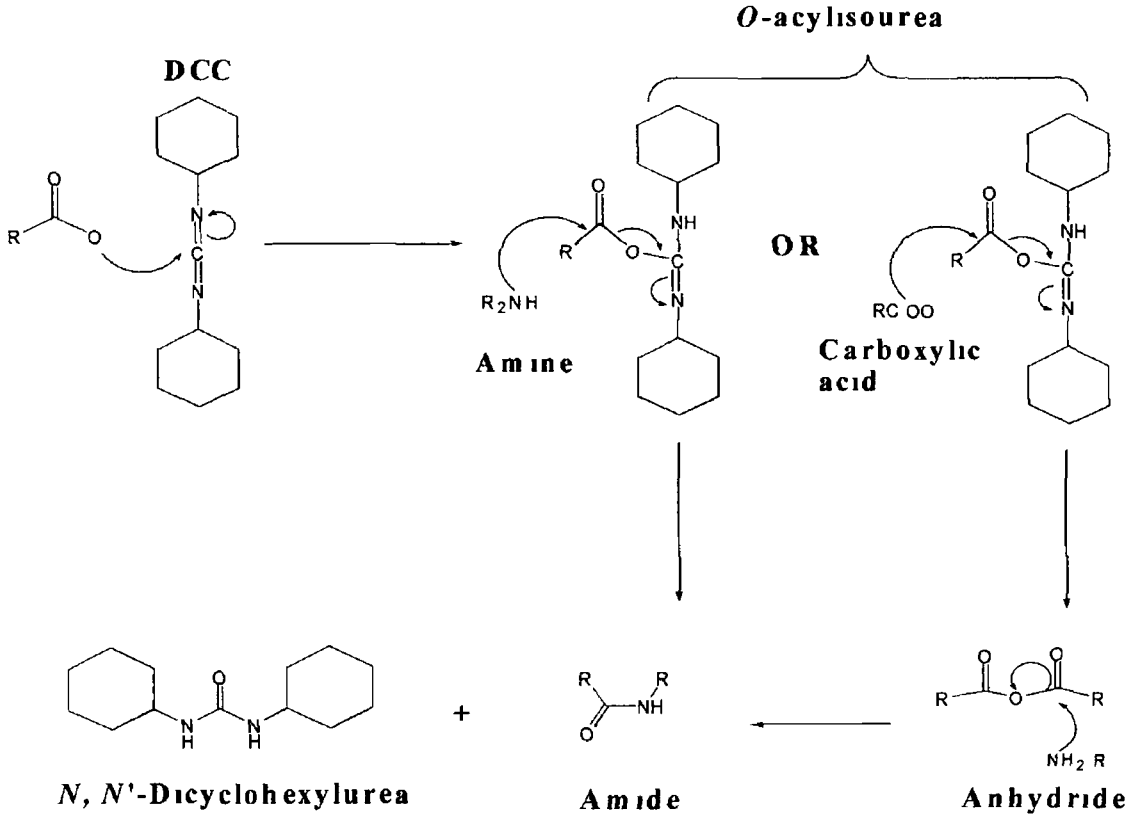

Fig 2 12 The mechanism of the synthesis of amide bonds using DCC

However, there are problems associated with this reaction The byproduct *N,N'*-dicyclohexylurea (DCU) is slightly soluble in dichloromethane and chloroform and often recrystallization and column chromatography are necessary to purify the product Intermediates that occur whilst using the DCC protocol are very reactive, and side reactions can interfere with yields and the purity of the product [13 19] Racemization can occur with susceptible carboxy components *via* a route schematically depicted in Figure 2 13 This happens when the reactive intermediate produced during the coupling reaction contains a basic centre, which causes an intramolecular proton transfer from the chiral carbon atom This results in rehybridization from sp^3 to sp^2 (a geometrically planar part of a molecule) and therefore, when the proton returns to its original position, racemization occurs due to the fact that it is equally likely to return to either face of the planar, sp^2 hybridized part of the molecule [19]

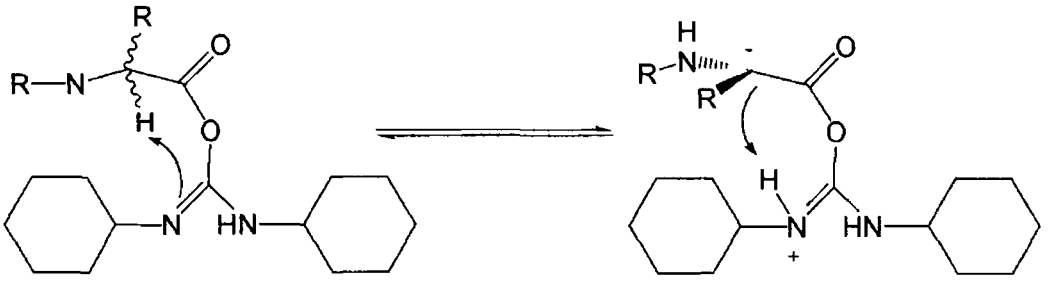

Fig 2 13 The process of proton exchange between chiral carbon and basic centre [19]

Furthermore, the collapse of the *O*-acylisourea by intramolecular acyl transfer to *N*-acylurea competes significantly with the desired attack from external nucleophiles (Figure 2 14) When this rearrangement occurs, the more inert *N*-acylurea is formed The formation of this by-product not only causes a reduction in yield, but also causes purification problems as its polarity tends to be almost identical to the required product [19]

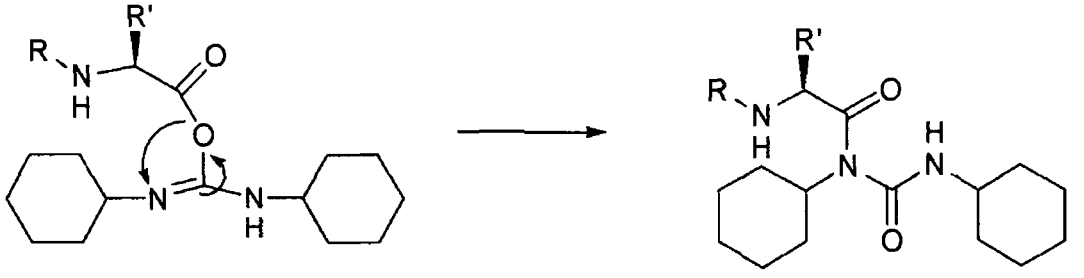

***O*-acylisourea** ***N*-acylurea**

Fig 2 14 The *O* to *N*-acyl transfer rearrangement [19]

The problems that are encountered when using DCC can be eradicated using an auxiliary nucleophile like 1-hydroxybenzotriazole (HOBt) [22] This compound carries out its function by reacting very quickly with the *O*-acylisourea (thereby shortening the lifetime of the intermediate, before undesirable side reactions can intervene) An acylating agent of lower potency is formed which is still reactive with respect to aminolysis, but is less prone to racemization or to other side reactions (Figure 2 15) [13 14]

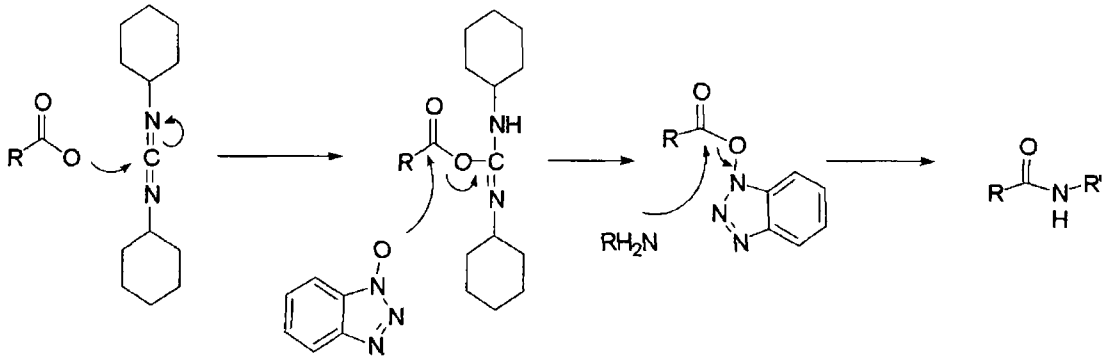

Fig 2 15 The participation of HOBt during the synthesis of an amide bond using the DCC protocol

Other carbodiimide reagents have been developed to avoid the difficulties encountered when trying to remove the final traces of DCU from the product For example, 1-{3-(dimethylammo)propyl}-3-ethylcarbodiimide (EDC) is increasingly employed as a coupling reagent The main attraction of EDC stems from the fact that it produces a water soluble urea byproduct, and any remaining traces of the 1-{3-(dimethylamino)propyl}-3-ethyl urea can be completely removed by using a dilute acid washing procedure [23]

2 4 The synthesis of *N*-{*para*-(ferrocenyl)benzoyl} amino acid alcohol derivatives

Reduction of the *N*-{*para*-(ferrocenyl)benzoyl} ammo acid ester derivatives to the corresponding *N*-{*para*-(ferrocenyl)benzoyl} amino acid alcohol using sodium borohydride and lithium chloride was also achieved for glycine, L-alanine, L-leucine and L-phenylalanine (Figure 2 16) Lithium chloride (LiCl) was employed to facilitate the reduction reaction [24] The respective yields of this reaction ranged from 59-65% and are summarized in Table 2 1

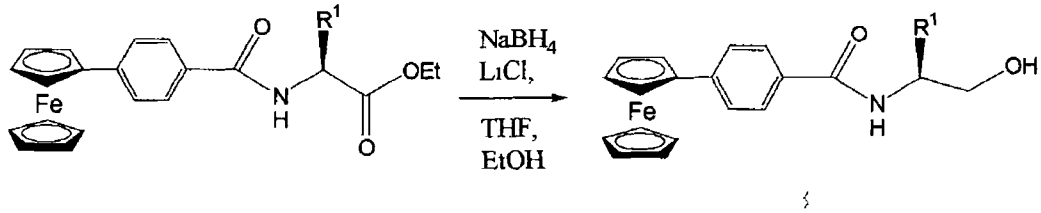

Fig 2 16 The reduction of *N*-{*p*ara-(ferrocenyl)benzoyl} ammo acid ethyl ester to the corresponding alcohol

2 5 The general structures of the *N*-(ferrocenyl)benzoyl amino acid derivatives

When the different amino acids *i e* glycine, L-alanine, L-leucine, L-phenylalanine, ±2-aminobutyric acid, β-alanine, 4-aminobutyric acid and isoaminobutyric acid are coupled to *ortho*-, *meta*- or *para*-ferrocenyl benzoic acid *via* the procedure outlined in Figure 2 17 the resultant product adopts one of the four general structures i-iv The yields for the reaction between ferrocenyl benzoic acid and the respective amino acid ester derivatives ranged between 40 and 68% and are summarized in Table 2 1

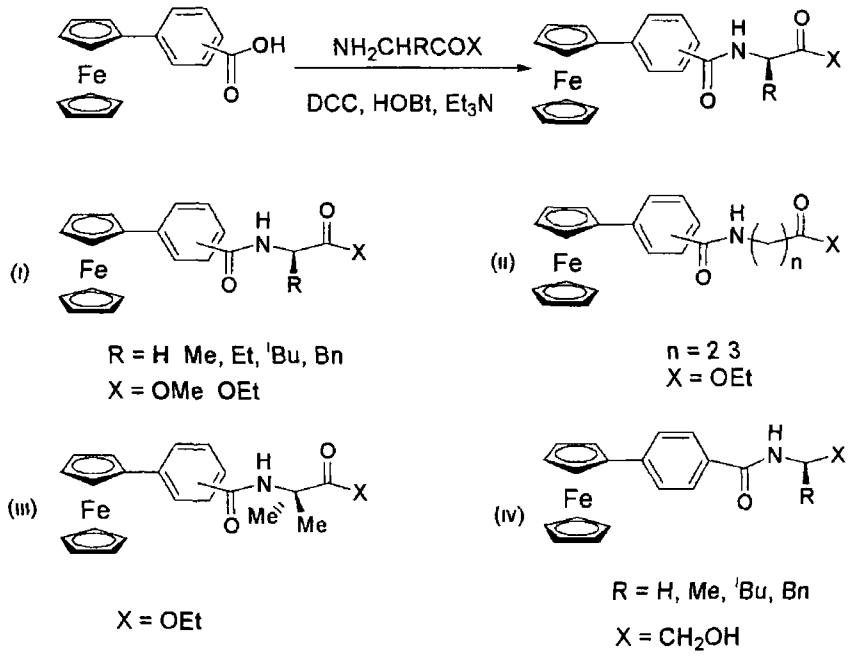

Fig 2 17 The reaction scheme and general structures (i)-(iv) for the *ortho*-, *meta*- and *para*- *N*-(ferrocenyl)benzoyl amino acid derivatives

(i) Represents the structures that include glycine (R = H), L-alanine (R = CH_3), L-leucine {R = $CH_2CH(CH_3)_2$}, L-phenylalanine (R = CH_2Ph) and ±2-aminobutyric acid (R = CH_2CH_3)

(ii) Represents the structures that incorporate β-alanine (n = 2) and 4-aminobutyric acid (n = 3)

(iii) Represents the structures that incorporate isoaminobutyric acid

(iv) The general structure of *N-para*-(ferrocenyl)benzoyl amino acid alcohol derivatives

Table 2 1 The *N*-(ferrocenyl)benzoyl amino acid derivatives

Compound	Gen structure	No	R	X	% yield
N-p-Fc-Bz gly-CO_2Me	I	**103**	H	OMe	52
N-p-Fc-Bz-L-ala-CO_2Me	I	**104**	Me	OMe	40
N-p-Fc-Bz-L-leu-CO_2Me	I	**105**	^tBu	OMe	40
N-p-Fc-Bz-L-phe-CO_2Me	I	**106**	Bn	OMe	45
N-p-Fc-Bz gly-CO_2Et	I	**107**	H	OEt	58
N-p-Fc-Bz-L-ala-CO_2Et	I	**108**	Me	OEt	58
N-p-Fc-Bz-L-leu-CO_2Et	I	**109**	^tBu	OEt	64
N-p-Fc-Bz-L-phe-CO_2Et	I	**110**	Bn	OEt	60
N-p-Fc-Bz-β-ala-CO_2Et	II	**111**	$(CH_2)_2$	OEt	52
N-p-Fc-Bz-4-aminobutyric-CO_2Et	II	**112**	$(CH_2)_3$	OEt	55
N-p-Fc-Bz ±2-aminobutyric-CO_2Et	I	**113**	Et	OEt	55
N-p-Fc-Bz isoaminobutyric-CO_2Et	III	**114**	Me, Me	OEt	48
N-p-Fc-Bz gly-CH_2OH	IV	**115**	H	CH_2OH	65
N-p-Fc-Bz-L-ala-CH_2OH	IV	**116**	Me	CH_2OH	62
N-p-Fc-Bz-L-leu-CH_2OH	IV	**117**	^tBu	CH_2OH	61
N-p-Fc-Bz-L-phe-CH_2OH	IV	**118**	Bn	CH_2OH	59
N-m-Fc-Bz gly-CO_2Me	I	**121**	H	OMe	59
N-m-Fc-Bz-L-ala-CO_2Me	I	**122**	Me	OMe	61
N-m-Fc-Bz-L-leu-CO_2Me	I	**123**	^tBu	OMe	62
N-m-Fc-Bz-L-phe-CO_2Me	I	**124**	Bn	OMe	56
N-m-Fc-Bz-β-ala-CO_2Et	II	**125**	$(CH_2)_2$	OEt	68
N-m-Fc-Bz-4-aminobutyric-CO_2Et	II	**126**	$(CH_2)_3$	OEt	61
N-m-Fc-Bz ±2-aminobutyric-CO_2Et	I	**127**	Et	OEt	55
N-m-Fc-Bz isoaminobutyric-CO_2Et	III	**128**	Me, Me	OEt	55
N-o-Fc-Bz gly-CO_2Et	I	**131**	^tBu	OEt	62
N-o-Fc-Bz-L-ala-CO_2Et	I	**132**	Me	OEt	60
N-o-Fc-Bz-L-leu-CO_2Et	I	**133**	^tBu	OEt	64
N-o-Fc-Bz-L-phe-CO_2Et	I	**134**	Bn	OEt	68
N-o-Fc-Bz-β-ala-CO_2Et	II	**135**	$(CH_2)_2$	OEt	59
N-o-Fc-Bz-4-aminobutyric-CO_2Et	II	**136**	$(CH_2)_3$	OEt	62
N-o-Fc-Bz ±2-aminobutyric-CO_2Et	I	**137**	Et	OEt	55

Footnote Compounds **101**, **102**, **119**, **120**, **129** and **130** are starting materials and hence, are not included in Table 2 1

2 6 ^{1}H NMR studies of *N*-(ferrocenyl)benzoyl amino acid derivatives

In the ^{1}H NMR spectra of the *N*-(ferrocenyl)benzoyl amino acid ethyl esters the aromatic signals varied depending on whether the *ortho, meta,* or *para-N*-(ferrocenyl)benzoic acid was used as the starting material For the *ortho* derivative, a doublet, triplet, triplet, doublet pattern is typically observed, with each peak integrating for one proton The *meta* derivative gives an aromatic peak pattern, which consists of a singlet, two doublets and a triplet with all peaks integrating for one proton each The pattern of the aromatic region for *para* derivatives is very distinctive, with two sets of doublets, both signals integrating for two protons each

The chemical shift of the amide proton depends greatly on the type of deuterated solvent used When the spectra were obtained in $CDCl_3$, the amide proton peaks appear between δ 5 8 and 6 83, however when d_6-DMSO was employed the amide proton peaks were shifted downfield to appear in the range δ 7 98 to 9 02 This shift is attributed to a hydrogen bond interaction between the amide proton and the polar S=O bond in the sulfoxide group of d_6-DMSO $CDCl_3$ however, does not have the same ability to form hydrogen bonds with the amide proton as d_6-DMSO and hence their signals appear in a relatively upfield position

The ^{1}H NMR spectra showed three peaks in the ferrocenyl region characteristic of a monosubstituted ferrocenyl derivative with the peaks typically appearing between δ 3 77 and 4 90 These signals are as a result of the presence of the *ortho* hydrogens on the cyclopentadienyl (η^5-C_5H_4) ring, which appear in the range δ 4 53 to 4 90, the *meta* hydrogens on the (η^5-C_5H_4) ring (δ 4 17-4 47), and the hydrogens of the (η^5-C_5H_5) ring (δ 3 77 to 4 06) The peaks due to the *ortho* and *meta* protons of the (η^5-C_5H_4) ring can appear either as fine triplets with coupling constants in the range 1 6-2 Hz, or as singlets with both signals integrating for two protons The (η^5-C_5H_5) ring in all cases appears as a singlet

Table 2 2 Selected ^{1}H NMR data (δ) for the *N*-(ferrocenyl)benzoyl amino acid derivatives

Compound No	NH	αH	$(\eta^5\text{-}C_5H_4)^{ortho}$	$(\eta^5\text{-}C_5H_4)^{meta}$	$(\eta^5\text{-}C_5H_5)$
103	8 88	n/a	4 85	4 38	3 98
110	8 8	4 54-4 68	4 88	4 41	4 02
115*	6 6	n/a	4 71	4 39	4 04
124	8 91	4 46-4 51	4 83-4 86	4 39-4 44	4 01
127	8 73	4 35	4 87	4 36	4 04
133	8 69	4 30-4 36	4 6	4 28, 4 12	4 05

* All NMR experiments were conducted in d_6-DMSO except in the case of compound **115** which was conducted in $CDCl_3$

2.6 1 ^{1}H NMR study of *N*-{*ortho*-(ferrocenyl)benzoyl}-L-alanine ethyl ester (132)

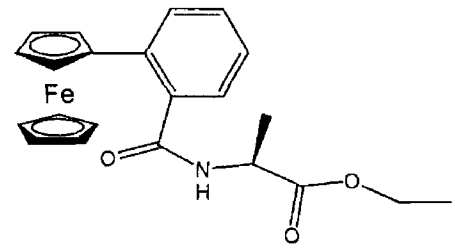

Fig 2 18 *N*-{*ortho*-(ferrocenyl)benzoyl}-L-alanine ethyl ester (**132**)

The ^{1}H NMR spectrum of *N*-{*ortho*-(ferrocenyl)benzoyl}-L-alanine ethyl ester was acquired in d_6-DMSO and hence, gave an amide peak at the relatively downfield position of δ 8 75 The signal due to the amide proton appears as a doublet due to coupling with the α-hydrogen The splitting pattern for the *ortho*-disubstituted phenyl ring is seen as a doublet at δ 7 79, a triplet at δ 7 41 that integrates for one proton, and a multiplet that occurs between δ 7 11 and δ 7 26 that integrates for two protons The *meta* and *ortho* peaks of the $(\eta^5\text{-}C_5H_4)$ ring appear as broad doublets at δ 4 27 and δ 4 63 respectively A characteristic singlet due to the unsubstituted $(\eta^5\text{-}C_5H_5)$ ring appears at δ 4 03 The α-hydrogen, integrating for one proton, appears as a quintet at δ 4 36 This splitting pattern can be attributed to its position beside both the amide proton and the methyl group of alanine The signal due to the L-alanine methyl group appears as a doublet at δ 1 31 The characteristic ethyl ester signals appear as a triplet and a quartet at δ 1 23 and δ 4 12, respectively

2 6 2 ^{1}H NMR study of *N*-{*meta*-(ferrocenyl)benzoyl}-L-alanine methyl ester (122)

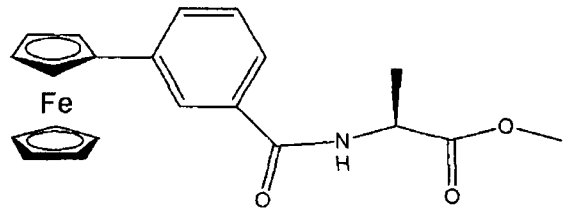

Fig 2 19 *N*-{*meta*-(ferrocenyl)benzoyl}-L-alanine methyl ester (**122**)

The ^{1}H NMR spectrum of *N*-{*meta*-(ferrocenyl)benzoyl}-L-alanine methyl ester was obtained in d_6-DMSO and hence, gave an amide peak at the relatively downfield field position of δ 8 85 and appears as a doublet due to coupling with the α-hydrogen The characteristic splitting pattern for the *meta*-disubstituted phenyl group with two different substituents is seen as a singlet at δ 7 98, a multiplet that integrates for two protons between δ 7 76 and δ 7 73 and a triplet at δ 7 41 that integrates for one proton The typical mono-substituted ferrocenyl pattern comprises two fine triplets that occur at δ 4 39 and δ 4 86 respectively while the singlet that integrates for five protons appears at δ 4 03 is due to the unsubstituted (η^5-C_5H_5) ring The α-hydrogen, which appears as a multiplet in the range δ 4 50-4 59, integrates for one proton The characteristic methyl ester signal appears as a singlet at δ 3 66 and integrates for three protons The L-alanine methyl group is coupled to the α-hydrogen and appears as a doublet at δ 1 44 with a coupling constant of 7 6 Hz

2 6.3 ^{1}H NMR study of *N*-{*para*-(ferrocenyl)benzoyl}-L-alanine ethyl ester (108)

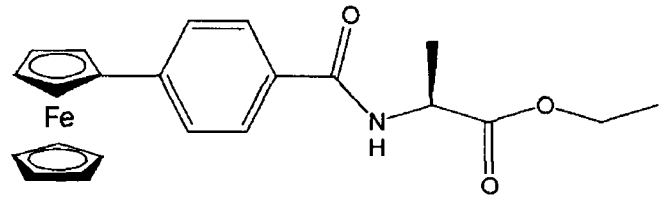

Fig 2 20 *N*-{*para*-(ferrocenyl)benzoyl}-L-alanine ethyl ester (**108**)

The ^{1}H NMR spectrum for *N*-{*para*-(ferrocenyl)benzoyl}-L-alanine ethyl ester (Figure 2 21) was obtained in d_6-DMSO and hence, gave an amide peak at δ 8 47 that appears as a doublet due to coupling with the α-hydrogen The characteristic splitting pattern for the

para-disubstituted benzene ring is seen as two doublets, both of which integrate for two protons at δ 7 38 and δ 7 56 respectively The ferrocenyl region comprises of two fine triplets that occur at δ 4 17 and δ 4 65 respectively while the large singlet that integrates for 5 protons due to the unsubstituted (η^5-C_5H_5) ring appears at δ 3 77 The α-hydrogen appears as a multiplet in the range δ 4 41-4 48 and integrates for one proton The L-alanine methyl group is coupled to the α-hydrogen and appears as a doublet at δ 1 48 with a coupling constant of 7 6 Hz The ethyl ester signals appear as a triplet and a quartet at δ 1 21 and δ 4 12 respectively

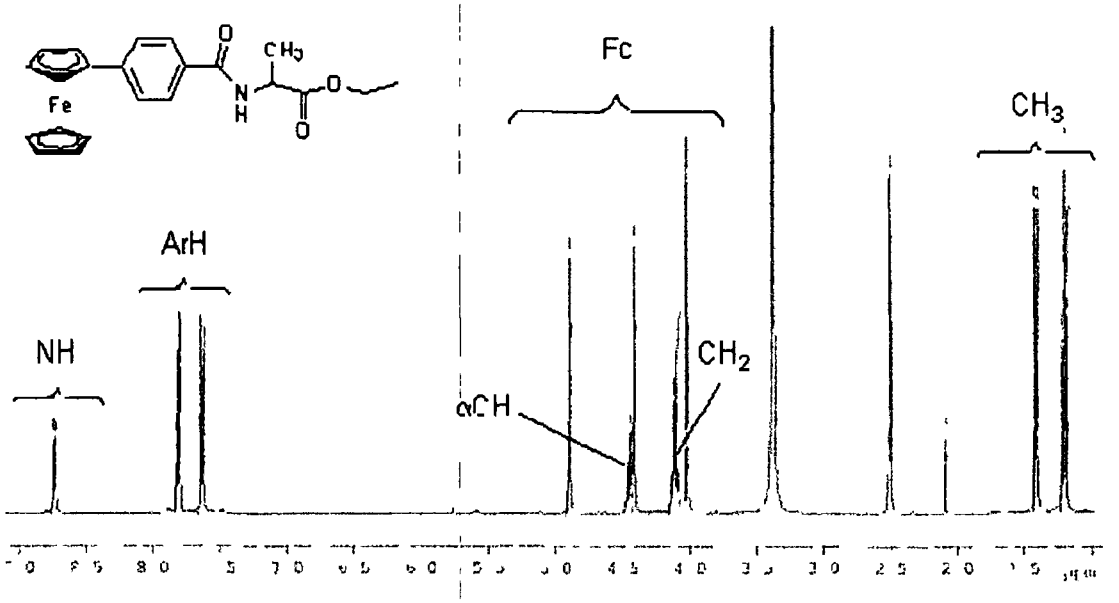

Fig 2 21 The ^{1}H NMR spectrum of *N*-{*para*-(ferrocenyl)benzoyl}-L-alanine ethyl ester (**108**)

2 6 4 ^{1}H NMR study of *N*-{*para*-(ferrocenyl)benzoyl}-L-alaninol (116)

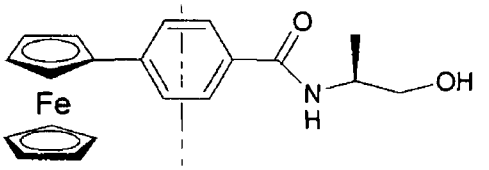

Fig 2 22 *N*-{*para*-(ferrocenyl)benzoyl}-L-alaninol (**116**)

The ^{1}H NMR spectrum of *N*-{*para*-(ferrocenyl)benzoyl}-L-alaninol (**116**) was acquired in d_6-DMSO and hence, the amide peak appeared as a doublet (due to coupling with the α-hydrogen) at the relatively downfield position of δ **8** 12 The characteristic splitting

pattern for the *para*-disubstituted phenyl ring is seen as two doublets at δ 7 66 and 7 84 respectively The *ortho* and *meta* peaks of the (η^5-C_5H_4) ring appear as singlets at δ 4 94 and δ 4 47 respectively The large characteristic singlet due to the unsubstituted (η^5-C_5H_5) ring appears at δ 4 08 The α-hydrogen, which integrates for one proton, appears as a multiplet in the range δ 4 76-4 85 This splitting pattern can be attributed to its position beside amide proton, the methylene group and methyl group of alanine The signal due to the methylene protons appears as a multiplet in the range δ 3 46-3 58 The peak due to the L-alanine methyl group appears as a doublet at δ 1 97 There was no signal corresponding to the hydroxyl proton and this may be attributed to proton-deuterium exchange with the solvent This spectrum provides evidence that the reduction procedure was successful as the characteristic ethyl ester peaks are not present

2 7 ^{13}C NMR and DEPT 135 study of the *N*-(ferrocenyl)benzoyl amino acid derivatives

A ^{13}C NMR and DEPT 135 study was carried out on all compounds synthesized In a DEPT 135 spectrum, methylene carbons appear as negative peaks *i e* appear below the resonance line, while methine and methyl carbons show up as positive peaks Carbonyl and quaternary carbons do not appear at all in a DEPT 135 spectrum [25]

In the ^{13}C spectra of these *N*-(ferrocenyl)benzoyl amino acid derivatives, the amide and ester carbonyl carbons appear at downfield positions usually between δ 166 0 and 175 4 In the aromatic region, depending on whether *ortho, meta* or *para*-(ferrocenyl) benzoic acid derivative is being used the number of peaks varies The *meta* and *ortho* derivatives both give rise to six aromatic peaks since none of the aromatic carbons are equivalent, however the *para* derivative only produces four signals (two peaks due to quaternary carbons and two peaks of roughly twice the intensity which are due to two carbons each) The aromatic quaternary carbons can be identified with the aid of DEPT 135 spectra (when compared to the conventional ^{13}C spectra as quaternary carbons disappear in the DEPT 135 spectra)

Signals due to the ferrocenyl protons appear between δ 67 0 and δ 85 7 The *ipso* carbon of the mono-substituted ferrocenyl group has a resonance in the range between δ 83 4 and 85 7 An intense peak at approximately δ 69 is attributed to the unsubstituted (η^5-C_5H_5) ring, and the signal due to the *meta* (η^5-C_5H_4) carbons generally overlaps with this peak

or appears in close proximity Slightly upfield at chemical shifts of the order of δ 66-68, the *ortho* carbons on the (η^5-C_5H_4) ring come into resonance

Since the DEPT 135 spectrum shows a negative peak at approximately δ 60-62 this peak can be assigned to the methylene carbon of the ethyl ester group The methyl carbon comes into resonance at approximately δ 14 as does the equivalent positive peak on the DEPT 135 spectrum

Table 2 3 Selected ^{13}C NMR data (δ) for *N*-(ferrocenyl)benzoyl amino acid derivatives

Compound No	C=O^1	C=O^2	(η^5-C_5H_4)^{ortho}	(η^5-C_5H_4)^{meta}	(η^5-C_5H_5)	(η^5-C_5H_4)^{ipso}
103	166 8	170 8	67	69 9	69 9	83 5
108	166 5	173 5	67	69 9	69 9	83 5
121	166 9	170 9	66 8	69 5	69 8	84 3
128	167 1	175 4	67	69 7	70 1	84 6
135	170 7	172 6	68 9	69 7	70 2	85 7
137	170 3	172 2	69	69 6	70 2	85 7

Footnote C=O^1, C=O^2 represent the chemical shifts for amide and ester carbonyls respectively

2 7 1 ^{13}C NMR and DEPT 135 study of *N*-{*ortho*-(ferrocenyl)benzoyl}-L-alanine ethyl ester (132)

The peaks at δ 172 9 and δ 169 8, respectively are due to the ester and amide carbonyl groups The *ortho*-disubstituted benzene ring, gives rise to six signals in the aromatic region The two quaternary carbons of the phenyl spacer group appear at δ 136 8 and 136 2, respectively, and do not appear in the DEPT 135 spectrum The four other aromatic peaks appear at δ 130 4, 129 2, 127 8 and 125 8, respectively The *ipso* carbon of the ferrocenyl group comes into resonance at δ 84 7 and is easily assigned as a quaternary carbon as it has no resonance in the DEPT 135 spectrum Upfield from the ferrocenyl *ipso* carbon signal, the (η^5-C_5H_5) ring appears at δ 69 8 while the signals due to the *meta* and *ortho* carbons appears at δ 69 6 and 68 6 respectively The methylene carbon of the ethyl ester carbon appears at δ 60 9 and gives a negative peak in the DEPT 135 spectrum while further upfield the α-carbon appears at δ 48 3 The methyl groups of the alanine sidechain and the ethyl ester are present at δ 17 and 14 5 respectively

2 7 2 ^{13}C and DEPT 135 NMR study of *N*-{*meta*-(ferrocenyl)benzoyl}-L-alanine methyl ester (122)

The ester carbonyl peak appears at δ 173 6 and the amide carbonyl appears at δ 166 5 The *meta*-disubstituted benzene ring gives rise to six signals The two quaternary carbons of the phenyl spacer group appear at δ 139 7 and 134 0, respectively, and show no signals in the DEPT 135 spectrum The four peaks at δ 129 4, 128 8, 125 4 and δ 124 7, respectively, are assigned as the four other aromatic carbons The methyl ester carbon appears at δ 52 3 while further upfield the α-carbon appears as a peak at δ 48 7 The chemical shifts of the ferrocenyl and L-alanine carbons are similar to those described for the *ortho* derivative in section 2 7 1

2.7.3 ^{13}C and DEPT 135 NMR study of *N*-{*para*-(ferrocenyl)benzoyl}-L-alanine ethyl ester (108)

The ester carbonyl peak appears at δ 173 2 and the amide carbonyl peak appears at δ 166 5 The *para*-disubstituted benzene ring, gives rise to four signals The peaks at δ 143 3 and 131 1 are assigned as the two quaternary carbons of the phenyl spacer group as there are no corresponding peaks on the DEPT 135 spectrum The two other peaks at δ 128 0 and 125 7 are assigned as the two sets of two equivalent aromatic carbons The chemical shifts of the ferrocenyl, L-alanine and the ethyl ester carbons are similar to those described for the *ortho* derivative in section 2 7 1 The ^{13}C and DEPT 135 spectra are presented in Figures 2 23 and 2 24 respectively

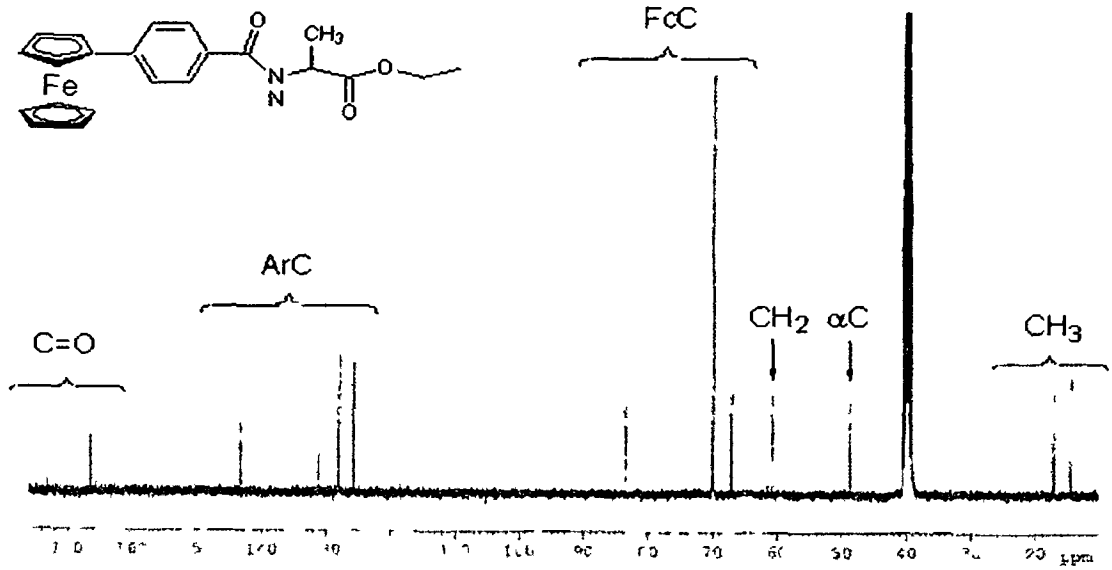

Fig 2 23 ^{13}C NMR spectrum of *N*-{*para*-(ferrocenyl)benzoyl}-L-alanine ethyl ester (108)

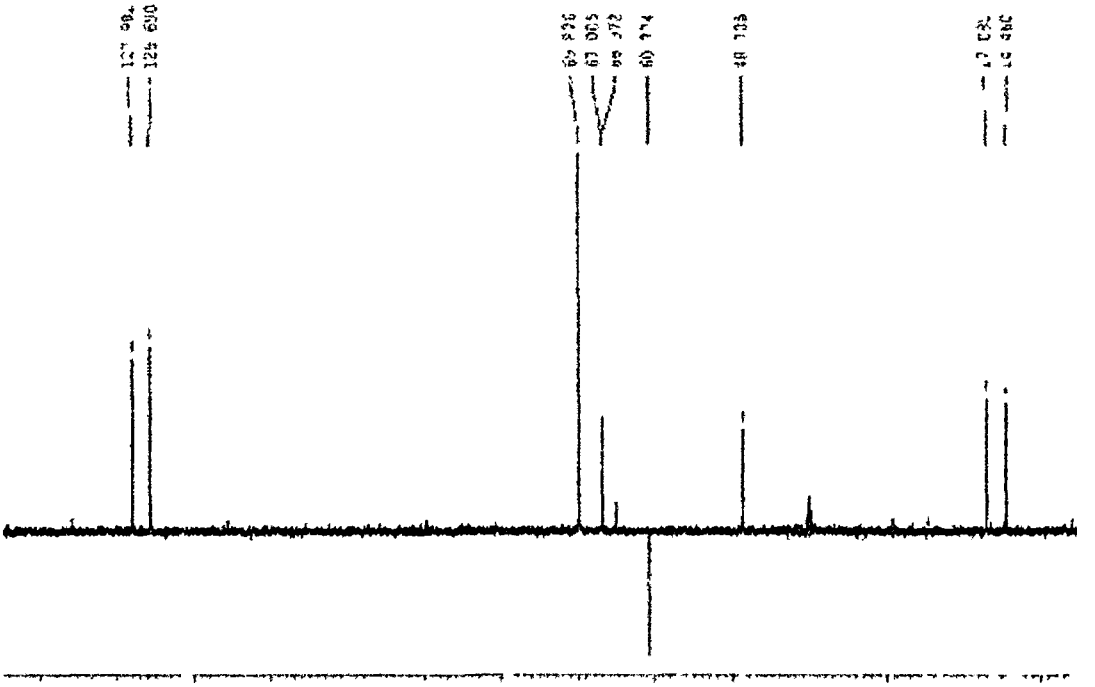

Fig 2 24 DEPT 135 spectrum of *N*-{*para*-(ferrocenyl)benzoyl}-L-alanine ethyl ester **(108)**

2 7 4 ^{13}C and DEPT 135 NMR study of *N*-{*para*-(ferrocenyl)benzoyl}-L-alaninol (116)

The amide carbonyl peak appears at δ 166 0 The *para*-disubstituted benzene ring gives rise to four signals The two quaternary carbons of the benzoyl spacer group appear at δ 142 7 and 132 1, respectively, and do not appear in the DEPT 135 spectrum The two other aromatic peaks appear at δ 127 1 and 125 2, respectively The *ipso* carbon of the ferrocenyl group comes into resonance at δ 85 7 and is easily assigned as a quaternary carbon as it has no resonance in the DEPT 135 spectrum Upfield from the ferrocenyl *ipso* carbon signal, the (η^5-C_5H_5) ring appears at δ 69 3 while the signals due to the *meta* and *ortho* carbons appears at δ 69 2 and 66 4, respectively The methylene carbon appears at δ 65 3 and gives a negative peak in the DEPT 135 spectrum while further upfield the peak due to the α-carbon appears at δ 47 5 The methyl group of the L-alanine sidechain appears at δ 16 2

2 8 HMQC study of *N*-{*para*-(ferrocenyl)benzoyl}-L-alanine methyl ester (104)

HMQC (Heteronuclear Multiple Quantum Coherence) is a 2D NMR technique used to facilitate the complete assignment of proton and carbon spectra and hence total structure elucidation can be achieved HMQC is a C-H correlation method that is frequently used to resolve the overlapping proton signals in complex structures [25] Since this technique correlates carbons and associated protons, no signals are observed for carbonyl or quaternary carbon atoms These spectra yield such useful information so as to remove many ambiguities regarding the structure of the compound that is being characterized The structure and HMQC spectrum of *N*-{*para*-(ferrocenyl)benzoyl}-L-alanine methyl ester is shown in Figures 2 25 and 2 26 respectively

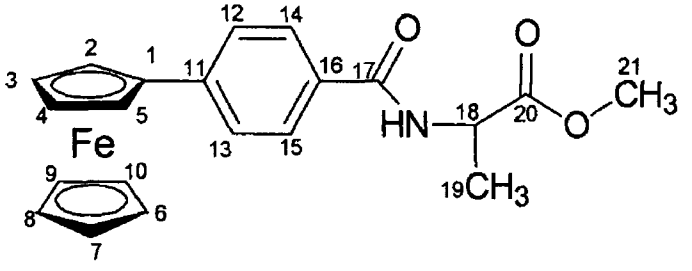

Fig 2 25 Structure of *N*-{*para*-(ferrocenyl)benzoyl}-L-alanine methyl ester (**104**)

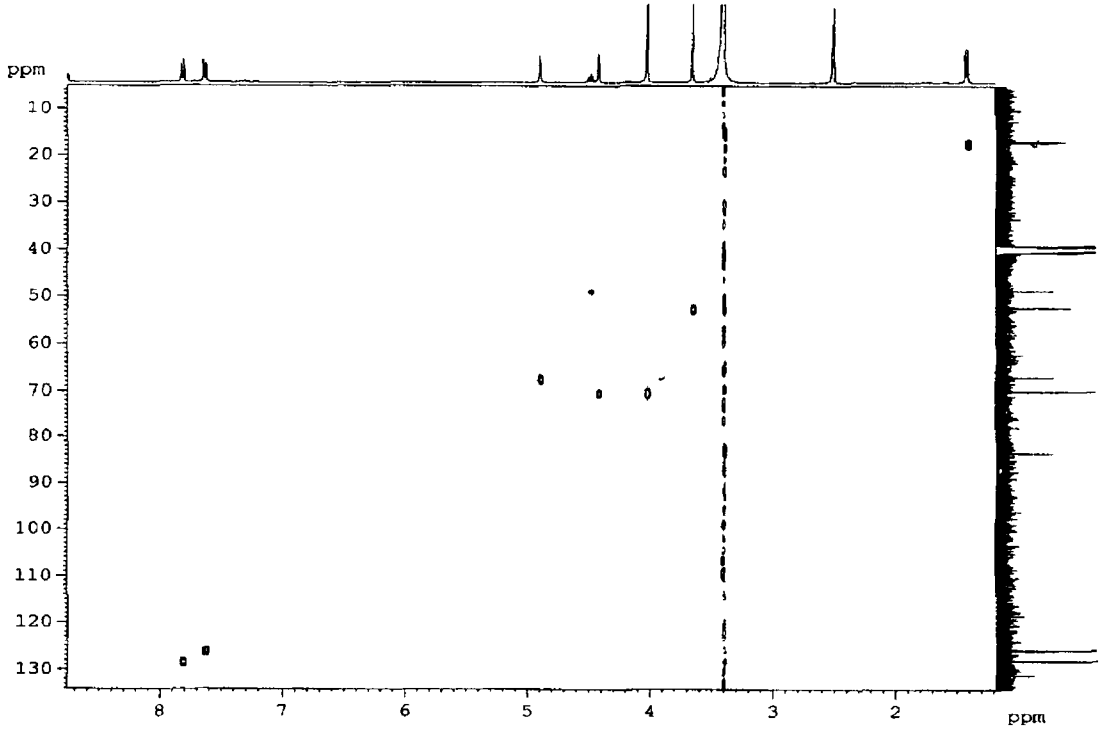

Fig 2 26 HMQC spectrum of *N*-{*para*-(ferrocenyl)benzoyl}-L-alanine methyl ester (**104**)

Table 2 4 HMQC data for *N*-{*para*-(ferrocenyl)benzoyl}-L-alanine methyl ester (**104**)

site	^{1}H	^{13}C	HMQC
1		83 5	
2, 5	4 9		67
3, 4	4 42		69 9
6 to 10	4 02		69 9
11		143 3	
12, 13	7 63		125 7
14, 15	7 81		128
16		131	
17		166 5	
18	4 46		48 6
19	1 41		17 1
20		173 7	
21	3 66		52 2

2 9 Infra red studies of the *N*-(ferrocenyl)benzoyl amino acid derivatives

Infra red (IR) spectroscopy is a spectroscopic method by which many functional groups can be identified Compounds can absorb IR radiation and hence various molecular vibrations are induced *e g* stretching, bending, rocking, etc These localized vibrations are very useful for the identification of key functional groups [25]

IR spectra are usually scanned from 600 to 4000 cm^{-1} The region above 1500 cm^{-1} usually provides the most informative data *i e* the characteristic absorbances associated with specific functional groups, while the region below 1500 cm^{-1} (*i e* the fingerprint region) contains very many peaks and hence, is of much less diagnostic value Often many of the peaks that appear in the region below 1500 cm^{-1} do not correspond to any fundamental vibration and are caused by overtone, combination or difference bands (which occur as a result of the interaction of two or more vibrations) and for this reason the fingerprint region is not often used to assign functional groups

The IR spectra of these compounds were obtained in potassium bromide The spectra of these compounds will typically show two bands between 3460 and 3400 cm^{-1} These bands are representative of secondary amide N-H groups, however, upon hydrogen bonding or if the sample is in the solid state these N-H groups will appear at a lower wavelength The appearance of two bands can be ascribed to two types of amide

absorptions *i e* amide I and amide II (Fig 2 27) Hydrogen bonding lowers and broadens N-H stretching frequencies albeit to a lesser degree than is the case with O-H groups as the intensity of the N-H absorption is usually less than that of O-H absorptions

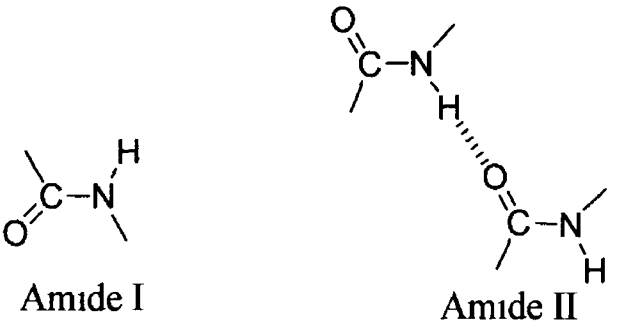

Fig 2 27 Configuration of amides giving rise to two bands in the IR spectrum

It is usual to observe the amide carbonyl (amide I) stretches between 1695 and 1680 cm^{-1} [21] Around 1540 cm^{-1}, N-H (amide II) bending usually occurs The ester carbonyl band usually appears between 1750 and 1735 cm^{-1} An IR spectrum can also give information about the substitution pattern on a benzene ring Six membered rings systems such as benzene produce bands in the 1600-1500 cm^{-1} and hence sometimes constitute a valuable identification for such a system Further bands due to aryl rings are present in the fingerprint region between 1225 and 950 cm^{-1} but are of little diagnostic value 'Out of plane' C-H bending vibrations produce a group of bands below 900 cm^{-1} The number of adjacent hydrogens determines the frequency of the C-H out-of-plane vibration and hence the frequency is a means of determining the substitution pattern For example, as an *ortho* disubstituted benzene ring has four adjacent hydrogens, it shows a band between 735 and 770 cm^{1} The *meta* disubstituted ring has three adjacent hydrogens and it shows a band between the frequencies of 750 and 810 cm^{-1}, while the *para* disubstituted benzene has only two adjacent hydrogens and it shows an absorbance between 860 and 800 cm^{1} However, in practice this peak assignment method is unreliable, as these bands, though strong, are not necessarily the strongest or even the only bands in that region, therefore assignments based on these criteria must be treated with caution [25]

Table 2 5 Selected IR values (cm^{-1}) for *N*-(ferrocenyl)benzoyl amino acid derivatives

Compound	N-H	$C=O^{amide}$	$C=O^{ester}$	Aryl C-H
107	3308	1685	1700	1560, 668
116	3326	1625	N/A	1560, 695
133	3324	1644	1744	1579, 1542, 692
136	3389	1647	1752	1542

2 10 UV-vis studies of *N*-(ferrocenyl)benzoyl amino acid derivatives

The visible and ultraviolet spectra of organic compounds are associated with transitions between electronic energy levels The transitions are generally between a bonding or a lone pair orbital and an unfilled non-bonding or anti-bonding orbital The wavelength of the absorption is then a measure of the separation of the energy levels of the orbitals concerned The most informative region in the UV-Vis range occurs from 300 nm, as this is where the excitation of electrons from *p*- and *d*-orbitals, π-orbitals and especially π-conjugated systems, gives rise to readily measured and informative spectra In the case of the compounds in this series, the visible region yields the most informative data The spectra of *ortho, meta* and *para* derivatives reflect this very clearly Of the three sets of derivatives, the *para* derivatives give the strongest absorptions in the visible region This is as a result of the benzene group lying roughly in the same plane as the (η^5-C_5H_4) group of ferrocenyl group This creates a larger conjugated entity *i e* chromophore, and as a rule, larger chromophores will give rise to stronger absorbances The *para* derivatives have local maxima at around 354 nm and at 453 nm, respectively The absorbance at 354 nm can be assigned to a π to π* transition of the phenylene spacer group This assertion is supported by the fact that such a transition is not observed in the *N*-ferrocenoyl series of compounds [26] The absorbance at 453 nm is attributed to a metal to ligand charge transfer band (MLCT) and is seen in the UV-Vis spectra of the *N*-ferrocenoyl compounds [26]

When comparing the corresponding values for the *ortho* and *meta* derivatives it is obvious that the absorbances are not as intense as is the case with the *para* systems and they typically appear at a shorter wavelengths The *meta* derivatives gives absorptions at around 329 nm and 446 nm, while the *ortho* derivative's local maxima are at 329 nm and 429 nm These values are consistent with the structures of the respective compounds and their decreasing degrees of conjugation *i e* the *para* derivatives display a much greater degree of co-planarity between the (η^5-C_5H_4) group and the phenyl ring system and hence

conjugation is more complete with respect to the *ortho* and *meta* derivatives However, the spectra of the *meta* and *ortho* analogues suggest that the substituted (η^5-C_5H_4) and phenyl groups do not lie in the same plane, hence presenting an increasing barrier to efficient conjugation

These absorbances also yield other interesting information Extinction coefficients are a function of how efficiently a chromophore absorbs UV or visible radiation The extent of conjugation therefore, is an important consideration The UV-vis spectrum shows a large disparity in the intensity of the absorbances between the *para* and the *ortho* and *meta* derivatives Since the *para* compounds are more conjugated than the *ortho* or *meta* derivatives, the bands in the visible region go from being fairly intense for the *para* compounds, to much less intense for the *ortho* and *meta* analogues Extinction coefficients are given by ε and can be calculated from the Beer-Lambert law *i e* A=εCl, where A is absorbance, C is concentration, l is the path length of the cell

In this UV-vis study, the spectra of all compounds were obtained at a concentration of 4 x 10^{-4} M

Table 2 6 Selected UV-vis data (nm) for *N*-(ferrocenyl)benzoyl amino acid derivatives

Compound no.	$\lambda_{max\,1}$(nm)	ε_1	λ_{max2}(nm)	ε_2
108	358	2670	454	860
116	356	2470	452	840
122	332	890	450	120
132	330	1130	450	290
133	334	1140	448	260
N*-Fc-A-COOEt	N/A	N/A	442	200

**N*-ferrocenoyl-L-alanine ethyl ester as prepared by Michael J Sheehy [26]

2 11 Mass spectrometric studies of the *N*-(ferrocenyl)benzoyl amino acids derivatives

Mass spectrometry (MS) enables the determination of the relative molecular mass of many different types of compounds and has been applied in many scientific fields and in industry [27]

Mass spectrometers can be divided into three fundamental parts, namely the ion source, the analyzer, and the detector The sample under investigation has to be introduced into

the ion source of the instrument Once inside the ion source, the sample molecules are ionized These ions are subsequently extracted into the analyzer region of the mass spectrometer where they are separated according to their mass (m) to charge (z) ratios (m/z) The mass spectrometer is maintained under high vacuum The separated ions are detected and these signals are processed by a data system where the m/z ratios are stored together with their relative abundance for presentation in the format of a mass spectrum [27] In this study, three MS techniques were employed, namely, Fast Atom Bombardment (FAB), Electrospray Ionization (ESI) and Matrix Assisted Laser Desorption Ionization (MALDI)

2.11 1 Fast Atom Bombardment Mass Spectrometry (FABMS)

Compounds **103-110** and **115-118**, were analysed by Fast Atom Bombardment Mass Spectrometry (FABMS) This soft ionization technique yields molecular mass information and in some cases structurally significant fragments ions are observed In FABMS, energy is provided by a beam of xenon (Xe) atoms of large translational energies When the fast xenon atoms impact into the solution of the sample in the matrix, the sample is desorbed (often as ions) by momentum transfer [27] Figure 2 28 depicts the impact of a fast Xe atom with the matrix/analyte mixture causing desorption and ionization

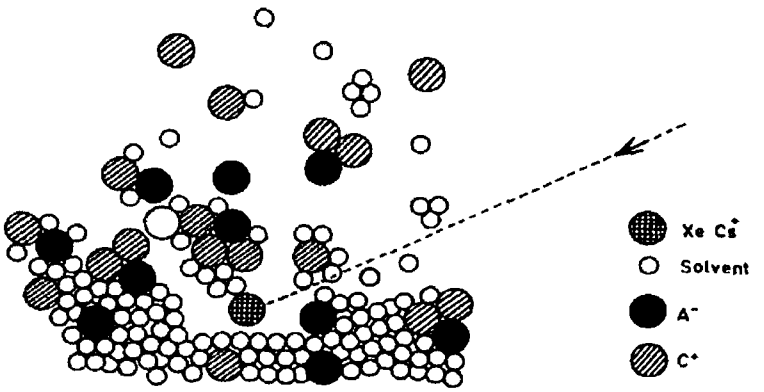

Fig 2 28 A schematic representation of the ionization process using FAB [28]

The plume of sample ions is then drawn into the mass analyser, the ions are separated according to their mass to charge ratio and the spectrum is generated The sample is usually dissolved in a matrix of low volatility Matrices commonly employed in FABMS include glycerol, 1-thioglycerol, 2-nitrophenyl octyl ether, triethanolamine and *meta*-nitro

benzyl alcohol [29] Often protonated oligomers of the matrix are desorbed along with the sample and may serve to mass mark the spectrum In this investigation *meta*-nitro benzyl alcohol (NBA) was employed as the liquid matrix [30]

Fig 2 29 The FAB spectrum of *N-para*-(ferrocenyl)benzoyl}-L-alaninol (**116**)

In the spectra of compounds **103-110** and **115-118** peaks appear at *m/z* 154, 307 and 460 etc which corresponds to protonated matrix (*meta*-nitrobenzyl alcohol) *i e* $[Mat + H]^+$, $[Mat_2 + H]^+$, $[Mat_3 + H]^+$ etc Examination of the mass spectra revealed the presence of intense radical-cation and an $[M + H]^+$ species Structurally important fragment ions were observed in the FAB mass spectra for all compounds analyzed

In the FAB mass spectrum for *N*-{*para*-(ferrocenyl)benzoyl}-L-alaninol (**116**) (Figure 2 29), a molecular radical cation species appears at *m/z* 363 A fragment ion is observed at *m/z* 289 and this signal corresponds to the ferrocenyl benzoyl fragment This peak also confirms the presence of the ferrocenyl benzoyl fragment at the *N*-terminus of the peptide The peak at *m/z* 261 is the same fragment less the carbonyl group The ion at *m/z* 289 is isobaric with an ion from the *meta*-nitrobenzyl alcohol $[Mat_2 + H]^+$-H_2O adduct Proof that the signal at *m/z* 289 is derived from the sample and not the matrix can be seen from the intense relative abundance when compared to the same ion observed from the neat matrix Addition of potassium iodide (KI) to the sample on a probe tip generated a signal of 39 mass units higher due to an $[M + K]^+$ adduct The fragment ions at *m/z* 289 and 261 were still present in the spectra, indicating the K^+ cation was co-ordinating at the *C* terminal moiety

2.11.2 Electrospray Ionization Mass Spectrometry (ESIMS).

Electrospray is a term that has come to refer to a small flow of liquid from a capillary needle when a potential difference is applied between the end of the capillary and a cylindrical electrode.[31] Under these conditions the sample leaving the capillary does not leave as a liquid but as a fine mist. The spray consists of droplets that are highly charged. These charges may be either positive or negative depending on the sign of the voltage applied to the capillary. Upon evaporation of the solvent droplets, a molecular ion of the sample molecule can be obtained in a desolvated state (Figure 2.30). These molecular ions are now carried into the ion analyzer by an electric field. The evaporation process produces either $[M+H]^+$ or $[M-H]^-$ adducts, and their generation promotes desolvation, as repulsive coloumbic forces become stronger than the cohesive forces of the droplet.

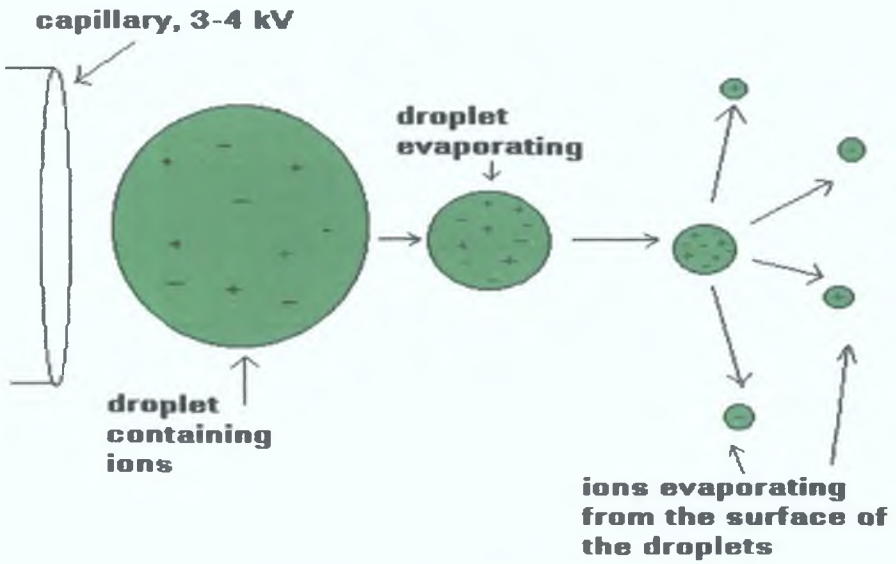

Fig 2.30 The process of desorption in electrospray.[32]

Electrospray ionization (ESI) is a particularly effective technique for the production of molecular ions from large polar molecules and it has also proved itself to be an invaluable tool in the analysis of large biopolymers as multiply charged ions are often produced (and mass spectrometry measures the mass to charge ratio).[33] ESI mass spectrometry was carried out on compounds **111**, **112** and **134**. Positive mode, negative mode, accurate mass and tandem MS data were obtained. The Micromass Q-TOF instrument was employed for these analyses.

The positive ion mode mass spectrum of the compound *N*-{*ortho*-(ferrocenyl)benzoyl}-L-phenylalanine-ethyl ester (**134**) shows an intense peak at *m/z* 481. The appearance of

this peak confirms the molecular mass of the compound and reveals the presence of a radical cationic species $[M]^{+\bullet}$ and an $[M+H]^+$ species at one mass unit higher Relatively intense peaks also appear at *m/z* 504 and 520 respectively The presence of these peaks can be attributed to sodium and potassium contamination of the sample (due to the use of both KOH and NaOH in the base hydrolysis of the ferrocene ethyl benzoate) Sodium and/or potassium cations may replace protons in the formation of positive ions during electrospray, yielding adducts of the form $[M + Na/K]^+$, which are separated from the fully protonated analogue, $[M+ H]^+$, by 22/38 mass units respectively

2 11 2 1 Tandem Mass Spectrometry (MS/MS)

Tandem mass spectrometry (MS/MS) is used to produce structural information from a compound by fragmenting specific sample ions inside the mass spectrometer and identifying the resulting fragment ions A tandem mass spectrometer is a mass spectrometer that has more than one analyzer, in practice usually two A collision cell (which functions by fragmenting the ions that were selected by the first analyzer) is positioned between the two analyzers

The first analyzer is used to select user specified sample ions arising from a particular component, usually the $(M+H)^+$ or $(M-H)^-$ ions These chosen ions pass into the collision cell, and are bombarded by the gas molecules, which cause fragment ions to be formed, and these fragment ions are analyzed according to their mass to charge ratios, by the second analyzer All the fragment ions arise directly from the precursor ions specified in the experiment, and thus produce a fingerprint pattern specific to the compound under investigation

This type of experiment is particularly useful for providing structural information concerning small organic molecules and for generating peptide sequence information

Positive mode tandem mass spectrometry (MS/MS) data was obtained for the compounds **111**, **112** and **134** In the MS/MS spectra of *N*-{*ortho*-(ferrocenyl)benzoyl}-L-phenylalanine ethyl ester (**134**) (Figure 2 31), a fragment ion is observed at *m/z* 416 This fragment ion is consistent with the loss of a (η^5-C_5H_5) ring from the ferrocenyl moiety The peaks that appear at *m/z* 370 and 342 respectively correspond with the loss of ethanol and subsequently a carbonyl moiety The suggested mechanism by which these fragment ions are formed is seen in Figure 2 32

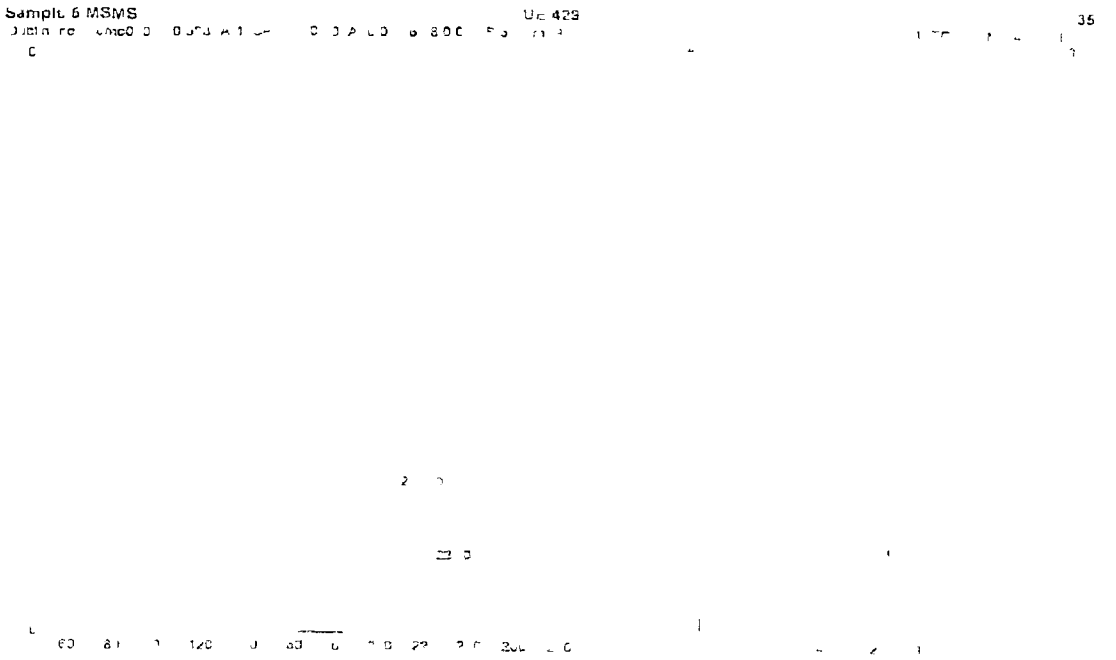

Fig 2 31 The MS/MS spectrum of *N*-{*ortho*-(ferrocenyl)benzoyl}-L-phenylalanine ethyl ester (**134**)

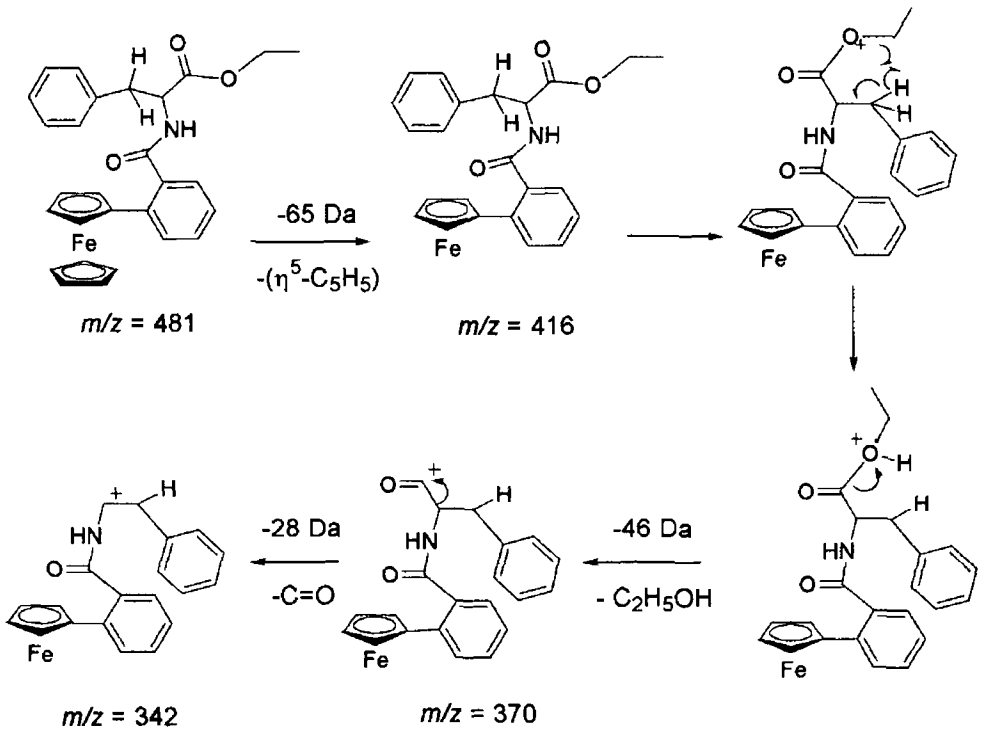

Fig 2 32 The proposed fragmentation pathway for the ions at *m/z* 416, 370 and 342 in the MS/MS spectra of *N*-{*ortho*-(ferrocenyl)benzoyl}-L-phenylalanine ethyl ester (**134**)

2 11 3 Matrix-Assisted Laser Desorption Ionization Time Of Flight Mass Spectrometry (MALDI-TOF MS)

During the last decade, matrix assisted laser desorption ionization (MALDI) has proved to be one of the most successful ionization methods for the mass spectrometric analysis of various compounds [34] MALDI allows for the vaporization and ionization of non volatile compounds from the solid phase directly into the gas phase [35]

As the term MALDI implies, matrices are employed in this mass spectrometry technique Matrices are small organic compounds that are co-crystallized with the analyte The matrix serves the purpose of absorbing the energy of the laser and hence, preventing decomposition of the compound being analyzed and this enables detection of intact molecules as large as one million Da Though it is not known how the matrix prevents the decomposition of the sample molecules, it is thought that since matrices are mostly acids, the transfer of a proton between the matrix and the analyte may play some part in promoting ionization Matrices are usually chosen with the nature of the analyte in mind For example, 3,5-dimethoxy-4-hydroxycinnamic acid or sinapinic acid (SA) is most commonly used for proteins of high mass, for peptides α-cyano-4-hydroxycinnamic acid (CHCA) is usually employed 2,5-Dihydroxy benzoic acid (DHA) is perhaps the most universal matrix as it can be used for proteins, peptides, glycoproteins, organic molecules, oligonucleotides and synthetic polymers [36] The matrix acts by mostly absorbing the energy arising from the laser and this minimizes the amount of sample damage that occurs Hence, MALDI is regarded as a soft ionization technique

Nitrogen lasers that operate at 337 nm are most commonly employed, as they are inexpensive and provide the most favorable combination of wavelength and power [37] The laser beam serves as the ionization and desorption source in MALDI Upon irradiation, part of the matrix/analyte mixture is vaporized (Figure 2 33) Ionization occurs by proton transfer between excited matrix molecules and analyte molecules both in the solid and gas phases It has also been reported that electron transfer as opposed to proton transfer occurs upon the application of the laser beam between the matrix and the ferrocene containing compounds [38] Once desorbed and ionized, the matrix plume carries the analyte into the analyzer

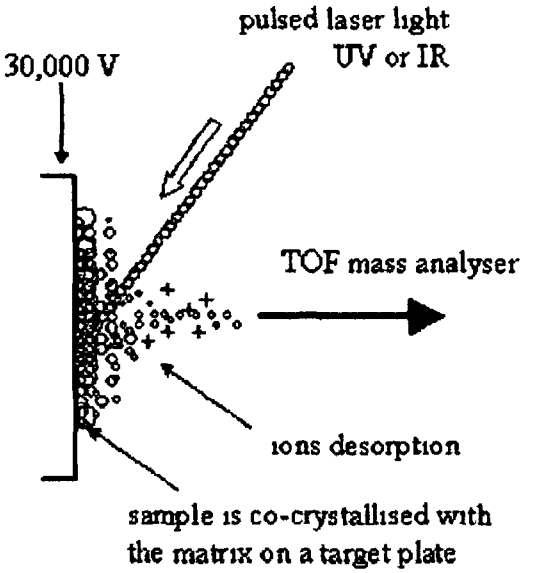

Fig 2 33 A schematic diagram of the ionization process in MALDI [39]

Time of flight (TOF) spectrometers are usually used in conjunction with the MALDI ionization technique These spectrometers work on the principle that all singly charged ions dropping through a potential difference V will acquire the same translational energy eV Hence, ions of smallest mass will have the highest velocities and they therefore have the shortest flight times The ions are accelerated by a potential difference between A and B (Figure 2 34) and subsequently pass into the field free flight tube They are separated in time, according to their m/z values and are collected at the mass detector D

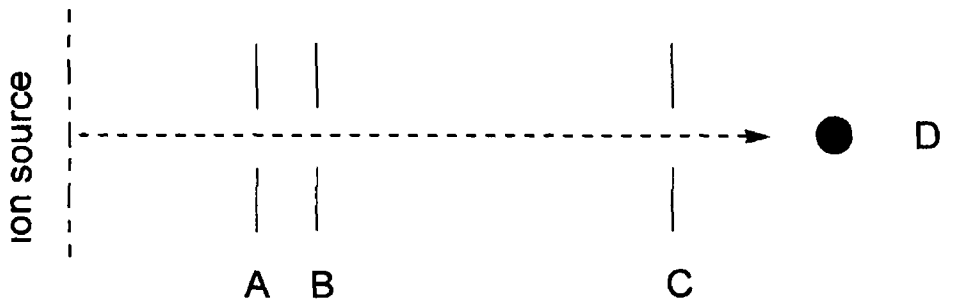

Fig 2 34 Schematic diagram of a TOF spectrometer

MALDI-TOF MS was carried out on compounds **111-114**, **121**, **123**, **125-128**, **131**, **132**, **and 135-138** Accurate mass data was also obtained All compounds analyzed gave spectra and molecular masses consistent with their respective structures

Three separate instruments *i e* a Bruker Ultraflex TOF-TOF, Applied Biosystems MALDI TOF and a Shimadzu AXIMA-CFR were used to obtain the required MS data Generally a matrix is required to facilitate the MALDI MS analysis of a sample and therefore, as a matter of routine dihydroxybenzoic acid (DHB) was employed as the matrix for MALDI MS using the Shimadzu AXIMA-CFR instrument However, analysis using the Bruker Q-TOF and Applied Biosystems instruments did not employ a matrix This is because ferrocene and hence, this series of ferrocenyl compounds are able to absorb the energy of the laser without decomposing and hence a matrix was thought to be superfluous to requirements

The mass spectrum of *N*-{*ortho*-(ferrocenyl)benzoyl}-β-alanine ethyl ester (**135**) (Figure 2 35) shows an intense peak corresponding to a molecular radical cation at *m/z* 405 This MS technique also generates $[M+H]^+$ species and this can be seen at *m/z* 406 The signal at *m/z* 340 confirms the loss of the (η^5-C_5H_5) fragment ion and this is typical behaviour for the spectra in the *ortho* series of compounds Similarly the $[M+H]^+$ minus the (η^5-C_5H_5) fragment is also seen at *m/z* 341 The $[M+Na]^+$ adduct is seen at *m/z* 428, 23 Da higher than the molecular ion peak

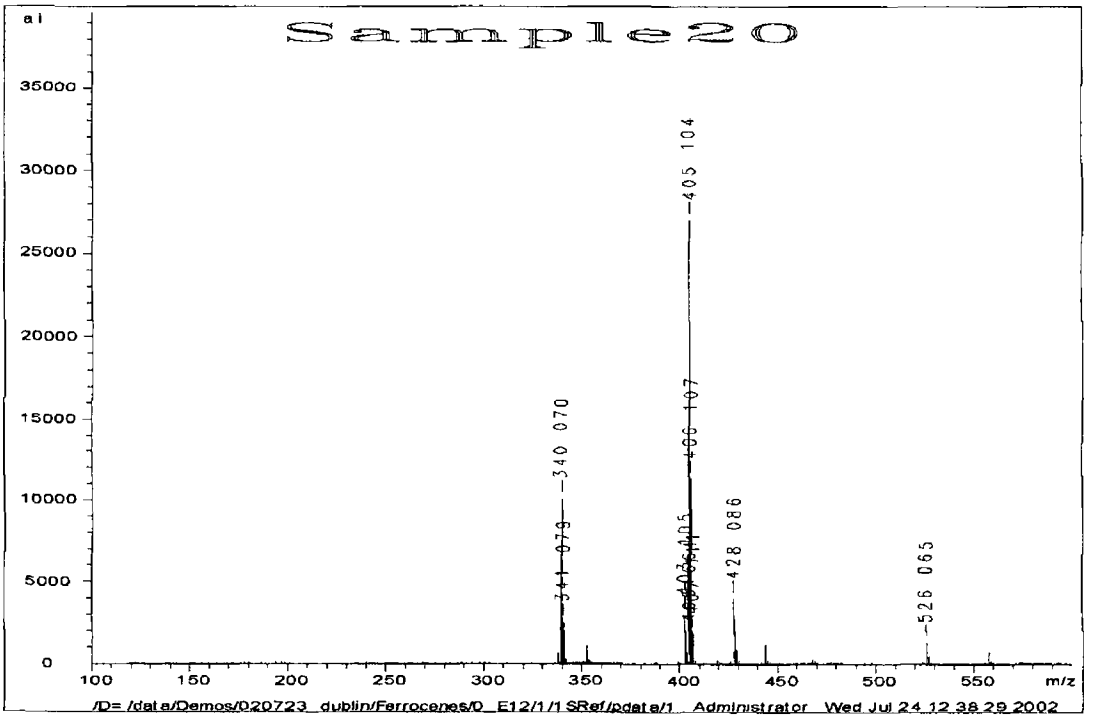

Fig 2 35 MALDI TOF spectrum of *N*-{*ortho*-(ferrocenyl)benzoyl}-β-alanine ethyl ester (**135**) (This spectrum was obtained by the Bruker TOF-TOF instrument)

2 12 X-ray crystallographic studies

Crystals are three dimensional ordered structures than can be described as a repetition of identical unit cells in three directions The unit cell is made up of the smallest possible volume that when repeated, is representative of the entire crystal The dimensions of a unit cell can be described with 3 edge lengths (a, b, c) and 3 angles (α, β, γ) The 3D location of atoms within a unit cell can be listed as their x, y, z Cartesian or fractional coordinates [40]

X-ray radiation is employed to determine the structure of crystals This is because in order for an object to be seen, its size needs to be at least half the wavelength of the light being used to see it Visible light has a wavelength much longer than the distance between atoms and therefore, it is ineffective in the acquisition of molecular crystal structures In order to obtain a definitive structure for a molecule, it is necessary to use a form of electromagnetic radiation whose wavelength is of the order of bond lengths and X-rays are ideal for such a task

Unfortunately, unlike with visible light, there is no known way to focus X-rays with a lens This causes an X-ray microscope to be unfeasible unless a way of focusing X-rays is found Until then, it is necessary to use X-rays to diffract through crystals and create a diffraction pattern that can be interpreted mathematically by a computer This turns the computer into a virtual lens, so on a monitor one can look at the structure of a molecule Crystals are important because by definition, they have a repeated unit cell within them The X-ray diffraction from one unit cell would not be significant Fortunately, the repetition of unit cells within a crystal amplifies the diffraction enough to give results that computers can yield a picture after mathematical interpretation of the results

When X-rays are beamed at the crystal, electrons diffract the X-rays, and this results in a diffraction pattern These patterns can subsequently be converted into electron density maps Since electrons surround atoms in a reasonably uniform manner, it is possible to determine where the atoms are located Hydrogen however, has only one electron, and therefore it is often difficult to locate To get a three-dimensional picture, the crystal is rotated while a computerized detector produces two dimensional electron density maps for each angle of rotation The third dimension comes from comparing the rotation of the crystal with the series of images Computer programs use this method to come up with three dimensional spatial coordinates [41]

2 12 1 X-ray crystallography study of *N*-(ferrocenyl)benzoyl ester and amino acid derivatives

para-Ferrocenyl methyl benzoate (**97**) crystallizes with one molecule in the asymmetric unit and unusually in space group Cc the molecular structure is depicted in Fig 2 36 The principal dimensions for **97** are carboxylate ester C-O 1 328(4) Å, C=O 1 199(4) Å, O-CH_3 1 430(4) Å and O-C=O 123 5(3)° The angle between the CO_2 carboxylate plane and the -C_6H_4- ring is 8 5(2)° and this aromatic system intersects the (η^5-C_5H_4) ring at 9 35(1)° There are no classical hydrogen bonds present and the only interaction of note is the (η^5-C_5H_4) O2=C1 contact where C13-H13 O2 forms a one-dimensional head-to-tail chain along the *a* axis with H13 O2 2 63 Å and C-H O 149°

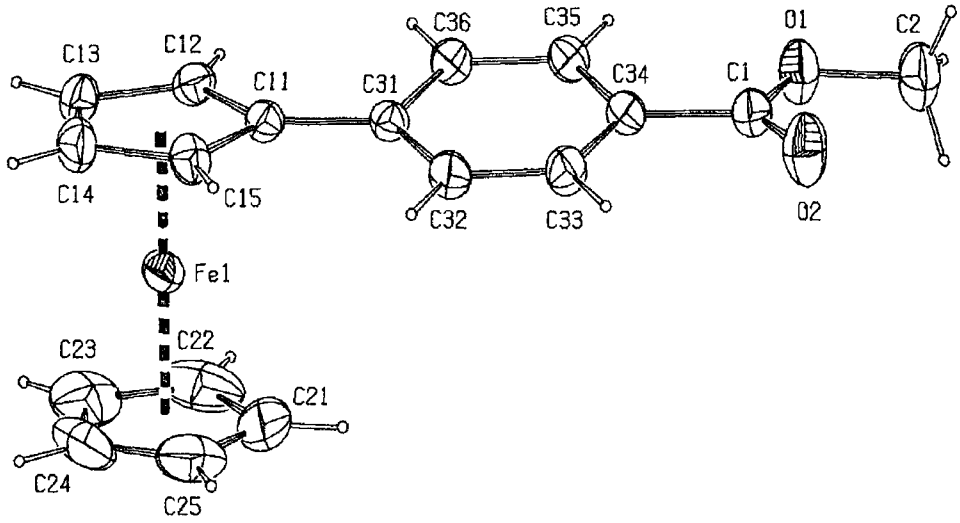

Fig 2 36 ORTEP drawing of *para*-ferrocenyl methyl benzoate (**97**)

For *N*-{*para*-(ferrocenyl)benzoyl}-L-alanine methyl ester **104** (Figure 2 38), the geometric parameters are amide C=O 1 223(2) Å, OC-NH 1 350(3) Å, HN-CH 1 451(2) Å and ester C=O/C-O 1 195(2)/1 340(2) Å, respectively, with N-H O=C(amide) as the primary intermolecular hydrogen bond, N O^{ii} 3 218(3) Å, N-H O^{ii} 158° (ii = -x, ½+y, -z) Two C-H O interactions are also present, C O 3 062(3), 3 454(3) Å along the *a*- and *b*-axes, respectively The angle between the -C_6H_4- ring and the three-atom plane O=C-N is 9 53(1)° and between the -C_6H_4- and (η^5-C_5H_4) rings of 4 92(10)° These results serve to demonstrate the co-planarity of the conjugated groups in **97** and **104** in the solid state The angle between the (η^5-C_5H_4) and the phenyl ring group is similar to that reported for 4-(*p*-

ferrocenylphenyl)pyridine (Figure 2 37) by Wong *et al* They found the angle between the two planar aromatic ring systems to be 3 1° [42]

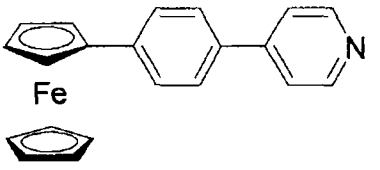

Fig 2 37 4-(*p*-Ferrocenylphenyl)pyridine prepared by Wong *et al* [42]

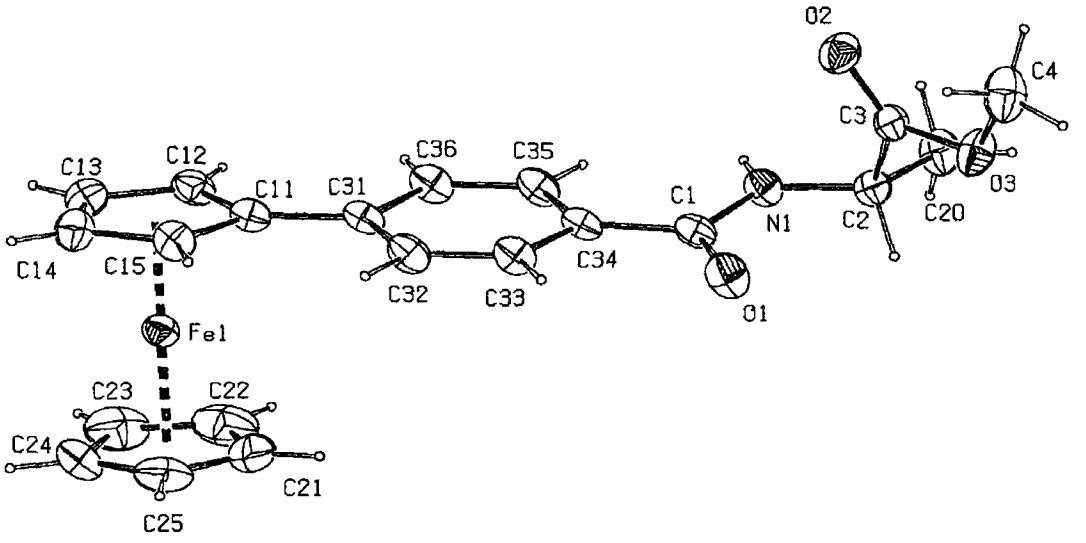

Fig 2 38 ORTEP drawing of *N*-{*para*-(ferrocenyl)benzoyl}-L-alanine methyl ester (**104**)

Table 2 7 Selected bond lengths and angles (Å, °) for molecules **97** and **104**

	97	**104**
Fe1 Cg1	1 6418(13)	1 6497(10)
Fe2 Cg2	1 6548(19)	1 6568(12)
Cg1 Fe1 Cg2	178 87(9)	179 16(7)
C1-O1	1 328(4)	1 223(2)
C1-O2/N1	1 199(4)	1 350(3)
C2-O1/N1	1 430(4)	1 451(2)
C1-N1	n/a	1 350(3)
C1-C34	1 489(3)	1 490(3)
Fe1-C11-C34	126 59(18)	125 55(14)
O1-C1-C34	112 2(3)	120 72(18)

Footnote Cg1 and Cg2 are the centroids of the (η^5-C_5H_4) and (η^5-C_5H_5) rings, respectively

Crystals suitable for X-ray crystallographic determination of *N*-{*para*-(ferrocenyl)benzoyl} glycine ethyl ester (**107**) were grown from ethyl acetate/petroleum ether (40-60°C) yielding orange needle shaped crystals Selected bond distances and angles of non hydrogen atoms are given in Table 2 8 and all pertinent crystallographic information is summarised in Table 2 9 Figure 2 39 shows the molecular structure and asymmetric unit of *N*-{*para*-(ferrocenyl)benzoyl}-glycine ethyl ester (**107**)

N-{*para*-(ferrocenyl)benzoyl}-glycine ethyl ester (**107**) crystallizes in the monoclinic space group $P2_1/c$, with two independent molecules per asymmetric unit The distances from Fe to the C atoms of the (η-C_5H_5)/(η-C_5H_4) rings are normal and compare well with other ferrocene structures [22] The range of the (η-C_5H_5) and (η-C_5H_4) internal C-C bond distances is 1 395(10) Å to 1 430(10) Å (mean 1 414 Å) and 1 360(11) to 1 409(12) Å (mean 1 395 Å) for the unsubstituted and substituted rings respectively Thus the C-C bond lengths in the (η-C_5H_4) ring are longer than in the (η-C_5H_5) ring for both molecules The distances of C11A/C11B to C31A/C31B *i e* the carbon on the substituted cyclopentadiene to the carbon on the phenyl groups are 1 470(9) Å and 1 478(8) Å respectively The distances from the amide carbonyl carbon to the phenyl carbon C34A-C1A 1 489(8) Å and C34B-C1B 1 498(8) Å are normal C-C distances The mean C-C bond length for the phenyl group in molecule A is 1 381 Å and in molecule B is 1 379 Å The carbonyl C=O bond distances for molecule A {1 248(7) Å} and molecule B {1 243(7) Å compare well with ferrocenoyl amino acids as prepared by Michael J Sheehy [25] The amide C(O)N distances C1A-N1A {1 328(7)Å} and C1B-N1B {1 327(7)Å} are typical of carbon to nitrogen bond lengths in amide bonds [26] The ester C=O bond lengths are 1 203(7) Å and 1 193(7) Å, while the ester C-O bond distances are 1 317(7) Å and 1 345(7) Å for molecules A and B, respectively

A noteworthy aspect of the asymmetric unit is the conformations which the two molecules adopt In molecule A, the ethyl ester group lies in the *trans* position with respect to the ferrocenyl group, however, in molecule B the ester lies in the *cis* position Calculations have shown that in molecule A the phenyl ring lies at an angle of 23 2(4)° with respect to the plane in which the cyclopentadienyl carbons lie, however, in molecule B, the angle between the previously mentioned planes is 18 93(4)° In comparison to values previously reported for ferrocenyl benzoyl compounds, these measurements for *N*-{*para*-(ferrocenyl)benzoyl}-glycine ethyl ester show that the interplanar angle between the C_5 and C_6 rings have increased [26 42] In molecule A, the angle between the C(O)N and

C_6H_4 planes is 23 8(3)° This makes the three atom plane O=C-N almost co-planar with respect to the (η^5-C_5H_4) ring system The carboxylate planes *i e* C2A-C3A-O2A-O3A and C2B-C3B-O2B-O3B lie almost orthogonally with respect to the amide planes

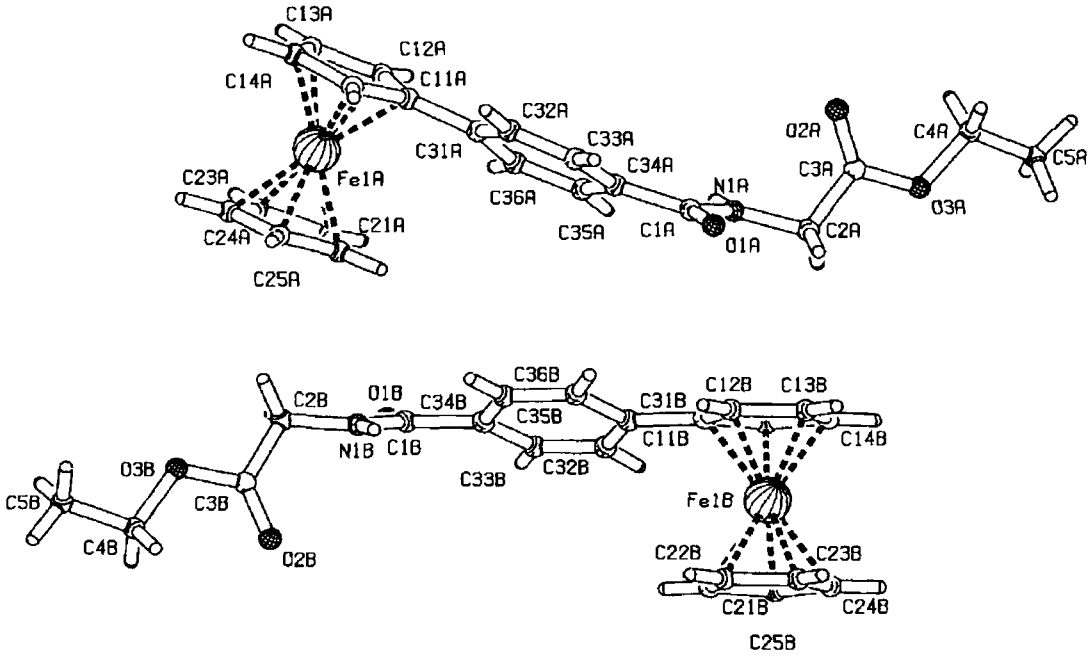

Fig 2 39 PLATON drawing of **107** This diagram shows both molecules of the asymmetric unit

Table 2 8 Selected bond distances (Å) and bond angles (degrees/°) for **107** with estimated standard deviations (e s d) in parentheses

	Molecule A	**Molecule B**
(a) Bond Distances		
av Fe(1)-C	2 033 {for (η^5-C_5H_4)R}	2 035{for (η^5-C_5H_4)R}
av Fe(1)-C	2 028 (for {η^5-C_5H_5)}	2 026 {for (η^5-C_5H_5)}
O1=C1	1 248(7)	1 243(7)
C(34)-C(1)	1 489(8)	1 498(8)
N(1)-C(2)	1 328(7)	1 327(7)
(b)Bond Angles		
O(1)-C(1)-N(1)	121 0(6)	122 0(6)
C(1)-N(1)-C(2)	124 6(5)	124 6(6)
N(1)-C(1)-C(34)	117 3(6)	116 4(6)
C(2)-C(3)-O(2)	124 2(6)	126 1(6)

Table 2 9 Pertinent Crystal structure data

Details	97	104	107
Empirical formula	$C_{18}H_{16}O_2Fe$	$C_{21}H_{21}NO_3Fe$	$C_{42}H_{42}Fe_2N_2O_6$
M	320 16	391 24	782 17
Crystal colour, habit	red, block	red, plate	Orange, needle
Crystal System	Monoclinic	Monoclinic	Monoclinic
Space group	Cc	$P2_1$	$P2_1/C$
a/Å	11 989(3)	10 683(11)	15 417(2)
b/Å	20 564(5)	6 189(6)	9 712(3)
c/Å	5 935(8)	14 318(14)	25 084(4)
β/°	93 282(6)	107 81(7)	97 740(5)
V/Å^3	1461 09(17)	897 60(15)	3721 4(13)
Z	4	2	8
Temperature/K	295K	295	295K
D_{calc}/g cm^3	1 455	1 448	1 397
μ/cm^1	1 033	1 033	8 3
F_{000}	664	408	1632
Crystal dimensions/mm			0 375 x 0 175 x 0 05
Max and min Transmission	0 50-0 44	0 75-0 66	0 95-0 75
Refinement method[43]	SHELXL97	SHELXL97	SHELXL97
Reflections collected/unique	3014/2874	4059/3529	7332
Data/parameters	2755/191	3378/237	3336/471
Goodness of fit	1 17	1 07	1 03
Final R indices {I>3σ(I)}	0 027/0 084	0 024/0 057	0 07/0 138
Density range in final diff Map/e Å^3	0 22- -0 26e Å^3	0 22- -0 12e Å^3	0 35- -0 38e Å^3

2 13 Conclusion

Ferrocenyl peptide systems have been reported to have application in the fields of peptide mimetic studies, supramolecular chemistry and materials science [3] This project sought to prepare a series ferrocenyl benzoyl peptide systems incorporating an electroactive core, an aromatic linker moiety (that may be exploited as a spectroscopic or chromophoric marker) and an amino acid fragment (that can interact with other molecules *via* hydrogen bond interactions)

The synthesis of ferrocenyl benzoic acid was achieved by reacting ferrocene with the diazonium salt of methyl/ethyl amino benzoate, followed by base hydrolysis Using the conventional DCC/HOBt protocol, a series of amino acid ester moieties (including glycine, L-alanine, L-leucine, L-phenylalanine, β-alanine, 4-aminobutyric acid, ± 2-aminobutyric acid, isoaminobutyric acid) were synthesized

These novel ferrocenyl benzoyl amino acid ester derivatives were subsequently characterized by a number of spectroscopic techniques namely ^{1}H NMR, ^{13}C NMR,

DEPT 135, HMQC, IR, UV-Vis and mass spectrometry (FAB, ESI, MS/MS, MALDI) All gave spectra in accordance with their proposed structures In cases where crystals of sufficient quality were isolated X-ray diffraction studies were also carried out

References Chapter 2

1 Severin, K , Bergs, R , Beck, W , *Angew Chem Int Ed Eng* , **1998**, *37*, 1624
2 Togni, A , Hayashi, T , '*Ferrocenes*', **1994**, Wiley, VCH publications
3 Savage, D , Gallagher, J F , Ida, Y , Kenny, P T M , *Inorg Chem Comm* , **2002**, *5*, 1034
4 Gallagher, J F , Kenny, P T M , Sheehy, M J , *Inorg Chem Comm* , **1999**, *2*, 200
5 Gallagher, J F , Kenny, P T M , Sheehy, M J , *Inorg Chem Comm* , **1999**, *2*, 327
6 Degani Y , Heller A , *J Phys Chem* , **1987**, *91*, 1285
7 van Staveren, D R , Weyhermuller T , Metzler-Nolte, N, *J Chem Soc Dalton Trans* , **2003**, 210
8 Ranganathan, D , Lakshm C , *J Chem Soc Chem Comm* , **2001**, 1250
9 Dunn, B M , *Chem Rev* , **2002**, *102*, 4431
10 Brenner, M , Huber W , *Helv Chim Acta* , **1953**, *36* 1109
11 Cipera, J D , Nicholls, R V V , *Chem Ind* , **1955**, 16
12 Kenner, G W , *Angew Chem Int Ed Eng* , **1959**, *71*, 741
13 Bodansky, M , '*Principles of Peptide Synthesis*', **1993**, Springer Verlag publishers
14 Jones J , '*Amino Acids and Peptide* Synthesis', Oxford Science Publications No 7 **1992**
15 Castro, B , Dormoy, J R , Evin, G , Selve, C , *Tetrahedron Lett* , **1975**, 1219
16 Coste, J , Le-Nguyen, C , Castro, B , *Tetrahedron Lett* , **1990**, 205
17 Sheehan, J C , Hess, G , *J Am Chem Soc* , **1955**, *77*, 1067
18 Sheehan, J C , Goodman, M , Hess, G , *J Am Chem Soc* , **1956**, *78*, 1367
19 Klausner, Y S , Bodansky, M , *Synthesis Rev* , **1972**, *9*, 453
20 DeTar, D F , Silverstein, R , *J Am Chem Soc* , **1966**, *88*, 1013
21 DeTar, D F , Silverstein, R , *J Am Chem Soc* , **1966**, *88*, 1020
22 Hanson, R W , Law, H D , *J Chem Soc* , **1965**, 7285
23 Sheehan, J C , Cruickshank, P A , Boshart, G A, *J Org Chem* , **1956**, *26*, 2525
24 March, J '*Advanced Organic Chemistry*', 4th Ed, Wiley, New York, **1985**
25 Williams, D H , Fleming, I , '*Spectroscopic Methods in Organic Chemistry*', McGraw-Hill publishers, **1995**, 5th edition
26 Sheehy, M J , '*The Design and Synthesis of Novel Peptide Derivatives as Malarial Protease Inhibitors and Electrochemical Anion Sensing Receptors*', DCU, Ph D, Thesis, **1999**
27 Silverstein, R , Bassler, G C , Morrill, T C , '*Spectrometric Identification of Organic Compounds*', John Wiley and Sons, **1981**, 4th edition
28 http //ms mc vanderbilt edu/tutorials/ms/fig3 htm
29 Gower, J L , *Biomed Mass Spectrom* , **1985**, *12*, 191
30 Sunner, J , *Org Mass Spectrom* , **1993**, *28*, 803
31 Gaskell, S J , *J Mass Spectrom* , **1997**, *32*, 677
32 http //www astbury leeds ac uk
33 Fenn, J B , Mann, M , Meng, C K , Wong, S F , Whithouse, C M , *Science*, **1989**, *246*, 64
34 Tanaka, K , Waki, H , Akita, S , Yoshida, Y , Yoshida, T , *Rapid Comm Mass Spectrom* , **1988**, *2*, 151
35 Hillenkamp, F , Karas, M , Beavis, R C , Chait, B T , *Anal Chem* , **1991**, *63*, 1193

36 http //www srsmaldı com/MALDI html
37 Donovan-McCarley, T , McCarley, R L , Lımbach, P A , *Anal Chem* , **1998**, *70*, 4376
38 Fenselau, C , *Analytıcal Chemıcal News & Features*, **1997**, 661
39 Blackstock, W P , Weır, M P , *Trends ın Bıotechnology*, **1999**, *17*, 121
40 Smart, L , Moore, E , '*Solıd State Chemıstry*', Chapman and Hıll publıshers, **1992**
41 Whıston, C , '*X-ray Methods*', John Wıley and Sons, **1987**
42 Wong, W Y , Wong, W T , *J Chem Soc , Dalton Trans* , **1996**, 3209
43 Sheldrıck, G M , SHELXL97, Unıversıty of Gottıngen, Germany

Chapter 3

Results and discussion II

3 1 Synthesis of *N*-(ferrocenyl)benzoyl dipeptide derivatives

The synthesis of the *N*-(ferrocenyl)benzoyl dipeptide derivatives was undertaken in order to enable comparisons to be drawn with the *N*-(ferrocenyl) benzoyl monopeptide derivatives and other fundamentally similar compounds [1 3]

Conventional peptide chemistry was employed in order to prepare the dipeptide moieties and these were subsequently coupled to the ferrocenyl benzoic acid using the DCC/HOBt protocol

Equimolar quantities of *N*-Boc protected amino acids were reacted with amino acid ethyl ester hydrochloride salts, DCC, catalytic amounts of HOBt and Et_3N in dichloromethane at 0°C Upon completion of this reaction, the dipeptide was washed with water, 10% potassium hydrogen carbonate, and 5% citric acid Deprotection of the amino terminal was achieved by using trifluoroacetic acid (TFA) (Figure 3 1) The TFA acts by cleaving the *tert*-butoxycarbonyl group leaving the amine functionality unprotected and susceptible to reaction with the carboxyl functional group of the ferrocenyl benzoic acid The Boc group is easily identified in a ^1H NMR spectrum as the nine equivalent protons of the *tert*-butyl group give rise to a large singlet at approximately δ 1 0 and hence, evidence of protection or deprotection of the amino terminus is readily obtained by ^1H NMR measurements

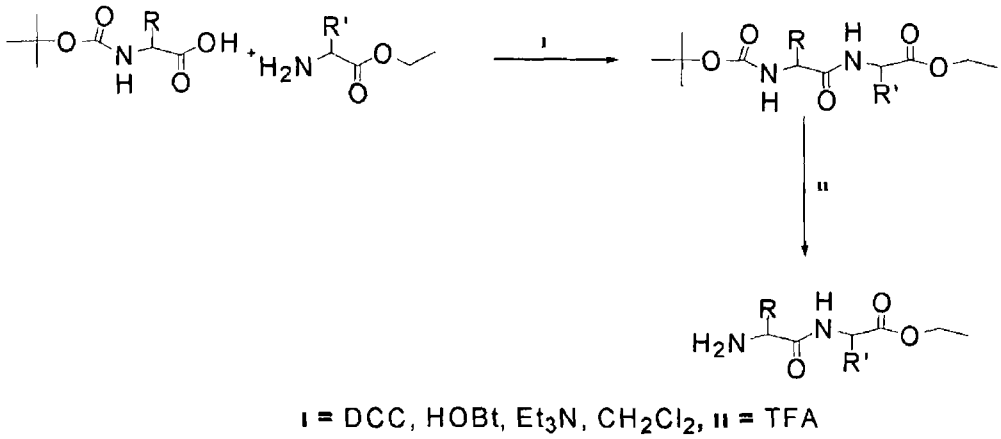

Fig 3 1 The synthesis and deprotection of a dipeptide

The deprotected dipeptide is subsequently coupled to ferrocenyl benzoic acid using equimolar amounts of DCC, and catalytic amounts of HOBt, and Et_3N [4] Only catalytic quantities of HOBt are employed as it competes significantly with the required dipeptide reaction yielding the byproduct ferrocenyl benzoyl benzotriazole ester (Figure 3 2)

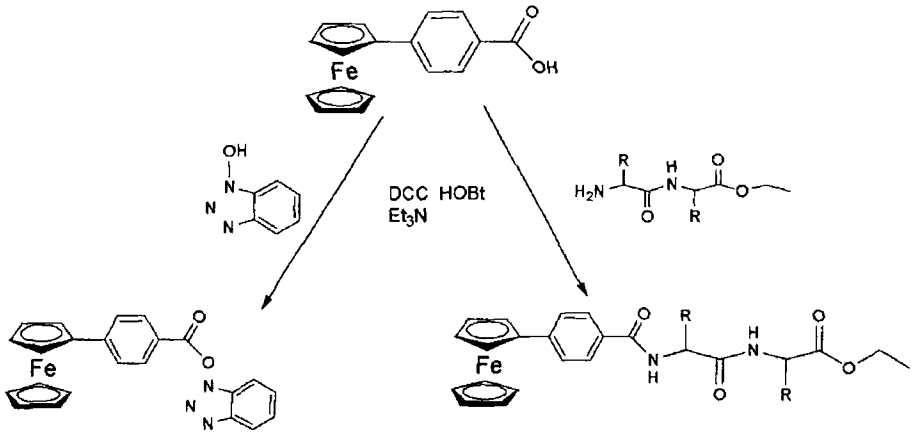

Fig 3 2 The competitive reaction between HOBt and dipeptide with ferrocenyl benzoic acid

Following the familiar washing procedure previously employed, a crude *N*-ferrocenyl benzoyl dipeptide ester molecule is isolated Separation using column chromatography furnishes the pure, required product, and in each case, the eluant was a 2 3 petroleum ether (40-60°C) ethyl acetate mixture

Yields varied depending on whether *ortho*, *meta* or *para*-ferrocenyl benzoic acid was employed In the cases of the *para* and *meta* derivatives the yields were roughly similar, ranging from 45-62%, however when the *ortho*-ferrocenyl benzoic acid was employed yields of only 25-47% were achieved and in some cases the required product was not isolated at all The reasons for the disparity in the yields can be rationalized by considering the respective approaches to the carboxylic acid hydroxyl group of the ferrocenyl benzoic acid On the *ortho*- and *meta*-ferrocenyl benzoic acids respectively, the carboxylic acid functionality is more sterically hindered than that on the *para* derivative This assertion is supported by the fact that the reaction of the least bulky dipeptide, glycine-glycine ethyl ester, with the *ortho*-, *meta*- and *para*-ferrocenyl benzoic acids proceeds without difficulty and yields are reasonably good *i e* 56-60%, however the yields of the glycine-L-leucine ethyl ester derivatives vary somewhat and in the case

of the reactions of glycine-L-leucine ethyl ester with *ortho*-ferrocenyl benzoic acid no reaction occurred at all and hence, this may provide evidence that a steric effect influences the outcome of the reaction Table 3 1 summarizes the yields of all the *N*-(ferrocenyl)benzoyl amino acid derivatives that have been prepared

Table 3 1 *N*-(ferrocenyl)benzoyl dipeptide derivatives

Compound	No	R	R	% Yield
N-p-Fc-Bz-L-ala-gly-CO_2Et	**138**	Me	H	58
N-p-Fc-Bz-L-ala-L-ala-CO_2Et	**139**	Me	Me	49
N-p-Fc-Bz-L-ala-L-leu-CO_2Et	**140**	Me	^{t}Bu	52
N-p-Fc-Bz-L-ala-L-phe-CO_2Et	**141**	Me	Bn	60
N-p-Fc-Bz-β-ala-β-ala-CO_2Et	**142**	CH_2	CH_2	49
N-m-Fc-Bz-L-ala-gly-CO_2Me	**143**	Me	H	51
N-m-Fc-Bz-L-ala-gly-CO_2Et	**144**	Me	H	52
N-m-Fc-Bz-L-ala-L-ala-CO_2Et	**145**	Me	Me	48
N-m-Fc-Bz-L-ala-L-leu-CO_2Et	**146**	Me	^{t}Bu	45
N-m-Fc-Bz-L-ala-L-phe-CO_2Et	**147**	Me	Bn	47
N-o-Fc-Bz-L-ala-gly-CO_2Et	**148**	Me	H	40
N-o-Fc-Bz-L-ala-L-phe-CO_2Et	**149**	Me	Bn	25
N-p-Fc-Bz gly-gly-CO_2Et	**150**	H	H	62
N-p-Fc-Bz gly-L-ala-CO_2Et	**151**	H	Me	58
N-p-Fc-Bz gly-L-leu-CO_2Et	**152**	H	^{t}Bu	60
N-p-Fc-Bz gly-L-phe-CO_2Et	**153**	H	Bn	62
N-m-Fc-Bz gly-gly-CO_2Et	**154**	H	H	56
N-m-Fc-Bz gly-L-ala-CO_2Et	**155**	H	Me	55
N-m-Fc-Bz gly-L-leu-CO_2Et	**156**	H	^{t}Bu	49
N-m-Fc-Bz gly-L-phe-CO_2Et	**157**	H	Bn	50
N-o-Fc-Bz gly-gly-CO_2Et	**158**	H	H	47
N-o-Fc-Bz gly-L-ala-CO_2Et	**159**	H	Me	46
N-o-Fc-Bz gly-L-phe-CO_2Et	**160**	H	Bn	40

3 2 The protection of the amino terminus of an amino acid

The synthesis of dipeptide molecules, as shown in Figure 3 1, requires the protection of the amino terminus of one amino acid and the protection of the carboxyl terminus of another prior to a coupling reaction between the two Therefore, when both the amino and carboxyl protected amino acids are coupled, only the required dipeptide is isolated

The protection of the amino group operates by either suppressing the nucleophilicity of the amino group (by draining its electron density away) and/or by preventing its reaction by using a barrier of steric hindrance The protecting group must also be able to be easily removed under mild conditions so as not to damage other potentially vulnerable parts of the molecule [5]

A variety of protecting groups have been employed for the protection of the amino terminal They are usually selected so as they are orthogonal to the rest of the molecule (*i e* can be added or removed without affecting the other susceptible functional groups)

3 2 1 The alkoxycarbonyl group series

Amino groups are easily converted to alkoxycarbonylamino derivatives (*i e* urethanes/carbamates) and hence, contain both amide and ester functional groups As amides, these compounds are no longer nucleophilic, therefore, they are inert to reaction with carbonyl functionalities and hence the alkoxycarbonyl protecting groups execute their role well (*i e* the prevention of reaction at the amino terminus) Carbamates decarboxylate very easily and for this reason, the regeneration of the parent amine is achieved by acyl-oxygen fission This can be brought about in a number of ways depending on the alkyl group [5 6]

3.2 1 1 The benzyloxycarbonyl group (Z/Cbz)

The benzyloxycarbonyl (Z/Cbz) group was one of the first amino protecting groups employed in peptide synthesis [7] The Z group can be introduced onto the peptide using either the chloroformate or the benzyloxybenzotriazole ester reagents (Figure 3 3)

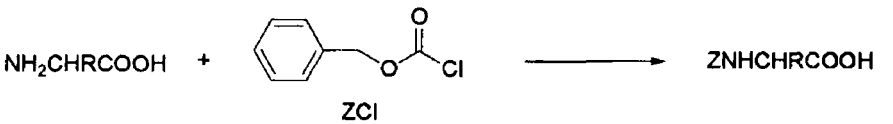

Fig 3 3 The protection of the amino terminal using the benzyloxycarbonyl group

This protecting group is generally inert to exposure from dilute alkali, or weakly nucleophilic moieties In addition the Z group is not affected by mildly acidic conditions *e g* trifluoroacetic acid The Z group is removed *via* treatment with HBr/AcOH (Figure 3 4) or catalytic hydrogenolysis

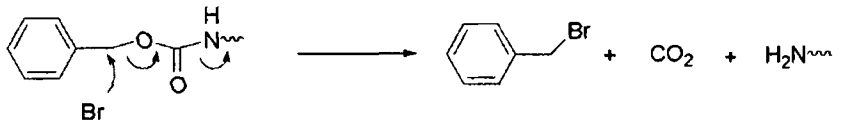

Fig 3 4 The deprotection of the Z group using HBr

This deprotection reaction occurs with ease and the amino acid can be precipitated as a hydrobromide salt on flooding with ether [5]

3 2 1 2 The *tert*-butoxycarbonyl group (Boc)

The *tert*-butoxycarbonyl group is probably the most universally used amino protecting group [23] This can be explained by the fact that it is easy to use, gives good yields and does not cause racemization Attempts were made to introduce the Boc group as its chloroformate derivative and subsequently as its hydrazide but safety problems associated with these procedures meant that they were unsuitable The standard method by which the Boc group is introduced onto the peptide is *via* its anhydride (Figure 3 5) This provides a fast and safe route to Boc-protected amino acids and peptides [8 9]

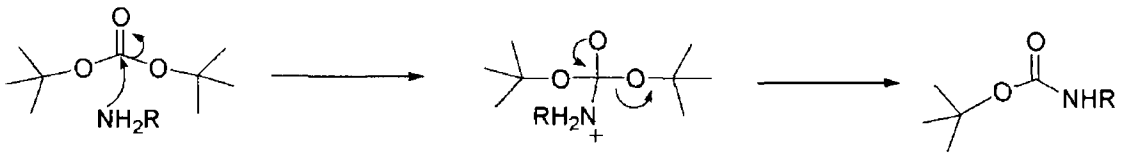

Fig 3 5 The introduction of the tert-butoxycarbonyl group using the anhydride derivative

The Boc group is stable towards catalytic hydrogenolysis, basic and nucleophilic reagent but is acid labile Hence, deprotection of the Boc group is easily achieved on exposure to TFA for 15 minutes (Figure 3 6) These are mild and reliable conditions The facility of this reaction is due to the stability of carbonium ion produced [8 9]

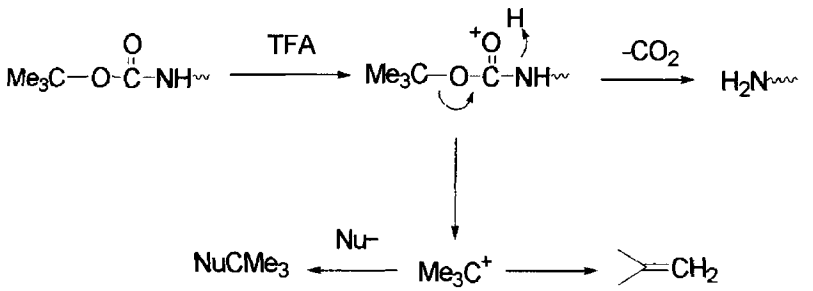

Fig 3 6 The reaction scheme for the removal of the Boc group

3 2 1 3 The 2-(4-biphenylyl)-isopropyloxycarbonyl group (Bpoc)

The 2-(4-biphenylyl)-isopropyloxycarbonyl (Bpoc) (Figure 3 7) group behaves in a similar fashion to the Boc group with the exception that it is more acid labile This is due to the fact the corresponding carbomum ion produced during the deprotection step is further stabilized by the biphenylyl subunit The Bpoc group is removed by using a dilute acetic acid in dichloromethane solution (conditions that would leave the Z and Boc groups intact) The Bpoc group is stable to bases and nucleophiles but it can be removed by catalytic hydrogenolysis [10]

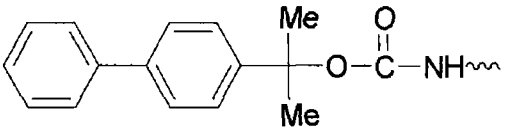

Fig 3 7 The Bpoc amino protecting groups

3 2 1 4 The 9-fluorenylmethoxycarbonyl group (Fmoc)

The 9-fluorenylmethoxycarbonyl (Fmoc) group is usually introduced onto an amino acid/peptide as its chloroformate [6] There are complications with this reaction however, as unwanted dipeptide byproducts may be formed (Figure 3 8)

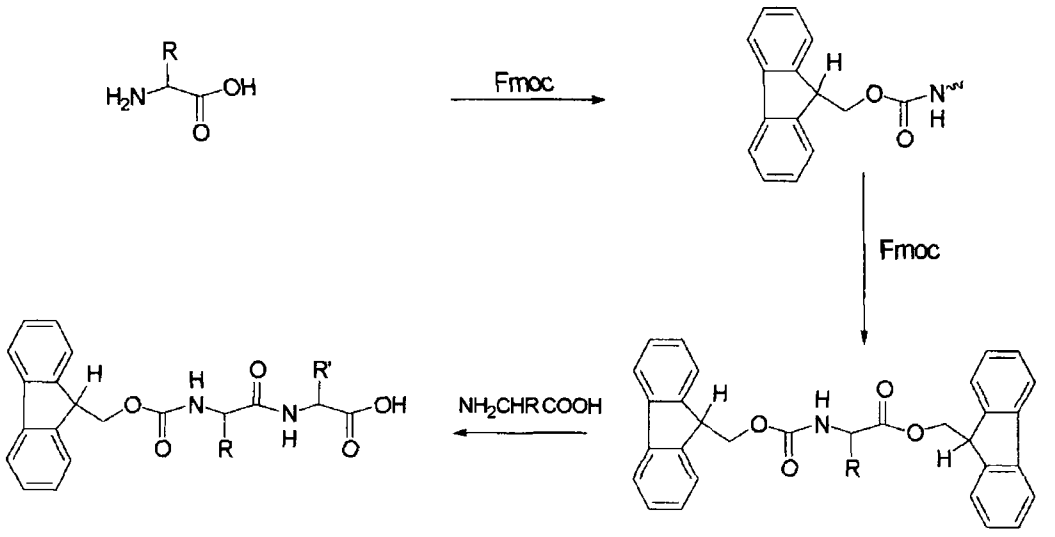

Fig 3 8 The undesirable dipeptide formation that may occur as a result of use of the Fmoc group

The Fmoc group is very stable to acidic reagents but is quickly removed when treated with basic solutions like piperidine or fluoride ion in dimethyl formamide (DMF) (Figure 3 9)

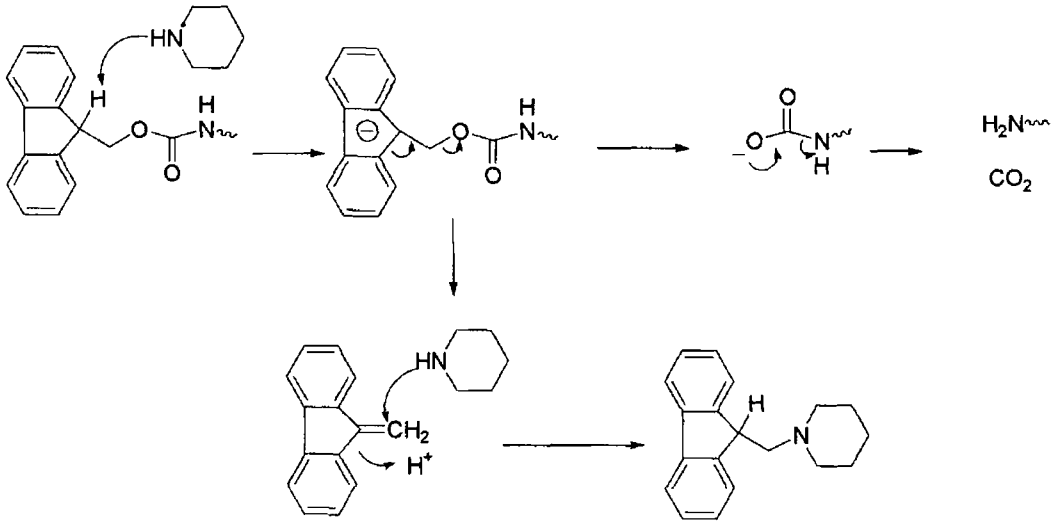

Fig 3 9 The deprotection of the Fmoc group by treatment with piperidine [5]

A huge variety of alkoxycarbonyl amino protecting groups exist, however, most have not been applied successfully in general peptide synthesis, and hence only the most successful examples are described here The fact that there is a selection of amino protecting groups, each of which can be selectively removed, is very important for the synthesis of peptides that might contain amino or other susceptible substituents [6]

3 2 2 The triphenylmethyl (trityl) protecting group

The triphenylmethyl (trityl) protected amino acids are usually prepared *via* the trimethyl silyl derivatives (Figure 3 10) as direct tritylation (*via* reaction of the amino acid with trityl chloride) is sluggish and usually gives poor yields [5]

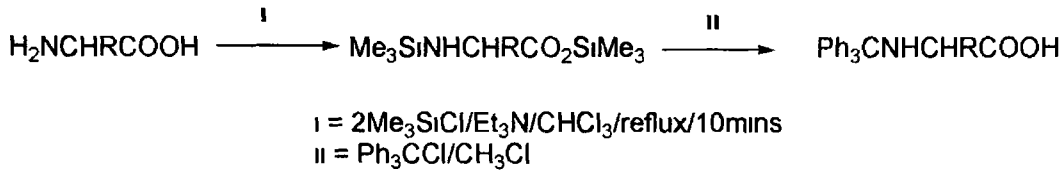

Fig 3 10 The protection of the amino terminus of an amino acid using the trityl group

The trityl group is very acid labile, and this is because the cation that is produced during the deprotection process (*i e* $^{+}CPh_3$) is very stable (Figure 3 11) The trityl group can be removed by acetic acid at pH 4 Catalytic hydrogenolysis also removes the trityl protecting group leaving the parent amine [6]

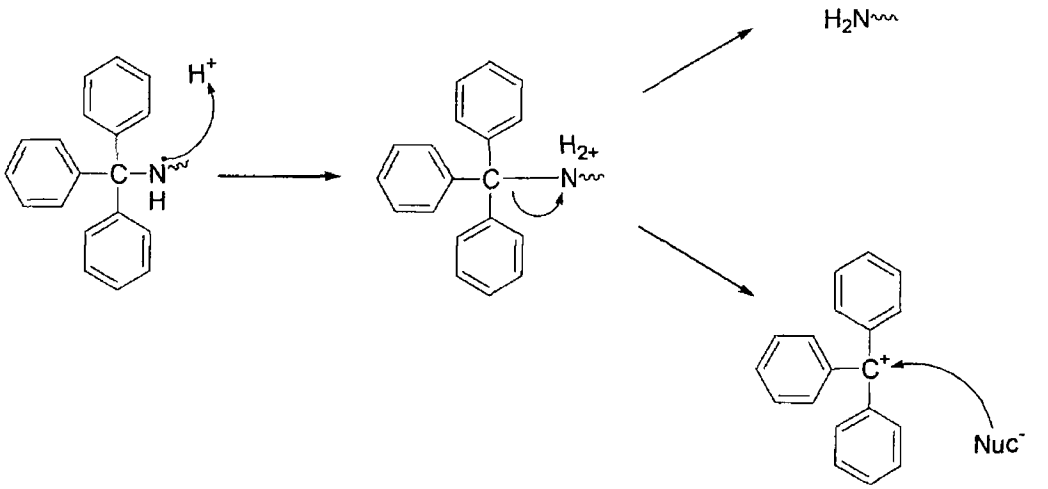

Fig 3 11 The deprotection of the trityl group

3 3 ^{1}H NMR study of *N*-(ferrocenyl)benzoyl dipeptide derivatives

In the ^{1}H NMR spectra of the *N*-(ferrocenyl)benzoyl dipeptide ethyl esters the aromatic peak patterns for the *ortho*, *meta* and the *para* derivatives are similar to those described in chapter 2 for the *N*-(ferrocenyl)benzoyl amino acid ester derivatives

Similarly, as with the *N*-(ferrocenyl)benzoyl amino acid ester compounds the chemical shifts at which the amide protons appear, depends on the solvent that is employed When the spectra were obtained in $CDCl_3$, the amide proton peaks appear between δ 6 50 and 7 67, however when d_6-DMSO is employed the amide proton peaks are shifted downfield to between δ 8 16 and 8 75

Three characteristic signals typically appear between δ 3 83 and 5 08 for a monosubstituted ferrocenyl moiety These signals are as a result of the presence of the *ortho* hydrogens on the (η^5-C_5H_4) ring (δ 4 48-5 08), the *meta* hydrogens on the (η^5-C_5H_4) ring (δ 4 09-4 66), and the (η^5-C_5H_5) hydrogens (δ 3 81-4 11) These chemical shifts values for a monosubstituted ferrocenyl group are in good agreement with *N*-ferrocenoyl amino acid derivative values quoted by Kraatz *et al* [11] and Sheehy *et al* [1,2] The peaks due to the *ortho* and *meta* protons of the (η^5-C_5H_4) ring can appear as fine triplets with coupling constants of 1 6-2 Hz and sometimes these peaks appear as singlets,

and both peaks integrate for two protons The large singlet due to the (η^5-C_5H_5) ring appears in the range δ 3 95-4 03 The spectra of the *N*-{*ortho*-(ferrocenyl)benzoyl} derivatives sometimes do not give the pattern typical of the ferrocenyl region in the ^{1}H NMR spectrum In the example of *N*-{*ortho*-(ferrocenyl)benzoyl}-L-alanine-L-phenylalanine ethyl ester, the signal representmg the *ortho* protons on (η^5-C_5H_4) ring, appear as two singlets The chemical shifts of the respective substitutents that make up the ethyl group are consistently similar, with the methylene signal appearing in the range δ 3 87 to 4 24, and the methyl group between δ 0 92-1 30

Table 3 2 Selected ^{1}H NMR data (δ)

Compound No	CONH^1	CONH^2	(η^5-C_5H_4)^{ortho}	(η^5-C_5H_4)^{meta}	(η^5-C_5H_5)
138	7 6	7 45	4 63	4 32	3 96
143*	8 62	8 39	4 87	4 39	4 04
145	7 83	7 06	4 62	4 26	3 96
147	7 82	7 46	4 63-4 66	4 29	3 98
151	7 34	7 19	4 61	4 3	3 95
159	7 8	6 72	4 50-4 52	4 29	4 11

* ^{1}H NMR spectra obtained in d_6-DMSO

3 3 1 The ^{1}H NMR spectrum of *N*-{*ortho*-(ferrocenyl)benzoyl} glycine-glycine ethyl ester (158)

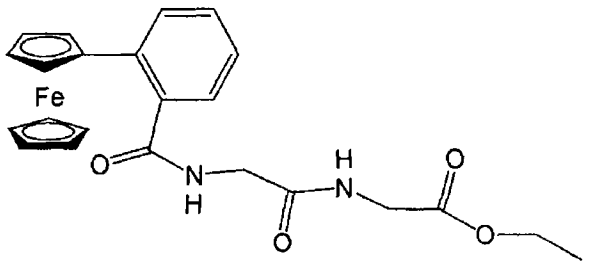

Fig 3 12 *N*-{*ortho*-(ferrocenyl)benzoyl} glycine-glycine ethyl ester (**158**)

The ^{1}H NMR spectrum of *N*-{*ortho*-(ferrocenyl)benzoyl} glycine-glycine ethyl ester (**158**) (Figure 3 13) was obtained in d_6-DMSO and hence, the two amide proton peaks are positioned at the downfield position of δ 8 18 and 8 51 respectively Both of these signals integrate for one proton each and appear as triplets due to the adjacent glycine methylene

groups The signals in the aromatic region confirm the presence of four protons, which appear between δ 7 42 and 7 78

The characteristic monosubstituted ferrocenyl splitting pattern is observed (for this series of compounds) between δ 4 06 and 4 64 The peak due to the *ortho* protons on the (η^5-C_5H_4) ring appears as the furthest downfield ferrocenyl signal and is observed as a fine triplet at δ 4 64 with a coupling constant of 2 Hz Similarly the signal due to the *meta* (η^5-C_5H_4) protons also appears as a fine triplet at δ 4 27 Both the *ortho* and *meta* peaks integrate for two hydrogens each At δ 4 06 there is a large singlet due to the (η^5-C_5H_5) ring that integrates for five protons

The methylene group of the ethyl ester appears as a quartet at δ 4 18 Between δ 3 93 and 3 99 there are two doublets, integrating for two protons each These peaks are assigned to the methylene groups of the two glycine residues respectively The methyl group of the ethyl ester function appears as a triplet at δ 1 29 and integrates for three protons

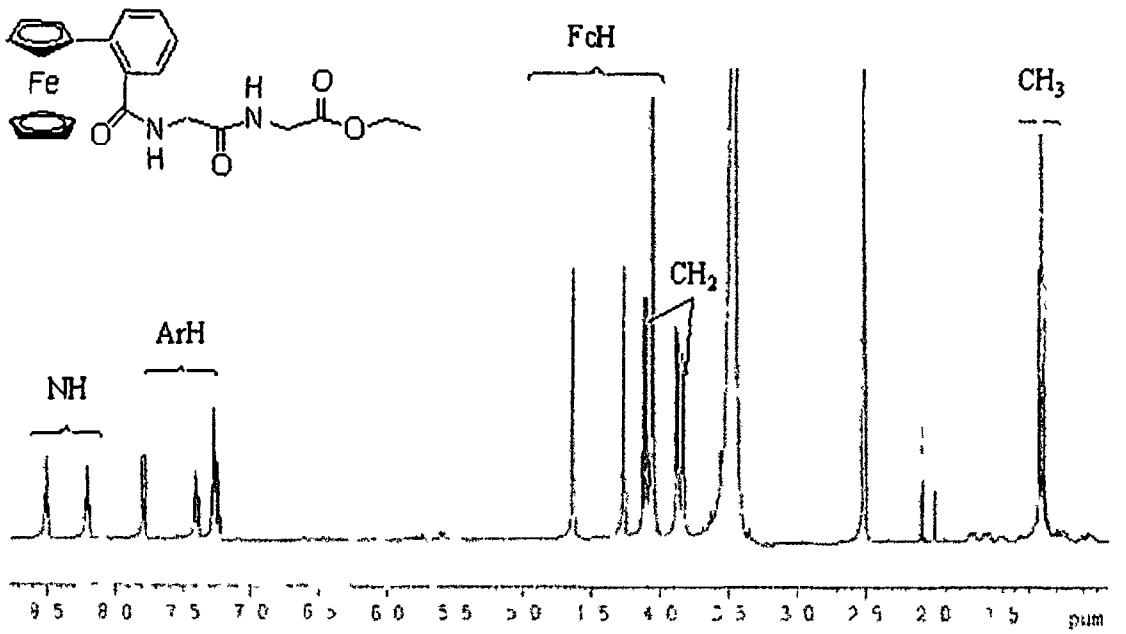

Fig 3 13 ^{1}H NMR spectrum of *N*-{*ortho*-(ferrocenyl)benzoyl} glycine-glycine ethyl ester **(158)**

3 3 2 The ^{1}H NMR spectrum of *N*-{*meta*-(ferrocenyl)benzoyl} glycine-glycine ethyl ester (154)

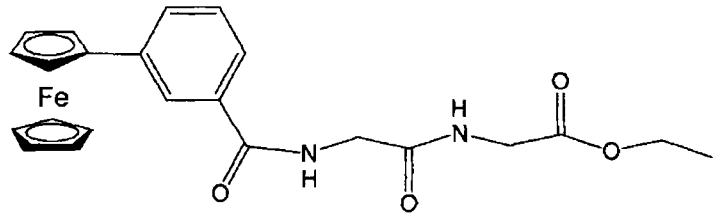

Fig 3 14 *N*-{*meta*-(ferrocenyl)benzoyl} glycine-glycine ethyl ester (**154**)

The ^{1}H NMR spectrum for *N*-{*meta*-(ferrocenyl)benzoyl} glycine-glycine ethyl ester (**154**) was acquired in $CDCl_3$ and hence, the two amide proton peaks are positioned at the relatively upfield position of δ 6 89 and 7 20 respectively Both of these signals integrate for one proton and appear as broad singlets The aromatic region confirms the presence of four protons, which appear between δ 7 26 and 7 87 As is typical with *meta* disubstituted benzene groups with two different substituents, the spectrum shows a triplet at δ 7 28, a multiplet (two overlapping doublets) integrating for two protons between δ 7 54 and 7 57, and a singlet at δ 7 87

In the ferrocenyl region, the peak due to the *ortho* protons on the (η^5-C_5H_4) ring appears as the furthest downfield ferrocenyl signal This signal appears as a fine triplet at δ 4 63 with a coupling constant of 2 Hz Similarly, the *meta* protons of the (η^5-C_5H_4) ring appear as a fine triplet at δ 4 27 Both these peaks integrate for two hydrogens The large singlet at δ 3 97 {due to the (η^5-C_5H_5) ring} integrates for five protons

A multiplet, integrating for four protons is observed between δ 4 13 and 4 17, due to the methylenes of the glycine residue and the ethyl ester group, respectively The doublet due to the methylene group of the second glycine residue appears at δ 4 07 and integrates for two protons The methyl group of the ethyl ester appears as a triplet at δ 1 20 and integrates for three protons

3 3 3 The ^{1}H NMR spectrum of *N*-{*para*-(ferrocenyl)benzoyl} glycine-glycine ethyl ester (150)

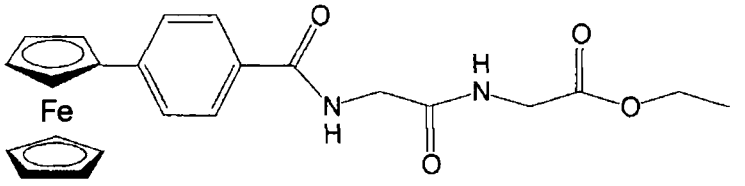

Fig 3 15 *N*-{*para*-(ferrocenyl)benzoyl} glycine-glycine ethyl ester (**150**)

The ^{1}H NMR spectrum for *N*-{*para*-(ferrocenyl)benzoyl} glycine-glycine ethyl ester (**150**) was obtained in $CDCl_3$ The two amide proton signals are present at the relatively upfield position of δ 6 85 and 7 09 Both of these signals integrate for one proton and appear as triplets due to the neighbouring methylene groups of the respective glycine residues The characteristic splitting pattern of the *para* disubstituted benzene groups shows two doublets integrating for two protons each at δ 7 45 and 7 69, respectively

In the ferrocenyl region, the typical splitting pattern for a mono substituted ferrocenyl group is observed The peaks of the *ortho* protons on the (η^5-C_5H_4) ring appear as the furthest downfield ferrocenyl signal This signal appears as a fine triplet at δ 4 63 with a coupling constant of 2 Hz Similarly, the signal due to the *meta* protons of the (η^5-C_5H_4) ring also appear as a fine triplet at δ 4 31 and both of these peaks integrate for two hydrogens each The (η^5-C_5H_5) ring is represented by a large singlet at δ 3 96 and integrates for five protons

Between δ 4 19 and 4 00, signals due to the glycine methylene and the ethyl ester methylene overlap to produce a multiplet that integrates for four protons The other glycine methylene group appears at δ 4 14 and gives rise to a doublet with a coupling constant of 5 6 Hz The methyl group of the ethyl ester integrates for three protons and is represented by a triplet at δ 1 21

3 4 ^{13}C NMR & DEPT 135 studies of *N*-(ferrocenyl)benzoyl dipeptide ester derivatives

In the ^{13}C spectra of these *N*-(ferrocenyl)benzoyl dipeptide derivatives, the amide and ester carbonyl carbons appear at downfield positions usually between δ 166 2 and 173 2

The number of peaks in the aromatic region varies depending on whether *ortho, meta* or *para*-(ferrocenyl) benzoic acid is being employed in the coupling procedure The *meta* and *ortho* derivatives both give rise to six aromatic peaks since none of the aromatic carbons are equivalent, however the *para* derivative only produces four signals (two peaks due to two quaternary carbons and two peaks of roughly twice the intensity which are attributed to two carbons each) The aromatic quaternary carbons can be identified with the aid of DEPT 135 spectra

The ferrocenyl region typically occurs between δ 67 and 85 6 The ferrocenyl *ipso* carbon has a resonance usually at around δ 84 An intense peak at approximately δ 70 is attributed to the (η^5-C_5H_5) ring, and almost overlapping with this peak, the signal due to the *meta* carbons on the (η^5-C_5H_4) ring typically appear Slightly upfield, at chemical shifts of the order of δ 67, the *ortho* carbons of the (η^5-C_5H_4) ring usually come into resonance

The DEPT 135 spectrum shows a negative peak at approximately δ 62 and is assigned as the methylene peak of an ethyl ester group The methyl carbon comes into resonance at around δ 14 5 as does the equivalent positive peak on the DEPT 135 spectrum

Table 3 3 Selected ^{13}C NMR (δ) data

Compound No	C=O	C=O	C=O	*ipso* C	$(\eta^5\text{-}C_5H_4)^{ortho}$	$(\eta^5\text{-}C_5H_4)^{meta}$	$(\eta^5\text{-}C_5H_5)$
138	173	170	167 5	85 4	67 2	70 1	70 2
145	173 1	172 5	167 6	84 4	67	69 7	70 1
147	172 2	171 6	167 5	84 5	67 1	69 8	70 1
149	172 6	171 7	169 5	85	68 5, 68 7	69 5	69 8
153	171 7	169 2	167 9	83 9	67 2	70 1	70 2
159	173	171 3	168 4	85 6	69 2	69 6	69 7

3 4 1 ^{13}C and DEPT NMR study of *N*-{*ortho*-(ferrocenyl)benzoyl} glycine-glycine ethyl ester (158)

The three peaks that occur between δ 169 7 and 170 5 are due to three carbonyl groups It is not possible however, to assign the ester and amide carbonyl groups

The aromatic region shows six individual peaks, as an *ortho*-disubstituted benzene group with two different substituents will inevitably have six inequivalent carbons The two quaternary carbon atoms appear at δ 136 4 and 136 6 and the four aromatic primary

carbon signals appear at δ 125 8, 127 8, 129 1, 130 4, respectively As carbonyl and quaternary carbons do not appear in a DEPT 135 spectrum it allows these peaks to be easily assigned in the ^{13}C spectrum

Similarly, the signal at δ 84 8 is not observed in the DEPT 135 spectrum and therefore it is assigned as the *ipso* ferrocenyl carbon The (η^5-C_5H_5) ring appears as an intense signal at δ 69 8, beside which is the peak at δ 69 1 due to the *meta* carbons on the (η^5-C_5H_4) ring The *ortho* carbons on the (η^5-C_5H_4) ring appear as the furthest upfield ferrocenyl peaks and in this case they come into resonance at δ 68 6 ^{13}C NMR studies undertaken by Kraatz *et al* [11] would concur with the trends seen in Table 3 3 Their studies suggested that the ^{13}C NMR chemical shift values for the ferrocenyl group do not vary much despite there being different amino acid residues attached

At δ 60 9 the negative peak on the DEPT 135 spectrum is attributed to the methylene carbon on the ethyl ester group Similarly, at δ 41 0 and 41 3 two methylene carbons of the respective glycine residues give negative peaks in the DEPT 135 spectrum and thus are easily assigned The methyl carbon of the ethyl ester appears at δ 14 4

3 4 2 ^{13}C and DEPT 135 NMR study of *N*-{*meta*-(ferrocenyl)benzoyl} glycine-glycine ethyl ester (154)

The ^{13}C and DEPT 135 spectra of *N*-{*meta*-(ferrocenyl)benzoyl} glycine-glycine ethyl ester (**154**) can be seen in Figures 3 16 and 3 17 respectively The three carbonyl peaks appear between δ 170 2 and 168 4

The aromatic region shows six individual peaks, as a *meta*-disubstituted benzene group with two different substituents will have six inequivalent carbons The two aromatic quaternary carbons of the benzoyl group appear at δ 140 8 and 134 and the four other aromatic signals appear at δ 129 8, 129 0, 125 1, and 124 7 respectively

The signal at δ 84 4 is not present in the DEPT 135 (Figure 3 17) spectrum and therefore it is assigned as the *ipso* ferrocenyl carbon The (η^5-C_5H_5) ring appears as an intense signal at δ 70 1, beside which is the peak at δ 69 7 due to the *meta* carbons of the (η^5-C_5H_4) ring The *ortho* carbons on the (η^5-C_5H_4) ring appear as the furthest upfield peaks in the ferrocenyl region and in this instance they come into resonance at δ 67

At δ 62 1 the negative peak on the DEPT 135 spectrum is attributed to the methylene carbon of the ethyl ester group Similarly at δ 44 0 and 41 8 the two methylene carbons of

the respective glycine residues give rise to two negative peaks in the DEPT 135 spectrum and hence, are easily assigned The methyl carbon of the ethyl ester group appears at δ 14 5

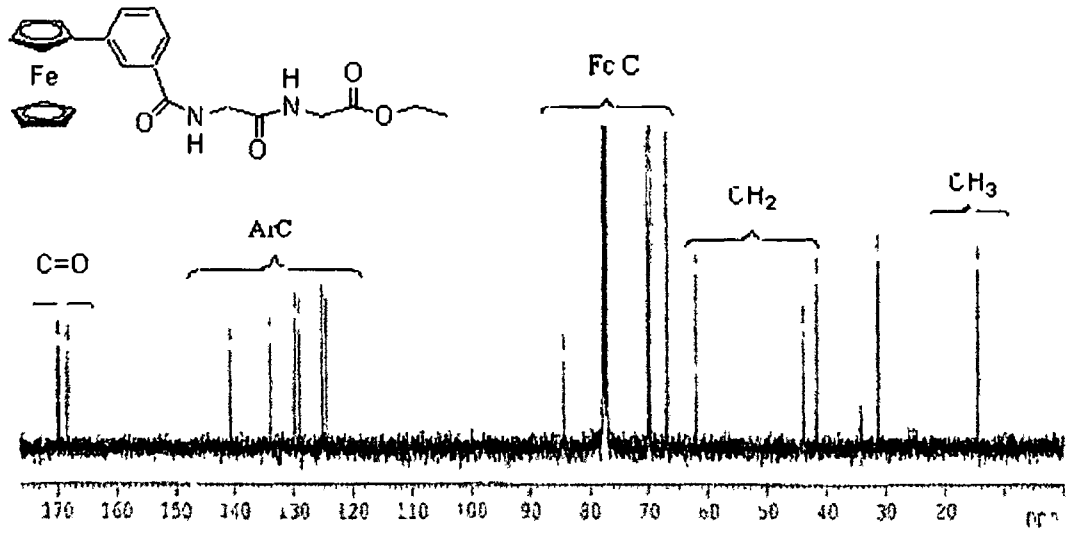

Fig 3 16 ^{13}C NMR spectrum of *N*-{*meta*-(ferrocenyl)benzoyl} glycine-glycine ethyl ester (**154**)

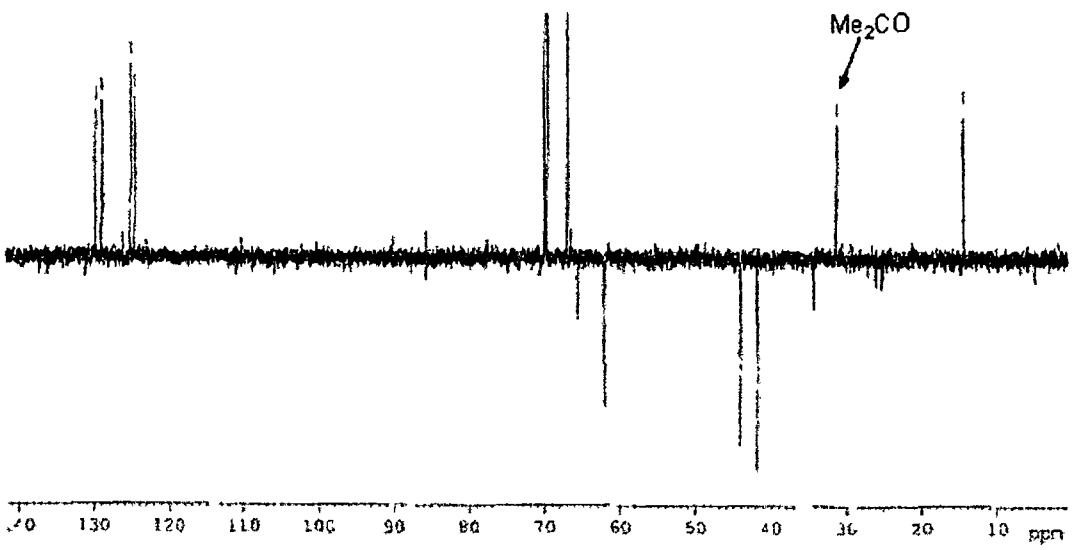

Fig 3 17 DEPT 135 spectrum of *N*-{*meta*-(ferrocenyl)benzoyl} glycine-glycine ethyl ester (**154**)

3 4.3 ^{13}C and DEPT 135 NMR study of *N*-{*para*-(ferrocenyl)benzoyl} glycine-glycine ethyl ester (150)

In the ^{13}C spectrum of *N*-{*para*-(ferrocenyl)benzoyl} glycine-glycine ethyl ester, as is typical for *para*-disubstituted, there are only four aromatic peaks This can be explained

by the fact that there are two sets of two equivalent carbons and two inequivalent quaternary carbons The two quaternary carbons of the aryl ring appear at δ 130 8 and 144 5 and the two other aromatic signals appear at δ 126 3 and 127 7 respectively

The signal at δ 83 7 does not show up in the DEPT 135 spectrum and therefore it is assigned as the *ipso* ferrocenyl carbon The (η^5-C_5H_5) ring appears as an intense signal at δ 70 1, beside which is the peak at δ 70 2 representing the *meta* carbons on the (η^5-C_5H_4) ring The *ortho* carbons on the (η^5-C_5H_4) ring appear as the furthest upfield ferrocenyl peaks and in this case they come into resonance at δ 67 2

At δ 62 1 the negative peak on the DEPT 135 spectrum is attributed to the methylene carbon on the ethyl ester group The signals at δ 41 8 and 44 0 are due to the two glycine methylene carbons and give rise to two negative peaks in the DEPT 135 spectrum The signal for the methyl group carbon of the ethyl ester appears at δ 14 5

3 5 HMQC study of *N*-{*para*-(ferrocenyl)benzoyl} glycine-glycine ethyl ester (150)

A HMQC study was undertaken for the *N*-(ferrocenyl)benzoyl dipeptide compounds and the spectrum for *N*-{*para*-(ferrocenyl)benzoyl glycine-glycine ethyl ester is shown in Figure 3 19 This enabled all the protons and carbons of the increasingly more complex structures to be unambiguously assigned [12] The results of the HMQC study for *N*-{*para*-(ferrocenyl)benzoyl glycine-glycine ethyl ester (**150**) (Figure 3 18) and are summarized in Table 3 4

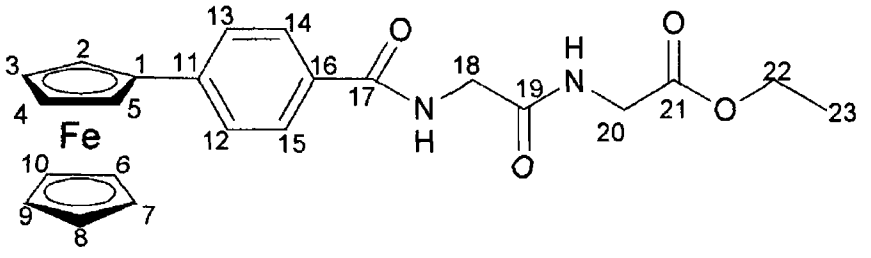

Fig 3 18 Structure of *N*-{*para*-(ferrocenyl)benzoyl} glycine-glycine ethyl ester (**150**)

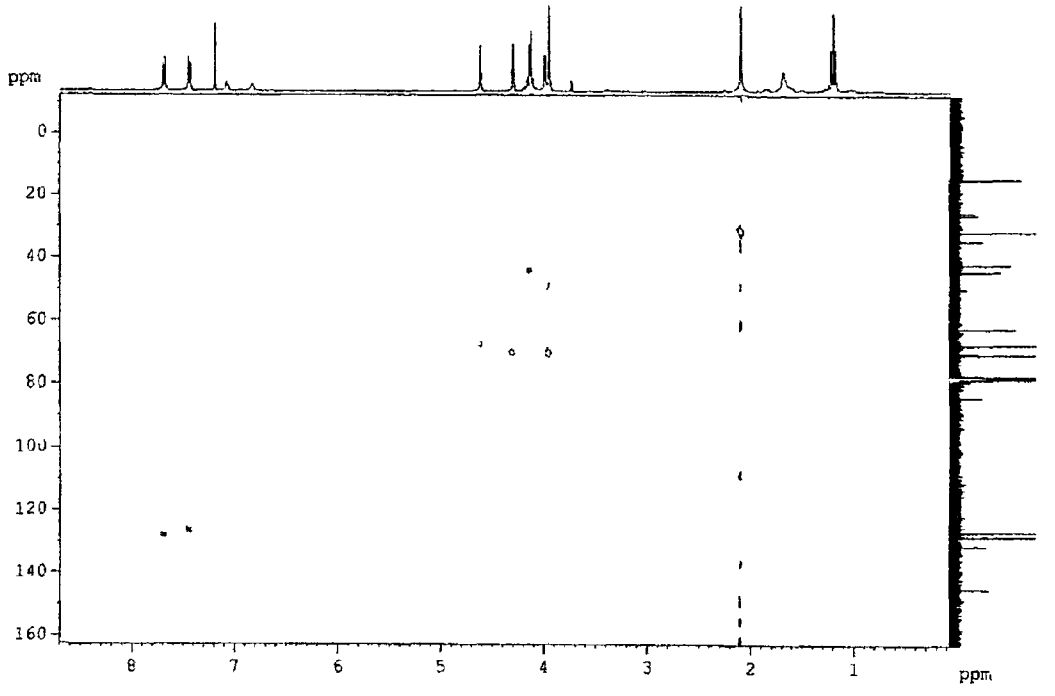

Fig 3 19 HMQC spectrum of *N*-{*para*-(ferrocenyl)benzoyl} glycine-glycine ethyl ester (**150**)

Table 3 4 C-H correlation data taken from the HMQC spectrum

position	^{1}H NMR	^{13}C NMR	HMQC
1		83 7	
2,5	4 63		67 1
3,4	4 31		70 1
6 to 10	3 96		70 2
11		144 5	
12,13	7 45		126 3
14,15	7 69		127 7
16		130 8	
17		168 1	
18	[a]4 14		44
19		[a]170 1	
20	[b]4		41 8
21		[b]169 8	
22	4 13		62 1
23	1 21		14 5

* Signals a and b may be reversed

3 6 Infrared (IR) studies of the *N*-(ferrocenyl)benzoyl dipeptide ester derivatives

IR spectroscopy is a technique that induces molecular vibrations *via* the application of infrared radiation Molecular vibrations of particular functional groups are induced at specific wavelengths Hence, absorbances at certain wavelengths in an IR spectrum are regarded as a means of confirming the presence of functional groups in a compound

3 6 1 IR study of *N*-{*ortho*-(ferrocenyl)benzoyl} glycine-glycine ethyl ester (158)

The IR spectrum of *N*-{*ortho*-(ferrocenyl)benzoyl} glycine-glycine ethyl ester (**158**), was obtained in potassium bromide (KBr) The spectrum showed peaks at 3397 and 3315 cm^{-1} These peaks correspond with frequencies expected for secondary amide N-H stretching At 3083 cm^{-1}, a band due to aryl C-H bonds is observed The ester carbonyl shows an intense peak at 1737 cm^{-1}, this frequency is entirely consistent with the expected value for a carbonyl in a O=C-O system [12] The amide carbonyl groups appear at 1657 and 1650 cm^{-1}, again these are roughly anticipated values Characteristic bands of six membered aromatic ring systems (in this case benzene) appear at 1560, 1524 and 1486 cm^{-1} respectively The C-O bond shows a strong band at 1202 cm^{-1} as expected, while the fingerprint region of this spectrum shows a complicated pattern of peaks and cannot easily be interpreted

Table 3 5 Selected IR data The values quoted are in cm^{-1}

Compound	N-H	$C=O^{amide}$	$C=O^{ester}$	Aryl C-H
140	3327, 3198	1629, 1609	1741	1543, 1507,
146	3287	1653, 1638	1750	1537, 692
149	3326, 3178	1656, 1638	1753	1529, 1509, 762
150	3321	1684, 1622	1735	1575, 1503
154	3380, 3265	1691, 1637	1729	1580, 1552, 692
155	3358, 3257	1687, 1639	1735	1561, 1542
160	3397, 3331	1654, 1648	1736	1523, 1502, 701

3 7 UV-Vis study of *N*-(ferrocenyl)benzoyl dipeptide ester derivatives

UV-Vis spectroscopy has been employed for the structural characterization of the *N*-(ferrocenyl)benzoyl dipeptide ester derivatives This study has yielded informative structural data pertaining to the varying degrees of conjugation observed in the *ortho*, *meta* and *para* *N*-(ferrocenyl)benzoyl dipeptide ester derivatives

3 7 1 A comparative study of the UV-Vis spectra of *N*-{*ortho*, *meta* and *para*-(ferrocenyl)benzoyl} glycine-glycine ethyl esters

The UV-Vis spectrum of the *N*-{*para*-(ferrocenyl)benzoyl} glycine-glycine ethyl ester show local maxima at 352 nm and 447 nm respectively These local maxima have extinction coefficients (ε) of 2220 and 760 respectively This compares with its *ortho* and *meta* derivatives, which have much weaker absorbances at shorter wavelengths *i e* the *meta* derivative has its absorbances at 325 nm and 443 nm with extinction coefficient values of 1140 and 330, while the visible bands of the *ortho* derivative appear at 326 and 439 nm with ε values of 1520 and 310 respectively It can be concluded that these spectra yield structural information regarding the degree of conjugation of the three derivatives UV-Vis spectra of *N*-{*ortho*, *meta* and *para*-(ferrocenyl)benzoyl} glycine-glycine ethyl esters were obtained in acteonitrile When these spectra were compared to the analogous *N*-ferrocenoyl derivatives the obvious difference was the presence of the π-π^* transitions of the benzoyl group whose λ_{max} values usually occur at 340-360 nm [2]

Each sample was made up to a 4 x 10^{-4} M solution so as to enable the acquisition of extinction coefficients that can be compared The three spectra were then plotted on the same axis (Figure 3 20) The difference between the spectra of the *para* derivatives and the *ortho* and *meta* derivatives is striking It is noteworthy that all three compounds show very strong absorbances in the UV region, however in this case more useful information is obtained from the visible region *i e* at wavelengths greater than 264 nm

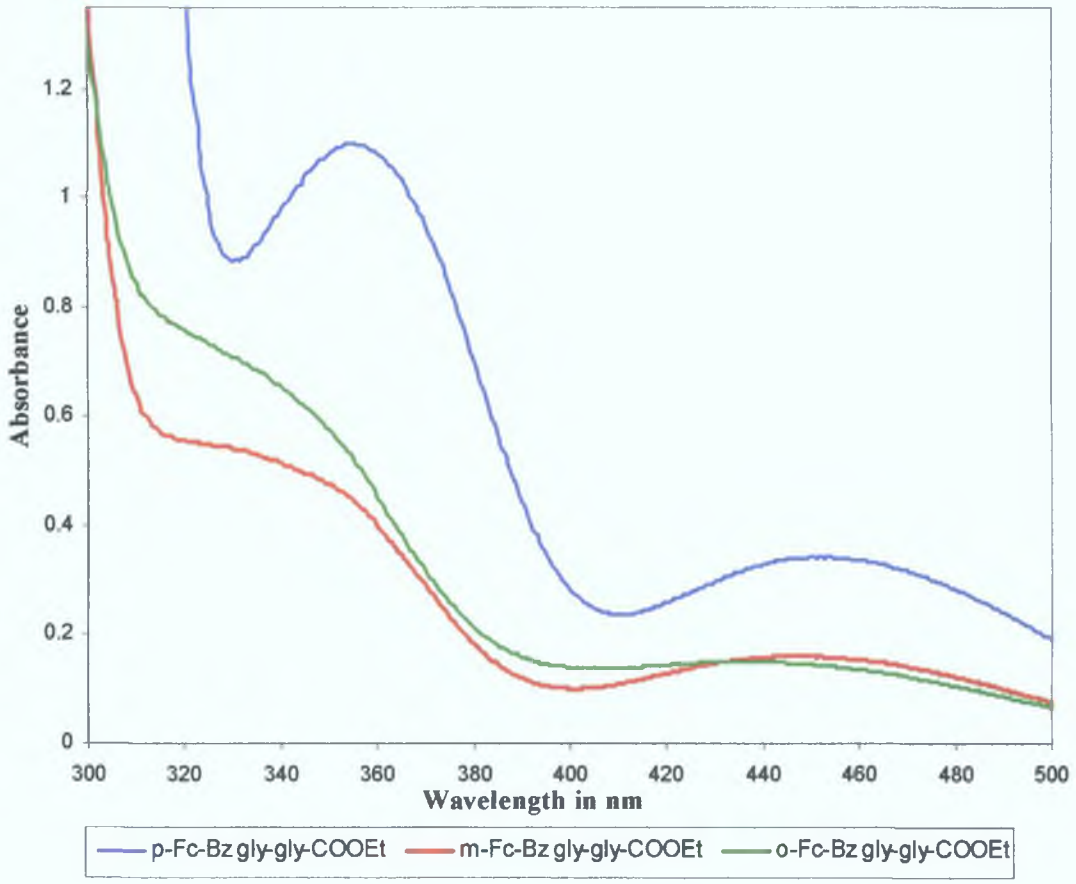

Fig 3.20 UV-Vis spectra of *N*-{*ortho, meta* and *para*-(ferrocenyl)benzoyl} glycine-glycine ethyl ester derivatives.

Table 3.6 Selected UV-Vis data. The values quoted below are in nm.

Compound no.	$\lambda_{max\,1}$(nm)	ε_1	λ_{max2}(nm)	ε_2
138	352	2400	450	720
141	352	2730	449	890
145	325	1540	443	430
146	321	1050	441	240
151	349	1870	447	560
155	325	1290	442	370
160	323	1570	440	360

3 8 A Mass Spectrometric study of the *N*-(ferrocenyl)benzoyl dipeptide ester derivatives.

Mass spectrometry is a spectroscopic technique that is employed in order to obtain relative molecular mass data In order to analyze non volatile *N*-(ferrocenyl)benzoyl dipeptide ester derivatives, soft ionization techniques such as fast atom bombardment, electrospray, and MALDI have been employed

3 8 1 Fast Atom Bombardment Mass Spectrometry (FABMS)

Fast atom bombardment mass spectroscopy was carried out on *N*-{*para*-(ferrocenyl)benzoyl glycine-glycine ethyl ester (**150**) Inspection of the mass spectrum (Figure 3 21) shows the presence of peaks due a radical cation species M^+ at *m/z* 448 and the protonated species $[M + H]^+$ at one mass unit higher Signals that appear at *m/z* 261 and 289 respectively are identical to those structurally important fragment ions generated in the FABMS of the *N*-(ferrocenyl)benzoyl amino acid derivatives (*i e* the ferrocenyl phenyl and ferrocenyl benzoyl subunits at *m/z* 261 and 289 respectively) This implies that the presence of the second glycine residue does not influence any alternative fragmentation pattern *Meta*-nitrobenzyl alcohol (NBA) was employed as the matrix, and as in the case of the FABMS for the *N*-(ferrocenyl)benzoyl amino acid derivatives, peaks corresponding to protonated matrix adducts *i e* $[Mat + H]^+$ and $[Mat_2 + H]^+$ appear at *m/z* 154 and 307 respectively The peak at *m/z* 136 corresponds to the $[Mat + H]^+ - H_2O$ adduct, however, the peak at *m/z* 289 which is due to the ferrocenyl benzoyl subunit is isobaric with the $[Mat_2 + H]^+ - H_2O$ adduct

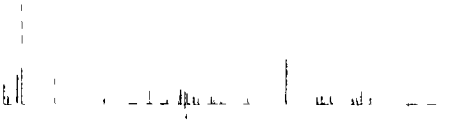

Fig 3 21 FABMS spectrum of *N*-{*para*-(ferrocenyl)benzoyl} glycine-glycine ethyl ester (**150**)

3 8 2 Electrospray Ionization Mass Spectrometry (ESIMS)

ESI mass spectrometry was carried out on compounds **139**, **141**, **146** The spectra were run in positive mode and negative mode Accurate mass and tandem MS data were also obtained

The positive ion mode mass spectrum of the compound *N*-{*para*-(ferrocenyl)benzoyl}-L-alanine-L-phenylalanine ethyl ester (**141**) shows an intense molecular ion peak at *m/z* 552 The appearance of this peak confirms the molecular mass of the compound and reveals the presence of a radical cationic species $[M]^{+\bullet}$ and an $[M+H]^+$ species at one mass unit higher Relatively intense peaks also appear at *m/z* 575 and 591 respectively The presence of these peaks can be attributed to there being sodium and potassium contaminants in the sample (due to the use of both KOH and NaOH in the base hydrolysis of the ferrocenyl ethyl benzoate synthetic step) Sodium and/or potassium ion cations may replace protons in the formation of positive ions during electrospray, yielding ions of the form $[M + Na/K]^+$, which are separated from the fully protonated analogue, $[M+ H]^+$, by 22/38 mass units respectively

The negative ion mode data typically shows an intense [M-H] molecular ion peak which in the case of *N*-{*meta*-(ferrocenyl)benzoyl}-L-alanine-L-leucine-ethyl ester (**146**) appears at *m/z* 517 The less intense radical anion peak $[M]^{-\bullet}$ appears as expected at *m/z* 518 and the appearance of this peak confirms the molecular mass of the compound in question

3 8 2 1 Tandem Mass Spectrometry (MS/MS)

Tandem mass spectrometry (MS/MS) experiments in both negative and positive mode were also preformed

In all the tandem MS spectra of these compounds, there is a fragment ion at *m/z* 261 confirming the presence of a ferrocenyl phenyl subunit at the *N*-terminal The signal at *m/z* 289 is due to cleavage at the benzoyl carbonyl group The signal at *m/z* 331 suggests that the fragmentation process has led to the generation of an a_1 ion in the *N*-(ferrocenyl)benzoyl peptide compounds in which the first residue is L-alanine (Figure 3 23) Evidence of the generation of an a_{-1} ion is also seen in the MS/MS mass spectra of *N*-(ferrocenyl)benzoyl peptide compounds in which glycine is the first amino acid residue In these cases the a_{-1} ion peak is shifted 14 mass units lower to *m/z* 317 The

appearance of the a_{-1} ions in peptide containing compounds is unusual It is unknown as of yet whether

1 The behaviour displayed by the *N*-(ferrocenyl)benzoyl-dipeptide compounds in which glycine and alanine are the first amino acid residues in the peptide sequence, extends to other amino acids

2 Ferrocene has an influence on the position of the bond cleavage and location of the resultant charge

The identification of fragment ions arising from MS/MS analysis of peptides has been facilitated by a nomenclature system which was devised by Roepstorff [13] The appearance of a, b, or c ions suggest that charge retention has occurred at the *N* terminal, while the appearance of x, y or z ions are consistent with charge retention at the *C* terminal A schematic depiction of this system is shown in Figure 3 22

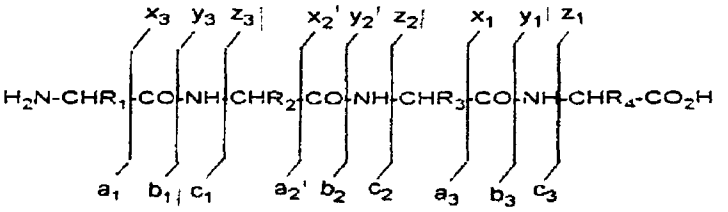

Fig 3 22 The suggested nomenclature for peptide fragment ions produced during MS/MS [30]

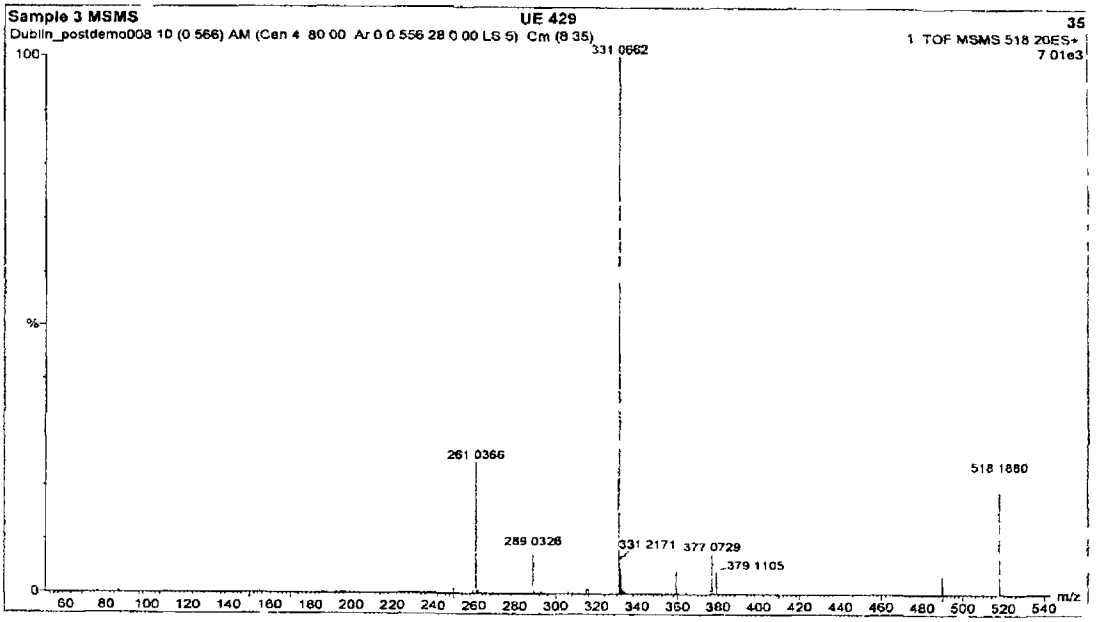

Fig 3 23 MS/MS spectrum of *N*-{*meta*-(ferrocenyl)benzoyl}-L-alanine-L-leucine ethyl ester (**146**) showing the structurally significant fragment peaks

3 8 3 Matrix-Assisted Laser Desorption Ionization Time Of Flight Mass Spectrometry (MADLI-TOF MS)

MALDI MS was carried out on compounds **138**, **140**, **142**, **143**, **145**, **147-149**, **152**, **154**, **156-160** MS/MS and accurate mass data were also obtained As with the MS/MS data obtained using the ESI technique, the familiar structurally significant fragment ions *i e* the ferrocenyl phenyl and the ferrocenyl benzoyl subunits, are observed at *m/z* 261 and 289 respectively In the case of *N*-{*ortho*-(ferrocenyl)benzoyl} glycine-L-phenylalanine ethyl ester (**160**), the mass spectrum not only shows the unusual a_1 ion fragment at *m/z* 317, but also the b_{-1} fragment ion at *m/z* 345 is apparent In the spectra of the *N*-{*ortho*-(ferrocenyl)benzoyl} dipeptide compounds there is a peak 65 Daltons lower than the molecular ion peak This corresponds with the loss of a cyclopentadiene (η^5-C_5H_5) group of the ferrocene moiety from the molecular ion and in the example in Figure 3 24 this signal is seen at *m/z* 473 The standard MALDI-TOF spectra are relatively simple for this class of compound The laser ionization technique does not initiate much fragmentation and hence is classified as a soft ionization technique Intense molecular ion peaks *i e* $[M]^+$ though are unusual in the MALDI MS of peptide molecules, are typically seen with this series of compounds Once again, the presence of sodium and potassium contammants is confirmed by the appearance of signals 23 and/or 39 mass units higher than the molecular ion, *i e* $[M + Na/K]^+$

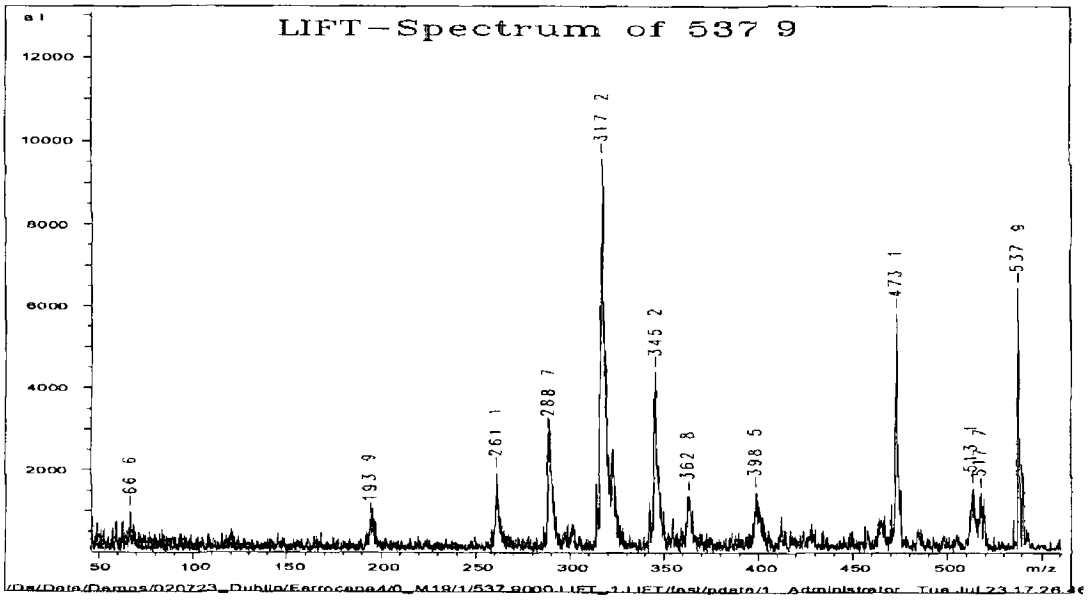

Fig 3 24 The MALDI-TOF MS/MS of *N*-{*ortho*-(ferrocenyl)benzoyl} glycine-L-phenylalanine ethyl ester (**160**)

3 9 X-ray diffraction study of *N-meta*-(ferrocenyl)benzoyl-L-alanine-L-leucine ethyl ester (146)

The structure of the dipeptide *N-meta*-(ferrocenyl)benzoyl-L-alanine-L-leucine ethyl ester (**146**) has been recently determined by single crystal diffraction methods Two molecules A and B are present in the asymmetric unit in space group $P2_12_12_1$ (Figures 3 25 and 3 26 below) These two molecules differ significantly and can best be described as having similar dipeptide conformations but with very different Fc-C_6H_4- orientations as depicted in Figure 3 27 This can best be evidenced by the interplanar angles between the C_5H_4 and C_6H_4 planes in A and B which are 3 6(3)° and 20 3(6)°, respectively The full experimental and structural description data for this structure will be reported in due course

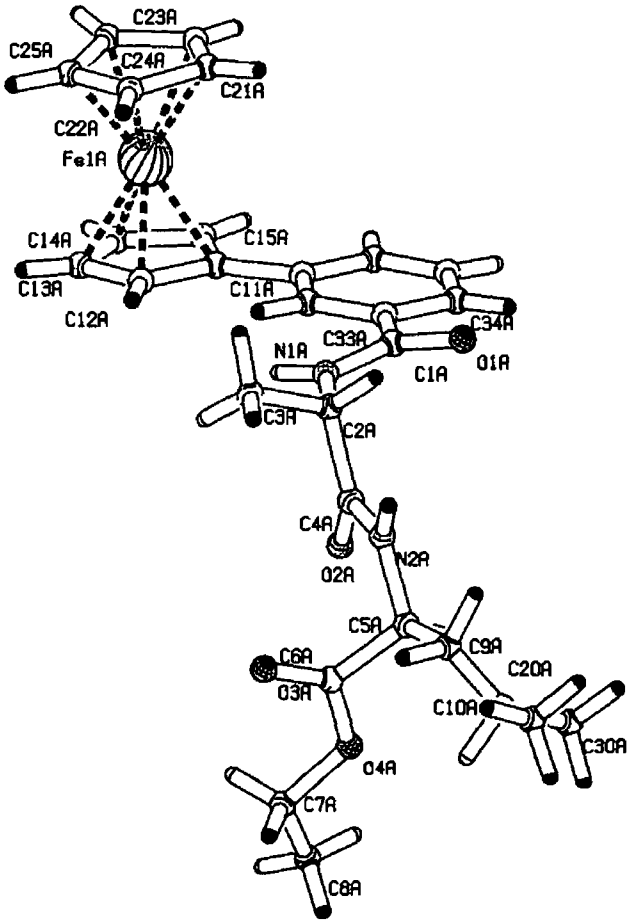

Fig 3 25 PLATON diagram of the *N-meta*-(ferrocenyl)benzoyl-L-alanine-L-leucine ethyl ester (**146**) molecule A [14]

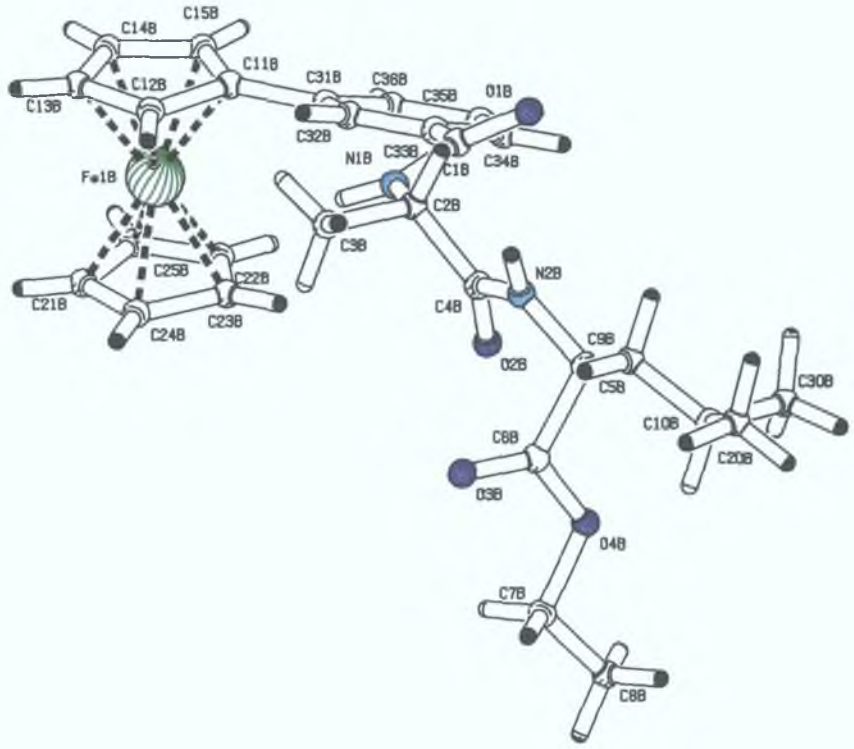

Fig. 3.26 PLATON diagram of the *N-meta*-(ferrocenyl)benzoyl-L-alanine-L-leucine ethyl ester (**146**) molecule B.[14]

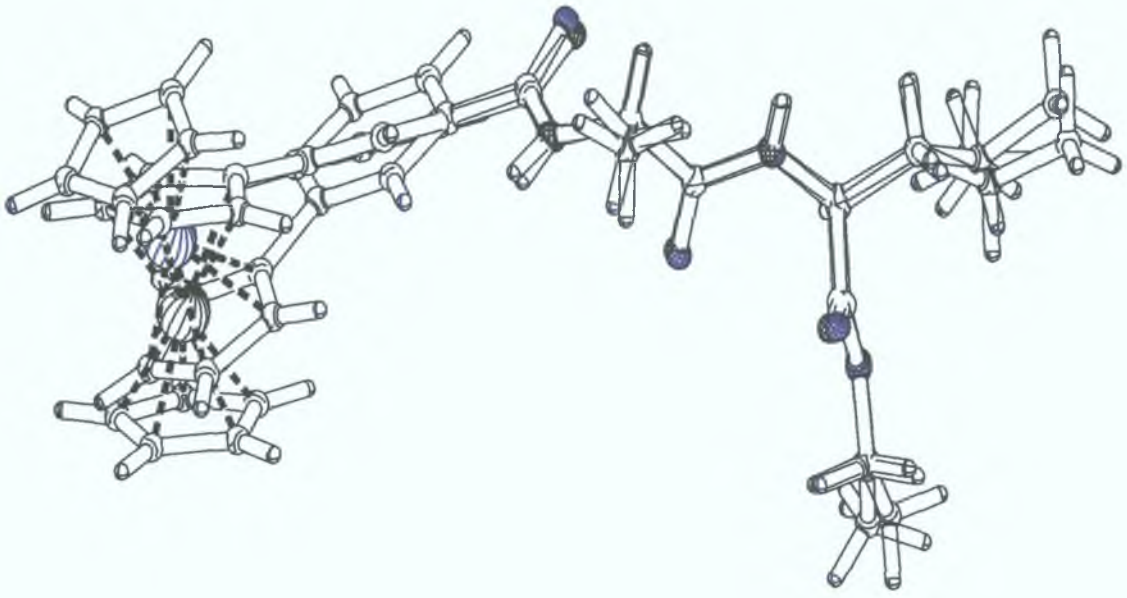

Fig. 3.27 PLATON diagram of the *N-meta*-(ferrocenyl)benzoyl-L-alanine-L-leucine ethyl ester (**146**) molecule A and B with best fit (most of the dipeptide coincides but the ferrocenylbenzoyl moiety is inverted from A to B).[14]

3 10 Conclusions

It is intended that the incorporation of organometallic fragments onto amino acids will lead to the development of new materials with innovative applications In this project, a ferrocenyl benzoyl moiety has been attached to ammo acid or dipeptide fragments using standard peptide chemistry [4] Though there are more than one potential uses for these new amino acid derivatives, the presence of both hydrogen bond donating amide and redox active moieties would suggest that they should be cheap and effective anion sensing/recognition compounds and this may be their most financially exploitable application

The synthesis of the *N*-(ferrocenyl)benzoyl ammo acid and dipeptide derivatives employed established organic chemistry and easily accessible, safe and inexpensive starting products were used to furnish unusual bio-organometallic structures In general, the products were isolated in moderately good yields The *N*-(ferrocenyl)benzoyl amino acid and dipeptide derivatives gave spectroscopic data in accordance with their structures and compared favourably (in terms of spectroscopic data) with the *N*-ferrocenyl amino acids and dipeptides which have been previously prepared and reported by Kraatz *et al* [11] and Sheehy and co-workers [12]

In future work, the yields of the *N*-(ferrocenyl)benzoyl amino acid and dipeptide derivatives may be improved by the use of more reactive coupling reagents especially in the case the *N-ortho*-(ferrocenyl)benzoyl amino acid and dipeptide derivatives In addition, the need for purification procedures may be eradicated by employing 1-{3-(dimethylamino)-propyl}-3-ethylcarbodiimide (EDC) (the coupling reagent that produces the water soluble urea byproduct) instead of DCC [6] An alternative strategy to avoid problems with steric hindrance especially when preparing the *N*-{*ortho*-(ferrocenyl)benzoyl}dipeptide ester compounds would be to couple individual amino acids to the *N*-(ferrocenyl)benzoyl ammo acid derivatives one by one instead of attaching bulky peptide chains *en masse* directly to the ferrocenyl benzoic acid moiety

References Chapter 3

1 Gallagher, J F , Kenny, P T M , Sheehy, M J , *Inorg Chem Comm* , **1999**, *2*, 327
2 Sheehy, M J , '*The Design and Synthesis of Novel Peptide Derivatives as Malarial Protease Inhibitors and Electrochemical Anion Sensing Receptors*', DCU, PhD, Thesis, **1999**
3 Savage, D , Gallagher, J F , Ida, Y , Kenny, P T M , *Inorg Chem Comm* **2002**, *5*, 1034
4 Degani, Y , Heller, A , *J Phys Chem* , *91*, 6, **1987**, 1285
5 Jones, J , '*Amino Acids and Peptide Synthesis*', Oxford Science Publications No 7 **1992**
6 Bodansky, M , '*Principles of Peptide Synthesis*', **1993**, Springer Verlag publishers
7 Begmann, M , Zervas, L , *Ber dtsch Chem Ges* , **1932**, *65*, 1192
8 Carpino, L A , *J Am Chem Soc* , **1957**, *79*, 4427
9 Anderson, G W , McGregor, A C , *J Am Chem Soc* , **1957**, *79*, 6180
10 Sieber, P , Iselin, B , *Helv Chim , Acta* , **1968**, *51*, 614, 622
11 Kraatz, H-B , Lusztyk, J , Enright, G D , *Inorg Chem* , **1997**, *36*, 2400
12 Williams, D H , Fleming, I , '*Spectroscopic Methods in Organic Chemistry*', McGraw-Hill publishers, **1995**, 5th edition
13 Roepstorff, P , Fohlman, J , *Biomed Mass Spectrom* , **1984**, *11*, 601
14 Spek, A L , PLATON, 1998, University of Utrecht, The Netherlands

Chapter 4

Anion Binding studies

4 1 Introduction

The design of molecular receptors that have the ability to selectively bind and sense cationic, anionic or even neutral guests *via* a macroscopic physical response is currently an area of intense research [1,2] The possibility of producing new materials that advance the field of molecular sensors has led to considerable interest in the development of redox active molecules in which the redox centre is in close proximity to a cation or anion binding site The utility of these systems is based upon the principle that the complexation of anionic species will cause a measurable shift in the oxidation potential of the redox active groups and hence, form the basis of useful, electrochemical sensors [3] The extent to which this shift may occur is also an important consideration in the development of amperometric devices, as this may indicate a degree of selectivity of one target over another

In investigations carried out by Beer and co-workers, hydrogen bond donating amide moieties (in the ferrocenyl complexes that were synthesized) were shown to be essential components of anion sensing molecules [4] The contribution that hydrogen bonding makes to the complexation process is usually important and can be determined by carrying out ^{1}H NMR titration studies If there are hydrogen bond interactions between the anion and the amide proton, a downfield shift of the amide proton signal from its original position is observed [5-8] ^{1}H NMR data has also shown that there are hydrogen bond interactions between the (η^5-C_5H_5) ring and the anion however, these are considerably weaker (Figure 4 1) [9]

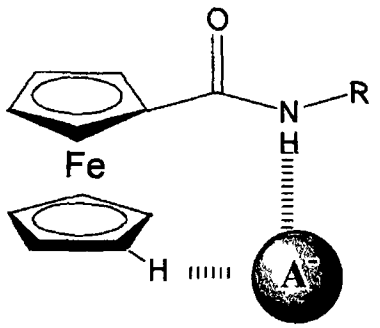

Fig 4 1 Hydrogen bonding between anion and receptor

A variety of organometallic redox active centres have been successfully incorporated into various host frameworks and shown to electrochemically detect charged and neutral guest species Of the organometallic redox active centres used, the most prevalent have been the metallocene moieties of cobaltocene and ferrocene [1] Ferrocene, because of its robustness and the simplicity of its structure is a very popular redox active building block [10] It displays almost ideal redox properties, and it is purported that its redox potential can be tuned dependmg on the nature of groups attached to it [5] The inclusion of ferrocene in anion receptor molecules therefore has a dual purpose When the ferrocene in a receptor is oxidized electrochemically to the cation, ferricenium, the receptor is in effect switched on The presence of the positive charge on the iron atom enables the ferricenium moiety to interact electrostatically with the anion It is intended that a cathodic shift will be observed in the voltammogram (with respect to the oxidation peak potential of the uncomplexed receptor) when anion complexation has occurred

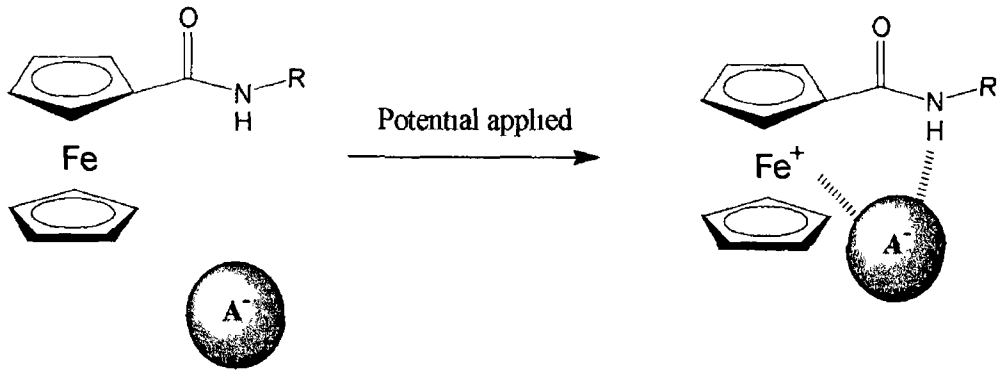

Fig 4 2 Electrochemical sensing of anions

Beer *et al* have prepared ferrocenyl amide compounds and have tested their anion recognition abilities They found that anions are bound by a combination of hydrogen bonding from amide, pyrrole or amine functionalities, and electrostatic interactions with the positively charged ferricenium moiety [4]

Similarly, Sheehy and co-workers synthesised a series of novel ferrocenoyl amino acids and dipeptides and their anion sensing capabilities were measured by a combination of electrochemistry and ^{1}H NMR titration experiments [7 8 12] The most dramatic result showed significant cathodic shifts when *N*-ferrocenoyl glycine methyl ester was in the presence of

dihydrogen phosphate anion It was reported that other receptors *e g* *N*-ferrocenoyl-phenylalanine ethyl ester did not bind anions as efficiently [7]

A study was undertaken testing the anion binding capabilities of molecules that are derivatives of those synthesized by Sheehy and co-workers This derivatisation was achieved by the inclusion of a benzoyl spacer group between the ferrocenyl and the amino acid moieties

As a result of the inclusion of a benzoyl spacer group between the redox centre and hydrogen bond donating amide groups, three different type cavities are possible, *i e* the amide functionality may be in the *ortho, meta* or *para* position with respect to ferrocene (Figure 4 3)

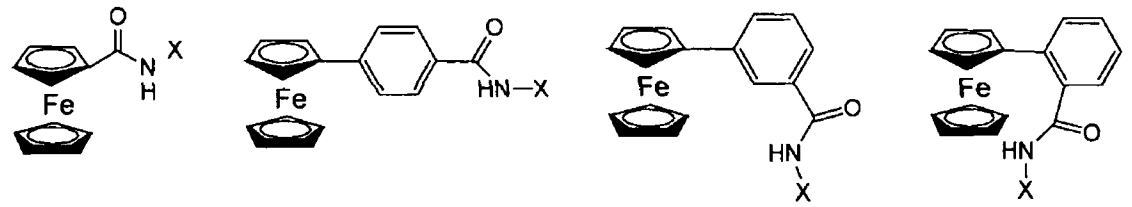

N-ferrocenoyl *para-* *meta-* *ortho-*

X = -{CH(R)CONH}$_n$-

Fig 4 3 Inclusion of phenyl spacer group enables variation in cavity size

It was anticipated that by varying the distance between the redox centre and the amide moiety, *niches* of different sizes are prepared and that it would be possible to bind anions selectively depending on which of the three derivatives was being used The receptors in this study were tested with three different anions, *i e* chloride, bromide and dihydrogen phosphate anions This study allows a comparison of the anion sensing abilities of *N*-ferrocenoyl and the *N*-ferrocenyl benzoyl derivatives and hence an evaluation of the contribution of the benzoyl spacer group to the complexation process can be made

4 2 ^{1}H NMR anion co-ordination studies of *N*-(ferrocenyl)benzoyl amino acid and dipeptide derivatives

^{1}H NMR spectroscopic studies were preformed to investigate the interaction between the neutral *N*-ferrocenyl benzoyl amino acid derivatives and various anions ^{1}H NMR provides a method of determining the non-covalent attraction between a guest and host molecules

Upon successful complexation of anionic species, a downfield shift of the amide proton signal is expected

Remarkable downfield shifts of the respective amide proton signal ranging from δ 0 5 to 2 5 have been reported in experiments involving similar receptors [7 8] This behaviour has been exhibited by *N*-ferrocenoyl glycine methyl ester upon addition of chloride, bromide and dihydrogen phosphate as their tetrabutylammonium salts ($Bu^n_4N^+X^-$, where X = Cl^-, Br^-, $H_2PO_4^-$) in $CDCl_3$ The *N*-ferrocenoyl glycine methyl ester was shown to sense halide and dihydrogen phosphate anions with a noteworthy selectivity, the trend being Cl >> $H_2PO_4^-$ > Br These results suggest that a significant CO-NH A hydrogen bonding interaction is contributing to the overall anion complexation process [11] These experiments have also shown that anions have significantly more affinity for the *N*-ferrocenoyl glycine derivative than for the L-alanine, L-leucine or L-phenylalanine derivatives [7] It was suggested that the extent of hydrogen bonding between the amide proton and the anion may be dependent on the steric bulk of the sidechain on the amino acid and hence, is only available for hydrogen bonding when an *N*-ferrocenoyl amino acid ester derivative incorporates the simplest amino acid *i e* glycine [12]

Similarly ^{1}H NMR titration experiments were conducted with *N*-ferrocenoyl dipeptide derivatives The *N*-ferrocenoyl glycine-glycine methyl ester derivative displayed the most dramatic downfield shifts of its respective amide protons upon addition of anions [8 11] This would again suggest that the amide hydrogen bonding interaction with the anion is sterically inaccessible when hydrophobic groups are attached to the amino acid It was shown to sense anions with a noteworthy selectivity, the trend bemg $H_2PO_4^-$ > Cl^- > Br

An anion coordinating study was undertaken between chloride, bromide and dihydrogen phosphate as the guest molecules and mono and dipeptide derivatives of *N*-{*ortho, meta* and *para*-(ferrocenyl)benzoyl} glycine and β-alanine as the host molecules Glycine and β-alanine amino acid derivatives were chosen for this study, as it had already been established that the most effective receptors had the simplest amino acid side-chains, *i e* the hydrogen atom, and therefore, access to the redox centre and the amide proton is not sterically hindered Also of interest was the extent to which the inclusion of a phenylene spacer group influences the anion binding properties of the *N*-(ferrocenyl)benzoyl glycine and β-alanine ester compounds

4.2.1 ^{1}H NMR anion co-ordinating studies of *N*-(Ferrocenyl)benzoyl amino acid derivatives.

The anion co-ordination abilities of these novel *N*-(ferrocenyl)benzoyl amino acid ester receptors were investigated by ^{1}H NMR anion titration experiments *via* the following general procedure:

A series of samples containing a 0.01 mol dm^{-3} solution of the respective receptor molecules were prepared. To these samples, solutions of varying anion concentrations, *i.e.* 0, 0.2, 0.4, 0.6, 0.8, 1, 2, 3 and 4 equivalents respectively, were added and their ^{1}H NMR spectra were subsequently recorded. The result of the experiments was a plot of displacement in chemical shift of the amide proton (from its position in the spectrum with zero equivalents of anion) as a function of the amount of anion added.

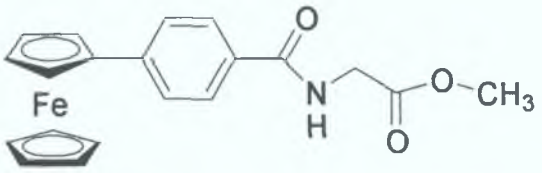

Fig 4.4 The structure of *N*-{*para*-(ferrocenyl)benzoyl} glycine methyl ester

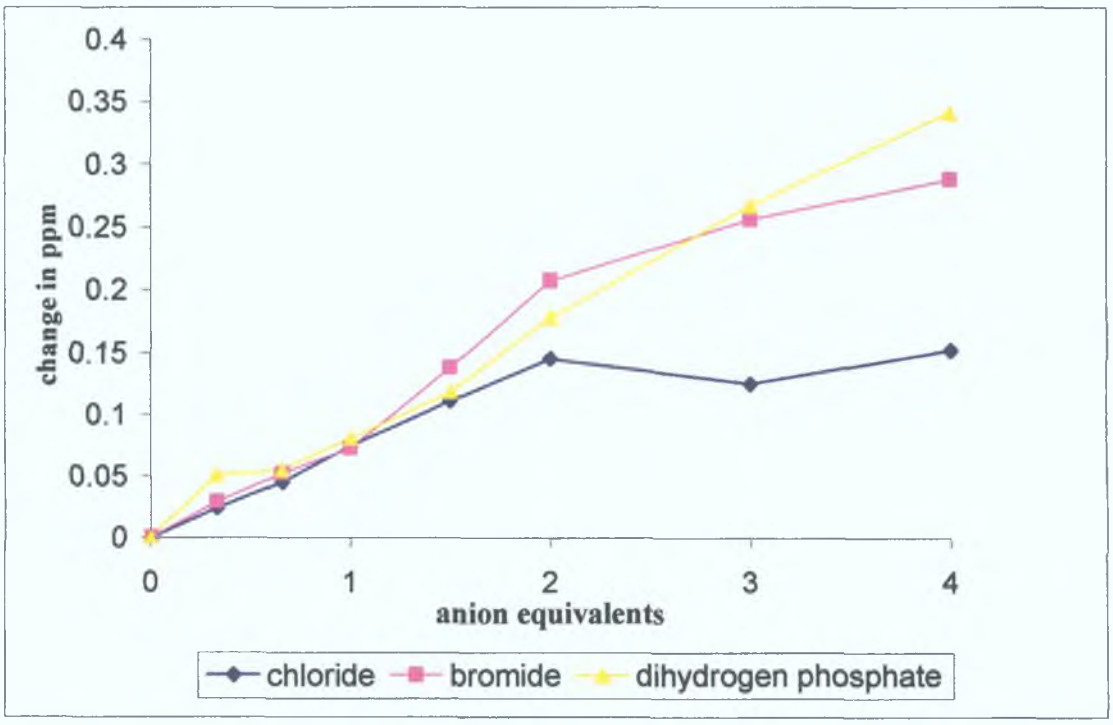

Fig 4.5 ^{1}H NMR titration curves representing the downfield shift of the amide proton of *N*-{*para*-(ferrocenyl)benzoyl} glycine methyl ester (**103**) upon treatment with various anions introduced as their tetrabutylammonium salts in $CDCl_3$.

The above plot of chemical shift of the amide proton signal versus equivalents of anion added indicates that the extent to which anion complexation occurs is very small When compared to the titration curve of *N*-ferrocenoyl glycine methyl ester derivative, (where there were quite significant downfield shifts of 2 5 ppm in the case of the titration with chloride ion), there appears to be a stark difference in its ability to form hydrogen bonds and hence complex anions [7] Furthermore, although there is a very slight downfield shift of the amide proton signal upon addition of a 2-4 equivalents of anion, there does not seem to be any selectivity at all This contrasts sharply with the *N*-ferrocenoyl glycine derivative where the receptor shows more affinity for the chloride ions than for either dihydrogen phosphate or bromide ion [7] Hence, it is possible to conclude from the results of these ^{1}H NMR titration experiments that *N*-{*para*-(ferrocenyl)benzoyl} glycine methyl ester does not selectively bind or even form hydrogen bonds efficiently with chloride, bromide or dihydrogen phosphate anions ^{1}H NMR titration experiments with *ortho* and *meta* *N*-(ferrocenyl)benzoyl glycine derivatives proved also to be poor anion receptors for the anion tested giving broadly similar results to those obtained for the *para* derivative

A similar series of experiments were carried out with the *N*-(ferrocenyl)benzoyl-β-alanine compounds It was thought that the extra methylene group (with respect to the glycine derivatives) may give the compound more flexibility to wrap around the potential host molecule and therefore enhance the degree to which it may complex guest molecules The ^{1}H NMR titration experiments were carried out as before

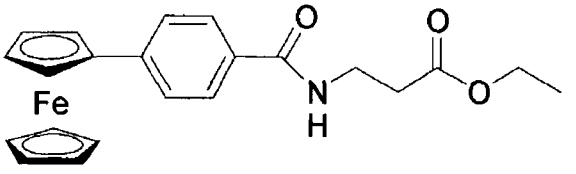

Fig 4 6 The structure of *N*-{*para*-(ferrocenyl)benzoyl}-β-alanine ethyl ester (**111**)

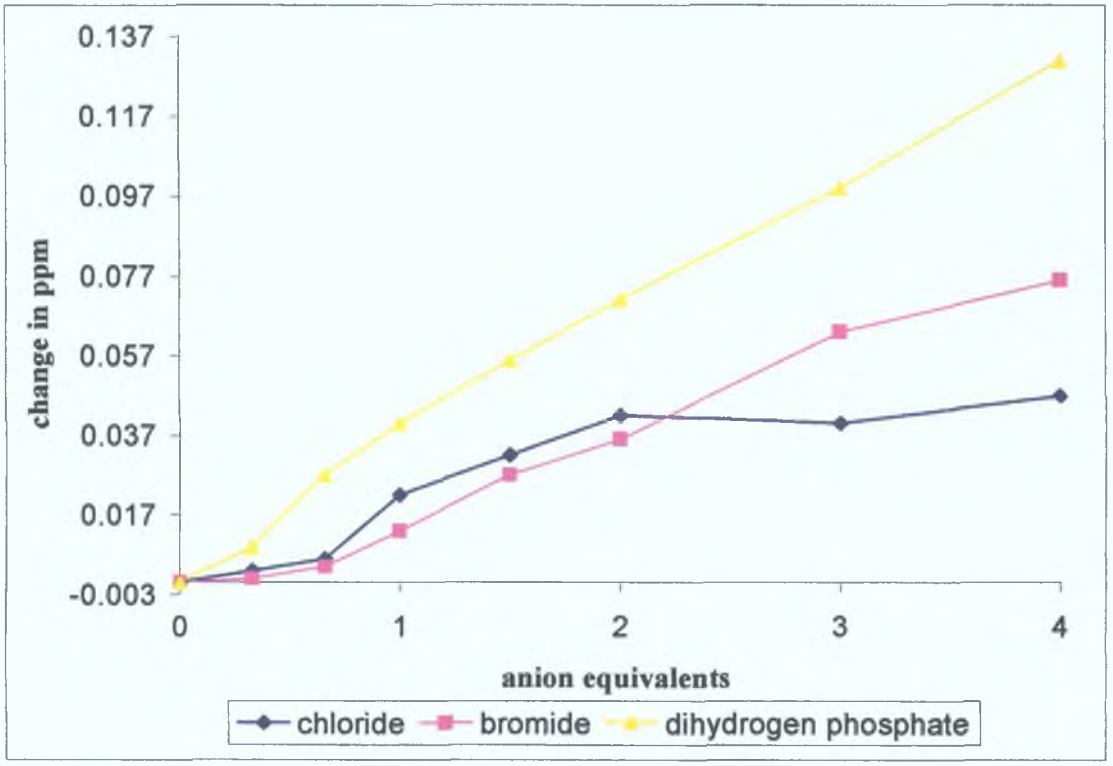

Fig 4.7 ^{1}H NMR titration curves representing the downfield shift of the amide proton of *N*-{*para*-(ferrocenyl)benzoyl}-β-alanine ethyl ester (**111**) upon treatment with various anions introduced as their tetrabutylammonium salts in $CDCl_3$.

This series of experiments shows that the receptor *N*-{*para*-(ferrocenyl)benzoyl}-β-alanine ethyl ester has very little affinity for the anions with which it is tested. Small downfield shifts of only 0.13 ppm for the dihydrogen phosphate anion are observed. These results indicate that there is actually a loss of binding ability in comparison to *N*-{*para*-(ferrocenyl)benzoyl} glycine methyl ester, so in effect the amide proton may have become less acidic and hence less available for hydrogen bonding with anions or other basic species. This could be an indication that the electron rich phenylene group is inductively feeding electron density to the carbonyl group and the amide proton as a result is not as acidic as in the *N*-ferrocenoyl compounds. However, despite the fact that this receptor does not complex anions as efficiently as the *N*-ferrocenoyl compound, perhaps some selectivity is seen. From the experimental results, it can be stated that the host molecule *N*-{*para*-(ferrocenyl)benzoyl}-β-alanine ethyl ester (**111**) has more affinity for the dihydrogen phosphate anion than for either the chloride or bromide ions.

The *meta* derivative was also examined. In this example the binding *niche* is made smaller by the positioning of the amide functionality closer to the redox centre.

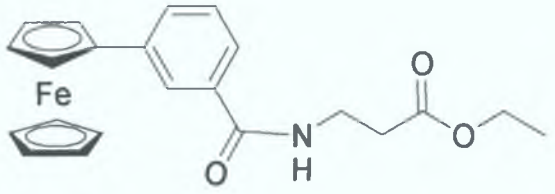

Fig 4.8 The structure of *N*-{*meta*-(ferrocenyl)benzoyl}-β-alanine ethyl ester (**125**).

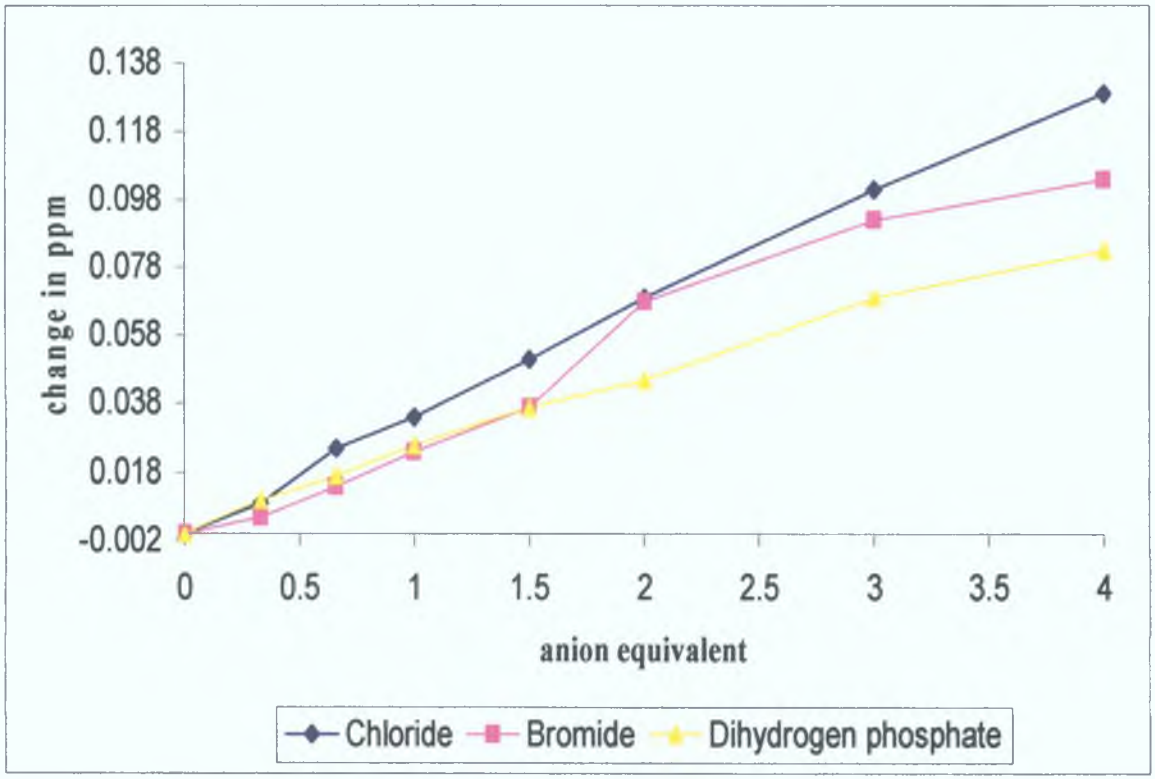

Fig 4.9 ^{1}H NMR titration curves representing the downfield shifts of the amide proton of *N*-{*meta*-(ferrocenyl)benzoyl}-β-alanine ethyl ester (**125**) when various anions are introduced as their tetrabutylammonium salts in $CDCl_3$.

Again, only very small downfield shifts are observed and this indicates poor interaction between the host and guest molecules. The extent to which the amide proton is shifted is very similar to the *para* derivative; however, selectivity seems to have been reversed. This time chloride ion has the strongest affinity with the host molecule, whereas dihydrogen phosphate is more weakly bound.

The *N*-{*ortho*-(ferrocenyl)benzoyl}-β-alanine ethyl ester (**135**) receptor behaves in a similar fashion *i.e.* small downfield shifts and a degree of selectivity favouring chloride ions is observed. In the case of *N*-{*ortho*-(ferrocenyl)benzoyl}-β-alanine ethyl ester (**135**), the binding *niche* is quite small and is unable to accommodate large anions like bromide or dihydrogen phosphate. However, due to the small size of the chloride ion it is complexed by the host molecule albeit to a very small degree.

4.2.2 ^{1}H NMR anion co-ordinating studies of *N*-(ferrocenyl)benzoyl dipeptide derivatives.

Anion co-ordination studies of these novel *N*-(ferrocenyl)benzoyl dipeptide receptors were investigated by ^{1}H NMR anion titration experiments. The solution of receptor was of the order of 0.01 mol dm^{-3} in deuterated $CDCl_3$. A series of samples with varying anion concentrations were prepared and their spectra were recorded. The result of the experiments was a plot of displacement in chemical shift of the amide proton signals as a function of equivalents of anion added.

The compound *N*-{*para*-(ferrocenyl)benzoyl}-β-alanine-β-alanine ethyl ester (**142**) was prepared. As this compound is a modified dipeptide, there are two amide moieties present, and hence it was intended that the extra ability to form hydrogen bonds with anions may enhance the binding process.

The results of the ^{1}H NMR titration experiments suggested that *N*-{*para*-(ferrocenyl)benzoyl}-β-alanine-β-alanine ethyl ester (**142**) did bind the selected anions to a significant degree. Downfield shifts of 1 ppm and 0.6 ppm respectively for the amide signals were observed upon addition of dihydrogen phosphate anion. These titration curves suggest that this receptor can selectively bind anions with the trend being $H_2PO_4^-$>Br^->Cl^-. These observations are rationalised in a number of ways.

1. The binding *niche* has been increased in size and as such, it may accommodate larger anions rather than smaller ones.
2. Because of the increase in size of the binding cavity, the steric bulk of the ferrocenyl and phenylene groups become less of a hindrance to complexation.
3. As this is a modified dipeptide, there are two amide moieties present that are available for hydrogen bonding with the respective anions. This is evident from the ^{1}H NMR

spectra, as both amide signals show downfield shifts and therefore, it is clear that both amide protons participate in the binding process.

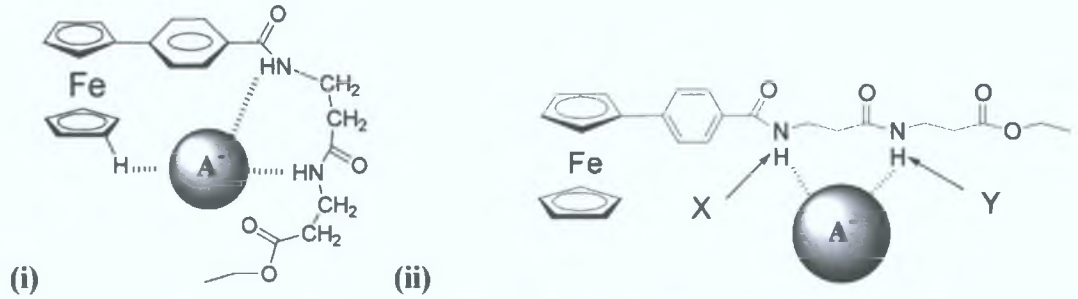

Fig 4.10 **(i)** Proposed interactions of anion with receptor molecule (**142**). **(ii)** Protons X and Y are the amide protons which contribute most to hydrogen bonding.

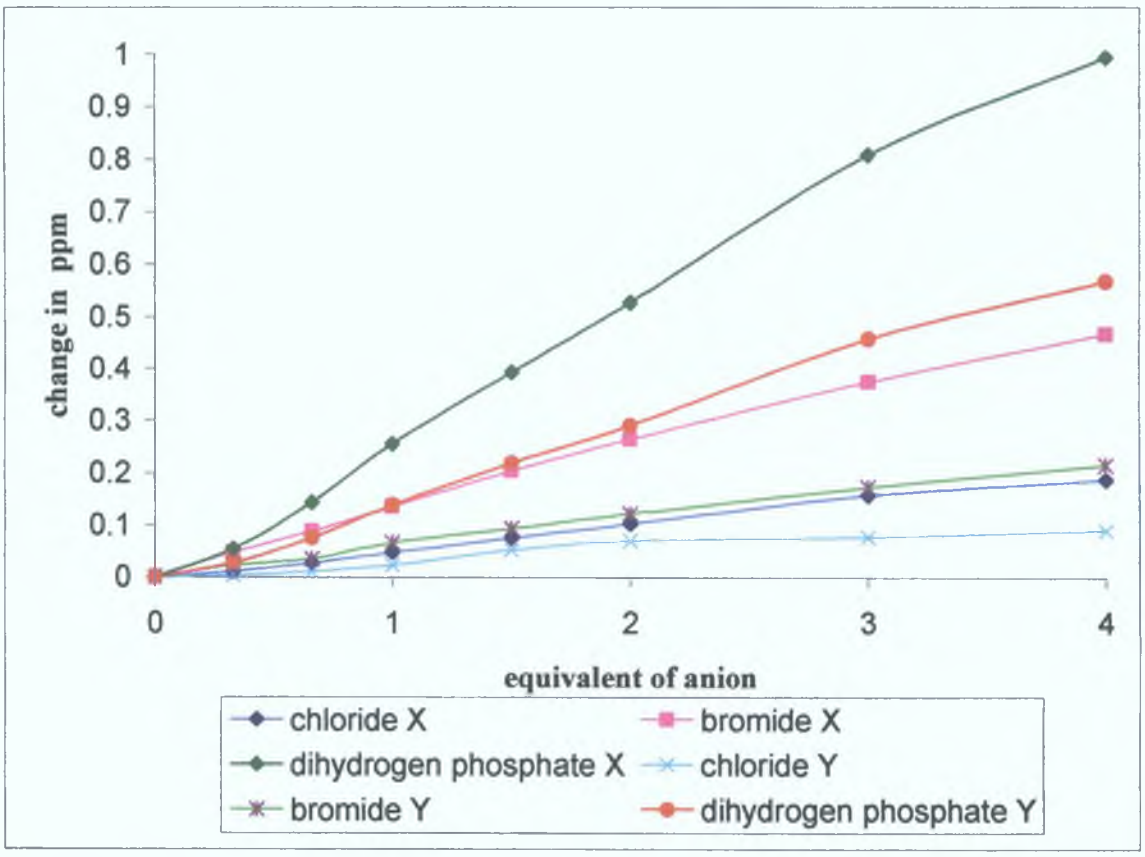

Fig 4.11 ^{1}H NMR titration curves of *N*-{*para*-(Ferrocenyl)benzoyl}-β-alanine-β-alanine ethyl ester (**142**) representing the shift of the furthest downfield amide proton upon treatment with various anions introduced as their tetrabutylammonium salts in $CDCl_3$.

From the above plot of "change in ppm versus anion equivalents", it is possible to state that anions have more affinity for amide proton X than for amide proton Y This is explained by comparing the relative downfield shifts of proton X and proton Y Proton X has been shifted 1 ppm downfield as opposed to the shift of 0 6 ppm as experienced by proton Y Unlike the result obtained in case of the *N*-ferrocenoyl glycine-glycine ethyl ester where ^{1}H NMR the titration curve indicates that two anions have been complexed, the shape of this anion titration curve does not yield information as to the ratio of host to guest

4 3 Electrochemical co-ordinating studies of *N*-(ferrocenyl)benzoyl amino acid derivatives

Cyclic voltammetry (CV) is perhaps the most versatile electroanalytical technique for the study of electroactive species [13 14] CV has been extensively exploited in order to establish redox properties of organometallic compounds [15] The redox behaviour of ferrocene is well established, and hence ferrocenyl compounds are ideal candidates for analysis by CV

In a CV experiment, the voltage applied to the working electrode is scanned from an initial value E_i (position A on the diagram Figure 4 9) to a predetermined limit $E_{\lambda 1}$ (position D on the diagram) These values are known as switching potentials *i e* the potentials at which the direction of the scan is reversed It is then possible to allow the instrument to scan between $E_{\lambda 1}$ and some other preselected value $E_{\lambda 2}$ (position A) as many times as is required The potential of the working electrode is controlled versus a reference electrode which in the case of these experiments is an Ag/Ag^{+} reference electrode [16]

A cyclic voltammogram is obtained by measuring the current at the working electrode during a potential scan The voltammogram is a plot of current (vertical axis) versus potential (horizontal axis)

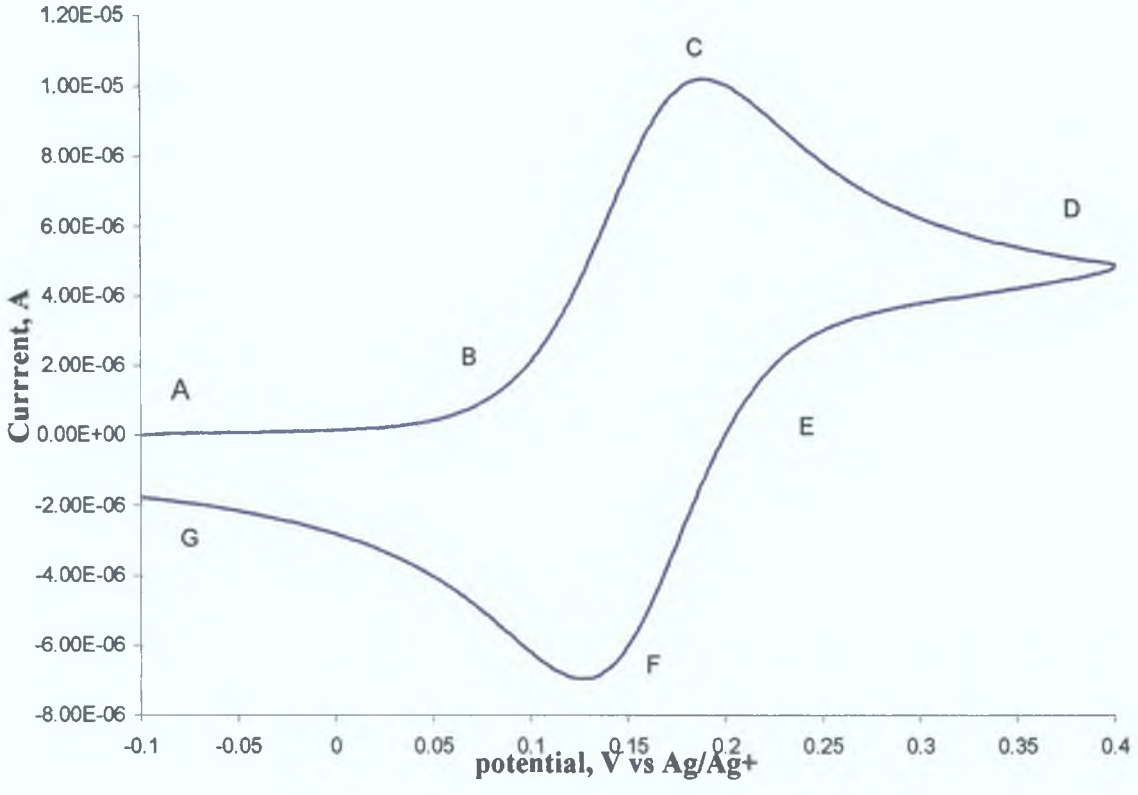

Fig 4.12 Typical cyclic voltammogram of a ferrocenyl compound.

A typical cyclic voltammogram is shown in Figure 4.12 for a platinum working electrode in a solution containing a ferrocenyl compound as the electroactive species. The switching potentials in this example are at 0.4 and -0.1 V, respectively.

A. The initial potential (E_i) is applied at -0.1 V. The potential is then scanned in a positively, *i.e.* the forward scan.

B. When the potential is sufficiently positive, the ferrocenyl compound starts to oxidize to the ferricenium compound, and as a consequence, the anodic current begins to increase.

C. The anodic current increases quickly until the concentration of ferrocenyl species at the electrode surface is diminished causing the current to peak. The current then decays as the solution surrounding the electrode is depleted of ferrocenyl compound due to its electrolytic conversion to the ferricenium species.

D. The scan direction is switched to negative at 0.4 V for the reverse scan. At this stage of the scan the ferricenium species starts to get reduced back to a ferrocenyl species, and thus the cathodic current begins.

E-G As is the case with redox systems that behave in an ideal fashion, the reverse scan roughly mirrors everything that happens on the forward scan The reverse scan ends when the current reaches the switching potential *i e* -0 1 V and if required the scan can be made cycle again

Many examples of ferrocenyl compounds electrochemically sensing anions have been reported in the literature [1,2] The CV curves for the compounds in this series of experiments exhibit the regular wave corresponding to the reversible ferrocene/ferricenium (Fc/Fc^+) redox couple (see Figure 4 12) When ferrocene functionalized receptors react with anions in non-aqueous solvents such as acetonitrile, several types of behaviour have been reported [5] For example, both the cathodic and anodic peaks of the reversible Fc/Fc^+ couple can be affected by the presence of anions that usually cause both oxidation and reduction peaks of ferrocene to undergo a cathodic shift The electrochemical shift of the oxidation peak of the ferrocenyl group to more negative potentials is attributed to the interaction of the receptor with the corresponding anion Another effect that could be observed is the cathodic shift of the reduction wave of ferrocenyl groups upon addition of anionic guests This is generally attributed to the interaction between the anionic guest and the Fc^+ cations produced upon oxidation

Important parameters of the CV include the magnitudes of the anodic peak potential (E_{pa}) and the cathodic peak potential (E_{pc}) A redox couple in which both species rapidly exchange electrons with the working electrode is termed an electrochemically reversible *couple* The formal reduction potential (E°) for a reversible couple is centred between E_{pa} and E_{pc} and is given by the equation

$$E^{O`} = \frac{E_{pa} + E_{pc}}{2}$$

The formal reduction potential can be defined as the potential at which the electrochemically active compound gains an electron and hence become reduced

It has been claimed by Beer *et al* that when ferrocene (which along with ferricenium is a well behaved redox couple) is substituted, the formal reduction potential is altered [12] Further research has shown that specific substituents yield specific deviations from the ideal Fc/Fc^+ formal reduction potential [17]

4 3.1 Electrochemical anion co-ordinating studies of *N*-(ferrocenyl)benzoyl amino acid derivatives

The anion co-ordination ability of these novel *N*-(ferrocenyl)benzoyl amino acid ester receptors was investigated by cyclic voltammetric anion titration experiments

The solutions of the *N*-(ferrocenyl)benzoyl amino acid and dipeptide derivatives were all made up to 1 mM concentrations with a 0 1 M TEAP (Tetraethyl ammonium perchlorate) solution in acetonitrile acting as supporting electrolyte The electrochemical cell consisted of a platinum working electrode, a Ag/Ag^{+} reference electrode and a platinum wire auxiliary electrode The measurements were all carried out at room temperature and the scan rate was 100 mV s^{1}

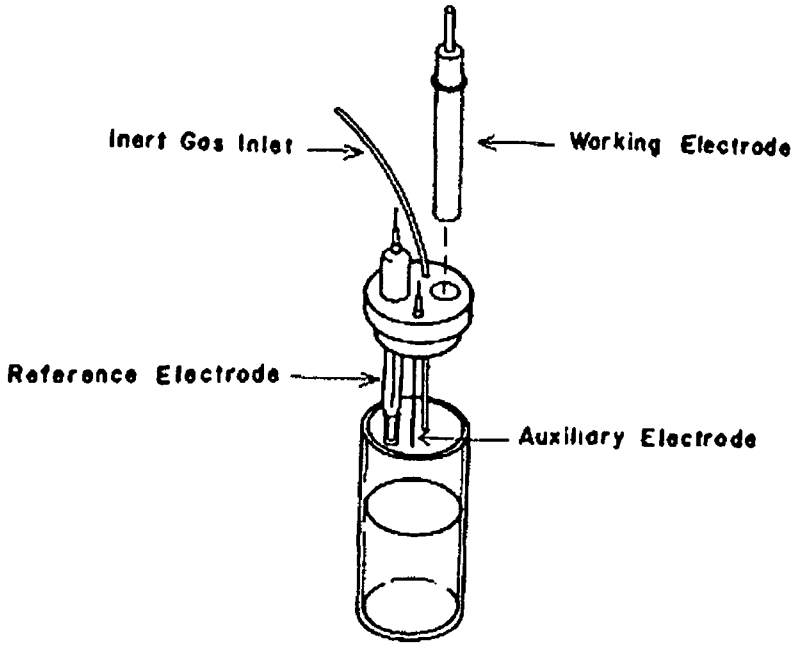

Fig 4 13 Schematic diagram of electrochemical cell as used in CV anion titration experiments **98**

The anion receptors were titrated against a series of concentrations of chloride, bromide and dihydrogen phosphate It was anticipated that the voltammogram would show the oxidation peak experiencing a shift to a more negative potential and that there would be the appearance of a two wave system upon the addition of the anions introduced as their tetra-alkyl-ammomum salts

As previously mentioned, the glycine and β-alanine derivatives were used in this series of titration experiments because the presence of hydrogen as the side group would minimize steric interference and therefore, would not inhibit possible host-guest interaction to any great degree. In addition, electrochemical anion titration data also serves to compliment the results of the ^{1}H NMR anion titration experiments.

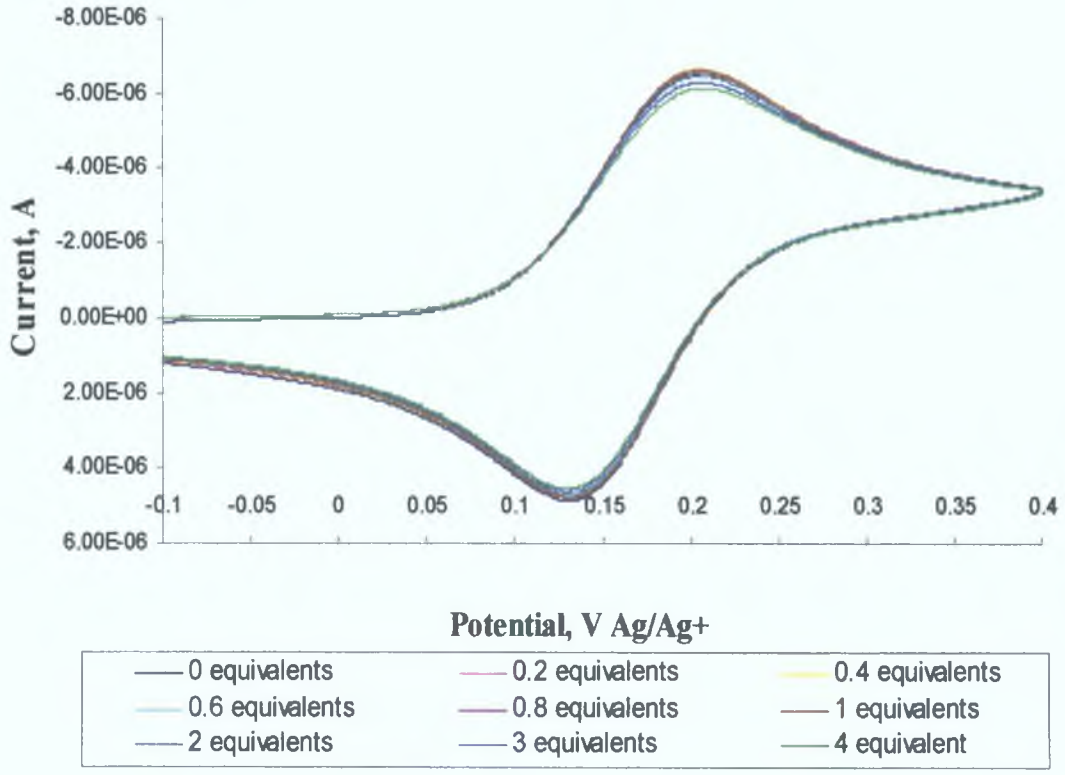

Fig 4.14 Cyclic voltammograms of titration of *N*-{*para*-(ferrocenyl)benzoyl} glycine methyl ester (**103**) with chloride ion.

The above cyclic voltammogram suggests that the receptor *N*-{*para*-(ferrocenyl)benzoyl}-glycine methyl ester (**103**) does not bind chloride ion at all. Neither the cathodic or anodic peak potentials have shifted even after the addition of four equivalents of chloride ion. The anionic size of the chloride ion is fairly small and as a consequence the positively charged iron atom and the amide proton may be too far apart to cooperatively bind the anion. In the *N*-ferrocenoyl glycine methyl ester derivatives, where the binding cavity is smaller, the chloride ion causes a cathodic shift of only 20 mV; therefore perhaps, the behaviour of this receptor towards chloride is not surprising.[7]

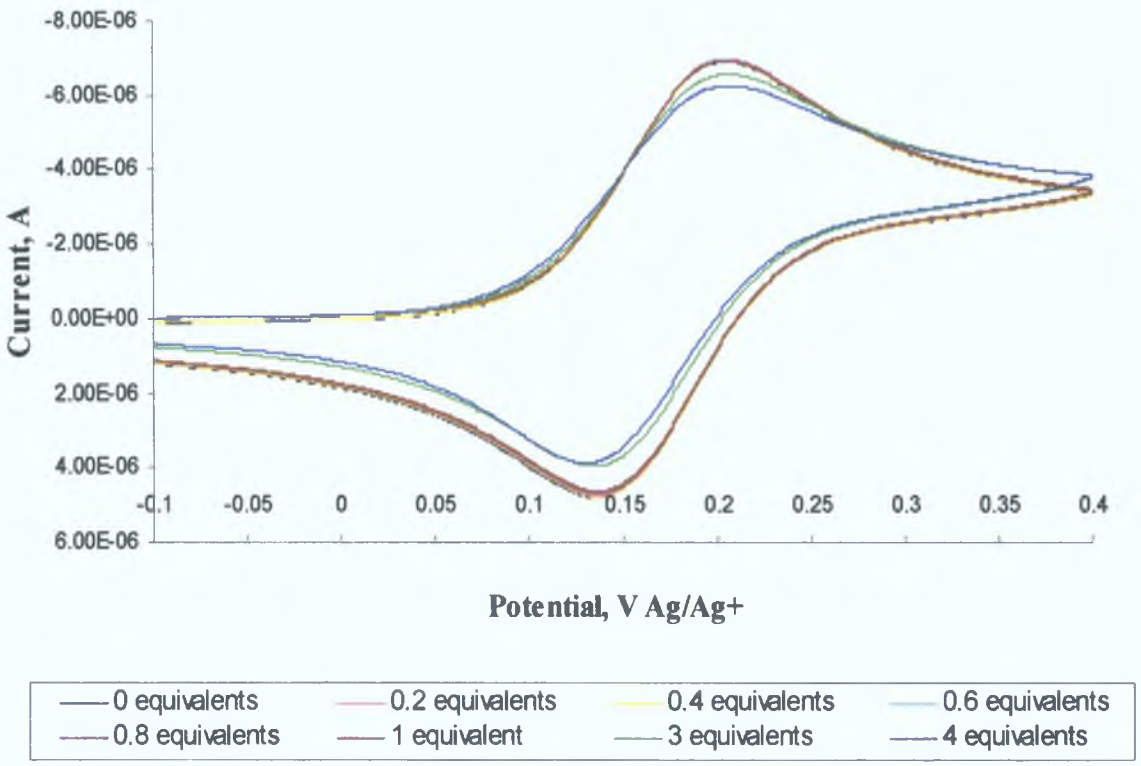

Fig 4.15 Cyclic voltammograms of titration of *N*-{*meta*-(ferrocenyl)benzoyl} glycine methyl ester (**121**) with dihydrogen phosphate ion.

The electrochemical titration of dihydrogen phosphate with the compound *N*-{*meta*-(ferrocenyl)benzoyl} glycine methyl ester (**121**) again shows no evidence of complexation. There is no anodic or cathodic shift of the peak potentials (Figure 4.15). As previously stated, the *N*-ferrocenoyl glycine ethyl ester showed a significant shift of 120 mV upon addition of dihydrogen phosphate anion. As the dihydrogen phosphate anion is fairly large, it is suggested that the anionic radius may not be the most important consideration when attempting to explain the inability of these compounds to electrochemically recognise anions.

Similar cyclic voltammetry experiments have shown that the receptor does not complex bromide ions as again no shifts in the potential are observed.

Cyclic voltammetry titration experiments were also carried out using other potential host molecules *i.e. ortho, meta* and *para N*-(ferrocenyl)benzoyl amino acid derivatives. However, none of the *N*-(ferrocenyl)benzoyl amino acid derivatives that were titrated

against chloride, bromide or dihydrogen phosphate ion showed any evidence of anion complexation.

4.3.2 Electrochemical anion co-ordinating studies of *N*-(ferrocenyl)benzoyl dipeptide derivatives.

Anion co-ordination ability of these novel *N*-(ferrocenyl)benzoyl dipeptide ester receptors was investigated by cyclic voltammetry anion titration experiments. Experimental conditions were identical to those employed for the electrochemical titrations with the *N*-(ferrocenyl)benzoyl amino acid derivatives.

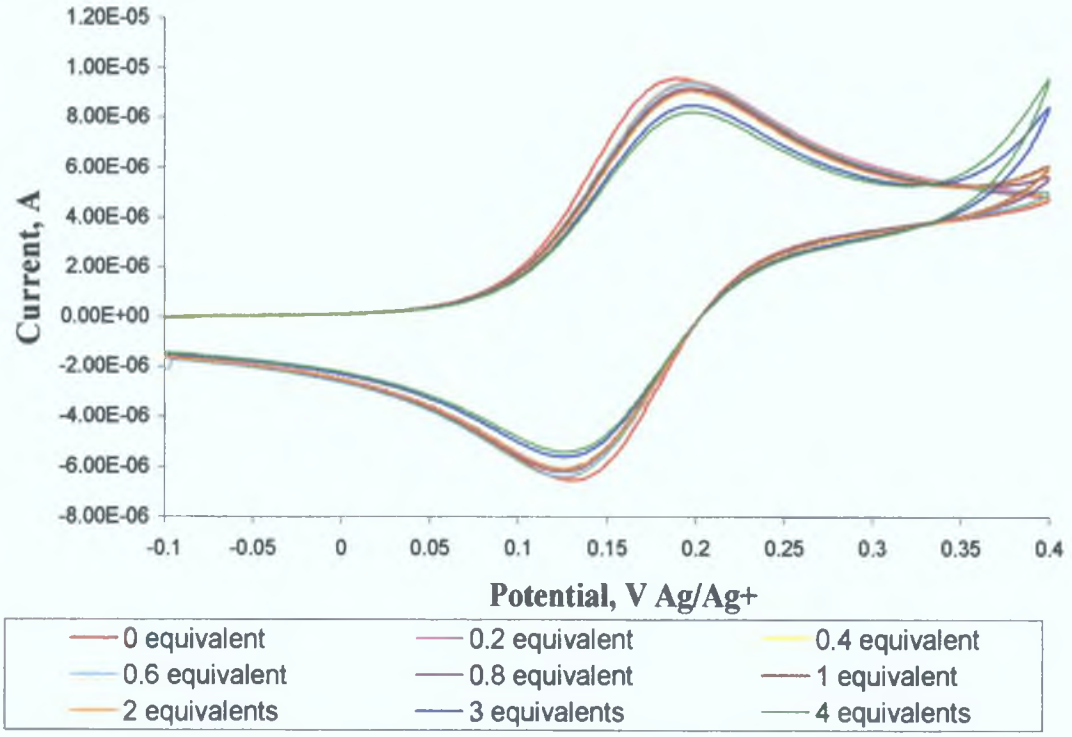

Fig 4.16 Cyclic voltammograms of titration of *N*-{*para*-(ferrocenyl)benzoyl}-β-alanine- β-alanine ethyl ester (**142**) with bromide ion.

These voltammograms show that no electrochemical recognition of anions is occurring. No shifts of the anodic or cathodic peak potentials are seen. This compares with shifts of up to 110 mV that were observed when the *N*-ferrocenoyl dipeptide derivatives were treated with various anions.[11]

All of the titrations carried out in this series of investigations show that there is no electrochemical recognition between the host *N*-(ferrocenyl)benzoyl dipeptide derivatives and the respective guest anionic species.

The data gained from the ^{1}H NMR and CV experiments suggest that the inclusion of the benzoyl spacer group into the *N*-ferrocenoyl receptors has a detrimental effect on their binding capabilities This assertion can be rationalised in a number of ways For example, as previously stated and as reported in the literature, both a redox centre and a hydrogen bond donor group are required for the successful electrochemical recognition and complexation of anions [4] The position of the benzoyl spacer group between the iron redox centre and the amide hydrogen bond donor may separate these two moieties to the extent where they are too far apart to cooperatively bind anionic species The benzoyl spacer group itself may also prevent successful binding of anionic species The steric bulk of the benzoyl group and its proximity to both redox centre and hydrogen bond donor group may prevent anions from gaining easy access to the binding *niche*

In the case of the *N*-{*para*-(ferrocenyl)benzoyl}-β-alanine-β-alanine ethyl ester (**142**) there is an apparent contradiction in the data obtained The ^{1}H NMR titration studies show that there is a degree of binding between the host molecule and dihydrogen phosphate in particular (Figure 4 11) However, in the electrochemical titration experiments there does not seem to be any complexation whatsoever This conflicting data suggests that any anion recognition that occurs is due primarily to hydrogen bond interactions between the amide moieties and the negatively charged dihydrogen phosphate anion Therefore, it can be inferred that the benzoyl group may prevent electrostatic interaction between the ferricenium moiety (generated upon electrochemical oxidation) and the anion in question

4 4 Conclusion

Whilst the recognition of cationic guest species has been extensively studied, the development of responsive ligand systems for anionic guest species is only now being researched in detail [18] The applications of an efficient and specific mode of anionic recognition would be of enormous benefit scientifically, environmentally and financially [19] Research carried out by Sheehy and co-workers demonstrated that *N*-ferrocenoyl peptides are inexpensive and effective anion sensing molecules [7 8 11] A series of host molecules were synthesised whereby a benzoyl spacer group was introduced in close proximity to both the redox centre and the hydrogen bond donating moiety This modification gave rise to a series of unusual ferrocenyl derivatives Cyclic voltammetry and ^{1}H NMR experiments provide data that would suggest that the *N*-(ferrocenyl)benzoyl peptide derivatives have very little if any affinity for the anions with which they were tested There was an

exception in the case of the *N*-{*para*-(ferrocenyl)benzoyl}-β-alanine-β-alanine ethyl ester (**142**) derivative where upon the two amide protons were shifted downfield by 1 ppm and 0 6 ppm respectively upon addition of dihydrogen phosphate This behaviour suggests that there was moderately good hydrogen bonding interaction between guest and host molecules

The CV data shows that no electrochemical recognition of anions occurs in any of the *N*-(ferrocenyl)benzoyl amino acid or dipeptide derivatives that were tested This information seems to indicate that the presence of the benzoyl group has altered the electrochemical anion sensing properties of the *N*-(ferrocenyl)benzoyl derivatives (with respect that of the *N*-ferrocenoyl series) [11] Because of the inclusion of the benzoyl group, the ferricenium no longer seems to participate m the anion complexation process This assertion can be made as no electrochemical response was evident from the CVs of the respective N-(ferrocenoyl)benzoyl amino acid or dipeptide derivative upon treatment with an anionic species Therefore, it is apparent that the redox moiety has been rendered redundant as an electrochemical signalling and anion binding device and hence, the series of receptors that were tested are ineffective host molecules

The inclusion of a less bulky spacer group such as methylene may achieve the required effect of being able to accommodate larger anions without sacrificing the contribution that the ferricemum makes to complexing and electrochemically recognising anions However, the inclusion of pyridine or pyrrole as the spacer group instead of the phenylene spacer would be a suitable aromatic substitute and may also provide hydrogen bond donating moieties and thus aiding anion complexation

References, chapter 4

1 Beer, P D , Cadman, J , *Coord Chem Rev* , **2000**, *205*, 131
2 Beer, P D , Gale, P A , *Angew Chem Int Ed Engl* , **2001**, *40*, 486
3 Beer, P D , Hazlewood, C , Hesek D , Hodacova J , Stokes, S E , *J Chem Soc* , *Dalton Trans* , **1993**, 1327
4 Beer, P D , Drew, M G B , Graydon, A R , Smith, D K , Stokes, S E , *J Chem Soc Dalton Trans* , **1995**, 403
5 Reynes, O , Maillard, F , Moutet, J C , Royal G , Saint-Aman, E , Stanciu, G , Dutosta J-P, Gosse, J , Mulatier, J-C , *J Organomet Chem* , **2001**, *637-639*, 356
6 Kingston, J E , Ashford, L , Beer, P D, Drew, M G B , *J Chem Soc Dalton Trans* , **1999**, 251
7 Gallagher, J F , Kenny, P T M , Sheehy, M J , *Inorg Chem Comm* , **1999**, *2*, 200
8 Gallagher, J F , Kenny, P T M , Sheehy, M J , *Inorg Chem Comm* , **1999**, *2*, 327
9 Beer, P D , Graydon, A R , Johnson, A O M , Smith, D K , *Inorg Chem* , **1997**, *36*, 2112
10 Togni, A , Hayashi, T , *Ferrocenes*, **1994**, VCH, Weinheim
11 Sheehy, M J , '*The Design and Synthesis of Novel Peptide Derivatives as Malarial Protease Inhibitors and Electrochemical Anion Sensing Receptors*', DCU, PhD, Thesis, **1999**
12 Beer, P D , Szemes, F , Balzani, V , Sala, C M , Drew, M G B , Dent, S W , Maestri, M , *J Am Chem Soc* , **1997**, *119*, 11864
13 Kissinger, P T , Heineman, W R , *J Chem Ed* , **1983**, *60*, 702
14 Van Benschloten, J J , Lewis, J Y , Hememan, W R , Roston, D A , Kissinger, P T , *J Chem Ed* , **1983**, *60*, 772
15 Chen, Z , Graydon, A R , Beer, P D , *J Chem Soc Faraday Trans* , **1996**, *92*, 97
16 Mabbott, G A , *J Chem Ed* , **1983**, *60*, 697
17 Kraatz, H B , Lusztyk, J , Enright, G D , *Inorg Chem* , **1997**, *36*, 2403
18 Fabbrizzi, L , Francese, G , Licchelli, M , Perrotti, A , Taglietti, A , *J Chem Soc Chem Comm* , **1997**, 581
19 Christiansson, D , Lipscomb W , *Acc Chem Res* , **1989**, 22, 62

Chapter 5

Experimental Details.

Experimental Note

Melting point determinations were carried on a Griffin melting point apparatus and are uncorrected Infra-red (IR) spectra were recorded using a Nicolet 405 FT-IR spectrophotometer Nuclear magnetic resonance (NMR) spectra were recorded on a Bruker AC 400 instrument operating at 400 MHz for ^{1}H NMR and 100 MHz for ^{13}C NMR All chemical shifts (δ) are reported in parts per million (ppm) and coupling constants (J) in Hz Ultraviolet (UV) spectra were recorded on a Shimadzu UV-Vis 3100 visible spectrometer Specific rotation $[\alpha]_D$ studies were recorded on a Perkin Elmer 241 polarimeter Fast atom bombardment (FAB) mass spectra were run on a Jeol SX 102 mass spectrometer with nitrobenzyl alcohol (NBA) as the matrix Electrospray ionisation (ESI) experiments were preformed on a Q-TOF Ultima equipped with a Waters 2790 LC system and on an Applied Biosystems Q-Star instrument MALDI TOF experiments were carried out on a Bruker Ultraflex TOF-TOF and the Shimadzu AXIMA-CFR (MALDI reflectron TOF mass analyzler) with 2,5-dihydroxy benzoic acid (DHS) as matrix Electrochemical measurements were carried out using the CHI 660 potentiostat Riedel-de Haen silica gel was used for thin layer and column flash chromatography All chemicals were purchased from the Sigma/Aldrich Company and were used without further purification The amino acid ester hydrochlorides were prepared by the method of Brenner (reference 10, chapter 2) by treating the amino acid with thionyl chloride and either methanol or ethanol Where necessary, solvents were purified prior to use and stored under nitrogen Dichloromethane was distilled from CaH_2 and triethylamine was distilled and stored over potassium hydroxide pellets Tetrahydrofuran (THF) was dried by heating under reflux over benzophenone and sodium metal until the mixture developed a deep purple colour (sodium benzophenone ketyl) followed by distillation

General procedure for the synthesis of the starting materials for the N-{para-(ferrocenyl)benzoyl} amino acid ester series

***para*-Ferrocenyl methyl benzoate 97**

Concentrated hydrochloric acid (6 ml) was added with intermittent cooling to a solution of methyl-4-aminobenzoate (3 g, 19 8 mmol) in 15 mls of water A solution of sodium nitrite (1 4 g, 20 3 mmol) in 15 ml of water was then added slowly to this mixture with stirring keeping the temperature below 5°C furnishing a pale yellow solution The resulting diazo salt was added to a solution of ferrocene (3 8 g, 20 4 mmol) in diethyl ether (90 ml) and allowed to react for 12 hours The reactant mixture was then washed with water, the ether layer was dried over $MgSO_4$ and the solvent was removed *in vacuo* to yield the crude product The crude product was purified by column chromatography (eluant 3 2 petroleum ether/diethyl ether) The crystals were of sufficient quality for an X-ray diffraction study

m p 100-102°C

I R ν_{max} (KBr) 2926, 1706, 1605, 1437, 1276, 1105 cm^{-1}

UV-Vis λ_{max} CH_2Cl_2 364 (ε 2190), 436 (810) nm

^1H NMR (400MHz) δ (DMSO) 7 64 (2H, d, J = 8 Hz, -ArH), 7 43 (2H, d, J = 8 Hz, -ArH), 4 66 {2H, t, J = 2 Hz, *ortho* on (η^5-C_5H_4)}, 4 21 {2H, t, J = 2 Hz, *meta* on (η^5-C_5H_4)}, 3 79 {5H, s, (η^5-C_5H_5)}, 3 61 (3H, s, -OCH_3)

^{13}C NMR (100MHz) δ (DMSO) 166 6, 145 5, 129 6, 126 9, 126 1, 83 0, 70 2, 68 1, 67 2, 52 3

***para*-Ferrocenyl benzoic acid 98**

Sodium hydroxide (0 3 g, 7 5 mmol) was added to *para*-ferrocenyl methyl benzoate (2 4 g, 7 5 mmol) in a 1 1 mixture of water/methanol and refluxed for three hours Concentrated HCl was added until pH 2 was reached The solution was allowed to cool and the product was isolated by filtration

m p (decomp) at 203°C

I R ν_{max} (KBr) 3449, 1678, 1607, 1284, 1105 cm^{-1}

UV-Vis λ_{max} CH_2Cl_2 368 (ε 1630), 460 (690) nm

^{1}H NMR (400MHz) δ (DMSO) 12 8 (1H, s, -COO*H*), 7 85 (2H, d, *J* = 8 Hz, -ArH), 7 64 (2H, d, *J* = 8 Hz, -ArH), 4 89 {2H, t, *J* = 2 Hz, *ortho* on (η^5-C_5H_4)}, 4 43 {2H, t, *J* = 2 Hz, *meta* on (η^5-C_5H_4)}, 4 03 {5H, s, (η^5-C_5H_5)}

^{13}C NMR (100MHz) δ (DMSO) 167 7, 145 0, 129 9, 127 3, 126 0, 83 2, 70 1, 69 9, 68 1, 67 1

General procedure for the synthesis of para-ferrocenyl benzoyl esters

para-Ferrocenyl ethyl benzoate 99

Concentrated sulfuric acid (0 5 ml) was added to *para*-ferrocenyl benzoic acid (0 3 g, 1 0 mmol) in ethanol (30 ml) and was allowed to reflux for 2-3 hours The excess solvent was subsequently removed in *vacuo* The resultant solid was redissolved in CH_2Cl_2 and was washed with water, 10% aqueous solution of sodium hydrogen carbonate and dried over $MgSO_4$ The resultant product was then purified using column chromatography {eluant 3 2 petroleum ether (40-60°C) diethyl ether} Recrystallization from diethyl ether furnished the title compound as an orange solid (0 21g, 65%)

I R ν_{max} (KBr) 2981, 2932, 1679, 1606, 1420, 1284 cm^{-1}

UV-Vis λ_{max} (MeCN) 360 (ε 2820), 454 (ε 940) nm

^{1}H NMR (400MHz) δ (DMSO) 7 86 (2H, d, *J* = 8 4 Hz, ArH), 7 66 (2H, d, *J* = 8 4 Hz, ArH), 4 90 {2H, s, *ortho* on (η^5-C_5H_4)}, 4 44 {2H, s, *meta* on (η^5-C_5H_4)}, 4 32 (2H, q, *J* = 6 Hz, -OC*H*$_2$CH$_3$), 4 03 {5H, s, (η^5-C_5H_5)}, 1 31 (3H, d, *J* = 6 Hz, -OCH$_2$C*H*$_3$)

^{13}C NMR (100MHz) δ ($CDCl_3$) 166 1, 145 5, 129 6, 127 2, 126 0, 83 0, 70 1, 69 9, 67 2, 60 9 (-ve DEPT), 14 6

para-Ferrocenyl propyl benzoate 100

For the compound **100**, propanol was used as both solvent and as a starting material (30 ml) The product was purified by column chromatography {eluant 3 2 petroleum ether (40-60°C) diethyl ether} Recrystallization from diethyl ether furnished the title compound as an orange solid (0 22g, 65%)

m p 84-86°C

I R ν_{max} (KBr) 1710, 1607, 1281, 1184 cm^{-1}

^{1}H NMR (400MHz) δ ($CDCl_3$) 7 89 (2H, d, J = 8 Hz, -ArH), 7 44 (2H, d, J = 8 Hz, -ArH), 4 63 {2H, t, J = 1 8 Hz, *ortho* on (η^5-C_5H_4)}, 4 31 {2H, t, J = 1 8 Hz, *meta* on (η^5-C_5H_4)}, 4 21 {2H, t, J = 6 8 Hz, -OCH_2CH$_2$CH$_3$}, 3 96 {5H, s, (η^5-C_5H_5)}, 1 73 {2H, sxt, J = 7 2 Hz, - OCH$_2$CH_2CH$_3$}, 0 98 {3H, t, J = 7 6 Hz, -OCH$_2$CH$_2$CH_3}

^{13}C NMR (100MHz) δ ($CDCl_3$) 167 2, 145 4, 130 1, 128 1, 126 0, 83 8, 70 2, 70 1, 67 3, 66 8, (-ve DEPT) 22 6 (-ve DEPT), 11 0

***para*-Ferrocenyl isopropyl benzoate 101**

For the compound **101**, isopropanol was used as both solvent and as a starting material (30 ml) The product was purified by column chromatography {eluant 3 2 petroleum ether (40-60°C) diethyl ether} Recrystallization from diethyl ether furnished the title compound as an orange solid (0 21 g,165%)

m p 76-78°C

I R ν_{max} (KBr) 2987, 2932, 1704, 1606, 1180, 1103, 821 cm^{-1}

UV-Vis λ_{max} (MeCN) 360 (ε 3020), 458 (ε 1120) nm

^{1}H NMR (400MHz) δ ($CDCl_3$) 7 87 (2H, d, J = 8 4 Hz, ArH), 7 43 (H, d, J = 8 4 Hz, ArH), 5 18 {1H, sept, J = 5 6 Hz, -CH(CH$_3$)$_2$}, 4 64 {2H, s, *ortho* on (η^5-C_5H_4)}, 4 32 {2H, s, *meta* on (η^5-C_5H_4)}, 3 96 {5H, s, (η^5-C_5H_5)}, 1 31 (6H, d, J = 6 Hz, -CH(CH_3)$_2$}

^{13}C NMR (100MHz) δ ($CDCl_3$) 166 6, 145 2, 130 0, 128 5, 126 0, 84 5 70 2, 70 1, 68 5, 67 3, 22 4

***para*-Ferrocenyl butyl benzoate 102.**

For the compound **102**, ^{n}butanol was used as both solvent and as a starting material (30 ml) The product was purified by column chromatography {eluant 3 2 petroleum ether (40-60°C) diethyl ether} Recrystallization from diethyl ether furnished the title compound as an orange solid (0 23 g, 65%)

m p 78-80°C

I R ν_{max} (KBr) 1708, 1606, 1272, 1181 cm^{-1}

UV-Vis λ_{max} (MeCN) 358 (ε 1790), 454 (ε 660) nm

^{1}H NMR (400MHz) δ ($CDCl_3$) 7 86 (2H, d, J = 8 Hz, ArH), 7 65 (2H, d, J = 8 Hz, ArH), 4 89 {2H, t, J = 2 Hz, *ortho* on (η^5-C_5H_4)}, 4 44 {2H, t, J = 2 Hz, *meta* on

(η^5-C_5H_4)}, 4 26 (2H, t, J = 6 8 Hz, -OCH_2CH$_2$CH$_2$CH$_3$), 4 03 {5H, s, (η^5-C_5H_5)}, 1 70 (2H, quint, J = 6 8 Hz, -OCH$_2$CH_2CH$_2$CH$_3$), 1 43 (2H, sxt, J = 6 8 Hz, -OCH$_2$CH$_2$CH_2CH$_3$), 0 94 (3H, t, J = 6 8 Hz, -OCH$_2$CH$_2$CH$_2$CH_3)

^{13}C NMR (100MHz) δ ($CDCl_3$) 166 1, 145 5, 129 6, 127 7, 126 1, 83 0, 70 2, 70 0, 67 2, 64 5 (-ve DEPT), 30 6 (-ve DEPT), 19 1 (-ve DEPT), 14 0

General procedure for the synthesis of N-{para-(ferrocenyl)benzoyl} amino acid esters

***N*-{*para*-(ferrocenyl)benzoyl} glycine methyl ester 103**

Glycine methyl ester hydrochloride (0 3 g, 2 4 mmol) and triethylamine (0 5 ml) were added to a solution of *para*-ferrocenyl-benzoic acid (**98**) (0 5 g, 1 6 mmol), 1-hydroxybenzotriazole (0 3g, 2 2 mmol) and 1,3-dicyclohexylcarbodiimide (0 45 g, 2 2 mmol) in CH_2Cl_2 (50 ml) at 0°C After 30 minutes the solution was raised to room temperature and allowed to proceed for 48 hours The precipitated *N, N'*-dicyclohexylurea was removed by filtration and the filtrate was washed with water, 10% potassium hydrogen carbonate, 5% citric acid and dried over $MgSO_4$ Recrystallization from petroleum ether (40-60°C) ethyl acetate furnished the title compound **103** as orange needles (0 32 g, 53%)

m p 116-117°C, $E_{½}$= 507 mV

Mass spectrum found $[M+H]^+$ 378 0774,

$C_{20}H_{20}N_1O_3Fe$ requires 378 0793

I R ν_{max} (KBr) 3308, 1763, 1701, 1636, 1561 cm^{-1}

UV-Vis λ_{max} CH_2Cl_2 356 (ε 1880), 454 (610) nm

^{1}H NMR (400MHz) δ (DMSO) 8 88 (1H, t, J = 5 6 Hz, -CON*H*-), 7 76 (2H, d, J = 8 Hz, -ArH), 7 60 (2H, d, J = 8 Hz, -ArH), 4 85 {2H, s, *ortho* on (η^5-C_5H_4)}, 4 38 {2H, s, *meta* on (η^5-C_5H_4)}, 3 98 {5H, s, (η^5-C_5H_5)}, 3 92 (2H, d, J = 5 6 Hz, -NHCH_2CO-), 3 63 (3H, s, -OCH_3)

^{13}C NMR (100MHz) δ (DMSO) 170 8, 166 8, 143 4, 131 0, 127 8, 125 8, 83 5, 69 9, 67 0, 52 1, 41 6 (-ve DEPT)

_N_-{*para*-(ferrocenyl)benzoyl}-L-alanine methyl ester 104

For compound **104**, L-alanine methyl ester hydrochloride (0 3 g, 2 2 mmol) was used as a starting material Recrystallization from petroleum ether (40-60°C) ethyl acetate furnished the title compound as orange needles The crystals were of sufficient quality for an X-ray diffraction study (0 28 g, 45%)

m p 137-138°C, $E_{½}$= 490 mV, $[\alpha]_D^{25}$ = +19° (c 2, CH_2Cl_2)

Mass spectrum found $[M+H]^+$ 392 0923,

$C_{21}H_{22}N_1O_3Fe$ requires 392 0949

I R ν_{max} ($CHCl_3$) 3409, 1742, 1654, 1500 cm^{-1}

UV-Vis λ_{max} CH_2Cl_2 356 (ε 1270), 452 (400) nm

^{1}H NMR (400MHz) δ (DMSO) 8 76 (1H, d, *J* = 6 8 Hz, -CON*H*-), 7 81 (2H, d, *J* = 8 Hz, -ArH), 7 72 (2H, d, *J* = 8 Hz, -ArH), 4 90 {2H, s, *ortho* on (η^5-C_5H_4)}, 4 46-4 50 {1H, m, -C*H*(CH_3)}, 4 42 {2H, s, *meta* on (η^5-C_5H_4)}, 4 02 {5H, s, (η^5-C_5H_5)}, 3 65 (3H, s, -OCH_3), 1 41 {3H, d, *J* = 7 2 Hz , -CH(CH_3)}

^{13}C NMR (100MHz) δ (DMSO) 173 7, 166 4, 143 3, 131 0, 128 0, 125 7, 83 5, 69 9, 67 0, 66 9, 52 3, 48 6, 17 1

_N_-{*para*-(ferrocenyl)benzoyl}-L-leucine methyl ester 105

For compound **105**, L-leucine methyl ester hydrochloride (0 3 g, 1 7 mmol) was used as starting material Recrystallization from petroleum ether (40-60°C) ethyl acetate furnished the title compound as a brown solid (0 28 g, 40%)

m p 96-98°C, $E_{½}$= 493 mV, $[\alpha]_D^{25}$ = + 4° (c 2, CH_2Cl_2)

Mass spectrum found $[M+H]^+$ 434 1399,

$C_{24}H_{28}N_1O_3Fe$ requires 434 1419

I R ν_{max} (KBr) 3327, 2929, 2851, 1627, 1610, 1547 cm^{-1}

UV-Vis λ_{max} CH_2Cl_2 356 (ε 1270), 454 (ε 360) nm

^{1}H NMR (400MHz) δ (DMSO) 8 69 (1H, d, *J* = 7 6 Hz, -CON*H*-), 7 81 (2H, d, *J* = 8 Hz, -ArH), 7 63 (2H, d, *J* = 8 Hz, -ArH), 4 90 {2H, t, *J* = 1 6 Hz, *ortho* on (η^5-C_5H_4)}, 4 48-4 54 [1H, m, -C*H*{$CH_2CH(CH_3)_2$}], 4 42 {2H, t, *J* = 1 6 Hz, *meta* on (η^5-C_5H_4)}, 4 02 {5H, s, (η^5-C_5H_5)}, 3 65 (3H, s, -OCH_3), 1 57-1 81 [3H, m, -CH{$CH_2CH(CH_3)_2$}], 0 93 [3H, d, *J* = 7 2 Hz, -CH{$CH_2CH(CH_3)_2$}], 0 90 [3H, d, *J* = 7 2 Hz, -CH{$CH_2CH(CH_3)_2$}]

^{13}C NMR (100MHz) δ ($CDCl_3$) 174 2, 167 4, 144 2, 131 4, 127 6, 126 2, 83 9, 70 2, 70 0, 67 2, 52 8, 51 5, 43 2 (-ve DEPT), 25 4, 23 3, 22 5

_N_-{*para*-(ferrocenyl)benzoyl}-L-phenylalanine methyl ester 106

For compound **106**, L-phenylalanine methyl ester hydrochloride (0 3 g, 1 4 mmol) was used as a starting material Recrystallization from petroleum ether (40-60°C) ethyl acetate furnished the title compound as orange crystals (0 29 g, 45%)

m p 151-152°C, $E_{½}$= 500 mV, $[\alpha]_D^{20}$ = -4° (c 1 4, CH_2Cl_2)

Mass spectrum found $[M+H]^+$ 468 1258,

$C_{27}H_{26}N_1O_3Fe$ requires 468 1262

I R ν_{max} (KBr) 3339, 2927, 1737, 1638, 1606, 1518 cm^{-1}

UV-Vis λ_{max} CH_2Cl_2 358 (ε 3370), 458 (ε 1110) nm

^{1}H NMR (400MHz) δ (DMSO) 8 83 (1H, d, J = 7 6 Hz, -CON*H*-), 7 73 (2H, d, J = 8 4 Hz, ArH), 7 61 (2H, d, J = 8 4 Hz, ArH), 7 20-7 34 (5H, m, ArH), 4 88 {2H, s, *ortho* on (η^5-C_5H_4)}, 4 64-4 72 {1H, m, -C*H*(CH_2Ph)}, 4 41 {2H, s, *meta* on (η^5-C_5H_4)}, 4 02 {5H, s, (η^5-C_5H_5)}, 3 65 (3H, s, -OC*H*$_3$), 3 11-3 17 {2H, m, -CH(C*H*$_2$Ph)}

^{13}C NMR (100MHz) δ (DMSO) 172 7, 166 7, 143 4, 138 1, 131 0, 129 4, 128 6, 127 9, 126 8, 125 8, 83 5, 69 9, 67 0, 54 7, 52 3, 36 7 (-ve DEPT)

_N_-{*para*-(ferrocenyl)benzoyl} glycine ethyl ester 107

For compound **107**, glycine ethyl ester hydrochloride (0 3 g, 2 2 mmol) was used as a starting material Recrystallization from petroleum ether (40-60°C) ethyl acetate furnished the title compound as orange needles The crystals were of sufficient quality for an X-ray diffraction study (0 351 g, 56%)

m p 102-104°C, $E_{½}$= 513 mV

Mass spectrum found $[M]^{+\bullet}$ 391,

$C_{21}H_{21}N_1O_3Fe$ requires 391

I R ν_{max} (KBr) 3308, 1735, 1700, 1685, 1211 cm^{-1}

UV-Vis λ_{max} CH_2Cl_2 358 (ε 2290), 454 (ε 740) nm

^{1}H NMR (400MHz) δ (DMSO) 8 90 (1H, d, J = 7 6 Hz -CON*H*-), 7 79 (2H, d, J = 8 Hz, ArH), 7 64 (2H, d, J = 8 Hz, ArH), 4 89 {2H, t, J = 2 Hz, *ortho* on (η^5-C_5H_4)}, 4 41 {2H,

t, J = 2 Hz, *meta* on (η^5-C_5H_4)}, 4 12 (2H, q, J = 7 2 Hz, -OCH_2CH$_3$), 4 02 {5H, s, (η^5-C_5H_5)}, 3 99 (2H, d, J = 5 6 Hz, -NHCH_2CO-), 1 21 (3H, t, J = 7 2 Hz, -OCH$_2$CH_3)

^{13}C NMR (100MHz) δ (DMSO) 170 4, 166 9, 143 4, 131 0, 127 8, 125 8, 83 5, 69 9, 67 0, 60 8 (-ve DEPT), 33 7 (-ve DEPT), 14 4

_N_-{*para*-(ferrocenyl)benzoyl}-L-alanine ethyl ester 108

For compound **108**, L-alanine ethyl ester hydrochloride (0 3 g, 2 0 mmol) was used as a starting material Recrystallization from petroleum ether (40-60°C) ethyl acetate furnished the title compound as an orange solid (0 38 g, 59%)

m p 104-106°C, $E_{½}$= 505 mV, $[\alpha]_D^{25}$ = 28° (c 2 1, EtOH)

Mass spectrum found $[M]^{+\bullet}$ 405,

$C_{22}H_{23}N_1O_3Fe$ requires 405

I R ν_{max} (KBr) 2928, 1750, 1648, 1509cm^{-1}

UV-Vis λ_{max} CH_2Cl_2 358 (ε 2670), 454 (ε 860) nm

^{1}H NMR (400MHz) δ (DMSO) 8 47 (1H, d, J = 6 8 Hz, -CONH-), 7 56 (2H, d, J = 8 Hz, ArH), 7 38 (2H, d, J = 8 Hz, ArH), 4 65 {2H, s, *ortho* on (η^5-C_5H_4)}, 4 41-4 48 {1H, m, -CH(CH$_3$)}, 4 17 {2H, s, *meta* on (η^5-C_5H_4)}, 4 12 (2H, q, J = 7 6 Hz, -OCH_2CH$_3$), 3 77 {5H, s, (η^5-C_5H_5)}, 1 48 {3H, d, J = 7 2 Hz , -CH(CH_3)}, 1 21 (3H, t, J = 7 6 Hz, -OCH$_2$CH_3)

^{13}C NMR (100MHz) δ (DMSO) 173 5, 166 5, 143 3, 131 1, 128 0, 125 7, 83 5, 69 9, 67 0, 60 8 (-ve DEPT), 48 7, 17 1, 14 5

_N_-{*para*-(ferrocenyl)benzoyl}-L-leucine ethyl ester 109

For compound **109**, L-leucine ethyl ester hydrochloride (0 3 g, 1 5 mmol) was used as a starting material Recrystallization from petroleum ether (40-60°C) ethyl acetate furnished the title compound as brown solid (0 46 g, 68%)

m p 127-129°C, $E_{½}$= 501 mV, $[\alpha]_D^{20}$ = + 3° (c 1 2, EtOH)

Mass spectrum found $[M]^{+\bullet}$ 447,

$C_{25}H_{29}N_1O_3Fe$ requires 447

I R ν_{max} (KBr) 3331, 2933, 1728, 1614 cm^{-1}

UV-Vis λ_{max} CH_2Cl_2 352 (ε 1550), 454 (ε 450) nm

^{1}H NMR (400MHz) δ (DMSO) 8 66 (1H, d, J = 7 6 Hz, -CON*H*-), 7 80 (2H, d, J = 8 Hz, -ArH), 7 62 (2H, d, J = 8 Hz, -ArH), 4 88 {2H, s, *ortho* on (η^5-C_5H_4)}, 4 50-4 6 [1H, m, -C*H*{$CH_2CH(CH_3)_2$}], 4 41 {2H, s, *meta* on (η^5-C_5H_4)}, 4 08 (2H, q, J = 6 8 Hz, -O*CH*$_2$CH$_3$), 4 02 {5H, s, (η^5-C_5H_5)}, 1 57-1 81 [3H, m, -CH{*CH*$_2$*CH*$(CH_3)_2$}], 1 19 (3H, t, J = 6 8 Hz, -OCH$_2$C*H*$_3$), 0 93 [3H, d, J = 6 4 Hz, -CH{CH_2CH(C*H*$_3$)$_2$}], 0 86 [3H, d, J = 6 4 Hz, -CH{CH_2CH(C*H*$_3$)$_2$}]

^{13}C NMR (100MHz) δ (DMSO) 173 1, 166 9, 143 3, 131 1, 128 0, 125 7, 83 5, 69 9, 67 0, 60 1(-ve DEPT), 51 4, 39 6 (-ve DEPT), 24 8, 23 2, 21 5, 14 5

_N_-{*para*-(ferrocenyl)benzoyl}-L-phenylalanine ethyl ester 110

For the compound **110**, L-phenylalanine ethyl ester hydrochloride (0 3 g, 1 3 mmol) was used as starting material Recrystallization from petroleum ether (40-60°C) ethyl acetate furnished the title compound as an orange solid (0 38 g, 61%)

m p 134-136°C, $E_{½}$= 498 mV, $[\alpha]_D^{20}$ = +48° (c 2 0, EtOH)

Mass spectrum found $[M]^{+\bullet}$ 481,

$C_{28}H_{27}N_1O_3Fe$ requires 481

I R ν_{max} (KBr) 2929, 1710, 1636, 1106 cm^{-1}

UV-Vis λ_{max} CH_2Cl_2 358 (ε 3370), 454 (ε 1070) nm

^{1}H NMR (400MHz) δ (DMSO) 8 80 (1H, d, J = 7 6 Hz, -CON*H*-), 7 73 (2H, d, J = 8 4 Hz, -ArH), 7 61 (2H, d, J = 8 4 Hz, -ArH), 7 21-7 32 (5H, m, -ArH), 4 88 {2H, s, *ortho* on (η^5-C_5H_4)}, 4 54-4 68 {1H, m, -C*H*(CH_2Ph)}, 4 41 {2H, s, *meta* on (η^5-C_5H_4)}, 4 10 (2H, q, J = 7 2 Hz, -O*CH*$_2$CH$_3$), 4 02 {5H, s, (η^5-C_5H_5)}, 3 11-3 17 {2H, m, -CH(C*H*$_2$Ph)}, 1 16 (3H, t, J = 7 2 Hz, -OCH$_2$C*H*$_3$)

^{13}C NMR (100MHz) δ (DMSO) 172 3, 166 8, 143 4, 138 0, 131 1, 129 4, 128 6, 127 9, 126 9, 125 7, 83 5, 69 9, 68 1, 67 1, 66 9, 61 0 (-ve DEPT), 54 8, 33 7 (-ve DEPT), 14 4

_N_-{*para*-(ferrocenyl)benzoyl} β-alanine ethyl ester 111

For compound **111**, β-alanine ethyl ester hydrochloride (0 3 g, 2 0 mmol) was used as a starting material Recrystallization from diethyl ether furnished the title compound as orange needles (0 34 g, 52%)

m p 137-138°C, E ° = 131 mV

Mass spectrum found $[M+H]^+$ 406 1106,

$C_{22}H_{24}N_1O_3Fe$ requires 406 1106

I R ν_{max} (KBr) 2930, 1708, 1651, 1629 cm^{-1}

UV-Vis λ_{max} CH_2Cl_2 354 (ε 1900), 452 (590) nm

^1H NMR (400MHz) δ (DMSO) 8 56 (1H, t, *J* = 5 2 Hz, -CON*H*-), 7 76 (2H, d, *J* = 8 Hz, -ArH), 7 61 (2H, d, *J* = 8 Hz, -ArH), 4 87 {2H, s, *ortho* on (η^5-C_5H_4)}, 4 39 {2H, s, *meta* on (η^5-C_5H_4)}, 4 07 (2H, q, *J* = 7 6 Hz, -OC*H*$_2$CH$_3$), 4 01 {5H, s, (η^5-C_5H_5)}, 3 50 (2H, q, *J* = 7 2 Hz, -C*H*$_2$CH$_2$-), 2 59 (2H, t, *J* = 7 2 Hz, -CH$_2$C*H*$_2$-), 1 18 (3H, t, *J* = 7 6 Hz, -OCH$_2$C*H*$_3$)

^{13}C NMR (100MHz) δ(DMSO) 171 7, 166 5, 143 0, 131 7, 127 7, 125 7, 83 6, 69 8, 66 9, 60 3 (-ve DEPT), 34 2 (-ve DEPT), 31 0 (-ve DEPT), 14 0

***N*-{*para*-(ferrocenyl)benzoyl}-4-aminobutyric acid ethyl ester 112**

For compound **112**, 4-aminobutyric acid ethyl ester hydrochloride (0 3 g, 1 8 mmol) was used as a starting material Recrystallization from diethyl ether furnished the title compound as orange needles (0 37 g, 55%)

m p 80-82°C, E ° = 132mV

Mass spectrum found $[M+H]^+$ 420 1264,

$C_{23}H_{26}N_1O_3Fe$ requires 420 1262

I R ν_{max} (KBr) 2930, 1733, 1623, 1547 cm^{-1}

UV-Vis λ_{max} CH_2Cl_2 354 (ε 1260), 450 (ε 370) nm

^1H NMR (400MHz) δ (DMSO) 8 45 (1H, t, *J* = 5 2 Hz, -CON*H*-), 7 77 (2H, d, *J* = 8 Hz, -ArH), 7 61 (2H, d, *J* = 8 Hz, -ArH), 4 88 {2H, s, *ortho* on (η^5-C_5H_4)}, 4 40 {2H, s, *meta* on (η^5-C_5H_4)}, 4 06 (2H, q, *J* = 7 6 Hz, -OC*H*$_2$CH$_3$), 4 02 {5H, s, (η^5-C_5H_5)}, 3 39 (2H, q, *J* = 7 2 Hz, -NHC*H*$_2$CH$_2$CH$_2$-), 2 36 (2H, t, *J* = 7 2 Hz, -NHCH$_2$CH$_2$C*H*$_2$-), 1 78 (2H, quint, *J* = 7 2 Hz, -NHCH$_2$C*H*$_2$CH$_2$-), 1 17 (3H, t, *J* = 7 6 Hz, -OCH$_2$C*H*$_3$)

^{13}C NMR (100MHz) δ(DMSO) 173 1, 166 4, 142 8, 131 9, 127 7, 125 7, 83 6, 69 8, 66 9, 60 1 (-ve DEPT), 33 7 (-ve DEPT), 31 4 (-ve DEPT), 24 9 (-ve DEPT), 14 5

***N*-{*para*-(ferrocenyl)benzoyl} ± 2-aminobutyric acid ethyl ester 113**

For compound **113**, ± 2-aminobutyric acid ethyl ester hydrochloride (0 3 g, 1 8 mmol) was used as a starting material Recrystallization from petroleum ether (40-60°) furnished the title compound as orange needles The crystals were of sufficient quality for an X-ray diffraction study (0 37 g, 55%)

m p 105-107°C, E ° = 136 mV

Mass spectrum found $[M]^{+\bullet}$ 419 105,

$C_{23}H_{25}N_1O_3Fe$ requires 419 118

I R ν_{max} (KBr) 3305, 2981, 2928, 1734, 1639, 1609, 1542, 1522 cm^{-1}

UV-Vis λ_{max} MeCN 350 (ε 1190), 451 (ε 350) nm

^{1}H NMR (400MHz) δ ($CDCl_3$) 7 66 (2H, d, *J* = 8 4 Hz, ArH), 7 44 (2H, d, *J* = 8 4 Hz, ArH), 6 69 (1H, d, *J* = 7 6 Hz, -CON*H*-), 4 72 {1H, q, *J* = 6 4 Hz, -C*H*(CH_2CH_3)}, 4 63 {2H, s, *ortho* on (η^5-C_5H_4)}, 4 31 {2H, s, *meta* on (η^5-C_5H_4)}, 4 18 (2H, q, *J* = 7 2 Hz, -OC*H*$_2$$CH_3$), 3 96 {5H, s, ($\eta^5$-$C_5H_5$)}, 1 91-1 98 {1H, m, -CH(C*H*$_2$$CH_3$)}, 1 74-1 89 {1H, m, -CH(C*H*$_2$$CH_3$)}, 1 24 (3H, t, *J* = 7 2 Hz, -OCH_2C*H*$_3$), 0 91 {3H, t, *J* = 7 2 Hz, CH(CH_2C*H*$_3$)}

^{13}C NMR (100MHz) δ ($CDCl_3$) 173 1, 167 3, 144 2, 131 5, 127 6, 126 2, 83 9, 70 2, 70 1, 67 2, 61 9 (-ve DEPT), 54 0, 26 2 (-ve DEPT), 14 6, 9 9

***N*-{*para*-(ferrocenyl)benzoyl} isobutyric acid ethyl ester 114**

For compound **114**, isobutyric acid ethyl ester hydrochloride (0 3 g, 1 8 mmol) was used as a starting material Recrystallization from diethyl ether furnished the title compound as an orange solid (0 22 g, 48%)

m p 130-132°C, E ° = 132 mV

Mass spectrum found $[M]^{+\bullet}$ 419 110,

$C_{23}H_{25}N_1O_3Fe$ requires 419 118

I R ν_{max} (KBr) 3223, 2928, 1741, 1621, 1610, 1567, 1521 cm^{-1}

UV-Vis λ_{max} MeCN 367 (ε 2900), 453 (ε 1060) nm

^{1}H NMR (400MHz) δ ($CDCl_3$) 7 64 (2H, d, *J* = 8 Hz, ArH), 7 44 (2H, d, *J* = 8 Hz, ArH), 6 77 (1H, s, -CON*H*-), 4 63 (2H, s, *ortho* on (η^5-C_5H_4)}, 4 31 {2H, s, *meta* on (η^5-C_5H_4)},

4 19 (2H, q, J = 7 2 Hz, -OCH_2CH$_3$), 3 97 {5H, s, (η^5-C$_5$H$_5$)}, 1 63 {6H, s, -C(CH_3)$_2$}, 1 23 (3H, t, J = 7 2 Hz, -OCH$_2$CH_3)

^{13}C NMR (100MHz) δ ($CDCl_3$) 175 4, 166 8, 143 9, 132 2, 127 5, 126 2, 83 9, 70 2, 70 0, 67 1, 62 1 (-ve DEPT), 57 3, 25 1, 14 6

General procedure for the synthesis of N-{para-(ferrocenyl)benzoyl} amino acid alcohols

N-{*para*-(ferrocenyl)benzoyl} glycinol 115

Lithium chloride (0 14 g, 3 2 mmol) and sodium borohydride (0 13 g, 3 7 mmol) were added to a solution of *N*-{*para*-(ferrocenyl)benzoyl}glycine ethyl ester (**107**) (0 43 g, 1 1 mmol) in dry THF (15 ml) and ethanol (15 ml) at 0°C The solution was stirred under nitrogen for 48 hours and then quenched with 1M HCl The reaction mixture was extracted with ethyl acetate and the organic phase was washed with water, 10% HCl, 10% $NaHCO_3$ and brine After drying over $MgSO_4$ the solvent was removed *in vacuo* Recrystallization from ethyl acetate furnished the title compound as an orange solid (0 25 g, 65%)

m p 155-157°C, $E_{½}$= 497 mV

Mass spectrum found $[M]^{+\bullet}$ 349,

$C_{19}H_{19}N_1O_2Fe$ requires 349

I R ν_{max} (KBr) 3318, 2926, 1653, 1636, 1550 cm^{-1}

UV-Vis λ_{max} EtOH 354 (ε 1840), 454 (ε 600) nm

^{1}H NMR (400MHz) δ ($CDCl_3$) 7 71 (2H, d, J = 8 Hz, -ArH), 7 51 (2H, d, J = 8 Hz, -ArH), 6 60 (1H, br s, -CON*H*-), 4 71 {2H, s, *ortho* on (η^5-C$_5$H$_4$)}, 4 39 {2H, s, *meta* on (η^5-C$_5$H$_4$)}, 4 04 {5H, s, (η^5-C$_5$H$_5$)}, 3 85-3 96 (2H, m, -CH$_2$CH_2OH), 3 65-3 71 (2H, m, -CH_2CH$_2$OH), 3 10 (1H, t, J = 5 6 Hz, -CH$_2$OH)

^{13}C NMR (100MHz) δ(DMSO) 166 5, 142 8, 132 0, 127 7, 125 7, 83 6, 69 8, 66 9, 60 2 (–ve DEPT), 42 5 (-ve DEPT)

N-{*para*-(ferrocenyl)benzoyl}-L-alaninol 116

For compound **116**, *N*-{*para*-(ferrocenyl)benzoyl}-L-alanine ethyl ester (**108**) (0 43g, 1 1 mmol) was employed as starting material Recrystallization from ethyl acetate furnished the title compound as an orange solid (0 25g, 62%)

m p decomp 110°C, $E_{½}$ = 490 mV, $[\alpha]_D^{20}$ -18° (c 1 9, EtOH)

Mass spectrum found $[M]^{+\bullet}$ 363,

$C_{20}H_{21}N_1O_2Fe$ requires 363

I R ν_{max} (KBr) 3433, 3326, 2927, 2853, 1625 cm^{-1}

UV-Vis λ_{max} CH_2Cl_2 , 356 (ε 2470), 452 (ε 840) nm

^{1}H NMR (400MHz) δ (DMSO) 8 12 (1H, d, *J* = 6 Hz, -CON*H*-), 7 84 (2H, d, *J* = 8 Hz, ArH), 7 66 (2H, d, *J* = 8 Hz , ArH), 4 94 {2H, t, *J* = 2 Hz, *ortho* on (η^5-C_5H_4)}, 4 76-4 85 {1H, m, -C*H*(CH_3)}, 4 47 {2H, t, *J* = 2 Hz, *meta* on (η^5-C_5H_4)}, 4 08 {5H, s, (η^5-C_5H_5)}, 3 46-3 58 (2H, m, - CH_2OH), 1 97 {3H, d, *J* = 6 4 Hz, -CH(CH_3)}

^{13}C NMR (100MHz) δ (DMSO) 166 0, 142 7, 132 1, 127 1, 125 2, 85 7, 69 3, 69 2, 66 4, 65 3 (-ve DEPT), 47 5, 16 2

***N*-{*para*-(ferrocenyl)benzoyl}-L-leucinol 117**

For compound **117**, *N*-{*para*-(ferrocenyl)benzoyl}-L-leucine ethyl ester (**109**) (0 49 g, 1 1 mmol) was employed as starting material Recrystallization from ethyl acetate furnished the title compound as an orange solid (0 27 g, 61%)

m p 98-99°C, $E_{½}$ = 488 mV, $[\alpha]_D^{25}$ = -23° (c 2 0, EtOH)

Mass spectrum found $[M]^{+\bullet}$ 405,

$C_{23}H_{27}N_1O_2Fe$ requires 405

I R ν_{max} (KBr) 3097, 1629, 1610, 1542, 1519 cm^{-1}

UV-Vis λ_{max} EtOH 354 (ε 2590), 454 (ε 450) nm

^{1}H NMR (400MHz) δ (DMSO) 7 98 (1H, d, *J* = 8 4 Hz, -CON*H*-) 7 47 (2H, d, *J* = 8 Hz, -ArH), 7 37 (2H, d, *J* = 8 Hz, ArH), 4 70-4 78 [1H, m, *J* = 6 Hz, -C*H*{$CH_2CH(CH_3)_2$}], 4 87 {2H, t, *J* = 2 Hz, *ortho* on (η^5-C_5H_4)}, 4 40 {2H, t, *J* = 2 Hz, *meta* on (η^5-C_5H_4)}, 4 03 {5H, s, (η^5-C_5H_5)}, 3 62-3 70 (2H, m, -CH_2OH), 1 62-1 72 [1H, m, -CH{$CH_2CH(CH_3)_2$}], 1 34-1 39 [2H, m, -CH{$CH_2CH(CH_3)_2$}], 0 78 [3H, d, *J* = 6 4 Hz, -CH{$CH_2CH(CH_3)_2$}], 0 70 {3H, d, *J* = 6 4 Hz, -CH{$CH_2CH(CH_3)_2$}]

^{13}C NMR (100MHz) δ (DMSO) 166 2, 142 6, 132 3, 127 8, 125 6, 83 7, 69 8, 69 7, 66 9, 63 0 (-ve DEPT), 48 2, 38 9 (-ve DEPT), 23 4, 21 0, 20 8

N-{*para*-(ferrocenyl)benzoyl}-L-phenylalaninol 118

For compound **118**, *N*-{*para*-(ferrocenyl)benzoyl}-L-phenylalanine ethyl ester (**110**) (0 53 g, 1 1 mmol) was employed as a starting material Recrystallization from ethyl acetate furnished the title compound as an orange solid (0 28 g, 59%)

m p 144-145°C, $E_{½}$= 482 mV, $[\alpha]_D^{20}$ = +59° (c 1 2, EtOH)

Mass spectrum found $[M]^{+\bullet}$ 439,

$C_{26}H_{25}N_1O_2Fe$ requires 439,

I R ν_{max} (KBr) 3256, 1631, 1610, 1104 cm^{-1}

UV-Vis λ_{max} EtOH 354 (ε 2130), 453 (ε 660) nm

^{1}H NMR (400MHz) δ ($CDCl_3$) 7 71 (2H, d, *J* = 8 Hz, ArH), 7 58 (2H, d, *J* = 8 Hz, ArH), 7 20-7 32 (5H, m, ArH), 6 90 (1H, d, *J* = 8 Hz, -CON*H*-), 4 80 {2H, s, *ortho* on (η^5-C_5H_4)}, 4 42 {2H, s, *meta* on (η^5-C_5H_4)}, 4 06 {5H, s, (η^5-C_5H_5)}, 3 59-3 73 (2H, m, -CH_2OH), 3 17 (1H, t, *J* = 5 6 Hz, -CH_2O*H*), 3 00-3 12 {2H, m, -CH(CH_2Ph)}

^{13}C NMR (100MHz) δ (CD_3CN) 171 4, 148 0, 145 1, 137 4, 134 7, 133 7, 133 0, 131 5, 130 8, 88 9, 75 1, 75 0, 72 1, 68 5 (-ve DEPT), 58 8, 42 1 (-ve DEPT)

General procedure for the synthesis of the starting materials for the N-{meta-(ferrocenyl)benzoyl} amino acid ester series.

***meta*-Ferrocenyl ethyl benzoate 119**

Concentrated hydrochloric acid (6 ml) was added with intermittent cooling to a solution of ethyl-3-aminobenzoate (3 g, 18 2 mmol) in 15 mls of water A solution of sodium nitrite (1 4 g, 20 3 mmol) in 15 ml of water was then added slowly to this mixture with stirring keeping the temperature below 5°C furnishing a pale yellow solution The resulting diazo salt was added to a solution of ferrocene (3 8 g, 20 4 mmol) in diethyl ether (90 ml) and allowed to react for 12 hours The reactant mixture was then washed with water, the ether layer was dried over $MgSO_4$ and the solvent was removed in *vacuo* to yield the crude product The crude product was purified using column chromatography (eluant 3 2 petroleum ether/diethyl ether)

m p 74-76°C

I R ν_{max} (KBr) 1719, 1299, 1243 cm^{-1}

UV-Vis λ_{max} MeCN 354 (ε 1280), 453 (ε 240) nm

^{1}H NMR (400MHz) δ (DMSO) 8 03 (1H, s, ArH), 7 84 (1H, d, J = 8 Hz, ArH), 7 79 (1H, d, J = 8 Hz, ArH), 7 46 (1H, t, J = 8 Hz, ArH), 4 84 {2H, s, *ortho* on (η^5-C_5H_4)}, 4 40 {2H, s, *meta* (η^5-C_5H_4)}, 4 34 (2H, q, J = 7 2 Hz, -OC*H*$_2$CH$_3$) 4 03 {5H, s, (η^5-C_5H_5)}, 1 34 (3H, t, J = 7 2 Hz, -OCH$_2$C*H*$_3$)

^{13}C NMR (100MHz) δ ($CDCl_3$) 165 7, 138 8, 131 4, 129 5, 129 2, 127 2, 125 8, 83 1, 68 6, 68 2, 67 0, 65 5 (-ve DEPT), 13 3

meta-Ferrocenyl benzoic acid 120

Sodium hydroxide (0 3 g, 7 5 mmol) was added to *meta*-ferrocenyl ethyl benzoate (**119**) (2 4 g, 7 2 mmol) in a 1 1 mixture of water/methanol and was refluxed for three hours Concentrated HCl was added until pH 2 was reached The solution was allowed to cool and the product was isolated by filtration

m p 159-161°C

I R ν_{max} (KBr) 3450, 1688 cm^{-1}

UV-Vis λ_{max} CH_2Cl_2 350 (ε 720), 436 (ε 290) nm

^{1}H NMR (400MHz) δ (DMSO) 13 2 (1H, s, -COO*H*), 8 03 (1H, s, ArH), 7 80 (1H, d, J = 8 Hz, ArH), 7 77 (1H, d, J = 8 Hz, ArH), 7 43 (1H, t, J = 8 Hz, ArH), 4 84 {2H, s, *ortho* on (η^5-C_5H_4)}, 4 39 {2H, s, *meta* on (η^5-C_5H_4)}, 4 03 {5H, s, (η^5-C_5H_5)},

^{13}C NMR (100MHz) δ (DMSO) 167 8, 140 0, 131 2, 130 7, 129 1, 127 1, 126 5, 84 0, 69 8, 69 6, 68 1, 66 8

General procedure for the synthesis of N-{meta-(ferrocenyl)benzoyl} amino acid esters

***N*-{*meta*-(ferrocenyl)benzoyl} glycine methyl ester 121**

Glycine methyl ester hydrochloride (0 3 g, 2 4 mmol) and triethylamine (0 5 ml) were added to a solution of *meta*-(ferrocenyl) benzoic acid (0 5 g, 1 6 mmol), 1-hydroxybenzotriazole (0 3 g, 2 2 mmol) and 1,3-dicyclohexylcarbodiimide (0 45 g, 2 2 mmol) in CH_2Cl_2 (50 ml) at 0°C After 30 minutes the solution was raised to room temperature and allowed to proceed for 48 hours The precipitated *N,N'*-dicyclohexylurea was removed by filtration and the filtrate was washed with water, 10% potassium hydrogen carbonate, 5% citric acid and dried over $MgSO_4$ Recrystallization from petroleum ether (40-60°C) ethyl acetate furnished *N*-{*meta*-(ferrocenyl)benzoyl} glycine methyl ester **121** as orange needles (0 36 g, 59%)

m p 109-111°C, E °= 132 mV

Mass spectrum found $[M]^{+\bullet}$ 377 068,

$C_{20}H_{19}N_1O_3Fe$ requires 377 071

I R ν_{max} (KBr) 1747, 1701, 1637, 1627, 1578 cm^{-1}

UV-Vis λ_{max} CH_2Cl_2 326 (ε 1460), 448 (ε 370) nm

^1H NMR (400MHz) δ (DMSO) 9 02 (1H, t, *J* = 5 6 Hz, -CON*H*-), 8 00 (1H, s, ArH), 7 76 (1H, d, *J* = 8 Hz, ArH), 7 72 (1H, d, *J* = 8 Hz, ArH), 7 42 (1H, t, *J* = 8 Hz, ArH), 4 86 {2H, s, *ortho* on (η^5-C_5H_4)}, 4 40 {2H, s, *meta* on (η^5-C_5H_4)}, 4 06 (2H, d, *J* = 5 6 Hz, -NHCH_2CO-), 4 04 {5H, s, (η^5-C_5H_5)}, 3 68 (3H, s, -OCH_3)

^{13}C NMR (100MHz) δ (DMSO) 170 9, 166 9, 139 8, 133 9, 129 3, 128 9, 125 2, 124 6, 84 3, 69 8, 69 5, 66 8, 52 1, 41 6 (-ve DEPT)

***N*-{*meta*-(ferrocenyl)benzoyl}-L-alanine methyl ester 122**

For the compound **122**, L-alanine methyl ester hydrochloride (0 3 g, 2 2 mmol) was used as a starting material Recrystallization from petroleum ether (40-60°C) ethyl acetate furnished the title compound as an orange solid (0 38 g, 61%)

m p 103-105°C, E ° = 128 mV, $[\alpha]_D^{20}$ = +3° (c 1 5, CH_2Cl_2)

I R ν_{max} ($CHCl_3$) 2928, 1750, 1636, 1628, 1542cm^{-1}

UV-Vis λ_{max} CH_2Cl_2 332 (ε 890), 450 (120) nm

^1H NMR (400MHz) δ (DMSO) 8 85 (1H, d, *J* = 6 4 Hz, -CON*H*-), 7 98 (1H, s, ArH), 7 70-7 86 (2H, m, ArH), 7 41 (1H, t, *J* = 8 Hz, ArH), 4 86 {2H, s, *ortho* on (η^5-C_5H_4)}, 4 50-4 59 {1H, m, -C*H*(CH_3)}, 4 39 {2H, s, *meta* on (η^5-C_5H_4)}, 4 03 {5H, s, (η^5-C_5H_5)}, 3 66 (3H, s, -OCH_3), 1 44 {3H, d, *J* = 7 2 Hz , -CH(CH_3)}

^{13}C NMR (100MHz) δ (DMSO) 173 6, 166 5, 139 7, 134 0, 129 4, 128 8, 125 4, 124 7, 84 3, 69 5, 68 1, 66 8, 52 3, 48 7, 17 1

***N*-{*meta*-(ferrocenyl)benzoyl}-L-leucine methyl ester 123**

For the compound **123**, L-leucine methyl ester hydrochloride (0 3 g, 1 7 mmol) was used as a starting material Recrystallization from petroleum ether (40-60°C) ethyl acetate furnished the title compound as a brown solid (0 43 g, 60%)

m p 154-156°C, E °=126 mV, $[\alpha]_D^{20}$ +5° (c 1 7, CH_2Cl_2)

Mass spectrum found $[M]^{+\bullet}$ 433 124,

$C_{24}H_{27}N_1O_3Fe$ requires 433 134

I R ν_{max} (KBr) 2930, 1745, 1630, 1579 cm^{-1}

UV-Vis λ_{max} CH_2Cl_2 330 (ε 1230),448 (ε 350) nm

^{1}H NMR (400MHz) δ (DMSO) 8 78 (1H, d, *J* = 7 6 Hz, -CON*H*-), 7 98 (1H, s, ArH), 7 69-7 83 (2H, m, ArH), 7 43 (1H, t, *J* = 8 Hz, ArH), 4 86 {2H, s, *ortho* on (η^5-C_5H_4)}, 4 50-4 58 (1H, m, - C*H*{$CH_2CH(CH_3)_2$}], 4 40 {2H, s, *meta* on (η^5-C_5H_4)}, 4 03 {5H, s, (η^5-C_5H_5)}, 3 67 (3H, s, -OC*H*$_3$), 1 61-1 82 [3H, m, -CH{C*H*$_2$C*H*$(CH_3)_2$}], 0 95 [3H, d, *J* = 6 4 Hz, -CH{CH_2CH(C*H*$_3)_2$}], 0 93 [3H, d, *J* = 6 4 Hz, -CH{CH_2CH(C*H*$_3)_2$}]

^{13}C NMR (100MHz) δ (DMSO) 171 6, 166 8, 139 7, 134 0, 129 4, 128 7, 125 4, 124 9, 84 5, 69 8, 69 5, 67 0, 52 3, 51 3, 39 6 (-ve DEPT), 24 4, 23 2, 21 6

***N*-{*meta*-(ferrocenyl)benzoyl}-L-phenylalanine methyl ester 124**

For the compound **124**, L-phenylalamne methyl ester hydrochloride (0 3 g, 1 4 mmol) was used as starting material Recrystallization from petroleum ether (40-60°C) ethyl acetate furnished the title compound as an orange solid (0 37 g, 56%)

m p 110-112°C, E ° = 130 mV, $[\alpha]_D^{20}$ -33 5° (c 1 4, CH_2Cl_2)

I R ν_{max} (KBr) 2929, 1751, 1635, 1534 cm^{-1}

UV-Vis λ_{max} CH_2Cl_2 328 (ε 1250), 448 (ε 310) nm

^{1}H NMR (400MHz) δ (DMSO) 8 91 (1H, d, *J* = 8 Hz, -CON*H*-), 7 90 (1H, s, ArH), 7 71 (1H, d, *J* = 8 Hz, ArH), 7 61 (1H, d, *J* = 8 Hz, ArH), 7 20-7 40 (6H, m, ArH), 4 80-4 96 {2H, m, *ortho* on (η^5-C_5H_4)}, 4 46-4 54 {1H, m, -C*H*(CH_2Ph)}, 4 39-4 48 {2H, m, *meta* on (η^5-C_5H_4)}, 4 01 {5H, s, (η^5-C_5H_5)}, 3 66 (3H, s, -OC*H*$_3$), 3 13-3 20 {2H, m, -CH(C*H*$_2$Ph)}

^{13}C NMR (100MHz) δ(DMSO) 172 7, 166 7, 139 7, 138 1, 134 0, 129 5, 129 3, 128 8, 128 6, 126 9, 125 3, 124 8, 84 3, 69 8, 69 5, 66 9, 66 7, 54 7, 52 4, 36 6 (-ve DEPT)

***N*-{*meta*-(ferrocenyl)benzoyl}-β-alanine ethyl ester 125**

For compound **125**, β-alanine ethyl ester hydrochloride (0 3 g, 2 0 mmol) was used as a starting material Recrystallization from petroleum ether (40-60°C) ethyl acetate furnished the title compound as orange needles (0 44 g, 68%)

m p 104-106°C, E ° = 128 mV

Mass spectrum found $[M]^{+\bullet}$ 405 104,

$C_{22}H_{23}N_1O_3Fe$ requires 405 103

I R ν_{max} (KBr) 3629, 2933, 1740, 1625, 1548, 1455, 1261, 1186 cm^{-1}

UV-Vis λ_{max} MeCN 324 (ε 1580), 448 (ε 410) nm

^{1}H NMR (400MHz) δ (DMSO) 8 62 (1H, t, *J* = 6 4 Hz, -CON*H*-), 7 39 (1H, s, ArH), 7 71 (1H, d, *J* = 7 6 Hz, ArH), 7 64 (1H, d, *J* = 7 6 Hz, ArH), 7 39 (1H, t, *J* = 7 6 Hz, ArH), 4 85 {2H, t, *J* = 1 2 Hz, *ortho* on (η^5-C_5H_4)}, 4 39 {2H, t, *J* = 1 2 Hz, *meta* on (η^5-C_5H_4)}, 4 08 (2H, q, *J* = 7 2 Hz, -OC*H*$_2$CH$_3$), 4 03 {5H, s, (η^5-C_5H_5)}, 3 51 (2H, q, *J* = 6 Hz, -NHC*H*$_2$CH$_2$-), 2 61 (2H, t, *J* = 7 2 Hz, -NHCH$_2$C*H*$_2$-), 1 19 (3H, t, *J* = 7 2 Hz, -OCH$_2$C*H*$_3$)

^{13}C NMR (100MHz) δ ($CDCl_3$) 173 4, 167 8, 140 6, 134 9, 129 5, 128 9, 125 2, 124 3, 84 6, 70 1, 69 7, 67 1, 61 3 (-ve DEPT), 35 7 (-ve DEPT), 34 3 (-ve DEPT), 14 6

***N*-{*meta*-(ferrocenyl)benzoyl}-4-aminobutyric acid ethyl ester 126**

For compound **126**, 4-aminobutyric acid ethyl ester hydrochloride (0 3 g, 1 8 mmol) was used as a starting material Recrystallization from diethyl ether furnished the title compound as orange needles (0 41 g, 60%)

m p 97-99°C, E ° = 124 mV

Mass spectrum found $[M]^{+\bullet}$ 419 119,

$C_{23}H_{25}N_1O_3Fe$ requires 419 118

I R ν_{max} (KBr) 3267, 2929, 1735, 1633, 1580, 1545, 1321, 1177 cm^{-1}

UV-Vis λ_{max} MeCN 322 (ε 1670), 447 (ε 450) nm

^{1}H NMR (400MHz) δ ($CDCl_3$) 7 84 (1H, s, ArH), 7 54 (1H, d, *J* = 7 6 Hz, ArH), 7 47 (1H, d, *J* = 7 6 Hz, ArH), 7 27 (1H, t, *J* = 7 6 Hz, ArH), 6 83 (1H, br s, -CON*H*-), 4 65 {2H, t, *J* = 1 6 Hz, *ortho* on (η^5-C_5H_4)}, 4 28 {2H, t, *J* = 1 6 Hz, *meta* on (η^5-C_5H_4)}, 4 08 (2H, q, *J* = 7 2 Hz, -OC*H*$_2$CH$_3$), 3 98 {5H, s, (η^5-C_5H_5)}, 3 47 (2H, q, *J* = 6 4 Hz, -NHC*H*$_2$CH$_2$CH$_2$-), 2 41 (2H, t, *J* = 6 4 Hz, -NHCH$_2$CH$_2$C*H*$_2$-), 1 93 (2H, quint, *J* = 6 8 Hz, -NHCH$_2$C*H*$_2$CH$_2$-), 1 18 (3H, t, *J* = 7 2 Hz, -OCH$_2$C*H*$_3$)

^{13}C NMR (100MHz) δ ($CDCl_3$) 174 5, 168 0, 140 6, 135 0, 129 3, 128 9, 125 0, 124 3, 84 6, 70 1, 69 7, 67 0, 61 2 (-ve DEPT), 40 3 (-ve DEPT), 32 6 (-ve DEPT), 24 7 (-ve DEPT), 14 6

_N_-{*meta*-(ferrocenyl)benzoyl} ± 2 aminobutyric acid ethyl ester 127

For compound **127**, ± 2 aminobutyric acid ethyl ester hydrochloride (0 3 g, 1 8 mmol) was used as a starting material Recrystallization from diethyl ether furnished the title compound as an orange solid (0 37 g, 55%)

m p 120-122°C, E ° = 130 mV

Mass spectrum found $[M]^{+\bullet}$ 419 114,

$C_{23}H_{25}N_1O_3Fe$ requires 419 118

I R ν_{max}(KBr) 3250, 2982, 1746, 1631, 1541, 1335, 1148 cm^{1}

UV-Vis λ_{max} MeCN 326 (ε 1430), 447 (ε 500) nm

^{1}H NMR (400MHz) δ (DMSO) 8 73 (1H, d, *J* = 6 8 Hz, -CON*H*-), 7 99 (1H, s, ArH), 7 68-7 80 (2H, m, ArH), 7 41 (1H, t, *J* = 8 Hz, ArH), 4 87 {2H, t, *J* = 1 6 Hz, *ortho* on (η^5-C_5H_4)}, 4 36 {2H, t, *J* = 1 6 Hz, *meta* on (η^5-C_5H_4)}, 4 35 {1H, q, *J* = 6 8 Hz, -C*H*(CH_2CH_3)}, 4 14 (2H, q, *J* = 7 2 Hz, -OC*H*$_2$CH$_3$), 4 04 {5H, s, (η^5-C_5H_5)}, 1 83-1 90 {1H, m, -CH(C*H*$_2$CH$_3$)}, 1 72-1 81 {1H, m, -CH(C*H*$_2$CH$_3$)}, 1 21 {3H, t, *J* = 7 6 Hz, -CH(CH_2C*H*$_3$)}, 0 99 (3H, t, *J* = 7 2 Hz, -OCH$_2$C*H*$_3$)

^{13}C NMR (100MHz) δ (DMSO) 172 6, 167 0, 139 6, 134 2, 129 3, 128 7, 125 4, 124 9, 84 4, 69 8, 69 5, 66 9, 66 8, 60 8 (-ve DEPT), 54 7, 24 3 (-ve DEPT), 14 5, 11 2

_N_-{*meta*-(ferrocenyl)benzoyl} isobutyric acid ethyl ester 128

For compound **128**, isobutyric acid ethyl ester hydrochloride (0 3 g, 1 8 mmol) was used as a starting material Recrystallization from diethyl ether furnished the title compound as an orange solid (0 38g, 57%)

m p 130-132°C, E °=127mV

Mass spectrum found $[M]^{+\bullet}$ 419 117,

$C_{23}H_{25}N_1O_3Fe$ requires 419 118

I R ν_{max}(KBr) 3265, 2981, 2937, 1749, 1636, 1542, 1547, 1542 cm^{-1}

UV-Vis λ_{max} MeCN 324 (ε 2100), 448 (ε 580) nm

^{1}H NMR (400MHz) δ ($CDCl_3$) 8 74 (1H, s, ArH), 7 54 (1H, d, J = 8 Hz, ArH), 7 47 (1H, d, J = 8 Hz, ArH), 7 27 (1H, t, J = 8 Hz, ArH), 6 82 (1H, br s, -CON*H*-), 4 63 {2H, t, J = 2 Hz, *ortho* on (η^5-C_5H_4)}, 4 28 {2H, t, J = 2 Hz, *meta* on (η^5-C_5H_4)}, 4 20 (2H, t, J = 7 2 Hz, -OC*H*$_2$CH$_3$), 3 97 {5H, s, (η^5-C_5H_5)}, 1 65 {6H, s, -C(C*H*$_3$)$_2$}, 1 24 (3H, t, J = 7 2 Hz, -OCH$_2$C*H*$_3$)

^{13}C NMR (100MHz) δ ($CDCl_3$) 175 4, 167 1, 140 7, 135 2, 129 5, 128 8, 125 1, 124 2, 84 6, 70 1, 69 7, 67 0, 62 1(-ve DEPT), 57 4, 25 0, 14 6

General procedure for the synthesis of the starting materials for the N-{ortho-(ferrocenyl)benzoyl} amino acid ester series

***ortho*-Ferrocenyl ethyl benzoate 129**

Concentrated hydrochloric acid (6 ml) was added with intermittent cooling to a solution of ethyl-2-aminobenzoate (3g, 18 2 mmol) in 15 ml of water A solution of sodium nitrite (1 4 g, 20 3 mmol) in 15 ml of water was then added slowly to this mixture with stirring keeping the temperature below 5°C furnishing a pale yellow solution The resulting diazo salt was added to a solution of ferrocene (3 8 g, 20 4 mmol) in diethyl ether (90 ml) and allowed to react for 12 hours The reactant mixture was then washed with water, the ether layer was dried over $MgSO_4$ and the solvent was removed in *vacuo* to yield the crude product The crude product was purified using column chromatography {eluant 2 3 petroleum ether (40-60°C) diethyl ether}

^{1}H NMR (400MHz) δ (DMSO) 7 88 (1H, d, J = 8 Hz, ArH), 7 50 (1H, t, J = 8 Hz, ArH), 7 39 (1H, d, J = 8 Hz, ArH), 7 30 (1H, t, J = 8 Hz, ArH), 4 46 {2H, s, *ortho* on (η^5-C_5H_4)}, 4 33 {2H, s, *meta* on (η^5-C_5H_4)}, 4 14 (2H, q, J = 7 2 Hz, -OC*H*$_2$CH$_3$), 4 09 {5H, s, (η^5-C_5H_5)}, 1 13 (3H, t, J = 7 2 Hz, -OCH$_2$C*H*$_3$)

^{13}C NMR (100MHz) δ (DMSO) 170 3, 138 7, 132 6, 131 7, 130 5, 128 8, 126 3, 86 6, 70 1, 69 7, 68 8, 61 5(-ve DEPT), 14 2

***ortho*-Ferrocenyl benzoic acid 130**

Sodium hydroxide (0 3 g, 7 5 mmol) was added to *ortho*-ferrocenyl ethyl benzoate (**129**) (2 4 g, 7 2 mmol) in a 1 1 mixture of water/methanol and was refluxed for three hours Concentrated HCl was added until pH 2 was reached The solution was allowed to cool and the product was isolated by filtration

m p 124-126°C

I R ν_{max} (KBr) 1693, 1607, 1402, 1227 cm^{-1}

UV-Vis λ_{max} CH_2Cl_2 356 (ε 1310), 450 (ε 430) nm

^1H NMR (400MHz) δ (DMSO) 12 8 (1H, s, -COO*H*), 7 83 (1H, d, *J* = 8 Hz, ArH), 7 44 (1H, t, *J* = 8 Hz, ArH), 7 37 (1H, d, *J* = 8 Hz, ArH), 7 27 (1H, t, *J* = 8 Hz, ArH), 4 55 {2H, s, *ortho* on (η^5-C_5H_4)}, 4 32 {2H, t, *meta* on (η^5-C_5H_4)}, 4 08 {5H, s, (η^5-C_5H_5)}

^{13}C NMR (100MHz) δ (DMSO) 171 2, 137 0, 133 4, 131 1, 129 9, 127 8, 126 1, 85 4, 69 9, 69 2, 68 6

General procedure for the synthesis of N-{ortho-(ferrocenyl)benzoyl} amino acid esters

***N*-{*ortho*-(ferrocenyl)benzoyl} glycine ethyl ester 131**

Glycine ethyl ester hydrochloride (0 3 g, 2 2 mmol) and triethylamine (0 5 ml) were added to a solution of *ortho*-ferrocenyl benzoic acid (0 5 g, 1 6 mmol), 1-hydroxybenzotriazole (0 3 g, 2 2 mmol) and 1,3-dicyclohexylcarbodiimide (0 45 g, 2 2 mmol) in CH_2Cl_2 (50 ml) at 0°C After 30 minutes the solution was raised to room temperature and allowed to proceed for 48 hours The precipitated *N,N'*-dicyclohexylurea was removed by filtration and the filtrate was washed with water, 10% potassium hydrogen carbonate, 5% citric acid and dried over $MgSO_4$ Recrystallization from petroleum ether (40-60°C) ethyl acetate furnished *N*-{*ortho*-(ferrocenyl)benzoyl} glycine methyl ester **131** as orange needles (0 39 g, 62%)

m p 99-101°C, E °=109mV

Mass spectrum found $[M]^{+\bullet}$ 391 089,

$C_{21}H_{21}N_1O_3Fe$ requires 391 087

I R ν_{max} (KBr) 3298, 1740, 1643, 1529 cm^{-1}

UV-Vis λ_{max} CH_2Cl_2 340 (ε 1060), 446 (ε 340) nm

^1H NMR (400MHz) δ (DMSO) 8 76 (1H, d, *J* = 5 6 Hz -CON*H*-), 7 81 (1H, d, *J* = 8 Hz, ArH), 7 43 (1H, t, *J* = 8 Hz, ArH), 7 20-7 28 (2H, m, ArH), 4 68 {2H, t, *J* = 2 Hz, *ortho* on (η^5-C_5H_4)}, 4 28 {2H, t, *J* = 2 Hz, *meta* on (η^5-C_5H_4)}, 4 16 (2H, q, *J* = 7 2 Hz, -OC$H_2$$CH_3$), 4 05 {5H, s, ($\eta^5$-$C_5H_5$)}, 3 92 (2H, d, *J* = 6 4 Hz, -NHCH_2CO-), 1 24 (3H, t, *J* = 7 2 Hz, -OCH_2CH_3)

^{13}C NMR (100MHz) δ (DMSO) 170 6, 170 2, 136 8, 136 0, 130 4, 129 3, 127 8, 125 8, 84 5, 69 8, 69 1, 68 6, 60 9(-ve DEPT), 41 4(-ve DEPT), 14 4

***N*-{*ortho*-(ferrocenyl)benzoyl}-L-alanine ethyl ester 132**

For compound **132**, L-alanine ethyl ester hydrochloride (0 3 g, 2 0 mmol) was used as the starting material Recrystallization from petroleum ether (40-60°C) ethyl acetate furnished the title compound as a yellow solid (0 39 g, 60%)

m p 54-56°C, E ° = 111 mV, $[\alpha]_D^{25}$ +9° (c 2, CH_2Cl_2)

Mass spectrum found $[M]^{+\bullet}$ 405 104,

$C_{22}H_{23}N_1O_3Fe$ requires 405 103

I R ν_{max} (KBr) 3323, 1757, 1635, 1530, 1459 cm^{-1}

UV-Vis λ_{max} MeCN 330 (ε 1130), 450 (ε 290) nm

^{1}H NMR (400MHz) δ (DMSO) 8 75 (1H, d, *J* = 6 8 Hz, -CON*H*-), 7 79 (1H, d, *J* = 8 Hz, ArH), 7 41 (1H, t, *J* = 8 Hz, ArH), 7 21-7 26 (2H, m, ArH), 4 63 (2H, d, *J* = 1 6 Hz, *ortho* on (η^5-C_5H_4)), 4 36 {1H, quint, *J* = 8 Hz, -C*H*(CH_3)}, 4 27 {2H, d, *J* = 1 6 Hz, *meta* on (η^5-C_5H_4)}, 4 12 (2H, q, *J* = 6 4 Hz, -OC*H*$_2$$CH_3$), 4 03 {5H, s, ($\eta^5$-$C_5H_5$)}, 1 31 {3H, d, *J* = 7 2 Hz, - CH(CH_3)}, 1 22 (3H, t, *J* = 6 4 Hz, -OCH_2C*H*$_3$)

^{13}C NMR (100MHz) δ (DMSO) 172 9, 169 8, 136 8, 136 2, 130 4, 129 2, 127 8, 125 8, 84 7, 69 8, 69 6, 68 7, 68 6, 68 5, 60 9 (-ve DEPT), 48 3, 17 0, 14 4

***N*-{*ortho*-(ferrocenyl)benzoyl}-L-leucine ethyl ester 133**

For compound **133**, L-leucine ethyl ester hydrochloride (0 3 g, 1 5 mmol) was used as the starting material Recrystallization from petroleum ether (40-60°C) ethyl acetate yielded the title compound as an orange solid The crystals were of sufficient quality for an X-ray diffraction study (0 46 g, 64%)

m p 88-90°C, E ° = 106 mV, $[\alpha]_D^{20}$ = +3° (c 1 2, CH_2Cl_2)

I R ν_{max} (KBr) 3324, 3266, 1744, 1644cm^{-1}

UV-Vis λ_{max} CH_2Cl_2 334 (ε 1140), 448 (ε 260) nm

^{1}H NMR (400MHz) δ (DMSO) 8 69 (1H, d, *J* = 7 6 Hz, -CON*H*-), 7 81 (1H, d, *J* = 8 Hz, ArH), 7 41 (1H, t, *J* = 8 Hz, ArH), 7 26 (1H, t, *J* = 8 Hz, ArH), 7 16 (1H, d, *J* = 8 Hz, ArH), 4 60 {2H, s, *ortho* on (η^5-C_5H_4)}, 4 30-4 42 [1H, m, -C*H*{$CH_2CH(CH_3)_2$}], 4 28

{1H, s, *meta* on (η^5-C_5H_4)}, 4 12 {1H, s, *meta* on (η^5-C_5H_4)}, 4 11 (2H, q, J = 6 4 Hz, -O$CH_2$$CH_3$), 4 05 {5H, s, ($\eta^5$-$C_5H_5$)}, 1 57-1 81 [3H, m, -{$CH_2CH$($CH_3$)$_2$}], 1 22 (3H, t, J = 6 4 Hz, -OCH$_2$$CH_3$), 0 87 [6H, t, J = 6 4 Hz, -CH{CH_2CH(CH_3)$_2$}]

^{13}C NMR (100MHz) δ (DMSO) 172 8, 170 3, 136 6, 136 3, 130 5, 129 1, 127 7, 125 8, 84 7, 69 8, 69 6, 68 5, 60 9 (-ve DEPT), 51 0, 39 5 (-ve DEPT), 24 6, 23 3, 21 4, 14 4

***N*-{*ortho*-(ferrocenyl)benzoyl}-L-phenylalanine ethyl ester 134**

For compound **134**, L-phenylalanine ethyl ester hydrochloride (0 3 g, 1 3 mmol) was used as a starting material Recrystallization from petroleum ether (40-60°C) ethyl acetate yielded the title compound as orange rhombs The crystals were of sufficient quality for an X-ray diffraction study (0 52 g, 68%)

m p 110-112°C, E ° = 95 mV, $[\alpha]_D^{20}$ = -6° (c 2, CH_2Cl_2)

Mass spectrum found $[M]^{+\bullet}$ 481 135

$C_{28}H_{27}N_1O_3Fe$ requires 481 134

I R ν_{max} (KBr) 2929, 1728, 1656, 1531 cm^{-1}

UV-Vis λ_{max} CH_2Cl_2 336 (ε 5750), 448 (ε 1440) nm

^{1}H NMR (400MHz) δ (DMSO) 8 75 (1H, d, J = 8 Hz, -CON*H*-), 7 66 (1H, d, J = 7 2 Hz, ArH), 7 20-7 41 (6H, m, ArH), 7 16 (1H, t, J = 7 2 Hz, ArH), 6 88 (1H, d, J = 7 2 Hz, ArH), 4 54-4 67 {1H, m, -C*H*(CH_2Ph)}, 4 49 {1H, s, *ortho* on (η^5-C_5H_4)}, 4 03-4 10 {5H, m, *meta* on (η^5-C_5H_4), *ortho* on (η^5-C_5H_4) and -O$CH_2$$CH_3$}, 3 76 {5H, s, ($\eta^5$-$C_5H_5$)}, 2 83-3 04 {2H, m, -CH(CH_2Ph)}, 0 99 (3H, t, J = 7 2 Hz, -OCH$_2$CH_3)

^{13}C NMR (100MHz) δ (DMSO) 171 9, 169 9, 137 9, 136 8, 136 1, 130 4, 129 5, 129 1, 128 6, 127 5, 126 9, 125 7, 84 4, 69 8, 69 0, 68 7, 68 5, 61 1 (-ve DEPT), 54 0, 31 1 (-ve DEPT), 14 4

***N*-{*ortho*-(ferrocenyl)benzoyl}-β-alanine ethyl ester 135**

For the compound **135**, β-alanine ethyl ester hydrochloride (0 3 g, 2 0 mmol) was used as a starting material Recrystallization from petroleum ether (40-60°C) ethyl acetate yielded the title compound as an orange solid (0 38 g, 59%)

E ° = 107 mV

Mass spectrum found $[M]^{+\bullet}$ 405 104,

$C_{22}H_{23}N_1O_3Fe$ requires 405 103

I R ν_{max} (KBr) 2932, 1735, 1670, 1520 cm^{-1}

UV-Vis λ_{max} MeCN 319 (ε 1590), 446 (ε 350) nm

^1H NMR (400MHz) δ ($CDCl_3$) 7 68 (1H, d, *J* = 7 6 Hz, ArH), 7 29-7 40 (2H, m, ArH), 7 14-7 18 (1H, m, ArH), 5 80 (1H, t, *J* = 5 6 Hz, -CON*H*-), 4 42 {2H, t, *J* = 1 6 Hz, *ortho* on (η^5-C_5H_4)}, 4 18 {2H, t, *J* = 1 6 Hz, *meta* on (η^5-C_5H_4)}, 3 94-4 04 {7H, m, -O$CH_2$$CH_3$, ($\eta^5$-$C_5H_5$)}, 3 43 (2H, q, *J* = 6 4 Hz, -NHC$H_2$$CH_2$-), 2 37 (2H, t, *J* = 6 4 Hz, -NHCH_2CH_2-), 1 13 (3H, t, *J* = 7 2 Hz, -OCH_2CH_3)

^{13}C NMR (100MHz) δ ($CDCl_3$) 172 6, 170 7, 136 5, 136 4, 131 2, 129 6, 128 1, 126 6, 85 7, 70 2, 69 7, 68 9, 61 0 (-ve DEPT), 35 3 (-ve DEPT), 34 0 (-ve DEPT), 14 6

***N*-{*ortho*-(ferrocenyl)benzoyl}-4-aminobutyric acid ethyl ester 136**

For the compound **136**, 4-aminobutyric acid ethyl ester hydrochloride (0 3 g, 1 8 mmol) was used as a starting material Recrystallization from diethyl ether yielded the title compound as a brown solid (0 42 g, 62%)

m p 62-63°C, E °= 108 mV

Mass spectrum found $[M]^{+\bullet}$ 419 108,

$C_{23}H_{25}N_1O_3Fe$ requires 419 118

I R ν_{max} (KBr) 3389, 3086, 2925, 1752, 1647, 1542, 1406, 1196 cm^{-1}

UV-Vis λ_{max} MeCN 325 (ε 1640), 445 (ε 280) nm

^1H NMR (400MHz) δ ($CDCl_3$) 7 78 (1H, d, *J* = 7 6 Hz, ArH), 7 38-7 41 (2H, m, ArH), 7 25-7 31 (1H, m, ArH), 5 51 (1H, br s, -CON*H*-), 4 53 {2H, s, *ortho* on (η^5-C_5H_4)}, 4 29 {2H, s, *meta* on (η^5-C_5H_4)}, 4 02-4 20 (7H, m, -O$CH_2$$CH_3$, ($\eta^5$-$C_5H_5$)), 3 28 (2H, q, *J* = 6 4 Hz, -NHC$H_2$$CH_2$$CH_2$-), 2 20 (2H, t, J = 7 2 Hz, -NH$CH_2$$CH_2CH_2$-), 1 68-1 76 (2H, m, -NHCH_2C$H_2$$CH_2$-), 1 24 (3H, t, J = 7 6 Hz, -OCH_2CH_3)

^{13}C NMR (100MHz) δ ($CDCl_3$) 173 6, 170 9, 136 5, 136 3, 131 2, 129 7, 128 2, 126 7, 85 7, 70 2, 69 8, 69 0, 60 9 (-ve DEPT), 39 6 (-ve DEPT), 32 0 (-ve DEPT), 24 6 (-ve DEPT), 14 6

***N*-{*ortho*-(ferrocenyl)benzoyl} ± 2 aminobutyric acid ethyl ester 137**

For the compound **137**, ± 2 aminobutyric acid ethyl ester hydrochloride (0 3 g, 1 8 mmol) was used as a starting material Recrystallization from diethyl ether furnished the title compound as orange needles (0 37 g, 55%)

m p 67-69°C, E ° = 111 mV

Mass spectrum found $[M]^{+\bullet}$ 419 107,

$C_{23}H_{25}N_1O_3Fe$ requires 419 118

I R ν_{max} (KBr) 3260, 2980, 1742, 1636, 1541, 1196, 1153 cm^{-1}

UV-Vis λ_{max} MeCN 323 (ε 1590), 444 (ε 360) nm

^1H NMR (400MHz) δ ($CDCl_3$) 7 72 (1H, d, *J* = 8 Hz, ArH), 7 31-7 45 (2H, m, ArH), 7 19 (1H, d, *J* = 8 Hz, ArH), 5 86 (1H, d, *J* = 7 6 Hz, -CON*H*-), 4 46-4 55 {3H, m, *ortho* on (η^5-C_5H_4), -C*H*(CH_2CH_3)], 4 19 {2H, s, *meta* on (η^5-C_5H_4)}, 4 07 (2H, q, *J* = 7 2 Hz, -O*CH*$_2$CH$_3$), 3 96 {5H, s, (η^5-C_5H_5)}, 1 64-1 73 {1H, m, -CH(C*H*$_2$CH$_3$)}, 1 55-1 64 {1H, m, -CH(C*H*$_2$CH$_3$)}, 1 17 (3H, t, *J* = 7 2 Hz, -OCH$_2$C*H*$_3$), 0 69 {3H, t, *J* = 7 2 Hz, -CH(CH$_2$C*H*$_3$)}

^{13}C NMR (100MHz) δ ($CDCl_3$) 172 2, 170 3, 136 8, 136 1, 131 4, 129 8, 128 2, 126 6, 85 7, 70 2, 70 1, 69 6, 69 0, 61 7 (-ve DEPT), 54 0, 25 8 (-ve DEPT), 14 6, 9 8

General procedure for the synthesis of N-{para-(ferrocenyl)benzoyl} dipeptide esters

***N*-{*para*-(ferrocenyl)benzoyl}-L-alanine-glycine ethyl ester 138**

L-alanine-glycine ethyl ester hydrochloride (0 2 g, 1 0 mmol) was added to a solution of *para*-ferrocenyl benzoic acid (**98**) (0 3 g, 1 0 mmol), 1-hydroxybenzotriazole (0 2 g, 1 5 mmol), triethylamine (0 5 ml), and dicyclohexylcarbodiimide (0 45g, 2 2 mmol) in 50 ml of dichloromethane at 0°C After 30 minutes the temperature was raised to room temperature and the reaction was allowed to proceed for 48 hours The precipitated *N,N'*-dicyclohexylurea was removed by filtration and the filtrate was washed with water, 10% potassium hydrogen carbonate, 5% citric acid, dried over $MgSO_4$ and the solvent was removed *in vacuo* The product was purified by column chromatography {eluant 2 3 petroleum ether (40-60°C) ethyl acetate} Recrystallization from petroleum ether (40-60°C) ethyl acetate furnished the title compound **138** as an orange solid (0 27 g, 59%)

m p 75-77°C, E ° = 137 mV, $[\alpha]_D^{20}$ = +5° (c 2, EtOH)

Mass spectrum found $[M+H]^+$ 463 1308,

$C_{24}H_{27}N_2O_4Fe$ requires 463 1320

I R ν_{max} (KBr) 3326, 1748, 1627, 1609, 1560, 1512, 1195 cm^{-1}

UV-Vis λ_{max} MeCN, 352 (ε 2400), 450 (ε 720) nm

^1H NMR (400MHz) δ ($CDCl_3$) 7 60 (2H, d, J = 8 Hz, ArH), 7 45 (2H, d, J = 8 Hz, ArH), 6 71-6 80 (2H, m, -CON*H*-, -CON*H*-), 4 69-4 81 {1H, m, -C*H*(CH_3)}, 4 63 {2H, t, J = 1 6 Hz, *ortho* on (η^5-C_5H_4)}, 4 32 {2H, t, J = 1 6 Hz, *meta* on (η^5-C_5H_4)}, 4 15 (2H, q, J = 7 2 Hz, -OC*H*$_2$$CH_3$), 3 99 (2H, d, J = 5 2 Hz, -NHC*H*$_2$CO-), 3 96 {5H, s, (η^5-C_5H_5)}, 1 47 {3H, d, J = 7 2 Hz, -CH(C*H*$_3$)}, 1 21 (3H, t, J = 7 2 Hz, OCH_2CH_3)

^{13}C NMR (100MHz) δ ($CDCl_3$) 173 0, 170 0, 167 5, 144 4, 131 0, 127 6, 126 2, 85 4, 70 2, 70 1, 67 2, 62 0 (-ve DEPT), 49 1, 41 8 (-ve DEPT), 18 7, 14 5

_N_-{*para*-(ferrocenyl)benzoyl}-L-alanine-L-alanine ethyl ester 139

For the compound **139**, L-alanine-L-alanine ethyl ester hydrochloride (0 2 g, 0 9 mmol) was used as a starting material The product was purified by column chromatography {eluant 2 3 petroleum ether (40-60°C) ethyl acetate} Recrystallization from petroleum ether (40-60°C) ethyl acetate furnished the title compound as orange needles (0 26 g, 61%)

m p 69-71°C, E ° = 140 mV, $[\alpha]_D^{20}$ = -1° (c 2, EtOH)

Mass spectrum found $[M]^{+\bullet}$ 476 139,

$C_{25}H_{28}N_2O_4Fe$ requires 476 140

I R ν_{max} (KBr) 3326, 2936, 1741, 1629, 1609, 1543, 1507 cm^{-1}

UV-Vis λ_{max} EtOH, 353 (ε 2640), 449 (ε 840) nm

^1H NMR (400MHz) δ ($CDCl_3$) 7 67 (2H, d, J = 8 4 Hz, ArH), 7 43 (2H, d, J = 8 4 Hz, -ArH), 7 19 (2H, t, J = 8 Hz, -CON*H*-), 4 74 {1H, quint, J = 7 2 Hz, -C*H* (CH_3)}, 4 62 {2H, t, J = 1 6 Hz, *ortho* on (η^5-C_5H_4)}, 4 47 (1H, quint, J = 7 2 Hz, -C*H*(CH_3)}, 4 31 {2H, t, J = 1 6 Hz, *meta* on (η^5-C_5H_4)}, 4 15 (2H, q, J = 7 2 Hz, -OC*H*$_2$$CH_3$), 3 96 {5H, s, ($\eta^5$-$C_5H_5$)}, 1 47 {3H, d, J = 7 2 Hz, -CH(C*H*$_3$)}, 1 36 {3H, d, J = 7 2 Hz, -CH(C*H*$_3$)}, 1 24 (3H, t, J = 7 2 Hz, $-OCH_2CH_3$)

^{13}C NMR (100MHz) δ ($CDCl_3$) 173 1, 172 5, 167 3, 144 3, 131 2, 127 7, 126 2, 83 8, 70 2, 70 1, 67 2, 61 9 (-ve DEPT), 49 5, 48 7, 19 3, 18 5, 14 6

***N*-{*para*-(ferrocenyl)benzoyl}-L-alanine-L-leucine ethyl ester 140**

For compound **140**, L-alanine-L-leucine ethyl ester hydrochloride (0 2 g, 0 7 mmol) was used as a starting material The product was purified by column chromatography {eluant 2 3 petroleum ether (40-60°C) ethyl acetate} Recrystallization from petroleum ether (40-60°C) ethyl acetate furnished the title compound as an orange solid (0 234 g, 64%)

m p 62-64°C, E ° = 138 mV, $[\alpha]_D^{20}$= +4° (c 1 8, EtOH)

Mass spectrum found $[M+H]^+$ 519 1973,

$C_{28}H_{35}N_2O_4Fe$ requires 519 1946

I R ν_{max} (KBr) 3336, 2958, 1737, 1655, 1629, 1562, 1510 cm^{1}

UV-Vis λ_{max} EtOH, 354 (ε 2350), 450 (ε 740) nm

^{1}H NMR (400MHz) δ ($CDCl_3$) 7 66 (2H, d, *J* = 8 Hz, ArH), 7 43 (2H, d, *J* = 8 Hz, ArH), 6 93 (1H, d, *J* = 7 2 Hz, -CON*H*-), 6 83 (1H, d, *J* = 7 2 Hz, -CON*H*-), 4 77 {1H, quint, *J* = 4 8 Hz, -C*H*(CH_3)}, 4 62 {2H, t, *J* = 2 Hz, *ortho* on (η^5-C_5H_4)}, 4 50-4 53 [1H, m, -C*H*{$CH_2CH(CH_3)_2$}], 4 31 {2H, t, *J* = 2 Hz, *meta* on (η^5-C_5H_4)}, 4 16 (2H, q, *J* = 7 2 Hz, -OC*H*$_2$$CH_3$), 3 96 {5H, s, ($\eta^5$-$C_5H_5$)}, 1 52-1 62 [3H, m, -CH{C*H*$_2$C*H*(CH_3)$_2$}], 1 47 {3H, d, *J* = 6 8 Hz, -CH(C*H*$_3$)}, 1 22 (3H, t, *J* = 7 2 Hz, -OCH$_2$C*H*$_3$), 0 83 [6H, t, *J* = 4 4 Hz, -CH{$CH_2CH(CH_3)_2$}]

^{13}C NMR (100MHz) δ ($CDCl_3$) 173 1, 172 8, 167 4, 144 3, 131 2, 127 6, 126 2, 83 8, 70 2, 70 1, 67 2, 61 8 (-ve DEPT), 51 4, 49 4, 41 6 (-ve DEPT), 25 2, 23 2, 22 2, 19 2, 14 6

***N*-{*para*-(ferrocenyl)benzoyl}-L-alanine-L-phenylalanine ethyl ester 141**

For the compound **141**, L-alanme-L-phenylalanine ethyl ester hydrochloride (0 2 g 0 7 mmol) was used as a starting product The product was purified by column chromatography {eluant 2 3 petroleum ether (40-60°C) ethyl acetate} Recrystallization from petroleum ether (40-60°C) ethyl acetate furnished the title compound as orange needles (0 25 g, 65%)

m p 169-171°C, E ° = 139 mV, $[\alpha]_D^{20}$= +9° (c 1 9, EtOH)

Mass spectrum found $[M]^+$ 552 171,

$C_{31}H_{32}N_2O_4Fe$ requires 552 171

I R ν_{max} (KBr) 3316, 3268, 1753, 1655, 1624, 1546, 1516 cm^{1}

UV-Vis λ_{max} EtOH, 352 (ε 2730), 449 (ε 890) nm

^{1}H NMR (400MHz) δ (DMSO) 8 26 (1H, d, *J* = 7 6 Hz, -CON*H*-), 8 16 (1H, d, *J* = 7 6 Hz, -CON*H*-), 7 64 (2H, d, *J* = 8 4 Hz, ArH), 7 46 (2H, d, *J* = 8 4 Hz, ArH), 7 04-7 17 (5H, m, ArH), 4 74 {2H, t, *J* = 1 6 Hz, *ortho* on (η^5-C_5H_4)}, 4 36 {1H, quint, *J* = 7 2 Hz, C*H*(CH_3)}, 4 24-4 30 {3H, m, -C*H*(CH_2Ph), *meta* on (η^5-C_5H_4)}, 3 73-3 92 {7H, m, -OCH_2CH_3, (η^5-C_5H_5)}, 2 81-2 94 {2H, m, -CH(CH_2Ph)}, 1 14 {3H, d, *J* = 7 6 Hz, -CH(CH_3)}, 0 92 (3H, t, *J* = 7 2 Hz, -OCH_2CH_3)

^{13}C NMR (100MHz) δ (DMSO) 173 0, 171 7, 166 2, 143 1, 137 4, 129 5, 128 6, 128 0, 126 9, 126 6, 125 6, 83 5, 69 9, 66 9, 60 8 (-ve DEPT), 54 1, 48 8, 41 0 (-ve DEPT), 18 1, 14 3

N-{*para*-(ferrocenyl)benzoyl}-β-alanine-β-alanine ethyl ester 142

For the compound **142**, β-alanine-β-alanine ethyl ester hydrochloride (0 2 g, 0 9 mmol) was used as a starting product The product was purified by column chromatography {eluant 2 3 petroleum ether (40-60°C) ethyl acetate} Recrystallization from petroleum ether (40-60°C) ethyl acetate furnished the title compound as a brown solid (0 21 g, 49%)

m p 111-113°C, E ° = 130 mV

Mass spectrum found $[M]^{+\bullet}$ 476 139,

$C_{25}H_{28}N_2O_4Fe$ requires 476 140

I R ν_{max} (KBr) 3303, 2928, 1735, 1638, 1546, 1272, 1186 cm^{-1}

UV-vis λ_{max} MeCN, 346 (ε 1950), 447 (ε 560) nm

^{1}H NMR (400MHz) δ (DMSO) 8 65 (1H, t, *J* = 5 6 Hz, -CON*H*-), 8 23 (1H, t, *J* = 5 6 Hz, -CON*H*-), 7 94 (2H, d, *J* = 8 4 Hz, ArH), 7 79 (2H, d, *J* = 8 4 Hz, ArH), 5 08 {2H, t, *J* = 1 6 Hz, *ortho* on (η^5-C_5H_4)}, 4 60 {2H, t, *J* = 1 6 Hz, *meta* on (η^5-C_5H_4)}, 4 21-4 32 {7H, m, -OCH_2CH_3, (η^5-C_5H_5)}, 3 63 (2H, q, *J* = 6 8 Hz, -CONHCH_2CH_2CONH-), 3 47 (2H, q, *J* = 6 8 Hz, -CH_2CH_2CONHCH_2CH_2-), 2 64 (2H, t, *J* = 6 8 Hz, -CONHCH_2CH_2CONH-), 2 55 (2H, t, *J* = 6 8 Hz, -CH_2CH_2CONHCH_2CH_2-), 1 38 (3H, t, *J* = 7 2 Hz, -OCH_2CH_3)

^{13}C NMR (100MHz) δ (DMSO) 171 7, 170 1, 166 3, 142 8, 131 9, 127 6, 125 7, 83 6, 69 8, 66 9, 60 3 (-ve DEPT), 36 4(-ve DEPT), 35 7 (-ve DEPT), 34 2 (-ve DEPT), 33 7 (-ve DEPT), 14 4

_N_-{*meta*-(ferrocenyl)benzoyl}-L-alanine-glycine methyl ester 143

Foe the compound **143**, L-alanme-glycme methyl ester hydrochloride (0 2 g, 1 0 mmol) was used as a starting material The product was purified by column chromatography {eluant 2 3 petroleum ether (40-60°C) ethyl acetate} Recrystallization from petroleum ether (40-60°C) ethyl acetate furnished the title compound as an orange solid (0 227 g, 51%)

m p 103 -105°C, E ° = 130 mV, $[\alpha]_D^{20}$= -20° (c 1 7, EtOH)

Mass spectrum found $[M]^{+\bullet}$ 448 109,

$C_{23}H_{24}N_2O_4Fe$ requires 448 109

I R ν_{max} (KBr) 3285, 2931, 1753, 1647, 1631, 1579, 1548 1240 1208 cm^{1}

UV-Vis λ_{max} EtOH, 353 (ε 2330), 449 (ε 737) nm

^{1}H NMR (400MHz) δ (DMSO) 8 62 (1H, **d**, *J* = 5 6 Hz, ArH), 8 39 (1H, t, *J* = 5 6 Hz, ArH), 8 02 (1H, s, ArH), 7 73-7 81 (2H, m, ArH, -CON*H*-), 7 40 (1H, t, *J* = 8 Hz, -CON*H*-), 4 87 {2H, t, *J* = 1 6 Hz, *ortho* on (η^5-C_5H_4)}, 4 57 {1H, quint, *J* = 7 2 Hz, -CH(C*H*$_3$)}, 4 39 {2H, t, *J* = 1 6 Hz, *meta* on (η^5-C_5H_4)}, 4 04 {5H, s, (η^5-C_5H_5)}, 3 85-3 90 (2H, m, -NHC*H*$_2$CO-), 3 64 (3H, s, -OC*H*$_3$), 1 39 {3H, **d**, *J* = 7 2 Hz, -CH(C*H*$_3$)}

^{13}C NMR (100MHz) δ (DMSO) 173 4, 170 7, 166 3, 139 5, 134 4, 129 2, 128 6, 125 5, 124 8, 84 5, 69 8, 69 4, 66 9, 66 8, 52 0, 49 0, 41 0 (-ve DEPT), 18 2

_N_-{*meta*-(ferrocenyl)benzoyl}-L-alanine-glycine ethyl ester 144

For the compound **144**, L-alanme-glycme ethyl ester hydrochloride (0 2 g, 1 0 mmol) was used as a starting material The product was purified by column chromatography {eluant 2 3 petroleum ether (40-60°C) ethyl acetate} Recrystalhzation from petroleum ether (40-60°C) ethyl acetate furnished the title compound as a yellow solid (0 236 g, 51%)

m p 151-153°C, E ° = 130 mV, $[\alpha]_D^{20}$= -18° (c 2, EtOH),

I R ν_{max} (KBr) 3300, 2937, 1751, 1657, 1632, 1580, 1543, 1199 cm^{-1}

UV-Vis λ_{max} MeCN, 234 (ε 580), 445 (ε 100) nm

^{1}H NMR (400MHz) δ ($CDCl_3$) 7 80 (1H, s, ArH), 7 54 (1H, d, *J* = 8 Hz, ArH), 7 48 (1H, d, *J* = 8 Hz, ArH), 7 27 (1H, t, *J* = 8 Hz, ArH), 6 83-6 93 (2H, m, -CON*H*-), 4 74 {1H, quint, *J* = 7 2 Hz, -C*H*(CH_3)}, 4 67 {2H, s, *ortho* on (η^5-C_5H_4)}, 4 31 {2H, s, *meta* on (η^5-C_5H_4)}, 4 14 (2H, q, *J* = 7 2 Hz, -OC$H_2$$CH_3$), 3 80-4 00 {7H, m, ($\eta^5$-$C_5H_5$), -NHC$H_2$CO-}, 1 48 {3H, d, *J* = 7 2 Hz, -CH(CH_3)}, 1 14 (3H, t, *J* = 7 2 Hz, -OCH$_2$CH_3)

^{13}C NMR (100MHz) δ ($CDCl_3$) 173 0, 170 0, 167 8, 140 8, 134 2, 129 8, 129 0, 125 1, 124 5, 84 5, 70 1, 69 8, 67 1, 67 0, 62 0 (-ve DEPT), 49 5, 41 8 (-ve DEPT), 18 8, 14 5

_N_-{*meta*-(ferrocenyl)benzoyl}-L-alanine-L-alanine ethyl ester 145

For the compound **145**, L-alanine-L-alanine ethyl ester hydrochloride (0 2 g, 0 9 mmol) was used as a starting material The product was purified by column chromatography {eluant 2 3 petroleum ether (40-60°C) ethyl acetate} Recrystallization from petroleum ether (40-60°C) ethyl acetate furnished the title compound as yellow needles (0 224 g, 53%)

m p 58-60°C, E ° = 130 mV, $[\alpha]_D^{20}$ = -37° (c 1 9, EtOH)

Mass spectrum found $[M]^{+\bullet}$ 476 136,

$C_{25}H_{28}N_2O_4Fe$ requires 476 140

I R ν_{max} (KBr) 3276, 2986, 2939, 1739, 1637, 1584, 1543, 1400, 1128 cm^{-1}

UV-Vis λ_{max} EtOH, 325 (ε 1540), 443 (ε 430) nm

^{1}H NMR (400MHz) δ ($CDCl_3$) 7 83 (1H, s, ArH), 7 50-7 56 (2H, m, ArH), 7 26 (1H, t, *J* = 8 Hz, ArH), 7 06 (2H, t, *J* = 7 6 Hz, -CON*H*-), 4 78 {1H, quint, *J* = 7 2 Hz, -C*H*(CH_3)}, 4 62 {2H, t, *J* = 1 2 Hz, *ortho* on (η^5-C_5H_4)}, 4 50 [1H, quint, *J* = 7 2 Hz, -C*H*(CH_3)], 4 26 {2H, t, *J* = 1 6 Hz, *meta* on (η^5-C_5H_4)}, 4 14 (2H, q, *J* = 7 2 Hz, -OC$H_2$$CH_3$), 3 96 {5H, s, ($\eta^5$-$C_5H_5$)}, 1 49 {3H, d, *J* = 6 8 Hz, -CH(CH_3)}, 1 37 {3H, d, *J* = 6 8 Hz, -CH(CH_3)}, 1 22 (3H, t, *J* = 7 2 Hz, -OCH$_2$CH_3)

^{13}C NMR (100MHz) δ (DMSO) 173 1, 172 5, 167 6, 140 7, 134 3, 129 8, 128 9, 125 1, 124 6, 84 4, 70 1, 69 7, 67 0, 62 0 (-ve DEPT), 49 6, 48 7, 19 4, 18 5, 14 5

_N_-{*meta*-(ferrocenyl)benzoyl}-L-alanine-L-leucine ethyl ester 146

For the compound **146**, L-alanine-L-leucine ethyl ester hydrochloride (0 2 g, 0 7 mmol) was used as starting material The product was purified by column chromatography

{eluant 2 3 petroleum ether (40-60°C) ethyl acetate} Recrystallization from petroleum ether (40-60°C) ethyl acetate furnished the title compound as an orange solid (0 203 g, 56%)

m p 110-112°C, E ° = 126 mV, $[\alpha]_D^{20}$= -25°C (c 1 8, EtOH)

Mass spectrum found $[M]^{+\bullet}$ 518 186,

$C_{28}H_{34}N_2O_4Fe$ requires 518 187

I R ν_{max} (KBr) 3286, 2963, 1750, 1637, 1537, 1450, 1180 cm^{-1}

UV-Vis λ_{max} EtOH, 323 (ε1430), 442 (ε 410) nm

^1H NMR (400MHz) δ (DMSO) 8 33 (1H, d, *J* = 7 6 Hz, -CON*H*-), 8 08 (1H, d, *J* = 7 6 Hz, -CON*H*-), 7 77 (1H, s, ArH), 7 42-7 56 (2H, m, ArH), 7 71 (1H, t, *J* = 8 Hz, ArH), 4 65 {2H, t, *J* = 2 Hz, *ortho* on (η^5-C_5H_4)}, 4 34 {1H, quint, *J* = 6 4 Hz, -C*H*(CH_3)}, 4 17 {2H, t, *J* = 1 6 Hz, *meta* on (η^5-C_5H_4)}, 3 97-4 05 [1H, m, C*H*{$CH_2CH(CH_3)_2$}], 3 83-3 87 (2H, m, -O*C*H_2CH_3), 3 81 {5H, s, (η^5-C_5H_5)}, 1 24-1 52 [3H, m, CH{*C*H_2*C*H(CH_3)$_2$}], 1 15 {3H, d, *J* = 7 2 Hz, CH(*C*H_3)}, 0 95 (3H, t, *J* = 7 2 Hz, -OCH_2*C*H_3), 0 69 [3H, d, *J* = 6 4 Hz, CH{CH_2*C*H(*C*H_3)$_2$}], 0 64 [3H, d, *J* = 6 4 Hz, CH{CH_2*C*H(*C*H_3)$_2$}]

^{13}C NMR (100MHz) δ (DMSO) 173 1, 172 8, 166 3, 139 5, 134 5, 129 1, 128 6, 125 5, 124 7, 84 4, 69 8, 69 4, 66 8, 60 7 (-ve DEPT), 50 8, 48 9, 40 0 (-ve DEPT), 24 6, 23 1, 21 8, 18 2, 14 4

_N_-{*meta*-(ferrocenyl)benzoyl}-L-alanine-L-phenylalanine ethyl ester 147.

For the compound **147**, L-alanine L-phenylalanine ethyl ester hydrochloride (0 2 g, 0 7 mmol) was used as a starting material The product was purified by column chromatography ({eluant 2 3 petroleum ether (40-60°C) ethyl acetate} Recrystallization from petroleum ether (40-60°C) ethyl acetate furnished the title compound as an orange solid (0 203 g, 52%)

m p 61-63°C, E ° = 139 mV, $[\alpha]_D^{20}$= -19°C (c 1 9, EtOH)

Mass spectrum found $[M]^{+\bullet}$ 552 169,

$C_{31}H_{32}N_2O_4Fe$ requires 552 171

I R ν_{max} (KBr) 3325, 2930, 1739, 1637, 1579, 1532, 1499, 1208 cm^{-1}

UV-Vis λ_{max} EtOH, 327 (ε 1440), 442 (ε 390) nm

^{1}H NMR (400MHz) δ ($CDCl_3$) 7 82 (1H, s, ArH), 7 58 (1H, d, *J* = 8 Hz, ArH), 7 46 (1H, d, *J* = 8 Hz, ArH), 7 29 (1H, t, *J* = 8 Hz, ArH), 7 10-7 17 (3H, m, ArH), 7 02-7 11 (2H, m, ArH), 6 67 (1H, d, *J* = 7 2 Hz, -CON*H*-), 6 50 (1H, d, *J* = 7 2 Hz, -CON*H*-), 4 78-4 90 [1H, m,-NHC*H*(CH_3)], 4 63-4 70 {3H, m, *ortho* on (η^5-C_5H_4), -NHC*H*(CH_2Ph)}, 4 29 {2H, s, *meta* on (η^5-C_5H_4)}, 4 24 (2H, q, *J* = 7 2 Hz, -OC*H*$_2$$CH_3$), 3 98 {5H, s, ($\eta^5$-$C_5H_5$)}, 3 03 {1H, dd, J_{ax} = 2 0 Hz, J_{ab} = 5 6 Hz, CH(C*H*$_2$Ph)}, 3 06 {1H, dd, J_{ax} = 2 0 Hz, J_{ab} = 5 6 Hz, CH(C*H*$_2$Ph)}1 62 {3H, d, *J* = 6 4 Hz, -CH(C*H*$_3$)}, 1 21 (3H, t, *J* = 7 2 Hz, -OCH$_2$C*H*$_3$)

^{13}C NMR (100MHz) δ ($CDCl_3$) 172 2, 171 6, 167 5, 140 8, 136 1, 134 2, 129 8, 129 7, 129 0, 127 5, 126 3, 125 1, 124 5, 84 5, 70 1, 69 8, 67 1, 67 0, 62 1 (-ve DEPT), 53 8, 49 6, 38 3 (-ve DEPT), 18 8, 14 5

***N*-{*ortho*-(ferrocenyl)benzoyl}-L-alanine-glycine ethyl ester 148**

For compound **148**, L-alanine-glycine ethyl ester hydrochloride (0 2 g, 1 0 mmol) was used as a starting material The product was purified by column chromatography {eluant 2 3 petroleum ether (40-60°C) ethyl acetate} Recrystallization from petroleum ether (40-60°C) ethyl acetate furnished the title compound as orange needles (0 181 g, 39%)

m p 55-57°C, E ° = 131 mV, $[\alpha]_D^{20}$ = +0 3° (c 2 05, EtOH)

Mass spectrum found $[M]^{+\bullet}$ 462 09,

$C_{24}H_{26}N_2O_4Fe$ requires 462 12

I R ν_{max} (KBr) 3326, 2933, 1752, 1655, 1638, 1509, 1200 cm^{-1}

UV-Vis λ_{max} EtOH, 321 (ε 1050), 441 (ε 240) nm

^{1}H NMR (400MHz) δ (DMSO) 8 35 (1H, d, *J* = 7 2 Hz, -CON*H*-), 8 18 (1H, t, *J* = 7 2 Hz, -CON*H*-), 7 80 (1H, d, *J* = 8 Hz, ArH), 7 41 (1H, t, *J* = 8 Hz, ArH), 7 24-7 38 (2H, m, ArH), 4 57-4 59 {2H, m, *ortho* on (η^5-C_5H_4)}, 4 41 {1H, quint, *J* = 7 6 Hz, -C*H*(CH_3)}, 4 25-4 29 {2H, m, *meta* on (η^5-C_5H_4)}, 4 01-4 13 {7H, m, -OC*H*$_2$$CH_3$, ($\eta^5$-$C_5H_5$)}, 3 78-3 93 (2H, m, -CONHC*H*$_2$-), 1 25 {3H, d, *J* = 7 6 Hz, -CH(C*H*$_3$)}, 1 17 (3H, t, *J* = 7 2 Hz, -OCH$_2$C*H*$_3$)

^{13}C NMR (100MHz) δ (DMSO) 173 0, 170 1, 169 7, 136 6, 136 5, 130 5, 129 0, 127 8, 125 8, 85 0, 69 8, 69 5, 68 8, 68 5, 68 4, 60 8 (-ve DEPT), 48 7, 41 1 (-ve DEPT), 18 0, 14 4

***N*-{*ortho*-(ferrocenyl)benzoyl}-L-alanine-L-phenylalanine ethyl ester 149**

For the compound **149**, L-alanine-L-phenylalanine ethyl ester hydrochloride (0 2 g, 0 7 mmol) was used as starting material The product was purified by column chromatography {eluant 2 3 petroleum ether (40-60°C) ethyl acetate} Recrystallization from petroleum ether (40-60°C) ethyl acetate furnished the title compound as an orange solid (0 102 g, 25%)

m p 137-139°C, E ° = 134 mV, $[\alpha]_D^{20}$ = +2° (c 2 05, EtOH)

Mass spectrum found $[M]^{+\bullet}$ 552 158,

$C_{31}H_{32}N_2O_4Fe$ requires 552 171

I R ν_{max} (KBr) 3397, 3309, 2932, 1742, 1645, 1509, 1496, 1210 cm^{-1}

UV-Vis λ_{max} EtOH, 323 (ε 1570), 440 (ε 340) nm

^{1}H NMR (400MHz) δ (DMSO) 8 37-8 46 (2H, m , -CON*H*-), 7 80 (1H, d, *J* = 7 2 Hz, ArH), 7 60 (1H, t, *J* = 7 2 Hz, ArH), 7 38-7 47 (7H, m, ArH), 4 76 {2H, t, *J* = 1 2 Hz, *ortho* on (η^5-C_5H_4)}, 4 60-4 76 {2H, m, -C*H*(CH_3), -C*H*(CH_2Ph)}, 4 42-4 50 {2H, m, *meta* on (η^5-C_5H_4)}, 4 21-4 30 {7H, m, (η^5-C_5H_5), -OC*H*$_2$$CH_3$}, 3 19-3 28 {2H, m, -CH(C*H*$_2$Ph)}, 1 35 {3H, d, *J* = 7 2 Hz, -CH(C*H*$_3$)}, 1 27 (3H, t, *J* = 7 6 Hz, -OCH$_2$C*H*$_3$)

^{13}C NMR (100MHz) δ (DMSO) 172 6, 171 7, 169 5, 137 3, 136 5, 130 5, 129 5, 129 1, 128 6, 128 5, 127 8, 126 9, 125 8, 85 0, 69 8, 69 5, 68 7, 68 5, 60 9 (-ve DEPT), 53 9, 48 6, 33 7 (-ve DEPT), 18 1, 14 4

***N*-{*para*-(ferrocenyl)benzoyl} glycine-glycine ethyl ester 150**

For the compound **150**, glycine-glycine ethyl ester hydrochloride (0 2 g, 1 0 mmol) was used as a starting material The product was purified by column chromatography {eluant 2 3 petroleum ether (40-60°C) ethyl acetate} Recrystallization from petroleum ether (40-60°C) ethyl acetate furnished the title compound as orange needles (0 253 g, 56%)

m p 165-167°C, E ° = 137 mV

Mass spectrum found $[M]^{+\bullet}$ 448 110,

$C_{23}H_{24}N_2O_4Fe$ requires 448 109

I R ν_{max} (KBr) 3321, 2924, 1742, 1622, 1574, 1501, 1311 cm^{-1}

UV-Vis λ_{max} EtOH, 352 (ε 2140), 447 (ε 620) nm

^{1}H NMR (400MHz) δ ($CDCl_3$) 7 69 (2H, d, *J* = 8 Hz, ArH), 7 45 (2H, d, *J* = 8 Hz, ArH), 7 09 (1H, br s, -CON*H*-), 6 85 (1H, br s, -CON*H*-), 4 63 {2H, s, *ortho* on (η^5-C_5H_4)}, 4 31 {2H, s, *meta* on (η^5-C_5H_4)}, 4 12-4 25 (4H, m, -OC$H_2$$CH_3$, -NHC$H_2$CO), 4 00 (2H, d, *J* = 5 2 Hz, -NHCH_2CO-), 3 96 {5H, s, (η^5-C_5H_5)}, 1 21 (3H, t, *J* = 7 6 Hz, -OCH_2CH_3)

^{13}C NMR (100MHz) δ ($CDCl_3$) 170 1, 169 8, 168 1, 144 5, 130 8, 127 7, 126 3, 83 7, 70 2, 70 1, 67 2, 62 1 (-ve DEPT), 44 0 (-ve DEPT), 41 8 (-ve DEPT), 14 5

_N_-{*para*-(ferrocenyl)benzoyl} glycine-L-alanine ethyl ester 151

For the compound **151**, glycine-L-alanine ethyl ester hydrochloride (0 2 g, 1 0 mmol) was used as a starting material The product was purified by column chromatography {eluant 2 3 petroleum ether (40-60°C) ethyl acetate} Recrystallization from petroleum ether (40-60°C) ethyl acetate furnished the title compound as orange needles (0 241 g, 52%), m p 67-69°C, E ° = 136 mV, $[\alpha]_D^{20}$ = -24° (c 0 79, EtOH)

Mass spectrum found $[M]^{+\bullet}$ 462 114,

$C_{24}H_{26}N_2O_4Fe$ requires 462 124

I R ν_{max} (KBr) 3327, 2929, 1736, 1656, 1630, 1609, 1561, 1509, 1208 cm^{-1}

UV-Vis λ_{max} EtOH, 349 (ε 1865), 446 (ε 560) nm

^{1}H NMR (400MHz) δ ($CDCl_3$) 7 70 (2H, d, *J* = 8 Hz, ArH), 7 43 (2H, d, *J* = 8 Hz, ArH), 7 34 (1H, t, *J* = 4 8 Hz, -CON*H*), 7 19 (1H, d, *J* = 7 2 Hz, -CON*H*), 4 61 {2H, t, *J* = 1 6 Hz, *ortho* (η^5-C_5H_4)}, 4 51 {1H, quint, *J* = 7 2 Hz, -C*H*(CH_3)}, 4 30 (2H, t, *J* = 1 6 Hz, *meta* on (η^5-C_5H_4)}, 4 09-4 15 (4H, m, -NHCH_2CO-, -OC$H_2$$CH_3$), 3 95 {5H, s, ($\eta^5$-$C_5H_5$)}, 1 37 {3H, d, *J* = 7 2 Hz, -CH(CH_3)}, 1 23 (3H, t, *J* = 7 2 Hz, -OCH_2CH_3)

^{13}C NMR (100MHz) δ ($CDCl_3$) 173 1, 169 3, 168 1, 144 3, 131 0, 127 8, 126 2, 83 8, 70 2, 70 1, 67 2, 62 0 (-ve DEPT), 48 8, 44 0 (-ve DEPT), 18 5, 14 5

_N_-{*para*-(ferrocenyl)benzoyl} glycine-L-leucine ethyl ester 152

For compound **152**, glycine L-leucine ethyl ester hydrochloride (0 2 g, 0 8 mmol) was used as starting material The product was purified by column chromatography {eluant 2 3 petroleum ether (40-60°C) ethyl acetate} Recrystallization from petroleum ether (40-60°C) ethyl acetate furnished the title compound an orange solid (0 254 g, 63%)

m p 135-137°C, E ° = 136 mV, $[\alpha]_D^{20}$= -43° (c 2 15, EtOH)

Mass spectrum found $[M+H]^+$ 505 1819,

$C_{27}H_{33}N_2O_4Fe$ requires 505 1790

I R ν_{max} (KBr) 3371, 2963, 1743, 1655, 1638, 1562, 1542, 1508 cm^{-1}

UV-Vis λ_{max} EtOH, 352 (ε 2440), 449 (ε 790) nm

^1H NMR (400MHz) δ ($CDCl_3$) 7 68 (2H, d, J = 8 Hz, ArH), 7 44 (2H, d, J = 8 Hz, ArH), 7 03 (1H, br s, -CON*H*-), 6 69 (1H, d, J = 8 Hz, -CON*H*-), 4 63 {2H, s, *ortho* on (η^5-C_5H_4)}, 4 51- 4 62 [1H, m, -C*H*{$CH_2CH(CH_3)_2$}], 4 32 {2H, s, *meta* on (η^5-C_5H_4)}, 4 09- 4 16 (4H, m, -CONHCH_2-, -OCH_2CH_3), 3 98 {5H, s, (η^5-C_5H_5)}, 1 52-1 63 [3H, m, -CH{CH_2C*H*(CH_3)$_2$}], 1 21 (3H, t, J = 7 6 Hz, -OCH_2CH_3), 0 88 [6H, t, J = 4 4 Hz, -CH{$CH_2CH(CH_3)_2$}]

^{13}C NMR (100MHz) δ ($CDCl_3$) 173 1, 169 3, 168 0, 144 4, 131 0, 127 7, 126 3, 83 8, 70 2, 70 1, 67 2, 61 9 (-ve DEPT), 51 4, 44 0 (-ve DEPT), 41 8 (-ve DEPT), 25 3, 23 2, 22 3, 14 5

***N*-{*para*-(ferrocenyl)benzoyl} glycine-L-phenylalanine ethyl ester 153**

For the compound **153**, glycine-L-phenylalanine ethyl ester hydrochloride (0 2 g, 0 7 mmol) was used as starting material The product was purified by column chromatography {eluant 2 3 petroleum ether (40-60°C) ethyl acetate} Recrystallization from petroleum ether (40-60°C) ethyl acetate furnished the title compound as an orange solid (0 252 g, 67%)

m p 67-69°C, E ° = 133 mV, $[\alpha]_D^{20}$= +10° (c 2, EtOH),

I R ν_{max} (KBr) 3321, 2928, 2852, 1739, 1631, 1609, 1507, 1465, 1401, 1377 cm^{-1}

UV-Vis λ_{max} EtOH, 351 (ε 2620), 450 (ε 870) nm

^1H NMR (400MHz) δ ($CDCl_3$) 7 67 (2H, d, J = 8 Hz, ArH), 7 44 (2H, d, J = 8 Hz, ArH), 7 13-7 14 (3H, m, ArH), 7 05-7 09 (3H, m, ArH, -CON*H*-), 6 81 (1H, d, J = 7 6 Hz, -CON*H*-), 4 72-4 83 {1H, m, -C*H*(CH_2Ph)}, 4 64 {2H, s, *ortho* on (η^5-C_5H_4)}, 4 32 {2H, s, *meta* on (η^5-C_5H_4)}, 4 03-4 12 (4H, m, -NHCH_2CO-, -OCH_2CH_3), 3 97 {5H, s, (η^5-C_5H_5)}, 3 02-3 10 {2H, m, -CH(CH_2Ph)}, 1 17 (3H, t, J = 7 2 Hz, -OCH_2CH_3)

^{13}C NMR (100MHz) δ ($CDCl_3$) 171 7, 169 2, 167 9, 144 4, 136 1, 130 9, 129 7, 129 0, 127 8, 127 5, 126 2, 83 9, 70 2, 70 1, 67 2, 62 1 (-ve DEPT), 53 8, 44 0 (-ve DEPT), 38 3 (-ve DEPT), 14 5

***N*-{*meta*-(ferrocenyl)benzoyl} glycine-glycine ethyl ester 154**

For the compound **154**, glycine-glycine ethyl ester hydrochloride (0 2 g, 1 0 mmol) was used as starting material The product was purified by column chromatography {eluant 2 3 petroleum ether (40-60°C) ethyl acetate} Recrystallization from petroleum ether (40-60°C) ethyl acetate furnished the title compound as an orange solid (0 246 g, 55%) m p 54-56°C, E °=127 mV

Mass spectrum found $[M]^{+\bullet}$ 448 05,

$C_{23}H_{24}N_2O_4Fe$ requires 448 10

I R ν_{max} (KBr) 3379, 3265, 2936, 1729, 1691, 1637, 1552, 1272, 1215 cm^{-1}

UV-Vis λ_{max} EtOH, 325 (ε 1140), 443 (ε 330) nm

^{1}H NMR (400MHz) δ ($CDCl_3$) 7 87 (1H, s, ArH), 7 53-7 57 (2H, m, ArH), 7 28 (1H, t, *J* = 7 6 Hz, ArH), 7 20 (1H, br s, -CON*H*-), 6 82 (1H, br s, -CON*H*-), 4 62 {2H, t, *J* = 2 Hz, *ortho* on (η^5-C_5H_4)}, 4 30 {2H, t, *J* = 2 Hz, *meta* on (η^5-C_5H_4)}, 4 13-4 24 (4H, m, -O$CH_2$$CH_3$, -NHC$H_2$CO-), 4 01 (2H, d, *J* = 5 6 Hz, -NHCH_2CO-), 3 67 {5H, s, (η^5-C_5H_5)}, 1 20 (3H, t, *J* = 7 6 Hz, -OCH_2CH_3)

^{13}C NMR (100MHz) δ ($CDCl_3$) 170 0, 169 8, 168 4, 140 8, 134 0, 129 8, 129 0, 125 1, 124 7, 84 4, 70 1, 69 7, 67 0, 62 1 (-ve DEPT), 44 0 (-ve DEPT), 41 8 (-ve DEPT), 14 5

***N*-{*meta*-(ferrocenyl)-benzoyl} glycine-L-alanine ethyl ester 155**

For the compound **155**, glycine-L-alanine ethyl ester hydrochloride (0 2 g, 1 0 mmol) was used as starting material The product was purified by column chromatography {eluant 2 3 petroleum ether (40-60°C) ethyl acetate} Recrystallization from petroleum ether (40-60°C) ethyl acetate furnished the title compound as orange needles (0 229 g, 50%) m p 87-89°C, E ° = 131 mV, $[\alpha]_D^{20}$ = -18° (c 2, EtOH)

I R ν_{max} (KBr) 3358, 3257, 3095, 2932, 1735, 1687, 1639, 1561, 1528, 1509 cm^{-1}

UV-Vis λ_{max} EtOH, 325 (ε 1290), 442 (ε 370) nm

^{1}H NMR (400MHz) δ ($CDCl_3$) 7 94 (1H, s, ArH), 7 64 (2H, d, *J* = 8 4 Hz, ArH), 7 36 (1H, t, *J* = 8 4 Hz, ArH), 7 31 (1H, t, *J* = 7 2 Hz, -CON*H*-), 7 09 (1H, d, *J* = 7 2 Hz, -

CONH-), 4 71 {2H, t, J = 2 Hz, *ortho* on (η^5-C_5H_4)}, 4 62 {1H, quint, J = 7 6 Hz, -CH(CH_3)}, 4 35 {2H, t, J = 2 Hz, *meta* on (η^5-C_5H_4)}, 4 19-4 27 (4H, m, -NHCH_2CO-, -OC$H_2$$CH_3$), 4 05 {5H, s, ($\eta^5$-$C_5H_5$)}, 1 74 {3H, d, J = 7 6 Hz, -CH(CH_3)}, 1 30 (3H, t, J = 7 6 Hz, -OCH_2CH_3)

^{13}C NMR (100MHz) δ ($CDCl_3$) 173 1, 169 1, 168 3, 140 7, 134 1, 129 8, 129 0, 125 1, 124 7, 84 4, 70 1, 69 7, 67 0, 62 0 (-ve DEPT), 48 8, 44 0 (-ve DEPT), 18 6, 14 5

N-{*meta*-(ferrocenyl)-benzoyl} glycine-L-leucine ethyl ester 156

For the compound **156**, glycine-L-leucme ethyl ester hydrochloride (0 2 g, 0 8 mmol) was used as starting material The product was purified by column chromatography {eluant 2 3 petroleum ether (40-60°C) ethyl acetate} Recrystallization from petroleum ether (40-60°C) ethyl acetate furnished the title compound as an orange solid (0 229 g, 57%)

m p 129-131°C, E ° = 131 mV, $[\alpha]_D^{20}$ = -28° (c 1 6, EtOH)

Mass spectrum found $[M]^{+\bullet}$ 504 12,

$C_{27}H_{32}N_2O_4Fe$ requires 504 17

I R ν_{max} (KBr) 3363, 3244, 2958, 1731, 1702, 1672, 1642, 1538, 1216, 1157 cm^{-1}

UV-Vis λ_{max} EtOH, 322 (ε 1610), 443 (ε 440) nm

^{1}H NMR (400MHz) δ ($CDCl_3$) 7 86 (1H, s, ArH), 7 54 (1H, d, J = 7 6 Hz, ArH), 7 20-7 29 (3H, m, ArH, -CONH-), 7 01 (1H, d, J = 8 Hz, -CONH-), 4 63 {2H, s, *ortho* on (η^5-C_5H_4)}, 4 51-4 59 [1H, m, -CH{$CH_2CH(CH_3)_2$}], 4 27 {2H, s, *meta* on (η^5-C_5H_4)}, 4 18 (2H, t, J = 5 6 Hz, -NHCH_2CO-), 4 12 (2H, q, J = 7 2 Hz, -OC$H_2$$CH_3$), 3 96 (5H, s, ($\eta^5$-$C_5H_5$)}, 1 55-1 63 [3H, m, -CH{CH_2CH(CH_3)$_2$}], 1 21 (3H, t, J = 7 2 Hz, -OCH_2CH_3), 0 86 [6H, d, J = 7 6 Hz, -CH{CH_2CH(CH_3)$_2$}]

^{13}C NMR (100MHz) δ ($CDCl_3$) 173 2, 169 4, 168 4, 140 7, 134 1, 129 8, 129 0, 125 1, 124 7, 84 5, 70 1, 69 7, 67 0, 61 9 (-ve DEPT), 51 6, 44 0(-ve DEPT), 41 7 (-ve DEPT), 25 3, 23 2, 22 3, 14 5

N-{*meta*-(ferrocenyl)benzoyl} glycine-L-phenylalanine ethyl ester 157

For the compound **157**, glycine-L-phenylalanine ethyl ester hydrochloride (0 2 g, 0 7 mmol) was used as the starting material The product was purified by column chromatography {eluant 2 3 petroleum ether (40-60°C) ethyl acetate} Recrystallization

from petroleum ether (40-60°C) ethyl acetate furnished the title compound as orange needles (0 210 g, 56%)

m p 84-86°C, E ° = 130 mV, $[\alpha]_D^{20}$ = +1° (c 2 1, EtOH)

Mass spectrum found $[M]^{+\bullet}$ 538 134,

$C_{30}H_{30}N_2O_4Fe$ requires 538 156

I R ν_{max} (KBr) 3358, 2928, 1735, 1704, 1640, 1543, 1209 cm^{-1}

UV-Vis λ_{max} EtOH, 328 (ε 1260), 445 (ε 360) nm

^1H NMR (400MHz) δ ($CDCl_3$) 7 83 (1H, s, ArH), 7 55 (1H, d, *J* = 7 6 Hz, ArH), 7 50 (1H, d, *J* = 7 6 Hz, ArH), 7 27 (1H, t, *J* = 7 6 Hz, ArH), 7 04-7 12 (6H, m, ArH, -CON*H*-), 6 73 (1H, d, *J* = 7 6 Hz, -CON*H*-), 4 80 {1H, q, *J* = 7 6 Hz, -C*H*(CH_2Ph)}, 4 66 {2H, s, *ortho* on (η^5-C_5H_4)}, 4 30 {2H, s, *meta* on (η^5-C_5H_4)}, 4 05-4 13 (4H, m, -CONHCH_2-, -OC$H_2$$CH_3$), 3 99 (5H, s, ($\eta^5$-$C_5H_5$)}, 3 09 [1H, dd, J_{ax} = 2 0 Hz, J_{ab} = 5 6 Hz, -CH(CH_2Ph)], 3 03 [1H, dd, J_{ax} = 2 0 Hz, J_{ab} = 5 6 Hz -CH(CH_2Ph)], 1 17 (3H, t, *J* = 7 2 Hz, -$OCH_2C$$H_3$)

^{13}C NMR (100MHz) δ ($CDCl_3$) 171 6, 169 1, 168 2, 140 7, 136 1, 134 0, 129 8, 129 7, 129 0, 128 9, 127 6, 125 1, 124 7, 84 7, 70,3, 60 9, 67 1, 62 1 (-ve DEPT), 53 8, 43 9 (-ve DEPT), 38 0(-ve DEPT), 14 5

_N_-{*ortho*-(ferrocenyl)benzoyl} glycine-glycine ethyl ester 158

For the compound **158**, glycine-glycine ethyl ester hydrochloride (0 2 g, 1 0mmol) was used as starting material The product was purified by column chromatography {eluant 2 3 petroleum ether (40-60°C) ethyl acetate} Recrystallization from petroleum ether (40-60°C)-ethyl acetate furnished the title compound as orange needles (0 198 g, 44%)

m p 69-71°C, E ° = 131 mV

Mass spectrum found $[M]^{+\bullet}$ 448 106,

$C_{23}H_{24}N_2O_4Fe$ requires 448 109

I R ν_{max} (KBr) 3397, 2983, 1737, 1657, 1650, 1524, 1379, 1202 cm^{-1}

UV-Vis λ_{max} EtOH, 326 (ε 1430), 439 (ε 290) nm

^1H NMR (400MHz) δ (DMSO) 8 50 (1H, t, *J* = 6 Hz, -CON*H*-), 8 70 (1H, t, *J* = 6 Hz, -CON*H*-), 7 79 (1H, d, *J* = 7 6 Hz, ArH), 7 40 (1H, t, *J* = 7 6 Hz, ArH), 7 24-7 29 (2H, m, ArH), 4 64 {2H, t, *J* = 2 Hz, *ortho* on (η^5-C_5H_4)}, 4 27 (2H, t, J = 2 Hz, *meta* on

(η^5-C_5H_4)}, 4 22 (2H, q, J = 7 2 Hz, -OCH_2CH$_3$), 4 06 (5H, s, (η^5-C_5H_5)}, 3 87 (2H, d, J = 5 6 Hz, -NHCH_2CO-), 3 83 (2H, d, J = 5 6 Hz, -NHCH_2CO-), 1 28 (3H, t, J = 7 2 Hz, -OCH$_2$CH_3)

^{13}C NMR (100MHz) δ (DMSO) 170 5, 170 1, 169 7, 136 6, 136 4, 130 4, 129 1, 127 8, 125 8, 84 8, 69 8, 69 1, 68 6, 60 9 (-ve DEPT), 42 3(-ve DEPT), 41 0(-ve DEPT), 14 4

***N*-{*ortho*-(ferrocenyl)benzoyl} glycine-L-alanine ethyl ester 159**

For the compound **159**, glycine-L-alanine ethyl ester hydrochloride (0 2 g, 1 0 mmol) was used as a starting material The product was purified by column chromatography {eluant 2 3 petroleum ether (40-60°C) ethyl acetate} Recrystallization from petroleum ether (40-60°C) ethyl acetate furnished the title compound as an orange solid (0 136 g, 29%)

m p 102-104°C, E ° = 132 mV, $[\alpha]_D^{20}$= -4° (c 1 9, EtOH)

Mass spectrum found $[M]^{+\bullet}$ 462 113,

$C_{24}H_{26}N_2O_4Fe$ requires 462 124

I R ν_{max} (KBr) 3376, 3281, 1720, 1647, 1480, 1370, 1293 cm^{-1}

UV-Vis λ_{max} MeCN, 224 (e 340), 445 (e 210) nm

^{1}H NMR (400MHz) δ ($CDCl_3$) 7 80 (1H, d, J = 7 6 Hz, ArH), 7 36-7 44 (2H, m, ArH), 7 27 (1H, t, J = 7 6 Hz, ArH), 6 72 (1H, d, J = 6 8 Hz, -CON*H*-), 6 15 (1H, br s, -CON*H*-), 4 50-4 62 {3H, m, *ortho* on (η^5-C_5H_4), -C*H*(CH_3)}, 4 29 (2H, s, *meta* on (η^5-C_5H_4)}, 4 20 (2H, q, J = 6 8 Hz, -OCH_2CH$_3$), 4 11 (5H, s, (η^5-C_5H_5)}, 3 97 (2H, t, J = 4 8 Hz, -CONHCH_2-), 1 39 {3H, d, J = 7 2 Hz, -CH(CH_3)}, 1 28 (3H, t, J = 6 8 Hz, -OCH$_2$CH_3)

^{13}C NMR (100MHz) δ ($CDCl_3$) 173 0, 171 3, 168 4, 136 9, 135 5, 131 3, 130 0, 128 3, 126 7, 85 6, 70 2, 69 7, 69 6, 69 2, 61 9(-ve DEPT), 48 5, 44 0(-ve DEPT), 18 7, 14 5

***N*-{*ortho*-(ferrocenyl)benzoyl} glycine-L-phenylalanine ethyl ester 160**

For the compound **160**, glycine-L-phenylalanine ethyl ester hydrochloride (0 2 g, 0 7 mmol) was used as a starting material The product was purified by column chromatography {eluant 2 3 petroleum ether (40-60°C) ethyl acetate} The resultant product was recrystallized from petroleum ether (40-60°C) ethyl acetate and furnished the title compound as orange needles (0 105 g, 28%)

m p 51-53°C, E ° = 133 mV, $[\alpha]_D^{20}$= +2° (c 2 1, EtOH)

Mass spectrum found $[M]^{+\bullet}$ 538 168,

$C_{30}H_{30}N_2O_4Fe$ requires 538 155

I R ν_{max} (KBr) 3331, 2933, 1735, 1654, 1648, 1523, 1376, 1216 cm^{-1}

UV-Vis λ_{max} EtOH, 323 (ε 1570), 440 (ε 360) nm

^1H NMR (400MHz) δ (DMSO) 8 29 (1H, t, *J* = 6 Hz, -CON*H*-), 8 18 (1H, d, *J* = 7 6 Hz, -CON*H*-), 7 62 (1H, d, *J* = 8 Hz, ArH), 7 32 (1H, t, *J* = 8 Hz, ArH), 7 03-7 15 (7H, m, ArH), 4 48 {2H, s, *ortho* on (η^5-C_5H_4)}, 4 30-4 45 {1H, m, -C*H*(CH_2Ph)}, 4 09 {2H, s, *meta* on (η^5-C_5H_4)}, 3 86-3 99 {7H, m, (η^5-C_5H_5), -O$CH_2$$CH_3$}, 3 64 (2H, t, *J* = 5 2 Hz, -NHCH_2CO-), 2 80-2 85 {2H, m, -CH(CH_2Ph)}, 0 92 (3H, t, *J* = 7 2 Hz, -OCH_2CH_3)

^{13}C NMR (100MHz) δ (DMSO) 171 7, 170 3, 169 2, 137 3, 136 6, 136 4, 130 7, 129 5, 129 1, 128 6, 127 7, 127 0, 125 7, 84 7, 69 8, 69 1, 68 6, 60 9 (-ve DEPT), 54 1, 42 2 (-ve DEPT), 37 3 (-ve DEPT), 14 3

Appendix I

Appendix I

Abbreviations

°C	Degrees celsius
Ala	Alanine
ATP	Adenosine triphosphate
Boc	*Tert*-butoxycarbonyl
BOP	Benzotriazolyl-1-oxy(dimethylamino)-phosphonium hexafluorophosphate
Bpoc	2-(4-Biphenylyl)-isopropyloxycarbonyl
$CDCl_3$	Deuterated chloroform
CFR	Circular field reflectron
CV	Cyclic voltammetry
Da	Dalton
DCC	Dicyclohexylcarbodiimide
DCU	*N,N'* Dicyclohexylurea
DEPT	Distortionless enhancement through polarization transfer
DHA	2,5-Dihydroxy benzoic acid
DMSO	Dimethyl sulfoxide
DNA	Deoxyribonucleic acid
E°'	Formal reduction potential
$E_{½}$	Half wave reduction potential
EAN	Effective atomic number
EDC	1-{3-(dimethylamino)-propyl}-3-ethylcarbodiimide
ESI	Electrospray ionization
Et_3N	Triethylamine
FABMS	Fast atom bombardment mass spectrometry
Fc	Ferrocene
Fmoc	9-Fluorenylmethoxycarbonyl
g	Gram
HBr	Hydrogen bromide
HF	Hydrogen fluoride

HMPA	Hexamethylphosphoramide
HMQC	Heteronuclear multiple quantum coherence
HOBt	1-Hydroxybenzotriazole
IR	Infrared
LiCl	Lithium chloride
M	Molar
m p	Melting point
MALDI-TOF	Matrix assisted laser desorption ionization Time of flight
MeOH	Methanol
ml	Millilitre
MLCT	Metal-ligand charge transfer
mmol	Millimole
MRSA	Multi-resistant staphylococci
MS	Mass spectrometry
mV	Millivolt
nm	Nanometre
NMR	Nuclear magnetic resonance
PCl_5	Phosphorous pentachloride
Phe	Phenylalanine
ppm	Parts per million
Pro	Proline
SA	Sinapinic acid
$SOCl_2$	Thionyl chloride
TBTU	*O*-Benzotriazolyl bis-(dimethylamino)uranium tetrafluoroborate
TFA	Trifluoroacetic acid
UV-Vis	Ultraviolet-visible
Z/CBz	Benzyloxycarbonyl

Appendix II

ELSEVIER

Inorganic Chemistry Communications 5 (2002) 1034–1040

INORGANIC CHEMISTRY COMMUNICATIONS

www.elsevier.com/locate/inoche

Semi-rigid *N-para*-ferrocenyl(benzoyl)amino-acid esters for biomaterials: synthesis and characterization of Fc-$C_6H_4CONHCH(R)CO_2Me$ where Fc = $(\eta^5\text{-}C_5H_5)Fe(\eta^5\text{-}C_5H_4)$ and R = H, CH_3, $CH_2CH(CH_3)_2$, $CH_2C_6H_5$ and the X-ray crystal structures of Fc-$C_6H_4CO_2Me$ and the L-alanine derivative Fc-$C_6H_4CONHCH(CH_3)CO_2Me$

David Savage [a], John F. Gallagher [a,*], Yoshiteru Ida [b], Peter T.M. Kenny [a,1]

[a] *School of Chemical Sciences, Dublin City University, Dublin 9, Ireland*
[b] *School of Pharmaceutical Sciences, Showa University, Hatanodai, Shinagawa-ku, Tokyo 142-8555, Japan*

Received 16 August 2002; accepted 9 September 2002

Abstract

A series of *N-para*-(ferrocenyl)benzoyl amino-acid esters, *para*-Fc(C_6H_4)CONHCH(R)CO_2CH_3 {Fc = $(\eta^5\text{-}C_5H_5)Fe(\eta^5\text{-}C_5H_4)$; R = H, CH_3, $CH_2CH(CH_3)_2$, $CH_2C_6H_5$}, **3–6** have been prepared by coupling *para*-(ferrocenyl)benzoic acid to the amino-acid esters (gly, L-Ala, L-Leu, L-Phe) using the standard 1,3-dicyclohexylcarbodiimide (DCC), 1-hydroxybenzotriazole (HOBt) protocol. The compounds were fully characterized by a range of spectroscopic techniques including FAB-MS. The X-ray crystal structures of the parent *para*-(ferrocenyl)benzoyl methyl ester, Fc-$C_6H_4CO_2Me$, **1** and a chiral derivative *N*-{*para*-(ferrocenyl)benzoyl}-L-alanine methyl ester, Fc-$C_6H_4CONHCH(CH_3)CO_2Me$, **4** have been determined.

Keywords: Ferrocene; Biomaterials; Bioorganometallic chemistry; FAB-MS; X-ray crystal structures; Amino-acid esters

1. Introduction

Research in the area of bioorganometallic chemistry and in particular ferrocenyl derivatives has seen a dramatic increase in attention over the past decade, primarily for the ultimate goals of achieving (i) novel biomaterial based sensors, (ii) peptide mimetic models and unnatural drugs [1–6]. In conjunction with these developments, the field of ferrocene chemistry continues to expand into new hybrid areas of research including (iii) non-linear optical materials, (iv) liquid crystals and (v) novel molecular sensors [1b,7–9]. Our primary interest in bioorganometallic chemistry stems from the synthesis and characterisation of unusual biological materials which combine several key moieties namely (a) an electro-active core, (b) a conjugated linker which can potentially act as a chromophore and (c) a biological marker, usually an amino-acid ester or dipeptide derivative which can bind or interact with a larger biological host species, e.g., a protein or an enzyme [4].

The present series reported herein comprises a ferrocenyl moiety linked directly to the amino-acid residue through a *para*-benzoyl group such that the molecular *cleft* between the ferrocenyl moiety and the terminal amino-acid ester residue is enlarged and conjugation effects can be monitored along the semi-rigid backbone. A full paper on the entire series of *para*-(ferrocenyl)benzoyl amino acid and dipeptide ester derivatives will be reported in due course [10].

* Corresponding author. Tel.: +353-1-7005114; fax: +353-1-7005503.
E-mail addresses: john.gallagher@dcu.ie (J.F. Gallagher), peter.kenny@dcu.ie (P.T.M. Kenny).
[1] Also corresponding author. Tel.: +353-1-7005689.

1387-7003/02/$ - see front matter © 2002 Elsevier Science B.V. All rights reserved.
PII: S1387-7003(02)00638-X

2 Experimental

2 1 General procedures

All chemicals were purchased from Sigma/Aldrich and used as received Commercial grade reagents were used without further purification, however, solvents were purified prior to use Ferrocene carboxylic acid was prepared according to the published procedure [11] Melting points were determined using a Griffin melting point apparatus and are uncorrected Infrared spectra were recorded on a Nicolet 405 FT-IR spectrometer and UV–Vis spectra on a Hewlett-Packard 8452A diode array UV–Vis spectrophotometer NMR spectra were obtained on a Bruker AC 400 NMR spectrometer operating at 400 MHz for ^{1}H NMR and 100 MHz for ^{13}C NMR The ^{1}H and ^{13}C NMR chemical shifts (ppm) are relative to TMS and all coupling constants (J) are in Hertz Positive ion fast atom bombardment mass spectra were obtained on a JEOL SX102 double focussing mass spectrometer employing *meta*-nitrobenzyl alcohol as the liquid matrix The single crystal X-ray data for **1** and **4** were collected on a Siemens P4 diffractometer at 294(1) K ω-scans for the θ range 2–26° Data reduction was standard and Ψ-scans were used for the absorption corrections to **1** (6 reflections with 4° increments) and **4** (4 reflections with 4° increments)

2 2 General procedure for the synthesis of the starting materials 1, 2

2 2 1 para-Ferrocenyl methyl benzoate 1

Concentrated hydrochloric acid (6 ml) was added with intermittent cooling to a solution of methyl-4-aminobenzoate (3 g, 18 2 mmol) in 15 ml of water A solution of sodium nitrite (1 4 g, 20 3 mmol) in 15 ml of water was then added slowly to this mixture with stirring keeping the temperature below 5 °C furnishing a pale yellow solution The resulting diazo salt was added to a solution of ferrocene (3 8 g, 20 4 mmol) in diethyl ether (90 ml) and allowed to react for 12 h The reactant mixture was then washed with water, the ether layer was dried over $MgSO_4$ the solvent was removed in vacuo to yield the crude product The crude product was purified by column chromatography (eluent 3 2 petroleum ether/diethyl ether) The crystals were of sufficient quality for an X-ray diffraction study m p 100–102°C IR ν_{max} (KBr) 2926, 1706, 1605, 1437, 1276, 1105 cm^{-1} UV–Vis λ_{max} CH_2Cl_2 364 (ε 2190), 436 (810) nm

^{1}H NMR (400 MHz) δ (DMSO) 7 64 (2H, d, J = 8 Hz, –ArH), 7 43 (2H, d, J = 8 Hz, –ArH), 4 66 {2H, t, J = 2 Hz, *ortho* on (η^5-C_5H_4)}, 4 21 {2H, t, J = 2 Hz, *meta* on (η^5-C_5H_4)}, 3 79 {5H, s, (η^5-C_5H_5)}, 3 61 (3H, s, –OC*H*$_3$)

^{13}C NMR (100 MHz) δ (DMSO) 166 6, 145 5, 129 6, 126 9, 126 1, 83 0, 70 2, 68 1, 67 2, 52 3

2 2 2 para-Ferrocenyl benzoic acid 2

Sodium hydroxide (0 3 g, 7 5 mmol) was added to *para*-ferrocene methyl benzoate (2 4 g, 7 5 mmol) in a 1 1 mixture of water/methanol and refluxed for 3 h Concentrated HCl was added until pH 2 was reached The solution was allowed to cool and the product was isolated by filtration m p (decomp) at 203 °C IR ν_{max} (KBr) 3449, 1678, 1607, 1284, 1105 cm^{-1} UV–Vis λ_{max} CH_2Cl_2 368 (ε 1630), 460 (690) nm

^{1}H NMR (400 MHz) δ (DMSO) 12 8 (1H, s, –COO*H*), 7 85 (2H, d, J = 8 Hz, –ArH), 7 64 (2H, d, J = 8 Hz, –ArH), 4 89 {2H, t, J = 2 Hz, *ortho* on (η^5-C_5H_4)}, 4 43 {2H, t, J = 2 Hz, *meta* on (η^5-C_5H_4)}, 4 03 {5H, s, (η^5-C_5H_5)}

^{13}C NMR (100 MHz) δ (DMSO) 167 7, 145 0, 129 9, 127 3, 126 0, 83 2, 70 1, 69 9, 68 1, 67 1

2 3 General procedure for the synthesis of N-{para-(ferrocenyl)benzoyl}amino-acid esters 3–6

2 3 1 N-{para-(ferrocenyl)benzoyl}glycine methyl ester 3

Glycine methyl ester hydrochloride (0 3 g, 2 3 mmol) and triethylamine (0 5 ml) were added to a solution of *para*-ferrocenyl benzoic acid (0 5 g, 1 6 mmol), 1-hydroxybenzotriazole (0 3 g, 2 2 mmol) and 1,3-dicyclohexylcarbodiimide (0 45 g, 2 2 mmol) in CH_2Cl_2 (50 ml) at 0 °C After 30 min the solution was raised to room temperature and allowed to proceed for 48 h The precipitated *N,N'*-dicyclohexylcarbourea was removed by filtration and the filtrate was washed with water, 10% potassium hydrogen carbonate, 5% citric acid and dried over $MgSO_4$ Recrystallization from petroleum ether (40–60 °C)/ethyl acetate furnished *N*-{*para*-(ferrocenyl)benzoyl}glycine methyl ester **3** as orange needles (0 32 g, 52%) m p 116–117 °C, $E_{1/2}$ = 507 mV Mass spectrum found $[M+H]^+$ 378 0774, $C_{20}H_{20}N_1O_3Fe$ requires 378 0793 IR ν_{max} (KBr) 3308, 1763, 1701, 1636, 1561 cm^{-1} UV–Vis λ_{max} CH_2Cl_2 356 (ε 1880), 454 (610) nm

^{1}H NMR (400 MHz) δ (DMSO) 8 88 (1H, t, J = 5 6 Hz, –CON*H*CH$_2$-), 7 76 (2H, d, J = 8 Hz, –ArH), 7 60 (2H, d, J = 8 Hz, –ArH), 4 85 {2H, s, *ortho* on (η^5-C_5H_4)}, 4 38 {2H, s, *meta* on (η^5-C_5H_4)}, 3 98 {5H, s, (η^5-C_5H_5)}, 3 97 (2H, d, J = 5 6 Hz, –NHC*H*$_2$CO–), 3 63 (3H, s, –OC*H*$_3$) ^{13}C NMR (100 MHz) δ (DMSO) 170 8, 166 8, 143 4, 131 0, 127 8, 125 8, 83 5, 69 9, 67 0, 52 1, 41 6 (-ve DEPT)

2 3 2 N-{para-(ferrocenyl)benzoyl}-L-alanine methyl ester 4

L-Alanine methyl ester hydrochloride (0 3 g, 2 2 mmol) was used Recrystallization from petroleum ether

(40–60 °C)/ethyl acetate yielded *N*-{*para*-(ferrocenyl)-benzoyl}-L-alanine methyl ester **4** as orange needles (0 28 g, 45%) which were of sufficient quality for an X-ray diffraction study m p 137–138 °C, $E_{1/2} = 490$ mV, $[\alpha]_D^{25} = +19°$ (c 2, CH_2Cl_2) Mass spectrum found $[M + H]^+$ 392 0923, $C_{21}H_{22}N_1O_3Fe$ requires 392 0949 IR $\nu_{max}(CHCl_3)$ 3409, 1742, 1654, 1500 cm^{-1} UV–Vis λ_{max} CH_2Cl_2 356 (ε 1270), 452 (400) nm

^1H NMR (400 MHz) δ (DMSO) 8 76 (1H, d, $J = 6$ 8 Hz, –CONHCH–), 7 81 (2H, d, $J = 8$ Hz, –ArH), 7 72 (2H, d, $J = 8$ Hz, –ArH), 4 90 {2H, s, *ortho* on (η^5-C_5H_4)}, 4 46–4 50 {1H, m, –CONHC*H*(CH_3)CO–}, 4 42 {2H, s, *meta* on (η^5-C_5H_4)}, 4 02 {5H, s, (η^5-C_5H_5)}, 3 65 (3H, s –OCH_3), 1 41 {3H, d, $J = 7$ 2 Hz, –CONHCH(CH_3)CO–} ^{13}C NMR (100 MHz) δ (DMSO) 173 7, 166 4, 143 3, 131 0, 128 0, 125 7, 83 5, 69 9, 67 0, 66 9, 52 3, 48 6, 17 1

2 3 3 N-{para-(ferrocenyl)benzoyl}-L-leucinemethyl ester **5**

L-Leucine methyl ester hydrochloride (0 3 g, 1 6 mmol) was used Recrystallization from petroleum ether (40–60 °C)/ethyl acetate furnished **5** as a brown solid (0 28 g, 45%) m p 96–98 °C, $E_{1/2} = 493$ mV, $[\alpha]_D^{25} = +4°$ (c 2, CH_2Cl_2) Mass spectrum found $[M + H]^+$ 434 1399, $C_{24}H_{28}N_1O_3Fe$ requires 434 1419 IR ν_{max} (KBr) 3327, 2929, 2851, 1627, 1610, 1547 cm^{-1} UV–Vis λ_{max} CH_2Cl_2 356 (ε 1270), 454 (ε 360) nm

^1H NMR (400 MHz) δ (DMSO) 8 69 (1H, d, $J = 7$ 6 Hz, –CONH–), 7 81 (2H, d, $J = 8$ Hz, –ArH), 7 63 (2H, d, $J = 8$ Hz, –ArH), 4 90 {2H, t, $J = 1$ 6 Hz, *ortho* on (η^5-C_5H_4)}, 4 48–4 54 (1H, m, –NHC*H*CO–), 4 42 {2H, t, $J = 1$ 6 Hz, *meta* on (η^5-C_5H_4)}, 4 02 {5H, s, (η^5-C_5H_5)}, 3 65 (3H, s, –OCH_3), 1 57–1 81 {3H, m, –$CH_2CH(CH_3)_2$}, 0 93 {3H, d, $J = 7$ 2 Hz, –$CH_2CH(CH_3)_2$}, 0 90 {3H, d, $J = 7$ 2 Hz, –$CH_2CH(CH_3)_2$} ^{13}C NMR (100 MHz) δ ($CDCl_3$) 174 2, 167 4, 144 2, 131 4, 127 6, 126 2, 83 9, 70 2, 70 0, 67 2, 52 8, 51 5, 43 2 (-ve DEPT), 25 4, 23 3, 22 5

2 3 4 N-{para-(ferrocenyl)benzoyl}-L-phenyl-alanine methyl ester **6**

Phenylalanine methyl ester hydrochloride (0 3 g, 1 4 mmol) was used Recrystallization from petroleum ether (40–60 °C)/ethyl acetate furnished **6** as orange crystals (0 29 g, 45%) m p 151–152 °C, $E_{1/2} = 500$ mV, $[\alpha]_D^{20} = -4°$ (c 1 4, CH_2Cl_2) Mass spectrum found $[M + H]^+$ 468 1258, $C_{27}H_{26}N_1O_3Fe$ requires 468 1262 IR ν_{max} (KBr) 3339, 2927, 1737, 1638 1606, 1518 cm^{-1} UV–Vis λ_{max} CH_2Cl_2 358 (ε 3370), 458 (ε 1110) nm

^1H NMR (400 MHz) δ (DMSO) 8 83 (1H d, $J = 7$ 6 Hz, –CONH–), 7 73 (2H, d, $J = 8$ 4 Hz, –ArH), 7 61 (2H, d, $J = 8$ 4 Hz, –ArH), 7 20–7 34 (5H, m, –ArH), 4 88 {2H, s, *ortho* on (η^5-C_5H_4)}, 4 64–4 68 (1H, m, –CONHC*H*CO–), 4 41 {2H, s, *meta* on (η^5-C_5H_4)}, 4 02 {5H, s, (η^5-C_5H_5)}, 3 65 (3H, s, –OCH_3), 3 11–3 17 {2H, m, –CONHC*H*(CH_2Ph)CO–} ^{13}C NMR (100 MHz) δ (DMSO) 172 7, 166 7, 143 4, 138 1, 131 0, 129 4, 128 6, 127 9, 126 8, 125 8, 83 5, 69 9, 67 0, 54 7, 52 3, 36 7 (-ve DEPT)

3 Results and discussion

3 1 Synthesis

The preparation of the *para*-ferrocenyl benzoic acid **2** employed conventional diazonium salt chemistry Treatment of methyl-4-aminobenzoate with sodium nitrite in the presence of HCl yielded the diazonium salt which was then reacted with ferrocene in situ to furnish the *para*-substituted ferrocenyl methyl benzoate **1** as a viscous oil Recrystallization from $CHCl_3$ yielded crystals of sufficient quality for an X-ray diffraction study Prior to coupling with the C-protected amino acids, the ester group was cleanly cleaved by treatment with 10% NaOH to yield the *para*-ferrocenyl benzoic acid **2** The ^1H NMR spectrum showed signals at δ 7 64 and δ 7 85 due to the aromatic ring protons and the COO*H* proton

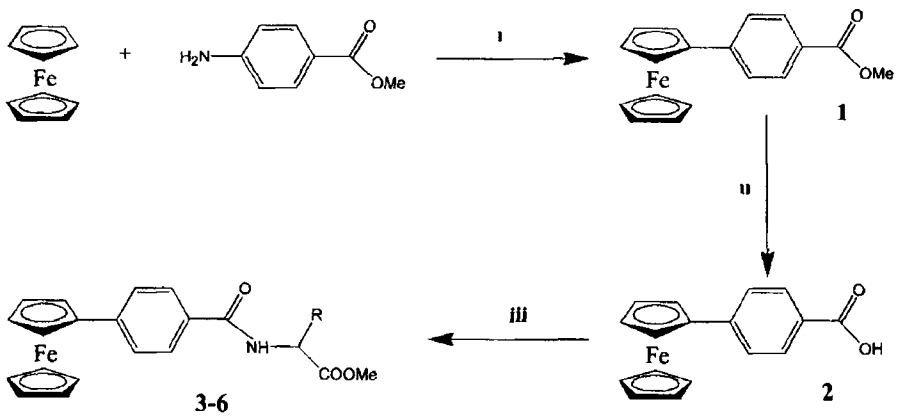

Scheme 1 Synthesis of the *N* ferrocenyl(benzoyl)amino-acid esters **3–6** (i) $NaNO_2$ HCl 5 °C (ii) NaOH/MeOH, (iii) DCC, HOBt, Et_3N, ($H_2NCH(R)CO_2Me$) where R = *H* **3** CH_3 **4** $CH_2CH(CH_3)_2$ **5** $CH_2C_6H_5$ **6**

was present at δ 12 8 The ferrocenyl *ortho* and *meta* protons on the (η^5-C_5H_4) ring were observed at δ 4 89 and δ 4 43, respectively, and at δ 4 03 for the (η^5-C_5H_5) ring The condensation of *para*-ferrocenyl benzoic acid with the free N-terminal amino-acid methyl esters of glycine, L-alanine, L-leucine and L-phenylalanine under basic conditions in the presence of dicyclohexylcarbodiimide (DCC) and 1-hydroxybenzotriazole (HOBt) cleanly led to the formation of yellow/orange coloured *N*-{*para*-(ferrocenyl)benzoyl}amino-acid esters, Fc-C_6H_4CONHCH(R)CO_2Me where R = H **3**, CH_3 **4**, $CH_2CH(CH_3)_2$ **5** and $CH_2C_6H_5$ **6** as outlined in Scheme 1, {Fc = (η^5-C_5H_5)Fe(η^5-C_5H_4)} The yields obtained ranged between 45% and 52% and all gave analytical and spectroscopic data in accordance with the proposed structures All of the *N-para*-(ferrocenyl)benzoyl derivatives were characterized by a combination of fast atom bombardment mass spectrometry (FABMS), ^{1}H NMR, ^{13}C NMR, DEPT-135 and ^{1}H-^{13}C COSY (HMQC) spectroscopy and for **1** and **4** by X-ray diffraction

3 2 *Mass spectrometry*

Since the introduction of soft ionization techniques such as fast atom bombardment mass spectrometry (FABMS), a wide range of thermolabile and non-volatile compounds can be subjected to mass spectrometric analysis [12a] As compounds **3–6** are not amenable to electron ionization studies, FAB was employed in the analysis FABMS confirmed the correct relative molecular mass for all the compounds and examination of the mass spectra revealed the presence of both intense radical-cation and an $(M + H)^+$ species This is a surprising observation as the vast majority of analytes which are subjected to analysis by FABMS yield protonated molecular ion species or cation adducts [12b] The relative abundance of the radical cation species is always greater than that of the $(M + H)^+$ species Addition of a dilute solution of potassium iodide (KI) to the sample and the liquid matrix on the probe tip generated a signal 39 Daltons higher due to an $[M + K]^+$ adduct Although sequence specific fragment ions are sometimes obscured by the background noise due to the liquid matrix employed in the ionization process, structurally significant fragment ions were observed in the FAB mass spectra for all the compounds analyzed A fragment ion is present at *m/z* 261 in all the mass spectra confirming the presence of a ferrocenylphenyl subunit at the N-terminal The signal at *m/z* 289 is due to cleavage at the benzoyl C=O function Even though this ion is isobaric with an ion from the *meta*-nitrobenzyl alcohol matrix, proof that it is due to the sample can be seen from the intense relative abundance when compared to the same ion observed from the neat matrix The abundance of the fragment ions at *m/z* 261 and *m/z* 289 increase in intensity relative to the chemical background ions due to the liquid matrix employed in the analysis upon addition of the KI solution this confirms that they originate from the sample molecules and not the *meta*-nitrobenzyl alcohol matrix employed in the analysis

Table 1
^{1}H and ^{13}C spectroscopic data for 4

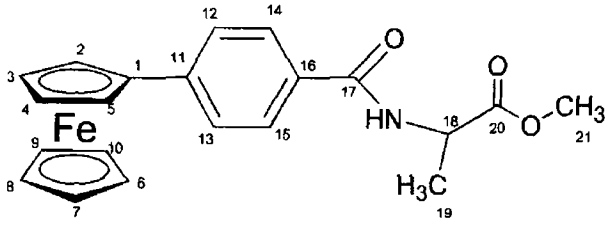

Site	^{1}H	^{13}C	HMQC
1		83 5	
2–5	4 9		67
3 4	4 42		66 9
6–10	4 02		69 9
11		143 3	
12, 13	7 63		125 7
14 15	7 81		128
16		131	
17		173 7	
18	4 46		48 6
19	1 41		17 1
20		166 5	
21	3 66		52 2

O=C–N is 9.53(14)° and between the $-C_6H_4-$ and (η^5-C_5H_4) rings of 4.92(10)°. These results serve to demonstrate the co-planarity of the conjugated groups in both **1** and **4** in the solid state (see Fig. 1).

Supplementary information

Crystallographic data for the structural analyses have been deposited with the Cambridge Crystallographic Data Centre, CCDC no. 189715 for **1** and CCDC no. 189716 for **4**. Copies of this information may be obtained free of charge from The Director, CCDC, 12 Union road, Cambridge, CB2 1EZ, UK (fax: +44-1223-336033, e-mail: deposit@ccdc.cam.ac.uk).

References

[1] (a) G. Jaouen (Ed.), J. Organomet. Chem., Bioorganometallic Chemistry (special issue), 589 (1999) 1–126.
(b) R.D. Adams (Ed.) J. Organomet. Chem., Ferrocene Chemistry (special issue), 619 (1999) 1–875.

[2] (a) V. Degani, A. Heller, J. Am. Chem. Soc. 110 (1988) 2615.
(b) M. Kira, T. Matsubara, H. Shinohara, M. Sisido, Chem. Lett. (1997) 89.

[3] (a) H.B. Kraatz, J. Lusztyk, G.D. Enright, Inorg. Chem. 36 (1997) 2400.
(b) H.B. Kraatz, D.M. Leek, A. Houmam, G.D. Enright, J. Lusztyk, D.D.M. Wayner, J. Organomet. Chem. 589 (1999) 38.

[4] (a) J.F. Gallagher, P.T.M. Kenny, M.J. Sheehy, Inorg. Chem. Commun. 2 (1999) 200.
(b) J.F. Gallagher, P.T.M. Kenny, M.J. Sheehy, Inorg. Chem. Commun. 2 (1999) 327.
(c) J.F. Gallagher, P.T.M. Kenny, M.J. Sheehy, Acta Crystallogr. C 55 (1999) 1257.

[5] (a) A. Nomoto, T. Moriuchi, S. Yamazaki, A. Ogawa, T. Hirao, J. Chem. Soc. Chem. Commun. (1998) 1963.
(b) T. Moriuchi, A. Nomoto, K. Yoshida, A. Ogawa, T. Hirao, J. Am. Chem. Soc. 123 (2001) 68.
(c) T. Moriuchi, A. Nomoto, K. Yoshida, T. Hirao, Organometallics 20 (2001) 1008.
(d) T. Itoh, S. Shirakami, N. Ishida, Y. Yamashita, T. Yoshida, H.S. Kim, Y. Wataya, Bioorg. Med. Chem. Lett. 10 (2000) 1657.

[6] (a) A. Hess, J. Schnert, T. Weyhermuller, N. Metzler-Nolte, Inorg. Chem. 39 (2000) 5437.
(b) O. Brosch, T. Weyhermuller, N. Metzler-Nolte, Inorg. Chem. 39 (2000) 323.

[7] (a) N.J. Long, Angew. Chem., Int. Ed. Engl. 34 (1995) 21.
(b) T. Verbiest, S. Houbrechts, M. Kauranen, K. Clays, A. Persoons, J. Mater. Chem. 7 (1997) 2175.
(c) J. Heck, S. Dabek, T. Meyer-Friedrichsen, H. Wong, Coord. Chem. Rev. (1999) 1217.
(d) J.A. Mata, E. Peris, S. Uriel, R. Llusar, I. Asselberghs, A. Persoons, Polyhedron 20 (2001) 2083.
(e) A.M. McDonagh, M.P. Cifuentes, M.G. Humphrey, S. Houbrechts, J. Maes, A. Persoons, M. Samoc, B. Luther-Davies, J. Organomet. Chem. 610 (2001) 145.
(f) M.H. Garcia, M.P. Robalo, A.P.S. Teixeira, A.R. Dias, M.F.M. Piedade, M.T. Duarte, J. Organomet. Chem. 632 (2001) 145.
(g) R.D.A. Hudson, I. Asselberghs, K. Clays, L.P. Cuffe, J.F. Gallagher, A.R. Manning, A. Persoons, K. Wostyn, J. Organomet. Chem. 637–639 (2001) 435.
(h) R.D.A. Hudson, A.R. Manning, D.F. Nolan, I. Asselberghs, R. Van Boxel, A. Persoons, J.F. Gallagher, J. Organomet. Chem. 619 (2001) 141.

[8] (a) J.S. Seo, Y.S. Yoo, M.G. Choi, J. Mater. Chem. 11 (2001) 1332.
(b) M. Even, B. Heinrich, D. Guillon, D.M. Guldi, M. Prato, R. Deschenaux, 7 (2001) 2595.

[9] (a) P.D. Beer, J.E. Nation, S.L.W. McWhinnie, M.E. Harman, M.B. Hursthouse, M.I. Ogden, A.H. White, J. Chem. Soc. Dalton Trans. (1991) 2485.
(b) J.E. Kingston, L. Ashford, P.D. Beer, M.G.B. Drew, J. Chem. Soc. Dalton Trans. (1999) 251.
(c) P.D. Beer, Acc. Chem. Res. 31 (1998) 71.

[10] (a) Unpublished results, D. Savage, School of Chemical Sciences, Dublin City University, Dublin 9, Ireland, 2002.
(b) J.F. Gallagher, P.T.M. Kenny, D. Savage, 2002 in preparation.

[11] P.C. Reeves, Org. Syn. 56 (1977) 28.

[12] (a) M. Barber, R.S. Bordoli, R.D. Sedgwick, A.N. Tyler, J. Chem. Soc. Chem. Commun. (1981) 325.
(b) P.T.M. Kenny, K. Nomoto, R. Orlando, Rapid Commun. Mass Spectrom. 11 (1997) 224.

[13] F.H. Allen, O. Kennard, Chem. Des. Automat. News 8 (1993) 1–31.

[14] G.M. Sheldrick, SHELXL97, University of Gottingen, Germany.

[15] A.L. Spek, PLATON, University of Utrecht, The Netherlands, 1998.

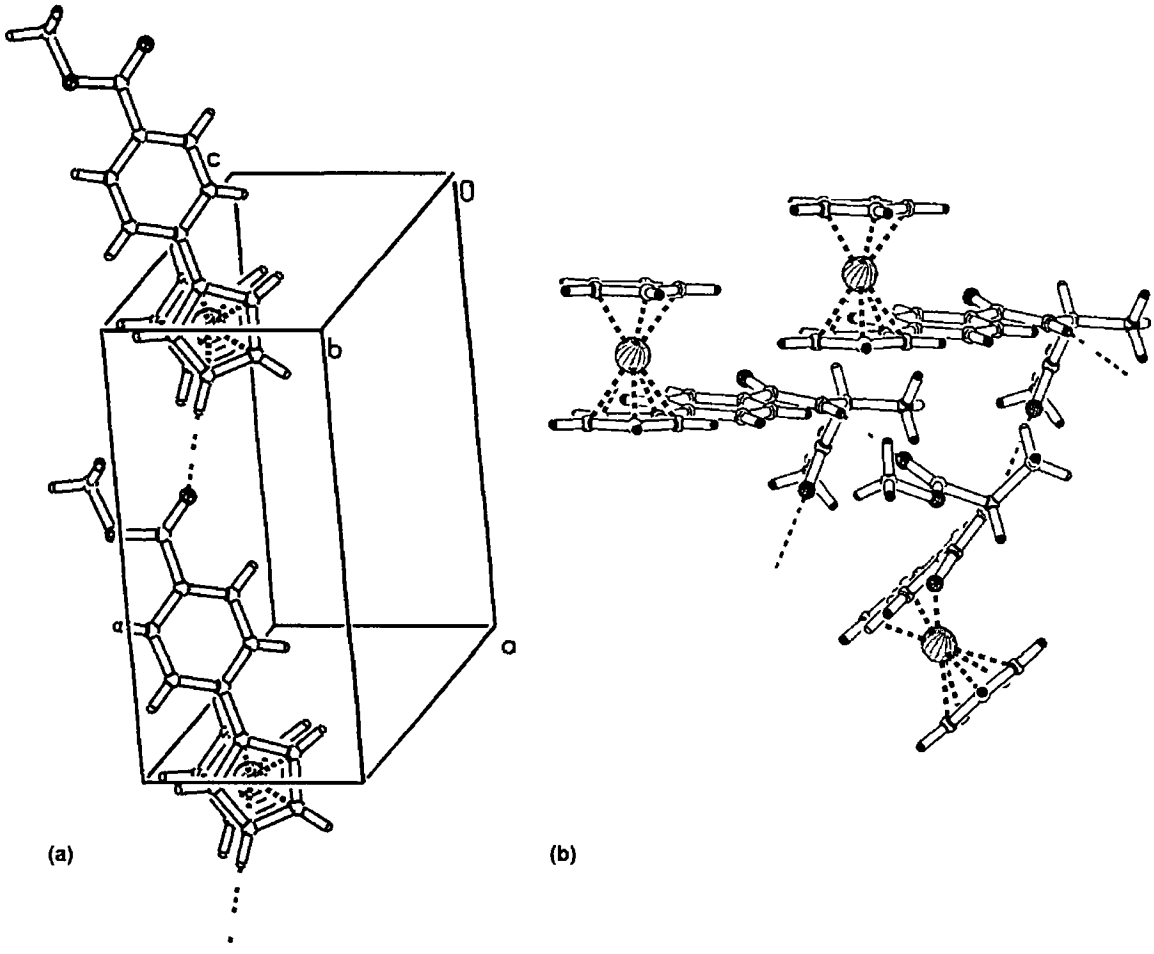

Fig 2 Views of the important intermolecular interactions in 1 (a) and 4 (b)

and angles listed in Table 2 [2] Despite the vast structural research available on ferrocenyl derivatives on the Cambridge Structural Database [13], compounds incorporating the Fc-C_6H_4-moiety are still relatively rare in comparison to the plethora of Fc derivatives reported

Compound 1 crystallises with one molecule in the asymmetric unit and *unusually* in space group Cc the molecular structure is depicted in Fig 1(a) The principal dimensions for 1 are carboxylate ester C—O 1 328(4) A, C=O 1 199(4) Å, O—CH_3 1 430(4) A and O—C=O 123 5(3)° The angle between the CO_2 carboxylate plane and the —C_6H_4— ring is 8 5(2)° and this aromatic system intersects the (η^5-C_5H_4) ring at 9 35(13)° There are no classical hydrogen bonds present and the only interaction of note is the (η^5-C_5H_4) O2=C1 contact where C13—H13 O2 forms a one-dimensional head-to-tail chain along the *a*-axis with H13 O2 2 63 A and C—H O 149° For 4, the geometric parameters are amide C=O 1 223(2) A, OC—NH 1 350(3) A, HN—CH 1 451(2) A and ester C=O/C—O 1 195(2)/1 340(2) A, respectively, with N—H O=C (ester) as the primary intermolecular hydrogen bond, N O^{II} 3 218(3) A, N—H O^{II} 158° (II = $-x, 1/2+y, -z$) Two C—H O interactions are also present, C O 3 062(3), 3 454(3) A along the *a*- and *b*-axis, respectively, Fig 2 The angle between the —C_6H_4— ring and the three-atom plane

[2] Crystallographic data 1 chemical formula $C_{18}H_{16}O_2Fe$ red block molecular weight 320 16 g mol^{-1} monoclinic space group Cc (No 9), $a = 11\ 9893(8)$ A $b = 20\ 5645(10)$ A, $c = 5\ 9358(5)$ A, $\beta = 93\ 282(6)°$, $V = 1461\ 09(17)$ A^3 $Z = 4$, density = 1 455 g cm^{-3} (calc), $F(000) = 664$ $\mu = 1\ 033$ mm^{-1} Flack parameter −0 013(18) Absorption correction range 0 440–0 496, 3014 reflections in the range 2–26° 2874 unique, $2755 > 2\sigma(I)$ 191 parameters R factor = 0 027 $wR_2 = 0\ 084$ GOF = 1 17 density range in the final difference map is −0 26 to +0 22 e A^{-3}

Crystallographic data 4 chemical formula $C_{21}H_{21}NO_3Fe$ red plate molecular weight 391 24 g mol^{-1} monoclinic space group $P2_1$ (No 4), $a = 10\ 6380(11)$ A $b = 6\ 1895(6)$ A $c = 14\ 3185(14)$ A $\beta = 107\ 810(7)°$, $V = 897\ 60(15)$ A^3, $Z = 2$, density = 1 448 g cm^{-3} (calc) $F(000) = 408$ $\mu = 1\ 033$ mm^{-1}, Flack −0 001(13), Absorption correction range 0 66–0 75 4059 reflections in the range 2–26° 3529 unique 3378 > $2\sigma(I)$, 237 parameters R factor = 0 024 $wR_2 = 0\ 057$ GOF = 1 07 density range in the final difference map is −0 12 to +0 22 e A^{-3}

Least squares refinement was undertaken using SHELXL97 [14] and the drawings were generated using PLATON [15]

Table 2
Selected bond lengths and angles (A, °) for molecules **1** and **4**

			1	4
Fe1	Cg1		1 6418(13)	1 6497(10)
Fe2	Cg2		1 6548(19)	1 6568(12)
Cg1	Fe1	Cg2	178 87(9)	179 16(7)
C1–O1			1 328(4)	1 223(2)
C1–O2/N1			1 199(4)	1 350(3)
C2–O1/N1			1 430(4)	1 451(2)
C1–N1			/	1 350(3)
C1–C34			1 489(3)	1 490(3)
Fe1–C11–C34			126 59(18)	125 55(14)
O1–C1–C34			112 2(3)	120 72(18)

Where Cg1 and Cg2 are the centroids of the (η^5 C_5H_4) and (η^5 C_5H_5) rings respectively

3 3 ^1H and ^{13}C NMR spectroscopic analysis

All the proton and carbon chemical shifts for compounds **3–6** were unambiguously assigned by a combination of DEPT-135 and ^1H-^{13}C-COSY (HMQC) The ^1H and ^{13}C NMR spectra for compounds **3–6** showed peaks in the ferrocene region characteristic of a mono substituted ferrocene moiety [3a,4] The protons in the *ortho* position of the substituted Cp ring appear in the region δ 4 85–4 9 whereas the protons in the *meta* position occur in the range δ 4 41–4 5 The unsubstituted Cp ring appears in the region δ 3 98–4 02 The protons of the *para*-disubstituted phenyl group appear as two doublets in the region δ 7 61–7 81 For example, in the case of the glycine derivative **3** the unsubstituted C_5H_5 ring appears as a singlet in the ^1H NMR spectrum at δ 3 98 The *ortho* and *meta* protons on the substituted Cp ring are present at δ 4 85 and δ 4 38, respectively The N*H* proton appears as a triplet at δ 8 88 (J = 5 6 Hz) whereas a doublet at δ 3 97 (J = 5 6 Hz) corresponds to the –NHC*H*$_2$CO– protons The aromatic protons are present as two doublets at δ 7 76 and δ 7 6 (J = 8 Hz) and a sharp singlet at δ 3 63 is due to the methyl ester

The ^{13}C NMR spectra show signals in the region δ 67–84 indicative of a monosubstituted ferrocene subunit with the *ipso* carbon of the substituted Cp ring appearing in a narrow range of δ 83 5–83 9 The methylene carbon atoms of derivatives **5** and **6** were identified by DEPT-135 A complete assignment of the ^1H and ^{13}C NMR spectra of *N*-{*para*-(ferrocenyl)benzoyl}-L-alanine methyl ester **4** is presented in Table 1

3 4 X-ray crystallographic studies of 1 and 4

The single crystal X-ray structures of compounds **1** and **4** have been determined with selected bond lengths

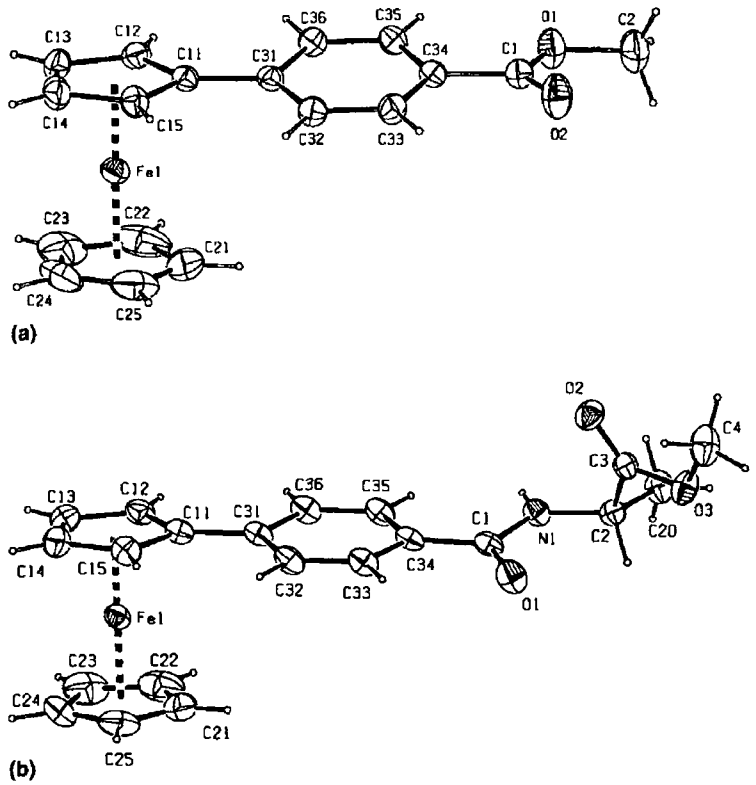

Fig 1 Molecular drawings of **1** (a) and **4** (b) using ORTEP displacement ellipsoids are drawn at the 30% probability level

Acta Crystallographica Section C
Crystal Structure Communications
ISSN 0108 2701

Ethyl and isopropyl 4-ferrocenylbenzoate

Frankie P. Anderson, John F. Gallagher, Peter T. M. Kenny, Clodagh Ryan and David Savage

Acta Crystallographica Section C
Crystal Structure Communications
ISSN 0108 2701

Ethyl and isopropyl 4-ferrocenylbenzoate

Frankie P Anderson,[a] John F Gallagher,[a]* Peter T M Kenny,[a]* Clodagh Ryan[b] and David Savage[b]

[a]School of Chemical Sciences National Institute for Cellular Biotechnology Dublin City University Dublin 9 Ireland and [b]School of Chemical Sciences Dublin City University Dublin 9 Ireland
Correspondence e mail john gallagher@dcu ie

Received 18 November 2002
Accepted 26 November 2002
Online 10 December 2002

The title compounds $[Fe(C_5H_5)(C_{14}H_{13}O_2)]$ and $[Fe(C_5H_5)(C_{15}H_{15}O_2)]$, respectively, contain the ferrocenyl $\eta^5(C_5H_4)$ and phenylene $-C_6H_4-$ rings in a nearly coplanar arrangement, with interplanar angles of 6 88 (12) and 10 5 (2)°, respectively Molecules of the ethyl ester form dimers through $\eta^5(C_5H_5)C-H\ O{=}C$ hydrogen bonds, with graph set $R_2^2(20)$, and, together with $Csp^3-H\ \pi(C_5H_5)$ interactions, generate a one dimensional column (irregular ladder) Molecules of the isopropyl ester aggregate through $\eta^5(C_5H_5)C-H\ \pi(C_6H_4)$ interactions

Comment

The design of new redox-active ligands for application in diverse research areas, such as medicinal chemistry and materials science, has engrossed scientists in recent years Ferrocene (Fc) derivatives, which are efficient redox systems, have been studied extensively in charge-transfer chemistry, hydrogen bonding and molecular-recognition science, peptide chemistry, non-linear optical materials, and liquid crystal research (Chesney *et al*, 1998, Glidewell *et al*, 1997, Zakaria *et al*, 2002, Kraatz *et al*, 1999, Gallagher *et al*, 1999*a*,*b*, Hudson, Asselsbergh *et al*, 2001, Hudson, Manning *et al*, 2001 Even *et al*, 2001, Seo *et al*, 2001) Our interest in ferrocenylbenzoyl derivatives stems from their use as precursors to ferrocenylbenzoyl amino acid ester and dipeptide derivatives We have recently reported the crystal structure of methyl 4 ferrocenylbenzoate, (I) (Savage *et al*, 2002)

An understanding of the interactions present in a given crystal structure can provide valuable information on the hydrogen-bonding and aggregation modes not just in the solid state but also in the liquid-crystalline state The structures of ethyl 4-ferrocenylbenzoate, (II), and the isopropyl analogue, (III), are reported herein for comparison with both the methyl analogue, (I), and our ongoing research on longer chain alkyl derivatives

The Fe1—C bond lengths for the $\eta^5(C_5H_4)$ ring of (II) are in the range 2 0341 (16)–2 0452 (14) A similar to the $\eta^5(C_5H_5)$ ring, with a range of 2 0315 (18)–2 0407 (17) A For (III), these values are in the ranges 2 024 (3)–2 044 (3) and 2 023 (4)–2 033 (4) A respectively In (II), the Fe1 *Cg*1 and Fe1 *Cg*2 distances are 1 6425 (8) and 1 6463 (9) A, respectively, and the *Cg*1 Fe1 *Cg*2 angle is 179 49 (5)°, where *Cg*1 and *Cg*2 are the centroids of the $\eta^5(C_5H_4)$ and $\eta^5(C_5H_5)$ rings respectively In (III), these values are 1 6413 (15) and 1 643 (2) A, and 178 88 (9)°, respectively In (II), the cyclopentadienyl C—C bond-length ranges are small being 1 413 (3)–1 435 (2) and 1 398 (3)–1 420 (3) A for the $\eta^5(C_5H_4)$ and $\eta^5(C_5H_5)$ rings, respectively In (III), these ranges are 1 407 (5)–1 428 (4) and 1 389 (6)–1 410 (6) A, respectively These results are as expected and highlight the similarity in the ferrocenyl bond lengths and angles in the esters (I) (Savage *et al*, 2002), and (II) and (III), described herein

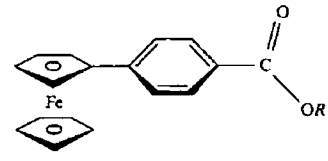

(II) R = ethyl
(III) R = isopropyl

The cyclopentadienyl rings deviate slightly from an eclipsed geometry in (II), as evidenced by the C1*n* *Cg*1 *Cg*2 C2*n* (*n* = 1–5) torsion angles ranging from 2 87 (14) to 3 61 (14)° In (III), the angles are in the range 6 1 (3)–7 0 (3)°, similar to the eclipsed geometry in (I), where the range is 0 8 (4)–2 3 (4)° In contrast, this range of angles is 13 7 (2)–15 4 (3)° in *para* ferrocenylbenzoyl- -alanine methyl ester (Savage *et al*, 2002)

The essentially linear molecular conformations adopted by (II) and (III) are comparable, with interplanar angles of 6 88 (12)° between the $\eta^5(C_5H_4)$ and $-C_6H_4-$ rings in (II), 10 5 (2)° in (III) and 9 35 (13)° in (I) The major differences are in the terminal O1—C1—C34—C33 torsion angles, the value of which is 0 8 (2)° in (II), 18 2 (5)° in (III) and 171 2 (3)° in (I) However, the disposition of the terminal alkoxy group, which gives a C1—O1—C2—C3 torsion angle of

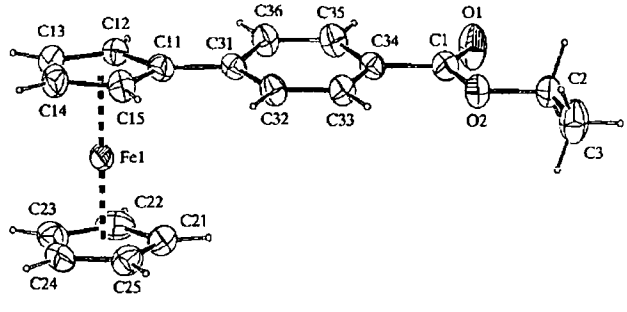

Figure 1
A view of the molecule of (II) with the atomic numbering scheme Displacement ellipsoids are drawn at the 30% probability level and H atoms are shown as small spheres of arbitrary radii

 DOI 10 1107/S0108270102021819

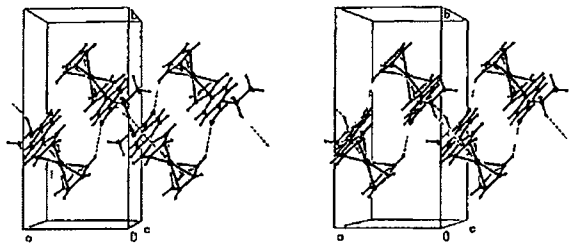

Figure 2
A stereoview of the interactions in the crystal structure of (II)

179 76 (16)° in (II) and 112 0 (5)° in (III), means that the methyl groups of the isopropyl moiety in (III) are oriented almost orthogonal to the ester CO_2 plane (Figs 1 and 3)

Analysis of the hydrogen bonding in (II) shows only two interactions of note, involving the substituted ring and the ester O=C group as $\eta^5(C_5H_4)C-H$ O=C interactions (Table 2 and Fig 2) Molecules of the ethyl ester form dimers through $\eta^5(C_5H_5)C-H$ O=C hydrogen bonds, graph set $R_2^2(20)$ and, together with Csp^3-H $\pi(C_5H_5)$ interactions, these generate a one-dimensional column (irregular ladder) The molecules of the isopropyl ester, (III), aggregate through $\eta^5(C_5H_5)C-H$ $\pi(C_6H_4)$ interactions (Table 4 and Fig 4)

Analysis of the April 2002 Version of the Cambridge Structural Database using *ConQuest* Version 1 4 (Allen, 2002) for the mono-substituted *para*-Fc-C_6H_4-*X* group (*X* is any atom) was undertaken for structures which fulfil the three-dimensional coordinates and $R < 0.10$ criteria A total of 13 relevant structures were found The interplanar angle between the C_5H_4 and C_6 rings varies between 2 2 and 29 1° for 17 examples, with a median of 12 8° (11 examples are within the range 7 7–19 3°) Our results above compare favourably with these values.

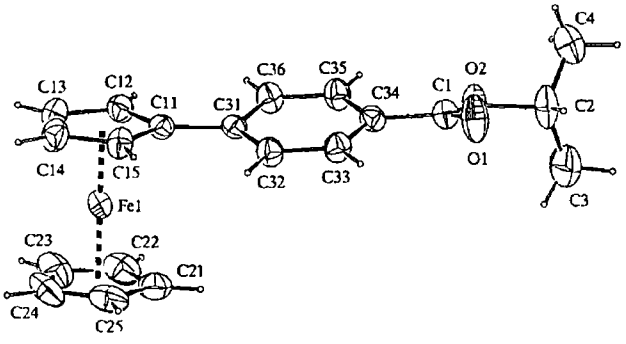

Figure 3
A view of the molecule of (III) with the atomic numbering scheme Displacement ellipsoids are drawn at the 30% probability level and H atoms are shown as small spheres of arbitrary radii

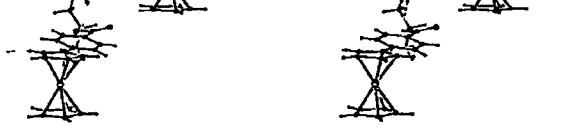

Figure 4
A stereoview of the interactions in the crystal structure of (III) For the sake of clarity the unit cell box has been omitted

Experimental

Compounds (II) and (III) were prepared according to standard literature procedures Analytical data for (II) m p 358–359 K (uncorrected), IR (KBr ν, cm $^{-1}$) 1678 (C=O) UV-vis, λ_{max} (CH_3CN) 360 (880), 445 (290) nm, ^{1}H NMR (400 MHz $CDCl_3$, δ, p p m) 7 86 (2H, *d*, *J* = 8 4 Hz, Ar H), 7 66 (2H, *d*, *J* = 8 4 Hz, Ar H) 4 89 [2H *t*, *J* = 1 8 Hz, *o* $\eta^5(C_5H_4)$] 4 44 [2H, *t*, *J* = 1 8 Hz, *m* $\eta^5(C_5H_4)$], 4 32 (2H, *q*, *J* = 7 Hz $-OCH_2CH_3$), 4 03 [5H, *s*, $\eta^5(C_5H_5)$] 1 33 (3H, *t*, $-OCH_2CH_3$), ^{13}C NMR ($CDCl_3$, δ, p p m) 166 1, 145 5, 129 6 127 2, 126 0, 83 0, 70 2, 69 9 67 2, 60 9 14 6 Analytical data for (III) m p 351–352 K (uncorrected), IR (KBr,ν, cm $^{-1}$) 1710 (C=O), UV-vis, λ_{max} (CH_3CN) 360 (1120), 458 (302) nm, ^{1}H NMR (400 MHz, $CDCl_3$, δ, p p m) 7 87 (2H, *d*, *J* = 8 4 Hz, Ar H), 7 44 (2H, *d*, *J* = 8 4 Hz, Ar H), 5 18 [1H, *m* $OCH(CH_3)_2$], 4 64 [2H, *s*, *o* $\eta^5(C_5H_4)$], 4 32 [2H, *s*, *m*-$\eta^5(C_5H_4)$], 3 96 [5H, *s*, $\eta^5(C_5H_5)$], 1 30 [6H *t* $OCH(CH_3)_2$], ^{13}C NMR ($CDCl_3$, δ p p m) 166 6, 145 2, 130 0 128 5 126 0 83 9 70 2, 70 1, 68 5, 67 3, 22 4

Compound (II)

Crystal data

$[Fe(C_5H_5)(C_{14}H_{13}O_2)]$	D_x = 1 425 Mg m $^{-3}$
M = 334 18	Mo $K\alpha$ radiation
Monoclinic $P2_1/c$	Cell parameters from 80 reflections
a = 7 9563 (5) A	θ = 5 5–20 7
b = 16 3464 (11) A	μ = 0 97 mm $^{-1}$
c = 12 0088 (10) A	T = 294 (1) K
β = 94 128 (5)	Block orange
V = 1557 78 (19) A^3	0 50 × 0 45 × 0 45 mm
Z = 4	

Data collection

Siemens *P4* diffractometer	R_{int} = 0 012
$\omega/2\theta$ scans	θ_{max} = 28°
Absorption correction ψ scan (North *et al* 1968)	h = 10 1
T_{min} = 0 629 T_{max} = 0 646	k = 21 1
4875 measured reflections	l = 15 15
3780 independent reflections	4 standard reflections
3276 reflections with $I > 2\sigma(I)$	every 296 reflections
	intensity variation ±1%

Table 1
Selected geometric parameters (A, °) for (II)

O1–C1	1 200 (2)	C1–C34	1 489 (2)
O2–C1	1 3282 (19)	C2–C3	1 486 (3)
O2–C2	1 4503 (19)	C11–C31	1 470 (2)
C1–O2–C2	115 63 (13)	O2–C2–C3	107 37 (15)
O1–C1–O2	123 17 (16)	C1–C34–C33	122 85 (14)
O1–C1–C34	124 07 (15)	C1–C34–C35	118 07 (14)
O2–C1–C34	112 76 (13)		
C2–O2–C1–C34	178 95 (13)	C12–C11–C31–C36	7 9 (2)
C1–O2–C2–C3	179 76 (16)	O1–C1–C34–C33	178 40 (17)

Refinement

Refinement on F^2	$w = 1/[\sigma^2(F_o^2) + (0.039P)^2 + 0.319P]$ where $P = (F_o^2 + 2F_c^2)/3$
$R[F^2 > 2\sigma(F^2)] = 0.028$	$(\Delta/\sigma)_{max} < 0.001$
$wR(F^2) = 0.079$	$\Delta\rho_{max} = 0.28$ e Å^{-3}
$S = 1.05$	$\Delta\rho_{min} = -0.30$ e Å^{-3}
3780 reflections	
200 parameters	
H atom parameters constrained	

Table 2
Hydrogen bonding and short contact geometry (Å, °) for (II)

*Cg*1 is the centroid of the substituted cyclopentadienyl ring

D—H···*A*	*D*—H	H···*A*	*D*···*A*	*D*—H···*A*
C22—H22···O1	0.93	2.54	3.360 (3)	147
C2—H2*A*···*Cg*1^{ii}	0.97	2.87	3.770 (2)	155

Symmetry codes: (i) $1+x, 1+y, z$; (ii) $x, 1+y, z$.

Compound (III)

Crystal data

$[Fe(C_5H_5)(C_{15}H_{15}O_2)]$	$D_x = 1.360$ Mg m^{-3}
$M_r = 348.21$	Mo $K\alpha$ radiation
Monoclinic, $P2_1/a$	Cell parameters from 72 reflections
$a = 9.3406$ (9) Å	$\theta = 6.1$–$15.3°$
$b = 10.1663$ (6) Å	$\mu = 0.89$ mm^{-1}
$c = 17.9072$ (10) Å	$T = 294$ (1) K
$\beta = 90.136$ (6)°	Block, red
$V = 1700.5$ (2) Å^3	0.39 × 0.26 × 0.15 mm
$Z = 4$	

Data collection

Siemens *P*4 diffractometer	$R_{int} = 0.006$
$\omega/2\theta$ scans	$\theta_{max} = 26°$
Absorption correction: ψ scan (North *et al.* 1968)	$h = -11 \rightarrow 1$
$T_{min} = 0.769$, $T_{max} = 0.875$	$k = -1 \rightarrow 12$
4440 measured reflections	$l = -22 \rightarrow 22$
3355 independent reflections	4 standard reflections
2439 reflections with $I > 2\sigma(I)$	every 296 reflections
	intensity variation: ±1%

Refinement

Refinement on F^2	$w = 1/[\sigma^2(F_o^2) + (0.0468P)^2 + 0.7638P]$ where $P = (F_o^2 + 2F_c^2)/3$
$R[F^2 > 2\sigma(F^2)] = 0.043$	$(\Delta/\sigma)_{max} < 0.001$
$wR(F^2) = 0.109$	$\Delta\rho_{max} = 0.33$ e Å^{-3}
$S = 1.04$	$\Delta\rho_{min} = -0.30$ e Å^{-3}
3355 reflections	
210 parameters	
H atom parameters constrained	

Table 3
Selected geometric parameters (Å, °) for (III)

O1—C1	1.186 (4)	C1—C34	1.485 (4)
O2—C1	1.321 (4)	C2—C3	1.440 (7)
O2—C2	1.481 (4)	C2—C4	1.448 (6)
C1—O2—C2	117.7 (2)	O2—C2—C4	108.2 (3)
O1—C1—O2	124.1 (3)	C3—C2—C4	114.8 (4)
O1—C1—C34	123.8 (3)	C1—C34—C33	118.2 (3)
O2—C1—C34	112.1 (3)	C1—C34—C35	123.7 (3)
O2—C2—C3	107.9 (4)		
C2—O2—C1—O1	5.9 (5)	C1—O2—C2—C3	112.0 (5)

Table 4
Hydrogen bonding and short contact geometry (Å, °) for (III)

*Cg*3 is the centroid of the phenylene ring system

D—H···*A*	*D*—H	H···*A*	*D*···*A*	*D*—H···*A*
C2—H2···O1	0.98	2.25	2.696 (4)	106
C12—H12···*Cg*3^{i}	0.93	2.75	3.658 (3)	167

Symmetry code: (i) $x, \frac{1}{2}-y, \frac{1}{2}+z$.

For compounds (II) and (III), space groups $P2_1/c$ and $P2_1/a$, respectively, were uniquely assigned from the systematic absences and confirmed by the analyses. H atoms were treated as riding atoms, with C—H distances in the range 0.93–0.98 Å.

For both compounds, data collection *XSCANS* (Siemens, 1994), cell refinement *XSCANS*, data reduction *XSCANS*, program(s) used to solve structure *SHELXS*97 (Sheldrick, 1997), program(s) used to refine structure *SHELXL*97 (Sheldrick, 1997), molecular graphics *ORTEP*III (Burnett & Johnson, 1996) and *PLATON* (Spek, 1998), software used to prepare material for publication *SHELXL*97 and *PREP*8 (Ferguson, 1998).

FPA thanks the National Institute for Cellular Biotechnology, for a studentship under the Irish Government PRTLI#3 funding scheme. JFG thanks Dublin City University for the purchase of a *P*4 diffractometer and computer system. DS thanks the School of Chemical Sciences and the Irish–American Partnership for funding to undertake chemical research.

Supplementary data for this paper are available from the IUCr electronic archives (Reference: GD1238). Services for accessing these data are described at the back of the journal.

References

Allen, F. H. (2002). *Acta Cryst.* B**58**, 380–388.

Burnett, M. N. & Johnson, C. K. (1996). *ORTEP*III. Report ORNL 6895. Oak Ridge National Laboratory, Tennessee, USA.

Chesney, A., Bryce, M. R., Batsanov, A. S., Howard, J. A. K. & Goldenberg, L. M. (1998). *J. Chem. Soc. Chem. Commun.* pp. 677–679.

Even, M., Heinrich, B., Guillon, D., Guldi, D. M., Prato, M. & Deschenaux, R. (2001). *Chem. Eur. J.* **7**, 2595–2604.

Ferguson, G. (1998). *PREP*8. University of Guelph, Canada.

Gallagher, J. F., Kenny, P. T. M. & Sheehy, M. J. (1999*a*). *Inorg. Chem. Commun.* **2**, 200–204.

Gallagher, J. F., Kenny, P. T. M. & Sheehy, M. J. (1999*b*). *Inorg. Chem. Commun.* **2**, 327–330.

Glidewell, C., Ahmed, S. Z., Gallagher, J. F. & Ferguson, G. (1997). *Acta Cryst.* C**53**, 1775–1778.

Hudson, R. D. A., Asselsbergh, I., Clays, K., Cuffe, L. P., Gallagher, J. F., Manning, A. R., Persoons, A. & Wostyn, K. (2001). *J. Organomet. Chem.* **637–639**, 435–444.

Hudson, R. D. A., Manning, A. R., Nolan, D. F., Asselsbergh, I., Van Boxel, R., Persoons, A. & Gallagher, J. F. (2001). *J. Organomet. Chem.* **619**, 141–151.

Kraatz, H. B., Leek, D. M., Houmam, A., Enright, G. D., Lustyk, J. & Wayner, D. D. M. (1999). *J. Organomet. Chem.* **589**, 38–49.

North, A. C. T., Phillips, D. C. & Mathews, F. S. (1968). *Acta Cryst.* A**24**, 351–359.

Savage, D., Gallagher, J. F., Ida, Y. & Kenny, P. T. M. (2002). *Inorg. Chem. Commun.* **5**, 1034–1040.

Seo, J. S., Yoo, Y. S. & Choi, M. G. (2001). *J. Mater. Chem.* **11**, 1332–1338.

Sheldrick, G. M. (1997). *SHELXS*97 and *SHELXL*97. University of Gottingen, Germany.

Siemens (1994). *XSCANS*. Version 2.2. Siemens Analytical X-ray Instruments Inc., Madison, Wisconsin, USA.

Spek, A. L. (1998). *PLATON*. University of Utrecht, The Netherlands.

Zakaria, C. M., Ferguson, G., Lough, A. J. & Glidewell, C. (2002). *Acta Cryst.* C**58**, m1–m4.